

Steam Enhanced Remediation Research for DNAPL in Fractured Rock Loring Air Force Base, Limestone, Maine



Steam Enhanced Remediation Research for DNAPL in Fractured Rock Loring Air Force Base, Limestone, Maine

Eva Davis
U.S. Environmental Protection Agency
Ada, Oklahoma 74820

Naji Akladiss & Rob Hoey
Maine Department of Environmental Protection
Augusta, Maine 04333

Bill Brandon & Mike Nalipinski
Region 1
U.S. Environmental Protection Agency
Boston, Massachusetts 02114

Steve Carroll & Gorm Heron
SteamTech Environmental Services, Inc.
Bakersfield, California 93308

Kent Novakowski
Queens University
Kingston, Ontario, Canada K7L3N6

Kent Udell
University of California, Berkeley
Berkeley, California 94720

State of Maine
Department of Environmental Protection
Augusta, Maine 04333

National Risk Management Research Laboratory
Office of Research and Development
U.S. Environmental Protection Agency
Cincinnati, Ohio 45268

Notice

The U.S. Environmental Protection Agency through its Office of Research and Development, Maine Department of Environmental Protection, United States Air Force, and SteamTech Environmental Services, Inc., funded, managed, and collaborated in the research described here. It has been subjected to the Agency's peer and administrative review and has been approved for publication as an EPA document. Mention of trade names or commercial products does not constitute endorsement or recommendation for use.

All research projects making conclusions or recommendations based on environmental data and funded all or in part by the U.S. Environmental Protection Agency are required to participate in the Agency Quality Assurance Program. This project was conducted under an approved Quality Assurance Project Plan. Information on the plan and documentation of the quality assurance activities and results are available from the lead author.

Preface

The Maine Department of Environmental Protection (MEDEP) understands that cleanup of fractured bedrock aquifers is difficult, expensive, and in many cases technically impracticable, but we still find technical impracticability difficult to accept. Therefore, when reasonable arguments arose against a technical impracticability waiver for the Quarry, MEDEP was anxious to find a technology that would reduce the mass of contaminant trapped in the bedrock. MEDEP conceived the Quarry project as a modest effort, meant to try innovative methods of mass reduction on a limited budget over a limited time. The Quarry location seemed ideal for trying out new technologies – remote, in a harsh climate, and far from receptors. As it turned out, the modest effort was nurtured by the expertise and resources of many agencies and individuals. I am grateful for their efforts and grateful I got the chance to work with them.

MEDEP would like to acknowledge the following parties who were crucial to the completion of the project:

Funding was provided by U.S. EPA, through its Superfund Innovative Technology Evaluation (SITE) program. Ms. Annette Gatchett of EPA (SITE program) provided excellent management skills in providing funding and oversight of the steam injection program.

Special thanks to Dr. Eva Davis of U.S. EPA for assuming the role of technical lead for the entire steam injection project. Dr. Davis' invaluable contribution to the project was the key to our success. She maintained the project on track, resolved many of the technical problems and tracked all project data. Dr. Davis was a major contributor to this report.

Mr. Paul Depercin of U.S. EPA (SITE program) provided a great deal of support in the field as well as contract management.

Mike Nalipinski and Bill Brandon of EPA Region I have provided the team with outstanding support. Mr. Nalipinski invested more than seven years into the Loring remediation; his input in to the program helped resolve many obstacles we encountered. Mr. Brandon's technical expertise in the field of structural geology and his knowledge of the site geology helped the team in the decision making process.

Mr. David Strainge of the U.S. Air Force provided crucial funding and project oversight. Mr. Strainge has been an invaluable resource to the Air Force and the people of Maine in the ten plus years since the base went Base Realignment and Closure (BRAC).

Many thanks to Rob Hoey and Robert Sypitkowski of the MEDEP for their contribution to the steam project in the area of geology and engineering. Mr. Hoey and Mr. Sypitkowski spent countless hours working on the project. Mr. Hoey was a great instrument in building a site map, the collection of ground water samples, and data processing.

SteamTech Environmental Services, Inc., contributed funding and technical expertise. SteamTech contributed a great deal to the success of the research project. Hank Sowers, Dr. Gorm Heron, Dr. Steve Carroll, and Gregg Crisp were great instruments in the design and operation of the steam injection at the Quarry.

This project would not be possible without the invaluable contribution of Dr. Kent Udell of the University of California at Berkeley and Dr. Kent Novakowski of Queen's University, Ontario, Canada.

EPA's Office of Environmental Measurement and Evaluation (Region I) made significant contributions to the success of the project in terms of technical expertise in vapor sampling, analysis of vapor samples, and validation of laboratory data.

Many thanks to the Maine Department of Human Services Laboratory for their efforts in analyzing aqueous phase samples and for providing the analytical data in a timely manner.



Naji Akladiss, P.E.
Loring Quarry Steam Injection Research Project Manager
Maine Department of Environmental Protection

Acknowledgments

Loring Quarry Steam Injection Research Project Team

U.S. Environmental Protection Agency:

Annette Gatchett, Associate Director for Technology,

ORD/NRMRL – Cincinnati, Ohio

Paul de Percin, SITE Project Manager, ORD/NRMRL – Cincinnati, Ohio

Dr. Eva Davis, Technical Lead, ORD/NRMRL – Ada, Oklahoma

Mike Nalipinski – Remedial Project Manager, Region 1

Bill Brandon – Geologist, Region 1

Maine Department of Environmental Protection:

Naji Akladiss, P.E., Project Manager

Rob Hoey, C.G., Geologist

Robert Sypitkowski, P.E., Engineer

SteamTech Environmental Services, Inc.:

Hank Sowers, CEO

Dr. Gorm Heron, Project Engineer

Dr. Steve Carroll, Project Geologist

Gregg Crisp, Field Manager

Air Force Base Conversion Agency:

David Strainge, Engineer

Experts from Acedemia:

Dr. Kent Novakowski, Queens University

Dr. Kent Udell, University of California - Berkeley

Executive Summary

This report details a research project on Steam Enhanced Remediation (SER) for the recovery of volatile organic contaminants (VOCs) from fracture limestone that was carried out at an abandoned quarry at the former Loring Air Force Base (AFB) in Limestone, Maine. The project was carried out by United States Environmental Protection Agency (U.S. EPA) Office of Research and Development (ORD) National Risk Management Research Laboratory (NRMRL), U.S. EPA Region I, Maine Department of Environmental Protection (MEDEP), SteamTech Environmental Services, Inc., the United States Air Force (USAF), and experts from academia on characterization of fractured rock and steam injection remediation. U.S. EPA's Superfund Innovative Technology Evaluation (SITE) program participated in this research project to evaluate the SER technology in the fractured rock setting.

Loring AFB was added to the Superfund National Priorities List in 1990, and the Quarry was one of more than 50 sites on base that were addressed. The Quarry had historically been used for the disposal of wastes from construction, industrial, and maintenance activities at the base, and during remedial activities in the 1990s, approximately 450 drums were removed. Subsequent investigations showed that both chlorinated organics and fuel-related compounds were present in the ground water beneath the Quarry. Tetrachloroethylene (PCE) was detected at concentrations indicative of the presence of Dense Non-Aqueous Phase Liquids (DNAPL). The Record of Decision (ROD), signed in 1999, recognized that it was currently impractical to restore ground water in fractured rock to drinking water standards. However, an agreement was made between the USAF, MEDEP, and EPA Region I to use the Quarry to conduct a research project to further the development of remediation technologies in fractured rock, and with the hope of recovering contaminant mass to reduce the timeframe for natural attenuation of the remaining contaminants. In addition, the regulatory agencies hoped to develop guidance on characterization techniques for fractured rock. A Request for Proposals (RFP) for technologies to be tested at the site was issued in 2001, and SER was chosen from the proposals received.

With a technology and a vendor chosen, additional technology specific objectives for the research project were developed, which included determining if SER could: 1) heat the target area for remediation, 2) enhance contaminant recovery, and 3) reduce contaminant concentrations in the rock and ground water. Secondary objectives included determining if contaminants were mobilized outside of the treatment area, documenting the ability of SteamTech's effluent treatment systems to meet discharge requirements, determining operating parameters for fractured rock, and documenting costs.

Characterization activities were initiated in 2001 with the installation of process boreholes based on the agreed on treatment area and the preliminary design of the treatment system. These borings were cored and logged, and rock chip samples were collected from fracture surfaces for determination of contaminant concentrations. Additional characterization activities included discrete interval transmissivity testing and ground water sampling, conventional borehole geophysical and acoustic televiewer (ATV) logging, and interconnectivity testing. Based on the results of all the characterization activities and an updated conceptual site model (CSM), the steam injection and extraction system was revised to include steam injection at the eastern side of the target area, with extraction along the center line and the western side of the target area.

Construction of the system was initiated in August 2002, and the extraction system starting operation on August 30. Steam injection was initiated on September 1, and continued until November 19, when funding for the project ran out. Extraction was terminated on November 26. Throughout operations, EPA's SITE program collected effluent vapor and water samples to document the contaminant recovery rate and amount of contaminants recovered. SteamTech collected temperature data using 22 thermocouple strings, and documented changes in subsurface resistivity caused by temperature increases or by steam replacing water in the fractures using electrical resistance tomography (ERT).

Early in operations, it became apparent that steam injection rates were much lower than anticipated due to low transmissivities in the injection intervals and sparsely spaced fractures. In an attempt to inject more steam and increase the rate of heating, three extraction wells were converted to injection wells during operations. Although this significantly increased the amount of steam being injected, the amount of energy that could be injected during the limited-time project was still low, and the entire target zone for treatment could not be heated. The highest recorded temperature away from the injection wells was approximately 50°C, which was recorded approximately 4.5 meters (15 feet) from the nearest injection well. ERT was found to be capable of monitoring the heatup of the subsurface during SER; however, the magnitude of the resistivity changes determined was not consistent with the expected change based on prior laboratory measurements of resistivity of limestone as a function of temperature. Based on the limited duration of steam injection during this project, it cannot be determined conclusively that

steam injection would be capable of heating the entire treatment area to the target temperature. However, since the rock chip sampling showed that most of the contaminants were located at the fracture surfaces or within 0.3 meter (1 foot) of the fracture surface, the heat that was injected was concentrated where the contaminants were found. It is possible that adequate treatment might have been achieved even without achieving target temperatures throughout the target zone.

Despite the limited heating that occurred, effluent vapor and water samples showed that after approximately three weeks of operations, the extraction rates started to increase, and they continued to increase for the duration of the project. The highest extraction rates were achieved at the end of the project, after steam injection had ceased and air injection was increased. This is believed to be due to air stripping of VOCs at the higher subsurface temperatures, which carried the vaporized contaminants to extraction wells. Effluent samples showed that more than 7.4 kg (16.2 lbs) of contaminants were recovered during the project, of which 5.0 kg (11.12 lbs) were chlorinated VOCs, 0.55 kg (1.22 lbs) were gasoline range organics (GRO), and 1.77 kg (3.9 lbs) were diesel range organics (DRO). Based on the high concentrations of PCE and DRO in some wells during the last round of sampling, it is believed that NAPL was about to be extracted.

Sampling of the effluent vapor and water streams just prior to discharge showed that the vapor and water treatment systems employed by SteamTech effectively treated these streams to meet discharge limitations. Ground water samples from two angled wells that extended below the treatment area showed that contaminants do not appear to have been moved downward by SER. Ground water samples from two wells just to the north and east of the treatment area showed that contaminants were not moved horizontally into those areas. Evaluation of operations data shows that higher steam injection pressure can be used in competent bedrock than are typically possible in unconsolidated media, and the importance of the co-injection of air and pressure cycling to enhance the transport of mobilized contaminants to extraction wells.

The evolution of the CSM as additional characterization information became available, and after the completion of the steam injection, allowed an evaluation of the importance of different characterization activities to understanding ground water and contaminant transport in fractured rock, and to the design and implementation of the SER system. It was determined that a variety of characterization activities are required to understand the flow system and contaminant distribution sufficiently for remediation system design and operation.

For large, simple-to-moderately complex fractured rock sites, SER may be an efficient and cost effective remediation technology for VOCs. However, for highly complex, low permeability fractured sites with low interconnectivity, such as the Loring Quarry, steam injection may not be the best method for remediation. In order for SER to be successful in such an environment, extensive characterization is needed, and extremely long injection times are likely necessary. Even with long injection times, heat losses may limit the ability to heat the entire target zone. For sites such as this, Thermal Conductive Heating (TCH) or Electrical Resistance Heating (ERH) may be more capable of uniformly heating the target zone, and may be effectively implemented with less characterization, resulting in an overall reduction in remediation costs. Further research is warranted on steam injection remediation in fractured rock in less complex sites, and on the application of ERH and TCH to contaminated fractured rock sites.

Contents

Preface	v
Acknowledgments	vi
Executive Summary	vii
Figures	xiii
Tables	xvi
Plates	xvii
Acronyms and Abbreviations	xviii
Chapter 1. Introduction	1
1.1. Site Description and History	2
1.1.1. Site Description	2
1.1.2. Administrative History	3
1.1.3. Technology Selection	3
1.1.4. Project Structure and Administration	3
1.2. Project Chronology	3
1.3. Objectives of Research Project	4
1.3.1. EPA's SITE Program	5
1.3.1.1. Primary Objectives	5
1.3.1.2. Secondary Objectives	6
1.3.2. Technology Objectives	7
1.3.2.1. Detailed Technology Objectives	7
1.3.2.2. Supplemental Technology Objectives	9
Chapter 2. Initial Hydrogeologic Conceptual Site Model	11
2.1. Introduction	11
2.2. Bedrock Structure	13
2.3. Hydraulic Conditions	15
2.4. Contaminant Distribution	16
2.5. Initial Conceptual Site Model	17
Chapter 3. General Description of Steam Injection	19
3.1. NAPL Source Zones and Plume Longevity	19
3.2. Steam Enhanced Remediation Technology Background	19
3.3. Thermal Remediation Mechanisms	20
3.4. Steam Injection Demonstrations and Remediations in Unconsolidated Media	21
3.5. Steam Demonstrations in Fractured Rock	22
Chapter 4. Characterization for Design and Implementation	23
4.1. Characterization Activities	24
4.1.1. Drilling Program	24
4.1.2. Rock Chip Sampling	24
4.1.3. Borehole Geophysics	34
4.1.4. Transmissivity Measurements	36
4.1.4.1. Method	36
4.1.4.2. Discussion of Results	37
4.1.5. Deep Monitoring Wells	47

4.1.5.1.	Drilling	47
4.1.5.2.	Well Installation and Hydraulic Testing	48
4.1.6.	Interconnectivity Testing	50
4.1.6.1.	Methods	51
4.1.6.2.	Results	52
4.1.7.	Ground Water Sampling	53
4.1.7.1.	Sampling of Treatment Area Boreholes	54
4.1.7.2.	Sampling of Deep Wells	59
4.1.7.3.	Ground Water Data QC Summary	61
4.2.	Pre-Operation Conceptual Model of Site	61
4.2.1.	Geology	62
4.2.2.	Contaminant Distribution	62
4.2.3.	Hydrogeology	64
Chapter 5.	Well Field, Process, and Subsurface Monitoring Design	71
5.1.	Injection and Extraction System (As-Built)	71
5.2.	Above-Ground Systems	76
5.2.1.	Steam Generation	76
5.2.2.	Effluent Extraction and Treatment Systems	78
5.2.2.1.	Vapor Extraction and Treatment System	78
5.2.2.2.	Water Extraction and Treatment System	79
5.3.	Subsurface Monitoring	79
5.3.1.	DigiTAM™ Temperature Monitoring System	79
5.3.2.	ERT System	79
5.4.	Modifications Made During Operations	81
Chapter 6.	Injection-Extraction Rates and Water-Energy Balances	83
6.1.	Injection Rates	83
6.1.1.	Steam Injection Rate	83
6.1.2.	Air Injection Rates	85
6.2.	Extraction Rates	86
6.2.1.	Vapor Extraction Rates	86
6.2.2.	Ground Water Extraction Rates	87
6.3.	Water Balance	88
6.3.1.	Methods	88
6.3.2.	Results	89
6.4.	Energy Balance	91
6.4.1.	Methods	91
6.4.2.	Results	91
Chapter 7.	Subsurface Temperature and ERT Monitoring Results	95
7.1.	Temperature Monitoring	95
7.1.1.	General Trends in Heating	95
7.1.2.	Temperature Data Supporting Interconnectivity Testing	98
7.1.2.1.	Profiles Showing a Constant Temperature Increase	99
7.1.2.2.	Profiles Showing a Post-Retrofit Temperature Increase	105
7.1.2.3.	Profiles Showing a Response that Suggests Vertical Heat Migration	105
7.1.2.4.	Profiles Showing Evidence of Long-Distance Thermal Migration	105
7.1.3.	Post-Steam Injection Temperature Monitoring	106
7.1.4.	Post-SER Borehole Investigation	106
7.2.	Subsurface ERT Monitoring	106
Chapter 8.	Effluent Sampling Results	117
8.1.	Ground Water and Process Stream Results	117
8.1.1.	Extraction Well PID Screening	117
8.1.2.	Extraction Well VOC Samples	119
8.1.3.	PID Screening of Process Streams	122
8.1.4.	Vapor Screening Results (FID)	123
8.2.	Contaminant Recovery Rates and Total Contaminants Recovered	123
8.2.1.	Vapor Phase Recovery	123

8.2.2. Aqueous Phase Recovery	133
8.2.3. Total Mass Recovered	139
8.3. Compliance Monitoring	139
8.3.1. Emitted Vapor Concentrations	139
8.3.2. Discharged Water Samples	141
Chapter 9. Post-Treatment Rock and Ground Water Sampling	143
9.1. Rock Chip Sampling Results	143
9.2. Ground Water Monitoring	148
9.2.1. May 2003 Monitoring Round	154
9.2.2. October 2003 Monitoring Round	154
9.2.3. May 2004 Monitoring Round	155
9.2.4. Ground Water QC Summary	155
9.2.5. Ground Water Summary	155
Chapter 10. Discussion and Interpretation	157
10.1. Post-Operational Conceptual Model	157
10.2. Discussion of Removal Mechanisms	163
10.3. Evaluation of Objectives	164
10.3.1. Discussion of EPA SITE Program Objectives	164
10.3.2. Discussion of Technology Objectives	167
10.3.3. Discussion of Additional Technology Objectives	170
Chapter 11. Conclusions	173
11.1. Lessons Learned	173
11.1.1. Characterization	173
11.1.1.1 Detailed Mapping	173
11.1.1.2 Coring	173
11.1.1.3 Borehole Geophysics	174
11.1.1.4 Acoustic Televiwer (ATV)	174
11.1.1.5 MERC Sampling	174
11.1.1.6 Discrete Interval Ground Water Sampling	174
11.1.1.7 Head Measurements	174
11.1.1.8 Discrete Interval Transmissivity Testing	175
11.1.1.9 Interconnectivity Testing	175
11.1.1.10 Deep Well Ground Water Sampling	175
11.1.2. Steam Enhanced Remedation	176
11.2. Technology Application	177
11.2.1. General Challenges for SER Applications in Fractured Rock	177
11.2.2. Recommended Approach for SER Implementation at Fractured Rock Sites	178
11.2.3. Amendments and Alternative Approaches	180
11.2.4. Conceptual Comparison of SER and TCH/ERH Costs for a Range of Site Complexity	181
Chapter 12. Recommendations for Future Research Related to Thermal Remediation in Fractured Rock	183
12.1. Rock Chip Samples to Determine Contaminant Distribution	183
12.2. Monitoring Methods	183
12.3. Evaluation of Existing Heat Flow Data	184
12.4. Mechanistic Laboratory Studies of Steam Flow in Fractures	184
12.5. Mechanistic Studies of TCH and ERH in Rock Settings	184
12.6. Effects of SER on the Dissolved Phase Plume	184
12.7. Effects of Injection and Extraction on a Larger Area	185
12.8. Use of Moveable, Inflatable Packers in Injection Wells	185
References	187

Appendices (Contained on Accompanying CD)

- A. Cost Summary
- B. Boring Logs
- C. Analytical Data
- D. Borehole Geophysical Data
- E. QA for Single Hole Transmissivity Tests
- F. Interconnectivity Data
- G. USGS Radar Tomography Paper
- H. Journal Articles
- I. Electrical Resistance Tomography Profiles and Temperature Profiles

Figures

Figure 1.1.1-1.	Location map for the former Loring Air Force Base and the Quarry site.	2
Figure 2.1-1.	Aerial view of the Loring Air Force Base Quarry.	11
Figure 2.1-2.	Results of previous ground water investigations at the Quarry.	12
Figure 2.2-1.	Bedrock geology of northeastern Aroostook County, Maine.	13
Figure 2.2-2.	Primary structural features of the Quarry.	14
Figure 2.2-3.	Diagrammatic cross-sectional representation of the fracturing of the Quarry.	15
Figure 2.4-1.	Loring Quarry PCE plume map.	16
Figure 4.0-1.	General site layout developed by SteamTech in April 2001.	23
Figure 4.1.4.1-1.	Schematic diagram illustrating the packer and standpipe configuration used for measuring transmissivity in the site boreholes.	36
Figure 4.1.4.2-1.	Location of wells and cross-sections plotted in Figures 4.1.4.2-2 to Figure 4.1.4.2-4.	45
Figure 4.1.4.2-2.	Transmissivity versus depth profiles for wells along central axis of site.	46
Figure 4.1.4.2-3.	Transmissivity versus depth profiles for wells in central part of site.	46
Figure 4.1.4.2-4.	Transmissivity versus depth profiles of wells on northern edge of site.	47
Figure 4.1.5.1-1.	Location and orientation of the deeper boreholes constructed around the periphery of the steam footprint.	48
Figure 4.1.5.2-1.	Hydraulic head with respect to elevation in each borehole.	49
Figure 4.1.5.2-2.	Transmissivity with respect to elevation in each deep borehole.	50
Figure 4.1.6.1-1.	Schematic diagram of the apparatus used for the pulse interference tests conducted using the slug test format.	51
Figure 4.1.6.2-1.	The source and observation response for an example pulse interference test.	52
Figure 4.2.1-1.	Conceptual model of geological structure at Quarry.	63
Figure 4.2.3-1.	Plan view of the basic interconnections determined for individual well bore pairs.	66
Figure 4.2.3-2.	Plan view of the injection and extraction well array showing the location of specific cross-sections.	66
Figure 4.2.3-3.	Interconnection along the northern perimeter of the site.	67
Figure 4.2.3-4.	Interconnections between I-4 and I-5.	67
Figure 4.2.3-5.	Profile view of fracture interconnections looking east.	68
Figure 4.2.3-6.	Fracture interconnections looking towards the northeast.	69
Figure 4.2.3-7.	Profile view of fracture interconnections looking north.	69
Figure 4.2.3-8.	Fracture interconnections looking down and towards north-northeast.	70

Figure 4.2.3-9.	Profile view of fracture interconnections looking downwards and towards the northeast.	70
Figure 5.1-1.	Well field layout.	71
Figure 5.1-2a.	Injection well design summary.	73
Figure 5.1-2b.	Extraction well design summary.	74
Figure 5.1-3.	Site layout, as-built.	75
Figure 5.2.1-1.	Steam generation and distribution system schematic.	76
Figure 5.2.2-1.	Extracted vapor and liquid treatment system schematic.	78
Figure 5.4-1.	Location of the concrete seal placed over the eastern part of the site in mid-October.	82
Figure 6.1.1-1.	Injection rate for each of the injection wells.	83
Figure 6.1.1-2.	Cumulative energy amounts injected into each injection well.	84
Figure 6.1.2-1.	Air injection pressure versus time.	85
Figure 6.1.2-2.	Air injection rate versus time.	85
Figure 6.2.1-1.	Extracted vapor flow rate.	87
Figure 6.2.2-1.	Extracted liquid flow rates for wellfield (calculated for point W-1 based on L-1 and KO-2 data).	87
Figure 6.2.2-2.	Cumulative water extraction from each of the extraction wells, based on corrected stroke counter measurements.	88
Figure 6.3.2-1.	Water flow rates for the various injection and extraction streams.	89
Figure 6.3.2-2.	Cumulative water volumes and balance.	90
Figure 6.4.2-1.	Enthalpy fluxes for the various streams during operations.	92
Figure 6.4.2-2.	Energy balance with cumulative energies for the various streams during operations.	92
Figure 6.4.2-3.	Calculation of average subsurface temperature in the test volume and estimated rock volumes that could be heated to 87 and 100°C.	93
Figure 7.1.1-1.	Background temperature profiles in site wells.	95
Figure 7.1.1-2.	Interpreted progression of heating across the site.	96
Figure 7.1.1-3.	Temperature profiles of wells in the eastern area.	97
Figure 7.1.1-4.	Temperature profiles of wells in central area showing heat up after October 14.	98
Figure 7.1.1-5.	Temperature profiles of wells in western area showing heat up after November 19.	99
Figure 7.1.1-6.	Temperature profiles of well I-8 and boring VEA-7 on southern boundary of site, showing rise in temperature of peripheral boring VEA-7 while adjacent steam injection well I-8 cools.	100
Figure 7.1.2.1-1.	Wells exhibiting constant temperature increase.	102
Figure 7.1.2.1-2.	Wells exhibiting post-retrofit temperature increase.	102
Figure 7.1.2.1-3.	Wells exhibiting evidence of vertical heat migration.	103
Figure 7.1.2.1-4.	Wells exhibiting long distance temperature response.	103
Figure 7.1.2.1-5.	Post-injection temperature monitoring profiles.	104
Figure 7.1.4-1.	Fracture at 23.4 meters (76.9 feet) bgs in BD I-5-6.	107

Figure 7.2-1.	Relationship of bulk resistivity to temperature (top) and bulk conductivity to temperature (bottom).	108
Figure 7.2-2.	Site map, showing location of ERT profiles listed in Table 5.3.2-1.	109
Figure 7.2-3.	Conductivity profiles of perimeter planes, November 30.	111
Figure 7.2-4.	Resistivity anomalies interpreted as indicating the passage of heated water across the perimeter of the treatment area.	112
Figure 7.2-5.	Examples of high conductivity anomalies parallel to VEA borings.	113
Figure 7.2-6.	Conductivity profiles of interior planes, November 30.	114
Figure 7.2-7.	Plane TC1-9-4, showing development of conductivity anomalies over time.	115
Figure 8.1.1-1.	Headspace PID screening data for the first subset of extraction wells.	118
Figure 8.1.1-2.	Headspace PID screening data for the second subset of extraction wells.	118
Figure 8.1.2-1.	PCE concentrations in the VOC grab samples from the extraction wells.	119
Figure 8.1.2-2.	TCE concentrations in the VOC grab samples from the extraction wells.	120
Figure 8.1.2-3.	Naphthalene concentrations in the VOC grab samples from the extraction wells.	121
Figure 8.1.2-4.	1,2,4-Trimethylbenzene concentrations in the VOC grab samples from the extraction wells.	121
Figure 8.1.3-1.	Results of PID headspace screening of process water samples.	122
Figure 8.1.4-1.	Results of continuous FID screening of vapors at location V-1 (untreated vapors).	123
Figure 8.2.1-1.	Vapor phase effluent concentrations over time.	132
Figure 8.2.1-2.	Vapor phase total VOC daily and cumulative recoveries.	132
Figure 8.2.2-1.	Aqueous phase effluent concentrations of total solvents, GRO, and DRO.	137
Figure 8.2.2-2.	Solvent concentrations in the aqueous phase and cumulative recoveries.	137
Figure 8.2.2-3.	GRO daily and cumulative recovery in the aqueous phase.	138
Figure 8.2.2-4.	DRO daily and cumulative recovery in the aqueous phase.	138
Figure 10.1-1.	Schematic cross-sections of site showing those fractures that showed a temperature increase during or after operations.	158
Figure 10.1-2.	Progressive sequence of heating observed at site, based on first evidence of temperature increase in temperature profiles presented in Appendix I and Plate 7.1.1-1.	159
Figure 10.1-3a.	PCE concentrations (micrograms/liter) in ground water, April 2002.	160
Figure 10.1-3b.	PCE concentrations (micrograms/liter) in ground water, May 2003.	160
Figure 10.1-4.	Interpretation of ground water flow paths under stressed conditions in effect during steam injection operations.	161
Figure 10.1-5.	Interpretation of ground water flow paths under ambient conditions.	162
Figure 11.2.4-1.	Sketch of comparative cost of site characterization and treatment costs for SER and TCH/ERH applications to sites with varying complexity.	182

Tables

Table 1.2-1.	Project Chronology	4
Table 1.3.2.1-1.	Primary Technology Objectives (Expanded from Work Plan)	8
Table 1.3.2.2-1.	Supplemental Technology Objectives (Defined During Course of Demonstration)	9
Table 4.1.1-1.	Well Drilling Details	25
Table 4.1.2-1.	Pre-Steam Injection MERC Sample Results	26
Table 4.1.3-1.	Summary of the Prominent Fractures as Determined from the Borehole Geophysics	35
Table 4.1.4.2-1.	Summary of Individual Well Transmissivity Profiles	38
Table 4.1.5.2-1.	Summary of Casing Intervals for SM-1, SM-2, and SM-3	49
Table 4.1.6.2-1.	Water Level Measurements Relative to a Datum at 225.6 meters (740 Feet) Above Mean Sea Level	53
Table 4.1.7.1-1.	Ground Water Sampling Intervals for Treatment Area Wells	55
Table 4.1.7.1-2.	Pre-Treatment Ground Water Sampling Results from Wells Within the Target Zone	56
Table 4.1.7.2-1.	Ground Water Sampling Intervals for Deep Wells	59
Table 4.1.7.2-2.	Pre-Treatment Ground Water Sampling Results from the Deep Boreholes	60
Table 4.2.3-1.	Wells Within Interconnected Areas	64
Table 5.2.1-1.	Major Design Parameters and Process Equipment Specifications	76
Table 5.3.2-1.	List of ERT Profiles	80
Table 8.2.1-1.	Analytical Results for Vapor Samples from Sample Point V-1	125
Table 8.2.2-1.	Analytical Results for Aqueous Phase Samples from Sample Location L-1	134
Table 8.2.3-1.	Summary of Contaminant Mass Recovered in Each Phase	139
Table 8.3.1-1.	Summary of Analytical Data on the Treated Vapor Emitted to the Atmosphere (Sample Location V-4)	140
Table 8.3.2-1.	Summary of Analytical Data on the Treated Water (Sample Location L-3)	142
Table 9.1-1.	Post-Treatment Rock Chip Sampling Results	144
Table 9.2.1-1.	Post-Treatment Ground Water Sampling Results	148

Plates (Contained on Accompanying CD)

- Plate 2.4-2. Cross-sectional representation of the contaminant distribution beneath the upper tier.
- Plate 4.1.2-1. PCE concentrations in rock chip samples.
- Plate 7.1.1-1. Temperature profiles during steam injection.
- Plate 7.1.1-2. Temperature profiles after steam injection.
- Plate 8.1.2-1. Effluent concentrations from each of the extraction wells.
- Plate 9.2.4-1. Summary of total VOC concentrations in ground water over the life of the project in wells used for extraction.

Acronyms and Abbreviations

AFB	Air Force Base
ALT	Advanced Logic Technologies
ARAR	Applicable or Relevant and Appropriate Standard
atm	atmosphere
ATV	Acoustic Televiewer
BCT	below casing top
BD	back drill
bgs	below ground surface
BIPS	Borehole Image Profiling System
BRAC	Base Realignment and Closure
BTEX	Benzene, toluene, ethyl benzene, and xylene
Btu	British thermal unit
CERCLA	Comprehensive Environmental Response, Compensation, and Liability Act
COC	Contaminant of Concern
CSM	Conceptual Site Model
CVOC	Chlorinated Volatile Organic Compound
DCA	Dichloroethane
DCE	Dichloroethylene
DEP	Department of Environmental Protection
DNAPL	Dense Non-Aqueous Phase Liquid
DRO	Diesel Range Organics
EM	Electromagnetic
EPA	Environmental Protection Agency
ER	Electrical resistivity
ERH	Electrical Resistance Heating
ERT	Electrical Resistance Tomography
EX	Extraction
FID	Flame Ionization Detector
FS	Feasibility Study
ft	feet
GAC	Granular activated carbon

gpm	gallons per minute
GRO	Gasoline Range Organics
HLA	Harding Lawson Associates
HPFM	Heat pulse flow meter
I	Injection
kg	kilograms
kJ/hr	kiloJoules per hour
kPa	kiloPascals
kWh	kiloWatt hours
lbs	pounds
LNAPL	Light Non-Aqueous Phase Liquid
lpm	liters per minute
m	meters
MCL	Maximum Contamination Level
MEDEP	Maine Department of Environmental Protection
MERC	Methanol extracted rock chip
mg/kg	milligrams per kilogram
mg/l	milligrams per liter
MS/MSD	Matrix spike/matrix spike duplicate
msl	mean sea level
NAPL	Non-Aqueous Phase Liquid
NFCS	Nonfracture control sample
NRMRL	National Risk Management Research Laboratory
ORD	Office of Research and Development
OTV	Optical televiewer
PCE	Tetrachloroethylene
PID	Photo-Ionization Detector
ppmv	parts per million volume
QAPP	Quality Assurance Project Plan
QC	Quality Control
RFP	Request for Proposals
RI	Remedial Investigation
ROD	Record of Decision
RPD	Relative Percent Difference
SARA	Superfund Amendments and Reauthorization Act of 1986
scfm	standard cubic foot per minute
scmm	standard cubic meter per minute
SER	Steam Enhanced Remediation

SITE	Superfund Innovative Technology Evaluation
SOP	Standard Operating Procedure
TC	Thermocouple
TCE	Trichloroethylene
TCH	Thermal Conduction Heating
TDS	Total Dissolved Solids
TI	Technical Impracticability
TIO	Technology Innovation Office
USAF	United States Air Force
USEPA	United States Environmental Protection Agency
USGS	United States Geological Survey
VEA	Vertical Electrode Array
VLf	Very low frequency
VOA	Volatile Organics Analysis
VOC	Volatile Organic Compound

Chapter 1. Introduction

This report details a field research project on the use of Steam Enhanced Remediation (SER) to recover volatile organic contaminants (VOCs) from fractured limestone. This project was carried out at an abandoned Quarry at the former Loring Air Force Base (AFB) in Limestone, Maine. Pre-operation characterization activities were initiated in Summer 2001, and steam injection operations took place from September 1 to November 19, 2002. Post-steam injection monitoring activities were initiated in Spring 2003 and were completed in Spring 2004.

Ground water in the fractured limestone bedrock beneath the Quarry has been contaminated with a variety of VOCs due to past disposal practices. The main chlorinated volatile organic compound (CVOC) identified was tetrachloroethylene (PCE), which was present at ground water concentrations that would indicate the likely presence of a dense non-aqueous phase liquid (DNAPL). Fuel-related compounds are also present in the Quarry as a light non-aqueous phase liquid (LNAPL) floating on the water table and dissolved in the ground water.

Loring AFB was added to the National Priorities List, otherwise known as Superfund, in February 1990. This research project was carried out to fulfill the requirements set forth in the final Record of Decision (ROD) for the Quarry ground water. In the ROD, which was signed in 1999, the AF agreed to make available \$250,000 for a limited scale implementation of DNAPL remediation technologies at the Quarry, and to coordinate with the United States Environmental Protection Agency (USEPA) Region I and Maine Department of Environmental Protection (MEDEP) to establish a program whereby the Quarry could be used to integrate Air Force (AF) funded mass reduction efforts with State and EPA supported research. The main objectives of this program were to develop an improved understanding of the mechanisms controlling DNAPL and dissolved phase contaminant behavior in fractured bedrock systems while reducing contaminant mass at the Quarry site.

A Request for Proposals (RFP) was issued in September 2000 soliciting remediation technologies to be tested at this site. After a technical review of the proposals received, Steam Enhanced Remediation (SER) was chosen as the technology to test at the Quarry. SER has been extensively tested in the laboratory and in the field for the remediation of volatile and semivolatile organic contaminants from unconsolidated soils, and several full-scale remediations in unconsolidated media have been successfully completed (See Chapter 3.). To date, however, SER had had only limited testing or use in fractured rock environments. This project was the first field-based research on the use of steam injection to remediate DNAPL in fractured limestone.

The original project scope and budgets had been set based on limited site characterization activities carried out in 1998 and 1999. After selecting SER, funding from MEDEP and EPA's Office of Research and Development (ORD) became available to augment funds provided by the AF. Estimates of steam injection rates based on a short-term pump test completed in 1998 indicated that the funding available should allow sufficient operation time for heating the entire target zone (which was approximately 15 meters (50 feet) wide and 45 meters (150 feet) in length) to the desired temperature. However, characterization activities completed prior to the initiation of steam injection showed that the target zone had significantly lower transmissivities than originally believed. Indeed, steam injection rates were much lower than initially anticipated. Also, the discovery of significant residual VOC contamination in some new boreholes and the limited interconnectivity of the boreholes caused a scaling back of the number of wells to be used for steam injection. Thus, steam injection rates were never as high as originally planned. Additional funding from MEDEP allowed the operation period to be extended from 60 days to 83 days; however, this time was still not sufficient to heat the entire target zone. At this time, effluent concentrations were high and still increasing. Despite this fact, when funding for the project ran out after 83 days of steam injection, the injection part of the system had to be shut down. The extraction system was operated for another seven days, and then the entire operation was shut down.

Thus, funding for this project was not sufficient to do all the desirable characterization, to study all possible aspects of the SER technology in fractured bedrock, or to extend the operation of the system sufficiently to complete the remediation. The project team worked together to define characterization and evaluation processes for the project that were as robust as possible within the funding and time constraints.

1.1. Site Description and History

1.1.1. Site Description

The former Loring Air Force Base is located in the northeastern portion of Maine and approximately 5 km (3 miles) west of the United States/Canada border (Figure 1.1.1-1). The main base covers approximately 3,640 hectares (9,000 acres) and was used by the Air Force from the late 1940s until September 1994. The Quarry is located near the northwestern boundary of the former base, at the periphery of the operational areas which supported the former air field, including a former jet engine test cell and the sprawling Nose Dock Area hangar complex. The greater Quarry, which includes the Quarry and the downgradient wetlands, is approximately 2.8 hectares (7 acres) in size. The site's topography and characteristics are reflective of past rock quarrying activities, which reportedly began with construction of the base in 1947 and ceased in 1985. Quarrying activities have generally removed much of the vegetative and soil cover which formerly existed at the site, together with a large volume of rock, leaving two "tiers" or "benches" which are open to the west and ringed on the other sides with rock outcrops or talus slopes. The site is located near a surface water drainage divide, and ground water and surface water are believed to flow generally westward from the site, into the wetlands which make up the headwaters to the West Branch of Greenlaw Brook.

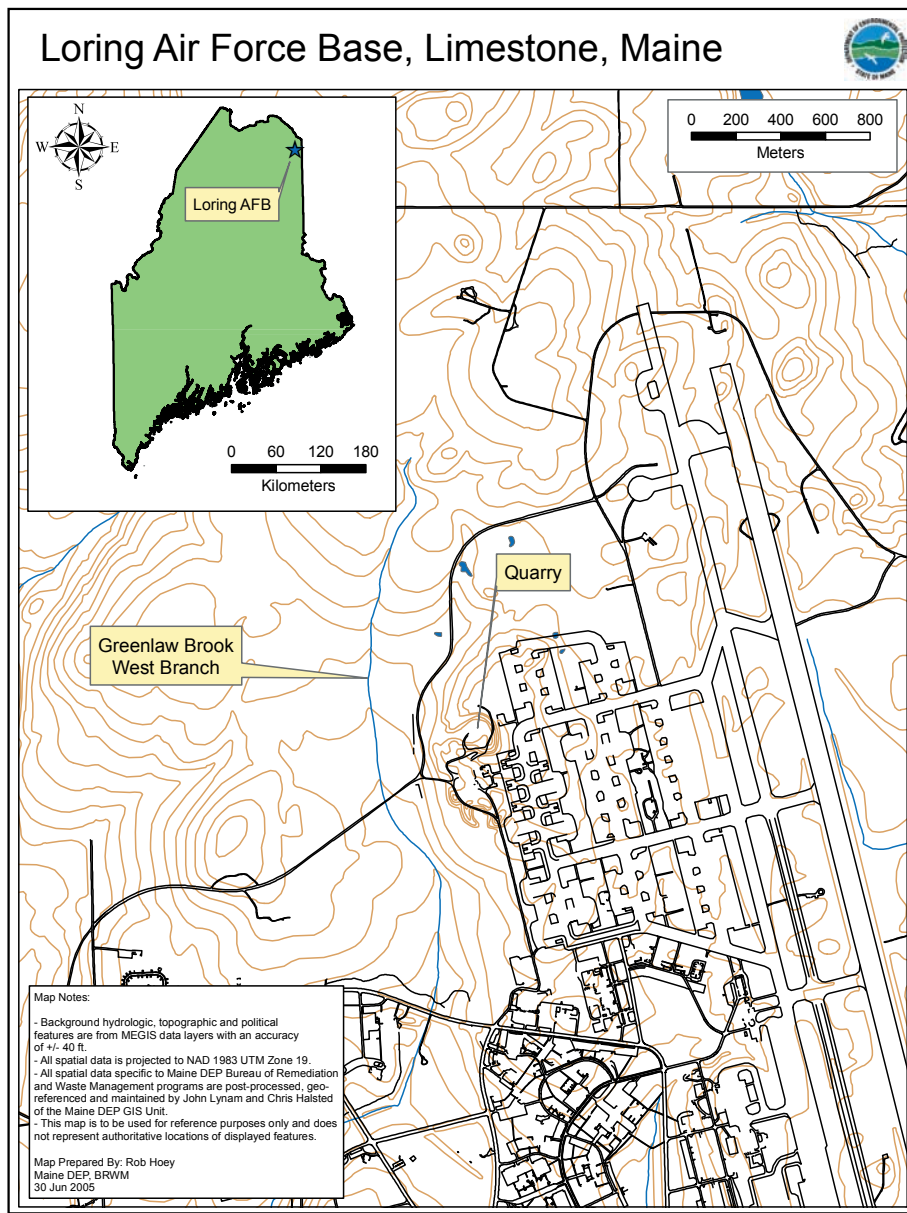


Figure 1.1.1-1. Location map for the former Loring Air Force Base and the Quarry site.

Historically, waste materials from construction projects, industrial and maintenance shops, and other base activities were stored or disposed of at the Quarry. A total of approximately 450 drums were removed during several removal actions during the 1980s and 1990s. Associated contaminated soils, sediments, and construction rubble were also removed at this time. Subsequent ground water investigations determined that both chlorinated and fuel-related compounds were present in the ground water, and concluded that PCE DNAPL was likely present in the bedrock.

1.1.2. Administrative History

Loring AFB was added to the Superfund National Priorities List in 1990. The Quarry site is one of the more than 50 sites on the base which have been addressed under the Comprehensive Environmental Response, Compensation, and Liability Act (CERCLA). In 1999 the remedial approach for the Quarry, which was part of Operable Unit 12, was finalized, and the final Feasibility Study, Proposed Plan, and ROD documents were completed (Harding Lawson Associates, 1999a, 1999b, 1999c). Associated remedial actions are either completed or in progress. To address MEDEP's inability to waive Applicable or Relevant and Appropriate Standards (ARARs), the AF included in the ROD \$250,000 for a research project to evaluate a DNAPL recovery technology at the Quarry, with the hope that the technology may become available at a later time for remediation of DNAPL in fractured rock.

1.1.3. Technology Selection

In order to conduct the research project on DNAPL recovery from fractured bedrock, an RFP was issued in 2001. In response to this RFP, six proposals were received. After evaluating proposals for in situ chemical oxidation, Steam Enhanced Remediation (SER), hot air thermal desorption, and electrical resistance heating, the project team selected SER as a promising innovative technology for the remediation research to be conducted at the Quarry.

Reasons for selecting SER include: 1) this technology has been demonstrated to be successful in overburden; 2) it was believed that the general robustness of the technology could potentially overcome the limited interconnectivity of the site; 3) the performance feedback and control offered by the use of electrical resistance tomography (ERT) and thermocouple monitoring networks; and 4) its use of multiphase extraction. Also, there was the expectation that a successful application of the technology would result in the removal of a significant portion of the VOC present mass in the subsurface.

1.1.4. Project Structure and Administration

This research project was a joint undertaking by MEDEP, U.S. EPA's ORD, EPA Region I, the Air Force Base Conversion Agency, and SteamTech Environmental Services. In addition, a complementary research project on the use of borehole radar tomography to monitor steam/heat migration was carried out concurrently by the United States Geological Survey (USGS). EPA's National Risk Management Research Laboratory (NRMRL) played a significant role in this research project through the Superfund Innovative Technology Evaluation (SITE) program and with technical expertise and project management provided by the Robert S. Kerr Environmental Research Center. The SITE program also funded participation by experts from academia in fractured rock characterization from Queen's University, in Ontario, Canada, and steam enhanced remediation from The University of California-Berkeley. Additional funding, as well as in-kind services, were provided by EPA ORD, EPA Region I, MEDEP, and SteamTech to augment the funds which the AF provided as agreed on in the ROD. Funding from EPA ORD's Technology Innovation Office (TIO) allowed additional characterization activities (interconnectivity testing) to be completed before the steam injection and for the radar tomography monitoring research conducted by the USGS.

1.2. Project Chronology

The project schedule changed substantially after the project was initiated. Initially, it was the intent of the project team to complete the pre-steam injection characterization as well as the steam injection in Summer and Fall 2001. However, after characterization activities were initiated, the project team decided to extend the characterization phase to allow additional characterization steps and data analysis to be completed, and then to complete the steam injection in Summer 2002. Post-treatment monitoring activities were then carried out in Spring and Summer 2003, with the final round of ground water sampling completed in Spring 2004. The chronology of the entire project is present in Table 1.2-1.

Table 1.2-1. Project Chronology

Phase	Task	Start	End	Description
Pre-Steam Injection Characterization	Borehole installation and rock chip sampling	5/15/01	6/21/01	All injection (I) and extraction (EX) wells, vertical electrode array (VEA) boreholes VEA-4, VEA-5, VEA-9, and thermocouple (TC) borehole TC-1 were cored and rock chip samples collected. Remaining VEA wells were installed by air hammer.
	Transmissivity testing	6/8/01	6/29/01	All newly installed wells plus existing wells in the target zone were tested on 3.2 meter (10 foot) intervals.
	Geophysical testing	8/7/01	8/9/01	Caliper logs, fluid resistivity, fluid temperature and acoustic televiewer logs were run on all I and EX wells.
	Deep boreholes	11/25/01	12/21/01	Included drilling, casing installation, and hydraulic testing.
	Ground water sampling	12/2/01	12/13/01	Wells within target area sampled.
		4/2/02	4/9/02	Wells within target area and deep boreholes sampled.
		6/10/02	6/10/02	Deep boreholes sampled.
Interconnectivity testing	5/23/02	7/12/02	Field work completed in two phases.	
Steam Injection Operations	Dual-phase extraction	8/30/02	11/01/02	Continuous extraction of liquid and vapor from all wells.
		11/04/02	11/26/02	Continuous extraction restarted after equipment failure.
	Air injection	8/31/02	9/01/02	Air injection into steam wells.
		9/21/02	9/23/02	Air injection resumed while steam system shut down.
		11/19/02	11/26/02	Air injection resumed at end of steam injection.
	Steam injection	9/01/02	9/21/02	Steam injection in wells I-4, I-5, and I-6.
		9/23/02	11/19/02	Steam injection resumed after equipment failure.
10/14/02		11/19/02	Steam injection in wells I-7, I-8, and VEA-5 (I-7 middle interval shut down on 11/9).	
Post-Steam Injection Monitoring	Ground water sampling	5/2/03	5/9/03	Wells within target area and deep wells sampled.
		10/20/03	10/22/03	Wells within target area and deep wells sampled.
		5/17/04	5/20/04	Wells within target area and deep wells sampled.
	Rock chip sampling	7/7/03	7/15/03	Eight drillback locations sampled.

1.3. Objectives of Research Project

Primary, guiding objectives for this research project that are broad in nature and thus independent of the technology implemented were established by the regulatory agencies at the time the ROD was signed. These objectives included: improving the understanding of the mechanisms controlling DNAPL and dissolved phase contaminant behavior in fractured bedrock systems; evaluating how a remediation technology could be successfully implemented and controlled in a fractured bedrock environment; reducing the mass of contaminants in the subsurface to reduce the overall remediation timeframe; and evaluating characterization needs for fractured bedrock systems. In addition, MEDEP and EPA Region I hoped to evaluate the effect of source zone treatment on plume longevity. However, plume longevity could not be evaluated due to the fact that sufficient information was not available prior to

the initiation of this project on the dissolved-phase plume, and the funds and time available for this project were not adequate to address this deficiency.

Once a technology and technology vendor had been chosen, additional specific objectives were developed by the vendor. Also, EPA's SITE program developed specific objectives in conjunction with the project team for the evaluation of the SER technology in fractured bedrock. The SITE program and technology vendor's objectives are described in detail below.

1.3.1. EPA's SITE Program

The purpose of EPA's SITE program is to accelerate the development, evaluation, and use of innovative remediation technologies. This program was initiated by the Superfund Amendments and Reauthorization Act (SARA) of 1986, which mandates implementing permanent solutions and the use of alternative, innovative treatment or resource recovery technologies to the maximum extent possible. The evaluation portion of the SITE program focuses on technologies in pilot- or full-scale stages of development, and are intended to collect performance data of known quality to evaluate system performance. To this end, primary and secondary objectives were developed for the evaluation of the SER technology at the Loring Quarry, and a Quality Assurance Project Plan (QAPP) was prepared to define the sampling and analytical procedures to be used to evaluate these objectives (U.S. EPA, 2002).

The Loring Quarry research team identified two primary objectives and six secondary objectives for the SITE program evaluation of the SER technology. The primary objectives focused on documenting the amount of contaminants that were recovered, recovery rates as a function of time by the SER technology, and the changes in ground water concentrations brought about by the contaminant recoveries. Data to support the evaluation of these objectives were collected by EPA, MEDEP, or their contractors. Secondary objectives included evaluating changes in contaminant concentrations in the rock, evaluating the ability of the technology to heat the rock and recover mobilized contaminants, and evaluating the ability of SteamTech's above ground treatment systems to treat the effluent streams so that discharges to the air and surface water met discharge permit requirements. Additional secondary objectives were to document the SER operating parameters used for this site and the costs of treatment. Some of the data to support these secondary objectives were collected by EPA, while the rest of the data were collected by SteamTech. The primary and secondary objectives for the SITE evaluation of the SER technology at the Loring Quarry are listed below as they are given in the QAPP. A brief summary of the evaluation method is also provided. After the QAPP was written, additional site characterization activities were completed. Based on the results of these characterization activities, the design of the steam injection and extraction system underwent considerable changes. These changes made it necessary to adjust some of the methods for evaluating the technology, and these changes are documented in four amendments to the QAPP.

Details on data collection for characterization are provided in Chapter 4, and details on data collection for evaluating mass recovery are given in Chapter 8. How well each of these objectives were met and the results of the evaluations are discussed in Chapter 10.

1.3.1.1. Primary Objectives

- P1. Determine the approximate reduction in contaminant of concern (COC) concentrations that occurs in ground water within the treatment zone as a result of SER treatment.*

This objective was evaluated by collecting ground water samples from discrete intervals of process boreholes before and after steam injection to evaluate the effectiveness of SER for reducing ground water contaminant concentrations. Packers were used to isolate the interval of interest, and low-flow sampling techniques were used to obtain the samples. In order to discern some of the temporal variations in ground water concentrations, two rounds of pre-treatment samples were obtained, in December 2001 and in April 2002. Three rounds of post-treatment samples were obtained, with the sampling events occurring in May 2003, October 2003, and May 2004. Approximately 25 ground water samples were collected during each round; however, because of changes in the use of many of the boreholes, it was not always possible to sample all the same intervals.

Ground water concentrations may also be affected by factors unrelated to this project (e.g., seasonal variations); thus, the effects of SER on ground water concentrations can only be approximated. The use of ground water samples to evaluate SER performance at this site was also limited by the fact that the extent of the source zone could not be determined prior to steam injection due to limitations in funding and time constraints. Also, it is likely that there were other, unidentified source zones within the greater Quarry area, and it is possible that they were in hydraulic connection with the treatment area, as discarded drums were removed from several areas of the Quarry. Thus, ground water sampling results may have been affected by contaminants drawn in from outside the treatment area.

- P2. Determine the mass removal of COC in all waste streams over the course of the SER treatment period.*

The principal means to evaluate steam injection for enhancing the recovery of VOCs from fractured limestone was through determining mass recovery rates as a function of time as the steam injection proceeded. Vapor and aqueous phase samples of the combined effluent streams were collected daily to determine mass recovery rates. Initial rates of recovery (while the target area was still mostly at ambient temperatures) were compared to recovery rates later in the project to determine if the rate of contaminant recovery increased in response to steam injection and the heating of the subsurface.

The total amount of mass recovered was also calculated based on these effluent samples and flow rate data; however, the use of mass recovery in evaluating SER performance is limited by the fact that the amount of contaminants in the subsurface within the

target area for SER implementation before and after treatment is not known. No attempt was made to estimate the amount of contaminant mass in the ground, as it is known that such estimations (even for unconsolidated media) contain significant errors due to the heterogeneity of the subsurface and thus, contaminant distribution. The errors are likely to be even greater for fractured rock. Without knowing the amount of contaminants in the ground before and after treatment, recovery efficiency cannot be determined. Thus, this objective focused on looking for changes in recovery rates due to steam injection.

The use of effluent concentrations to evaluate the effectiveness of the SER technology would be limited if contaminants from outside of the treatment zone were pulled into the extraction wells. It was known prior to treatment that contaminants existed just outside of the treatment zone. The initially-proposed design of the steam injection and extraction system would have effectively reduced the possibility of extracting contaminants from outside the treatment zone by surrounding the treatment zone with injection wells, thus blocking inward ground water flow from outside the treatment zone to the central extraction wells. However, changes to the design of the system in response to newly-acquired characterization data resulted in a system which concentrated injection at the eastern end of the site and extraction at the western end. The aggressive extraction system at the western end of the target area could have pulled contaminants in from outside the target area.

1.3.1.2. Secondary Objectives

- S1. Determine the approximate reduction in COC concentrations in potentially open fracture intervals within the treatment zone as a result of the SER treatment.*

Rock chip samples were collected both before and after the steam injection to determine the effect of SER on contaminant concentrations in the rock at the fracture surfaces. The method used to sample and analyze rock chips is described in detail in Chapter 4. There are no developed and tested methods for evaluating contaminant concentrations in fractured rock. The method used here was based on the rock chip sampling done at this site previously (HLA, 1998); however, the method has not been rigorously tested, and the extraction efficiency for volatile contaminants from limestone using this method has not been determined.

For soils, methods have been developed and standardized to an extent for determining contaminant concentrations. However, it is recognized that the heterogeneity of soils, and thus, the heterogeneity of contaminant concentrations in the soils, can lead to errors when trying to evaluate changes in contaminant concentrations brought about by remediation. It is likely that the error associated with determining contaminant concentrations in paired rock core samples is even greater than that associated with paired soil cores, as the heterogeneity in fractured rock is expected to be significantly greater than in most soils. Also, the conceptual model developed on the basis of data from this site envisages that contaminant NAPL that entered the fractured rock system flowed relatively freely through open apertures, but was trapped and absorbed into the rock matrix at places where the aperture narrowed or closed. This will further complicate any efforts to relate fracture surface concentrations from co-located cores obtained before and after the steam injection. Thus, the rock chip data presented here is viewed more qualitatively rather than quantitatively when looking for changes caused by remediation.

- S2. Determine if contamination is mobilized below, downgradient, or to the sides of the treatment zone as a result of the SER treatment.*

When a remediation technology is employed to mobilize contaminants for recovery, care must always be taken to design the system to collect all the contaminants that are mobilized. When the contaminant is a DNAPL, there is risk of downward mobilization of the contaminant during remediation as well as horizontal migration. The fractured rock environment may present significant challenges for collecting mobilized contaminants due to limited interconnectivity of the boreholes used for injection and extraction. To evaluate the efficiency of collecting mobilized contaminants, three deep boreholes were drilled to the sides of and below the target zone, and ground water samples were collected from discrete intervals both before and after steam injection. Two of these boreholes were drilled at a 45 degree angle from horizontal and approximately 70 meters (230 feet) in length, with the top of the boreholes to the north or south of the target area, and the bottom of the boreholes below the target area. The third borehole was drilled vertically and to the east of the target area. Bedding plane fractures (which potentially contain DNAPL) dip to the east, and thus, to the east is the likely direction of NAPL migration if it were to migrate from the treatment area. Before steam injection, ground water samples were obtained from these wells in April and June 2002. After steam injection, samples were obtained from these wells in May 2003, October 2003, and May 2004. Because all possible pathways for fluid movement away from the target area could not be monitored, these data provide only an indication of the potential for contaminant migration outside of the treatment area, but do not conclusively demonstrate that mobilization outside the treatment area did not occur.

- S3. Determine if the rock within the treatment zone can be heated to greater than 87°C (the co-boiling point of a water and PCE mixture) in the zones containing contaminants.*

In thermal remediation, heating the entire treatment zone to the temperature at which the nonaqueous phase liquid (NAPL) and water will boil is important for efficient recovery of the NAPL. The temperature at which water and another liquid will boil is always less than the boiling point of the liquids alone, and for water and PCE, the co-boiling point is 87°C (189°F). PCE NAPL in areas heated to this temperature should be completely vaporized. Unheated areas may collect mobilized contaminants by allowing vapors to recondense, thus reducing the efficiency of the remediation.

Although steam flow is expected to be very channelized in fractured rock, heat conduction from the steam in the fractures can be expected to heat the matrix blocks over time. To evaluate the ability of steam injection to heat the treatment area, SteamTech collected temperature data from thermocouple strings at approximately 23 locations within and around the target area. Thermocouples on the strings had a 1.5 meter (5 foot) vertical spacing, and temperature data was collected automatically every eight hours during the steam injection. The thermocouple data were augmented by electrical resistance tomography (ERT) data, which map changes in the resistivity of the subsurface caused by changes in temperature, fluid resistivity, and saturation.

S4. Document the ability of the ground water and vapor treatment system to treat the effluent streams and meet any discharge permits.

Once contaminants are brought to the surface, it is important to be able to separate the contaminants from the aqueous and vapor streams before discharge of the water and air. SteamTech employed skid-mounted treatment systems to treat effluent vapors and water. These systems cooled the effluent streams and separated water, NAPLs, and non-condensable vapors. The water and vapors were then treated by carbon adsorption before discharge. The treatment system has the ability to store NAPLs for subsequent disposal. SteamTech collected samples of the water and vapors weekly to determine the efficiency of the treatment systems and to determine if discharge criteria were met.

S5. Document the operating parameters during evaluation of the SteamTech SER technology.

Operational parameters that are commonly adjusted during SER to control heating rates and steam migration include injection locations and depth intervals, injection pressure/rate, air co-injection rates, and vapor and ground water extraction rates. Operating parameters employed during this project were documented by SteamTech, and changes in operating parameters were evaluated for their effect on the heating rate and steam migration, as well as their effect on contaminant recovery.

S6. Determine the cost of treatment for the SteamTech SER technology based upon the evaluation at LAFB.

Costs of each of the aspects of the application of the SER technology to this site, including drilling, sample collection and analysis, steam injection operation, effluent treatment, etc, were documented. A summary of the costs is provided in Appendix A.

1.3.2. Technology Objectives

The main technology objective was to determine the feasibility of using SER to significantly remediate ground water contaminated by PCE and other contaminants of concern (COC) in a fractured rock aquifer at the Quarry site on the former Loring AFB. The site exemplified many of the problems encountered at fractured bedrock sites. SER has been used successfully in unconsolidated media; the intention of this study was to identify technology modifications needed for applying SER to fractured rock in general, as well as to remove a significant mass of VOCs from the site.

Because the effectiveness of the technology is dependent on getting steam and/or heat to where the contaminants are, it is important to be able to determine the heat and steam distribution in the target area. Temperature changes caused by steam and hot water migration were monitored directly using DigiTAM digital thermocouple temperature sensors and indirectly using Electrical Resistivity Tomography (ERT). These techniques have been used successfully in unconsolidated media. Thus, another major objective of this project was to determine the applicability and value of these monitoring techniques in fractured media.

1.3.2.1. Detailed Technology Objectives

Detailed objectives of the demonstration were defined in the Work Plan (SteamTech, 2002) and are summarized in Table 1.3.2.1-1:

1. Document the application of steam injection technology and its ability to heat the fractured rock site to temperatures high enough to vaporize any DNAPL present in fractures and matrix.
2. Heat a portion of the target pilot volume from below and from three sides using multiple injection wells and intervals, and measure subsurface temperatures and electrical resistivity.
3. Identify operational parameters which govern heat-up rates and steam migration.
4. Extract liquid and vapors aggressively and recover as much of the NAPL constituents present in the test area as possible within the limitations of the technology, the resources available, and the time frame for operations.
5. Document removal rates and mass removal by detailed sampling and analyses.
6. Evaluate removal efficiency for PCE and other VOCs identified during sampling by pre- and post-test contaminant characterization.
7. Identify potential barriers to full-scale implementation at this site, and at fractured rock sites in general.

Table 1.3.2.1-1. Primary Technology Objectives (Expanded from Work Plan)

Primary Technology Objectives	Expected performance (pre-test)	Performance confirmation method
1. Document the application of steam injection technology and its ability to heat the fractured rock site to temperatures high enough to vaporize any DNAPL present in fractures and matrix.	Completion of data collection to allow for assessment	<ol style="list-style-type: none"> 1. Energy balance calculation to estimate volume of rock heated to target temperature. 2. Temperature data from Digitam sensors. 3. ERT data interpretation of heating patterns. 4. Chemical mass recovery trends – effect of the remediation on extracted water and vapor concentrations and NAPL presence.
2. Heat a portion of the target pilot volume from below and from three sides using multiple injection wells and intervals, and measure subsurface temperatures and electrical resistivity.	Target volume raised to target temperature	Direct temperature monitoring and approximation by ERT methods.
3. Identify operational parameters which govern heat-up rates and steam migration.	Collect well-field data on injection and extraction that supports the subsurface monitoring data	<ol style="list-style-type: none"> 1. Determine acceptable injection intervals from core data, geophysics, slug tests, and pulse interference (interconnectivity) testing. 2. Measure steam and air injection pressures and achievable rates. 3. Monitor extraction well data for signs of steam, condensate or air injection effects. 4. Determine potential air injection benefits. 5. Matrix heating: Calculations of thermal conduction timeframes for site heating compared to observed temperatures.
4. Extract liquid and vapors aggressively and recover as much of the NAPL constituents present in the pilot test area as possible within the limitations of the technology, the resources available, and the time frame for operations.	Operate system as designed, with proper adjustments to well-field and process equipment to keep the test and data collection continuous	<ol style="list-style-type: none"> 1. Monitor mass removal rates for NAPL, water and vapor. 2. Screen and sample individual wells for COC concentrations and headspace PID trends. 3. Inspect extracted fluids for NAPL presence. 4. Evaluate if the system was operated effectively and provided a fair test of the technology at this site. 5. Use collected data to estimate the most appropriate full-scale approach (based on lessons learned), and evaluate how close this test came to showing the mass removal we expect when sufficient time and funds are available.
5. Document removal rates and mass removal by detailed sampling and analyses.	Data collected	<ol style="list-style-type: none"> 1. Determine process stream vapor and liquid phase concentrations. 2. Calculate mass removal rate based on concentrations and flow rates. 3. Screen individual extraction well and analyze to determine trends in recovery rates.
6. Evaluate removal efficiency for PCE and other VOCs identified during sampling by pre- and post-test contaminant characterization.	Data collected by EPA SITE	Use pre- and post-treatment ground water and rock data to evaluate changes in COC concentrations (a SITE objective).
7. Identify potential barriers to full-scale implementation at this site, and at fractured rock sites in general.	Collect data set for discussion	Discussion based on holistic data interpretation, and data from related SER tests in fractured rock.

1.3.2.2. Supplemental Technology Objectives

During the field implementation, the following additional technology objectives were identified:

1. Determine the value of borehole tests and interconnectivity tests in determining the best use of each borehole interval for operation.
2. Study the mechanisms and importance of using air co-injection to improve the subsurface remediation.
3. Develop methods for pressure cycling in fractured rock with extraction hole temperatures below steam temperatures, and assess impacts on mass removal rates.
4. Study the effect of SER on mass removal rates at temperatures well below boiling, caused by mixing of cold and hot extraction borehole fluids.

The expected performance (pre-test) and performance confirmation method for each of these objectives are summarized in Table 1.3.2.2-1. How well each of the objectives was met will be discussed in Chapter 10.

Table 1.3.2.2-1. Supplemental Technology Objectives (Defined During Course of Demonstration)

Supplemental Technology Objectives	Expected performance (pre-test)	Performance confirmation method
1. Determine the value of borehole tests and interconnectivity tests in determining the best use of each borehole interval for operation.	Make best use of the data during implementation	Discussion based on holistic data review.
2. Study the mechanisms and importance of using air co-injection to improve the subsurface remediation.	Collect data for evaluation of potential benefits and downsides	<ol style="list-style-type: none"> 1. Compare steam injection rates with and without air injection. 2. Discuss extraction well responses to air injection following steam. 3. Discuss importance of air injection for reducing VOC condensation, and the risk and impact of spreading VOC-laden air.
3. Develop methods for pressure cycling in fractured rock with extraction hole temperatures below steam temperatures, and assess impacts on mass removal rates.	Use system as built to test pressure cycling options	<ol style="list-style-type: none"> 1. Observe well responses to vacuum adjustments to enhance de-pressurization. 2. Test borehole water level manipulations in support of SER. 3. Discuss options for pressure cycling without steam breakthrough to extraction wells.
4. Study the effect of SER on mass removal rates at temperatures well below boiling, caused by mixing of cold and hot extraction borehole fluids.	Collect data	Discussion based on holistic data interpretation.



Chapter 2. Initial Hydrogeologic Conceptual Site Model

2.1. Introduction

Figure 2.1-1 presents an aerial view of the Quarry site. The headwaters of the West Branch of Greenlaw Brook lie to the west, and the former Nose Dock Area lies to the east. The Quarry site is located near a topographic divide, with drainage generally to the west toward West Branch of Greenlaw Brook. Surface water drainage in the network of hangars and taxiways of the former Nose Dock Area to east of the Quarry is generally to the south and east (East Branch of Greenlaw Brook Drainage).

Past investigations at the Quarry have focused on the upper and lower tiers (Figure 2.1-2). The lower tier is approximately 0.81 hectare (2 acres) in size and contains water year round, which drains through an excavated ditch into the Greenlaw Brook wetland. The upper tier is approximately 1 hectare (2.5 acres) in size, is crescent-shaped, and is bordered on the north and east by rubble. Sloping bedrock escarpments rise approximately 9 meters (30 feet) to the unexcavated Quarry rim. To the west, the upper tier of the Quarry drops vertically approximately 9 meters (30 feet) to the lower tier.

Between 1983 and 1985, approximately 105 to 110 drums were removed from the upper tier. The contents of these drums were not determined, but their discovery launched a series of field investigations. Several phases of investigation took place starting in the late 1980's, culminating in a Final Remedial Investigation (RI) report in 1997 (ABB-ES, 1997). Development of a Feasibility Study (FS) was complicated by the late discovery of several hundred previously unidentified buried drums. During 1998, supplemental characterization studies were initiated, and a magnetometer survey (i.e., EM-34 and EM-61) identified a large anomaly along the eastern edge of the upper tier. Subsequent test-pitting and removal actions were focused on the wedge-shaped mass of talus, spoils, and soil which extended from the "rim" of the upper tier to the "floor." An additional 348 drums, 155 cubic meters (205 cubic



Figure 2.1-1. Aerial view of the Loring Air Force Base Quarry.

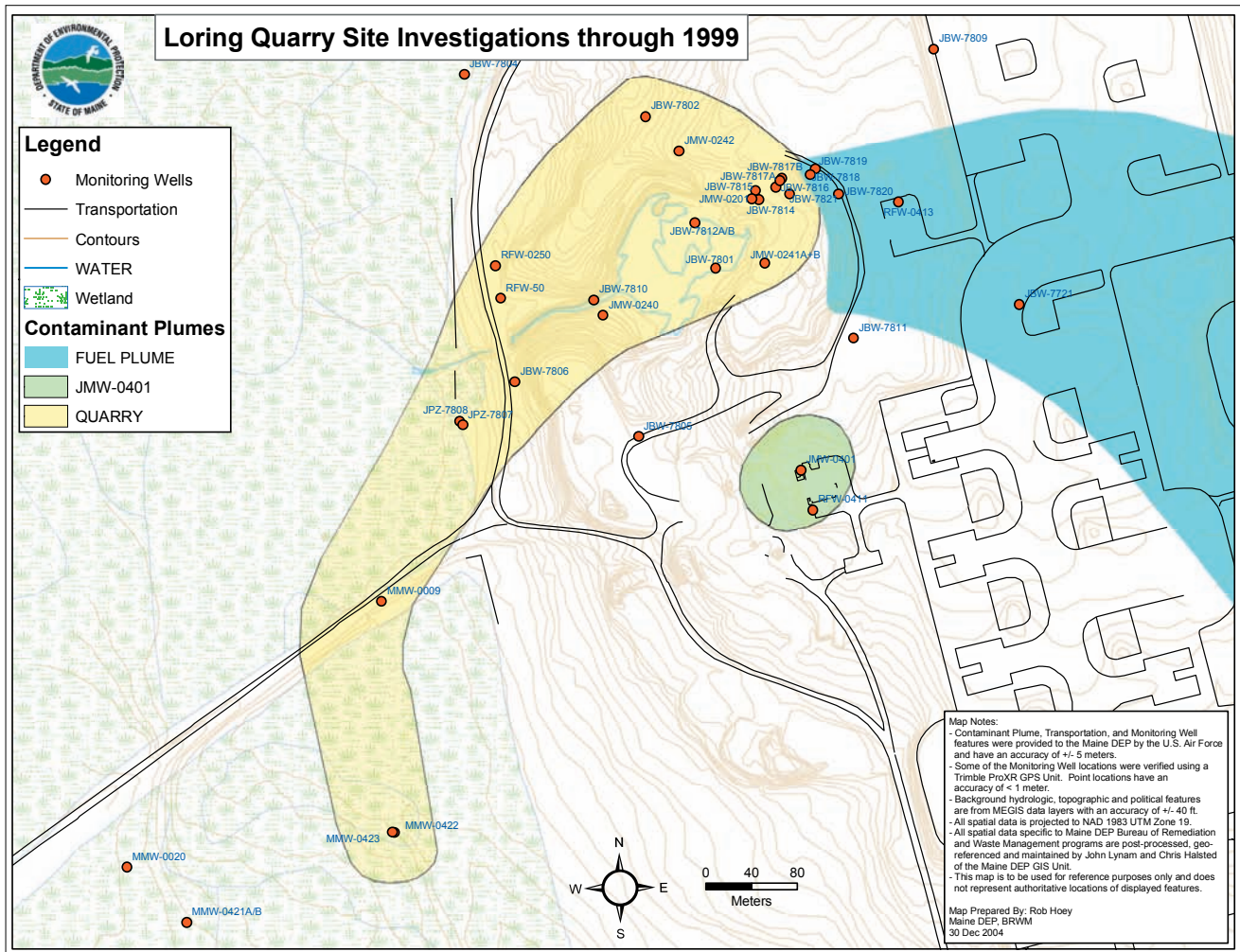


Figure 2.1-2. Results of previous ground water investigations at the Quarry.

yards) of contaminated soil, and approximately 3,800 liters (1,000 gallons) of waste oils, lubricants, and fuels were removed from this area. In 1999 a remedial approach was finalized, and final FS, Proposed Plan, and ROD documents were completed (HLA, 1999a; HLA, 1999b; U.S. EPA, 1999). The final remedy included a Technical Impracticability (TI) waiver for ground water restoration in the Quarry plume, but the TI waiver also included specific expectations regarding testing of remedial technologies at the site, thus setting the stage for the current research project.

The development of a conceptual model to describe fluid flow and contaminant distribution in the fractured limestone at the Quarry was an evolution resulting from a series of hydrogeologic investigations (HLA, 1998; HLA, 1999c) undertaken before the steam system was designed and the process wells drilled. The investigations employed surface geophysical methods including azimuthal resistivity; magnetometer surveys (EM-16, very low frequency (VLF), and EM-34); diamond-core rock drilling; borehole geophysics (caliper, electrical methods, acoustic televiwer (ATV), and borehole image processing system (BIPS)); specific capacity tests; and straddle packer sampling for ground water chemistry. The HLA reports summarize the conceptual model with three components: bedrock structure, hydraulic conductivity distribution, and contaminant distribution.

The initial conceptual model provided guidance on the presumed extent of the NAPL distribution, the distribution of subsurface geological features, and direction of ground water flow, and was the basis of the initial design of the steam injection study. The well locations, spacing, completion depths, and use (injection versus extraction) were chosen based on that model. However, as with most SER projects, the data obtained during the drilling of the steam injection and extraction wells, and the testing and operation of the wells once completed, allow a more accurate conceptual model of the subsurface hydraulic conductivity and contaminant distribution to be developed. Thus, the well pattern selected is not expected to be the optimum design since information obtained during implementation was not available during the design phase.

2.2. Bedrock Structure

Figure 2.2-1 presents bedrock structural geology at the regional scale. The bedrock of northeastern Maine is a sequence of volcanic and marine sedimentary formations of Ordovician-Devonian age. Beginning approximately 40 km (25 miles) west of Loring and traversing to the east, the bedrock formations include the Winterville basalt; sandstones and conglomerates of the Madawaska, Frenchville, and Jemmland Formations; the New Sweden calcareous siltstone; and the Carys Mills limestone. These rocks have been subjected to low-grade metamorphism and deformation associated with several orogenic events. Regional folding parallels the strike of lithologic contacts, which is oriented to the northeast. The folding occurs at several scales with the first-order folds represented by the regional anticlinoria and synclinoria with wavelengths of tens of kilometers. Second-order folds have wavelengths on the kilometer scale. Third-order folds with wavelengths on the order of tens of meters are evident in large outcrops such as the Loring Quarry (Roy, 1987). Mesoscopic folding with wavelengths on the order of centimeters and other manifestations of structural deformation are also commonly observed in outcrop and core samples.

Due to historical use of the site as a rock quarry, the overburden and shallow, weathered bedrock commonly observed across Loring have largely been removed. As a result, the geology in the Quarry consists of a competent, yet fractured, sequence of the Carys Mills Formation. This formation is primarily composed of interlayered argillaceous gray limestones and calcareous siltstones. The bedrock is micritic and thinly laminated with significant calcite infillings occurring along bedding and fracture planes.

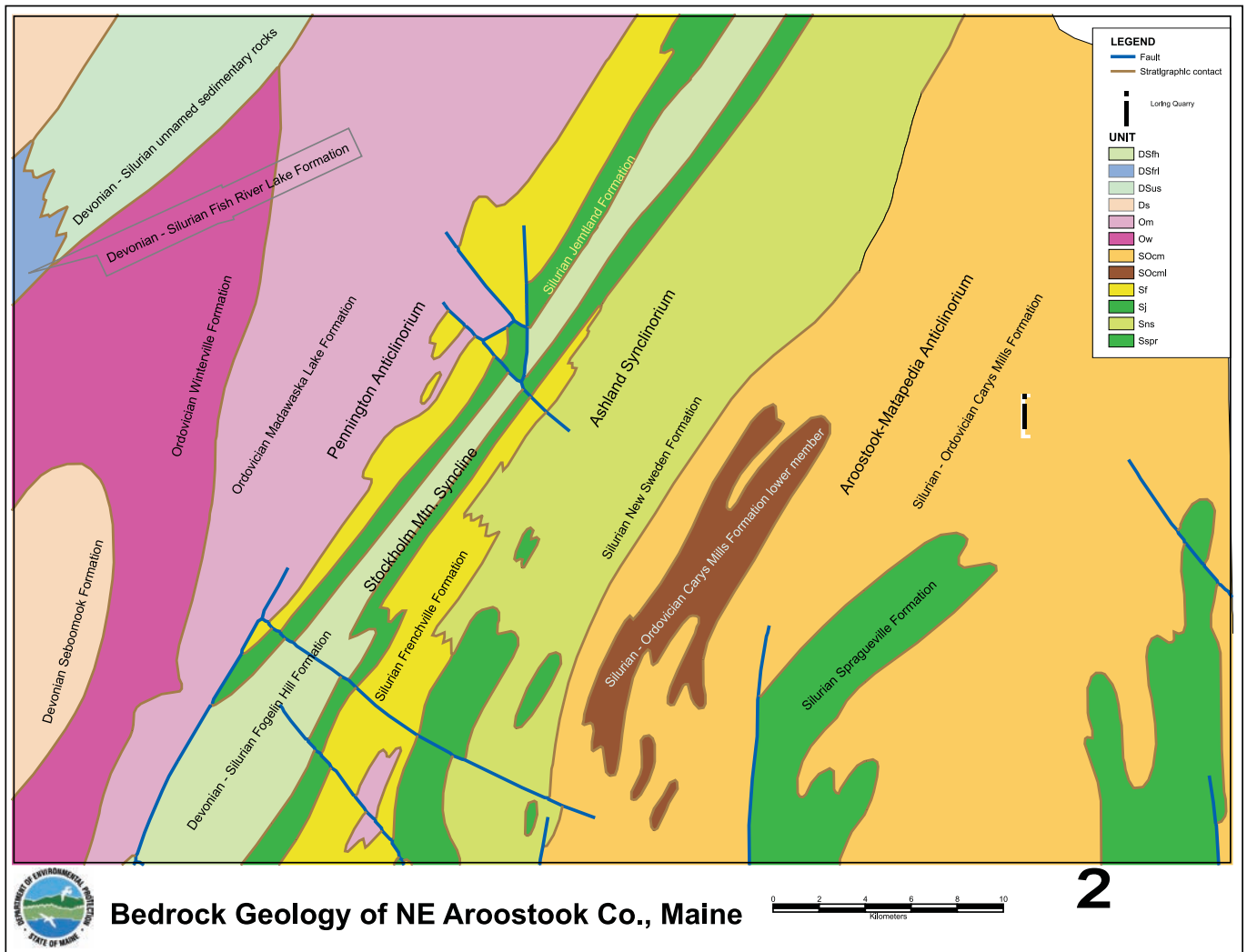


Figure 2.2-1. Bedrock geology of northeastern Aroostook County, Maine.

Figure 2.2-2 presents the primary structural features in the vicinity of the Quarry. Several major structural features are evident from exposures at the Quarry. The first is an anticline plunging N10E. The axial plane strikes north, dips steeply to the east, and bisects the lower tier of the quarry. This feature was interpreted from outcrop and borehole data of bedding orientation. Bedding in the western part of the Quarry dips steeply to the northwest. Bedding in the eastern portion of the lower tier and in the upper

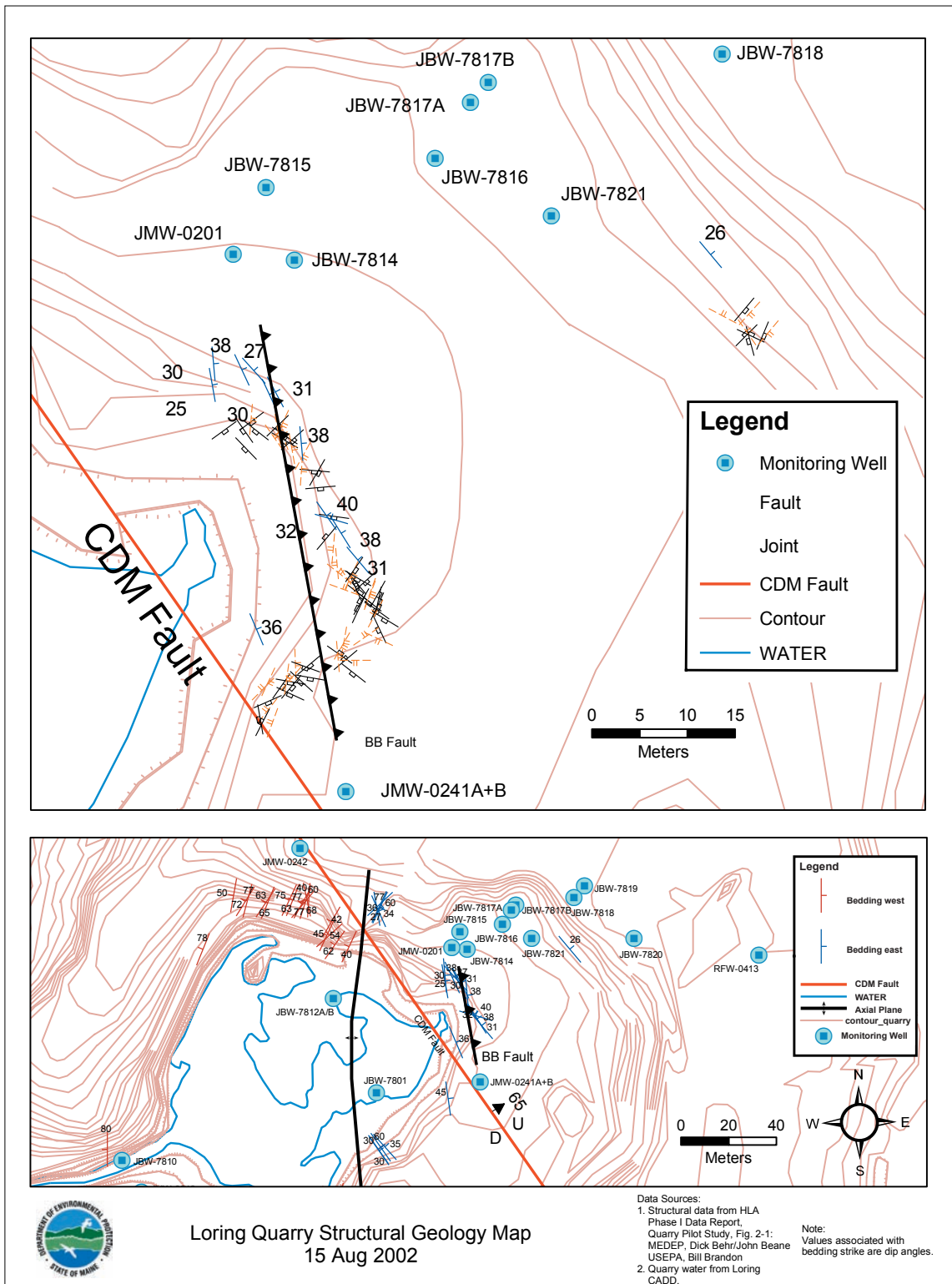


Figure 2.2-2. Primary structural features of the Quarry.

tier generally dips moderately to the northeast. A second major feature is a significant fault named the “CDM Fault,” which strikes north-northwest, dips steeply to the northeast, and more or less coincides with the boundary between the upper and lower tiers. Additionally, a number of low- to moderate angle “thrust” or “reverse” faults, which are generally parallel or sub-parallel to bedding, have been identified beneath the upper tier. Prominent among these features, the “BB fault” outcrops along the steep rock face separating the lower and upper tiers. The bedding-parallel features (BB Fault and related structures) which dip beneath the upper tier appear to be related to a major thrust/reverse fault which outcrops on the south Quarry wall in the lower tier, west of the trace of the CDM fault. The interrelationships between the CDM fault and the series of more gently dipping thrust/reverse faults (BB Fault, etc.) are not clear. However, all features appear to be pene-contemporaneous (i.e., related to the same paleo-stress field), with the last displacement of this type occurring along the CDM fault. A diagrammatic cross-sectional representation of the fracturing at the Quarry, which focuses on the upper tier, is shown on Figure 2.2-3.

In the upper tier, bedding plane fractures are one of three predominant fracture sets. The other two are northwest and northeast striking sets of steeply dipping fractures. The northwest trending fractures (N30W to N30E) cross the axis of the quarry fold at a high angle. The northeast trending fractures strike approximately N40E and thus generally coincide with the regional strike of the lithology and the first-order fold axes, but are oblique to the axis (N10E) of the third-order Quarry fold.

2.3. Hydraulic Conditions

Ground water in the upper tier is encountered at approximately 6 to 9 meters (20 to 30 feet) below ground surface (bgs). Ground water flow in the Quarry area is generally from a piezometric high in the Nose Dock Area (east of the Quarry) to the Greenlaw Brook wetland (approximately 300 meters (1,000 feet) west of the Quarry). The horizontal gradient over this area is 0.03, but it steepens significantly beneath the upper tier of the Quarry. Vertical gradients are downward in the zone beneath the upper tier and upgradient of the Quarry. Water level measurements downgradient of the Quarry indicate upward vertical gradients and discharge to the Greenlaw Brook wetland.

Specific capacity tests were conducted in several boreholes in and near the Quarry to provide a relative indication of the transmissivity distribution. The results of these tests range from 0.12 to 435 lpm/meter (0.01 to 35 gpm/ft). Within the upper tier, the range is 0.12 to 12.4 lpm/meter (0.01 to 1 gpm/ft), which is approximately equal to transmissivities of 1×10^{-6} to 1×10^{-4} m²/s (1.1×10^{-5} to 1.1×10^{-3} ft²/s). The higher values tended to be within 10 to 15 meters (30 to 50 feet) of the surface.

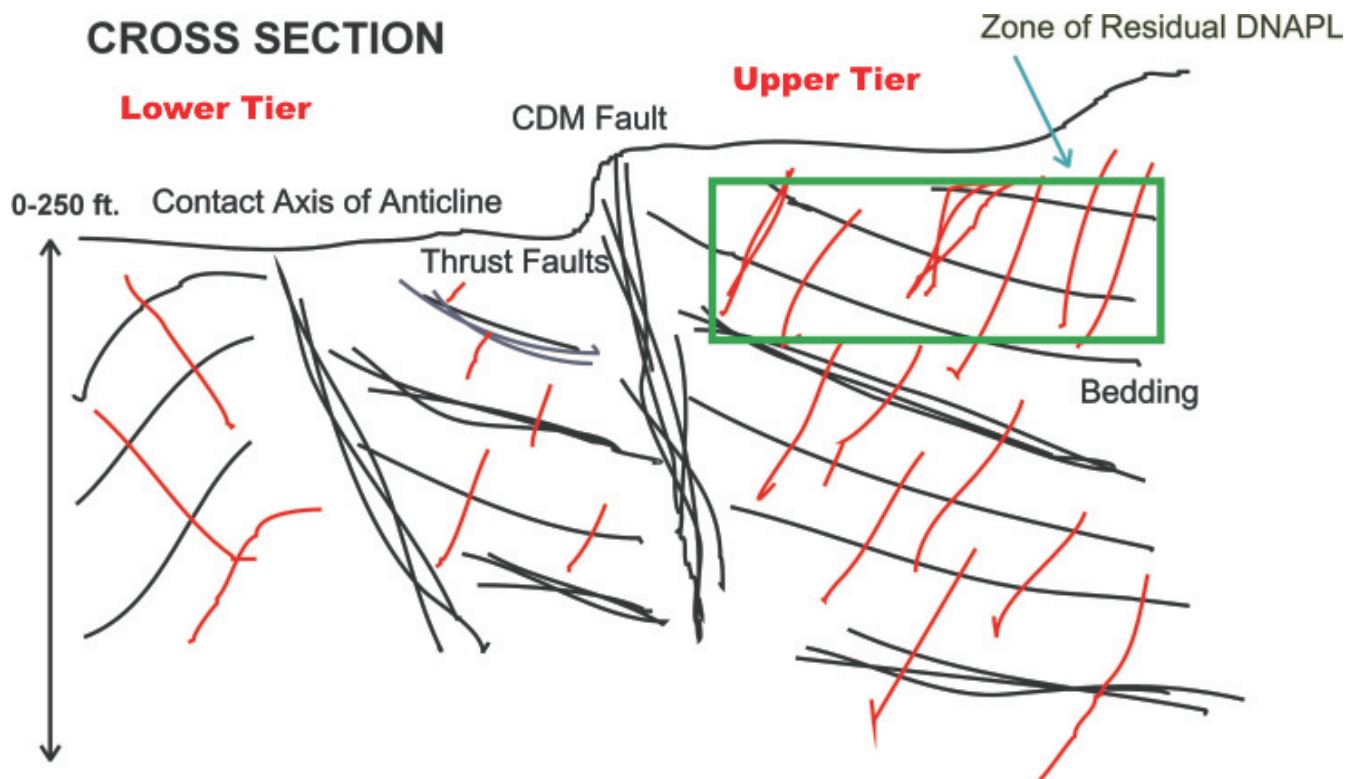


Figure 2.2-3. Diagrammatic cross-sectional representation of the fracturing of the Quarry.

2.4. Contaminant Distribution

Figure 2.4-1 presents a plan view of the Quarry area, showing wells used for characterization prior to the SER research project. Field programs between 1994 to 1998 defined a narrow plume of chlorinated solvents with a limited fuel component that originates in the upper tier and was initially believed to discharge into the Quarry wetland. Dissolved-phase concentrations within the upper tier are suggestive of the presence of DNAPL. PCE was the most-commonly detected chlorinated solvent, and the maximum concentration detected was 38 mg/l at 21 meters (70 feet) bgs in well JMW-0201. JMW-0201 also had the maximum concentrations found for trichloroethylene (TCE) (8.1 mg/l), cis-1,2-dichloroethylene (DCE) (5.5 mg/l), and vinyl chloride (0.076 mg/l). High concentrations of carbon tetrachloride (4.3 mg/l) were found in JBW-7821, while JBW-7817B contained the highest concentrations of benzene (24 mg/l) and toluene (360 mg/l). Other maximum ground water concentrations for the contaminants of concern include 1,2-dichloroethane (DCA), (0.021 mg/l) in JBW-7818 and naphthalene (0.018 mg/l) in JBW-7817A. Concentrations of PCE in the lower tier drop off by more than two orders of magnitude over a distance of approximately 45 meters (150 feet). Wells to the east of the upper tier contained fuel components, including benzene, toluene, ethylbenzene, and xylenes (BTEX), at high concentrations.

Plate 2.4-2 is true-scale cross-sectional representation of the contaminant distribution beneath the upper tier (HLA, 1999c). According to the Phase II Data Report and Interpretation (HLA, 1999c), it was believed that PCE was released in the area around JBW-7816, JBW-7817 and JMW-0201, and migrated vertically through axial plane and regional joint fracture systems to the bedding plane fractures, where a majority of the spent solvent appeared to be stored. The lateral extent of the PCE DNAPL was believed to be limited to the upper tier in this area, although its distribution was not well constrained, particularly to the north. The vertical distribution of CVOCs was generally thought to be limited primarily to the upper 30 meters (100 feet) of bedrock, although the only deeper borehole in the vicinity at that time, JBW-7816, showed concentrations of approximately 0.040 mg/l at depths up to 45 meters (149 feet) bgs. Based on color, relative observed viscosity, and chemical results, it was believed that LNAPL identified in JBW-7817 was an oil lubricant, and the LNAPL in JBW-7819 was a mixture of weathered fuel (presumably gasoline) and possibly

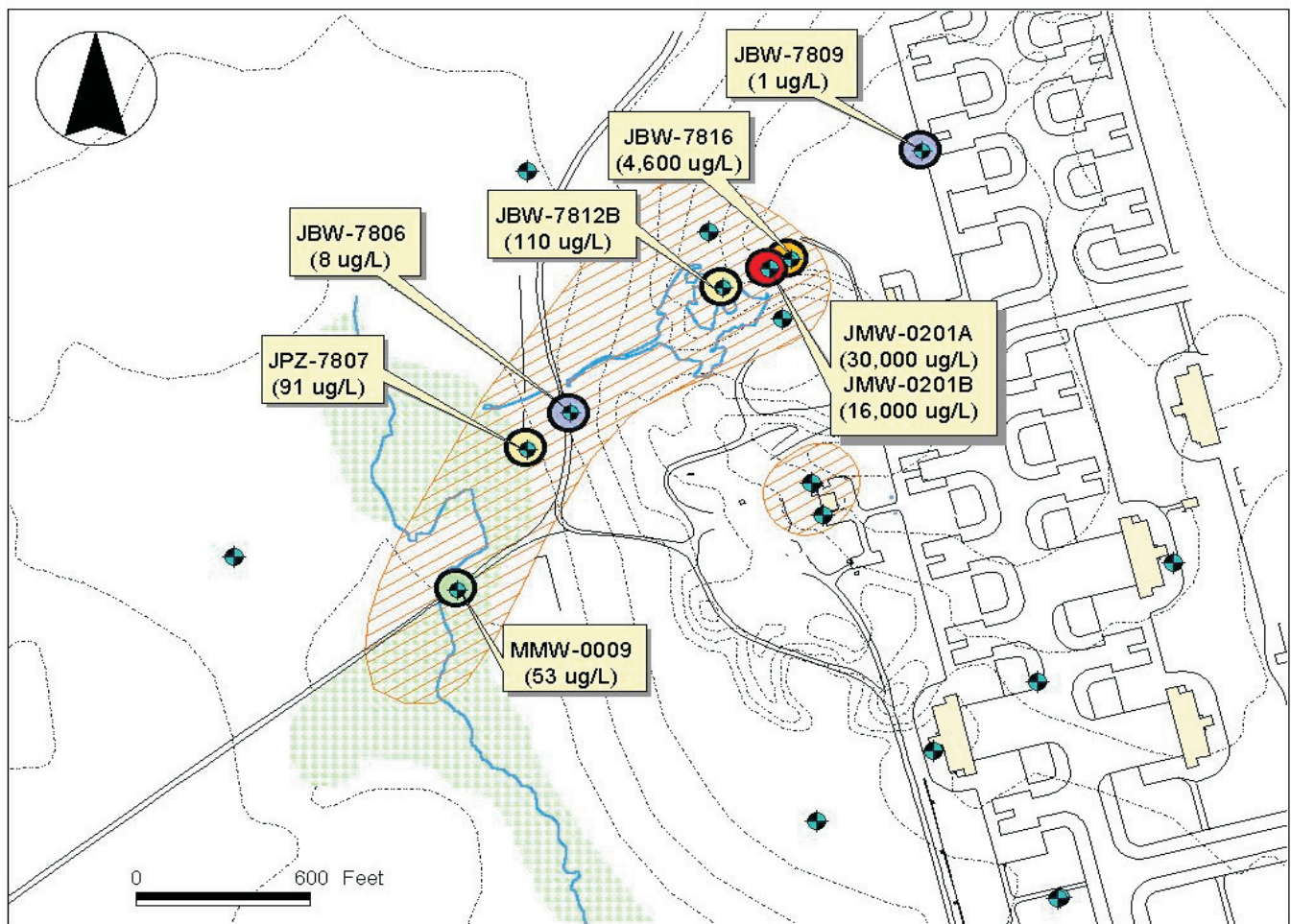


Figure 2.4-1. Loring Quarry PCE plume map.

lubricants. The detection of other chemical species, including carbon tetrachloride, carbon disulfide, and chloroform in wells JBW-7821 and JBW-7818, suggests a hydraulic and source relationship between these two wells that is not directly related to the source of PCE in JMW-0201, JBW-7816, and JBW-7817A.

2.5. Initial Conceptual Site Model

The conceptual site model (CSM) which emerged after the completion of the Phase I and II investigations can be summarized as follows. The upper tier was believed to be comprised of a more or less contiguous block of rock which was bound on the west by the CDM fault, and “flooded” by a series of bedding-parallel, NE-dipping, thrust and/or reverse faults. On the basis of outcrop observations, the CDM fault was thought to generally represent a significant geologic boundary. East of the CDM fault, in the upper tier, a complex but somewhat regular series of geologic features were identified, which included the following:

- **Bedding Plane Fractures:** parallel or subparallel to bedding and bedding-parallel faults, strike NW-SE, moderate dips to the NE;
- **Axial Plane Fractures** (i.e., those fractures parallel to the central axis of the regional fold system): strike NE-SW, dip steeply either to the NW or SE, with moderate to steep dips;
- **Regional Joint Fractures:** strike NW-SE and dip steeply either to the SW or NE at a variety of dip values (mainly steep dips).

Of these features, bedding plane fractures were believed to be the most significant with respect to ground water movement (and contaminant transport) as they accounted for over half of all fractures identified, contained the largest apertures observable from cores, and were believed to account for the majority of the responses measured during hydraulic testing.

Chemical weathering of the rock mass was generally observed to be quite limited, particularly as evidenced from fresh subsurface core samples, and fracturing was generally sparse. The bedrock ground water flow system was, therefore, generally conceptualized as a system dominated by fracture-controlled flow within a low permeability matrix. On a site-wide scale, ground water flow gradients were generally observed to be westward from the upper tier, toward the lower tier, the Quarry Wetlands, and the West Branch of Greenlaw Brook. Vertical gradients in the upper tier were generally downward, and upward gradients were observed in the vicinity of the surface water features to the west. However, this simple model did not consider hydrogeologic controls on ground water flow other than at the gross, site-wide scale. For example, the CDM fault’s relationship to ground water flow and contaminant transport was not examined, but the fault’s orientation and geologic character suggested that it might act to impede, or at least influence, the more generalized ground water movement from east to west. Bedding and the CDM fault both strike more or less orthogonally to the presumed east-to-west general ground water flow direction; however, the existing wellfield density was not sufficient to resolve the head-field gradients or to identify specific fracture-controlled ground water pathways in greater detail with respect to this feature or within the upper tier generally. Further resolution of ground water flow pathways was beyond the scope of the Phase I and II characterizations.

Contaminant distribution data from the upper tier suggested that it contained more than one source zone. Contaminants were believed to be located mostly in the hydraulically dominant bedding plane fractures. Ground water contaminant concentrations in the upper tier suggested that DNAPL was present (believed to be primarily residual DNAPL); however, it was believed that the residual DNAPL was confined to the upper tier, as concentrations in wells in the lower tier were lower by several orders of magnitude. Beneath the upper tier, the source zone was defined, mainly based on ground water samples, to generally coincide with a region of dissolved CVOC values greater than 1 mg/l. This source region was thought to be generally controlled by bedding parallel fracturing as it indicated a similar geometry to bedding, i.e., moderately dipping to the northeast. The high-concentration zone was identified from roughly 9 to 20 meters (30 to 65 feet) bgs on the western side of the upper tier, and deeper on the eastern side, from roughly 14 to 29 meters (45 to 95 feet) bgs.

While the rather strong influence of bedding dip on contaminant distribution was clear, it was less clear that this alone explained the source zone geometry, or whether these were the primary contaminant migration pathways within and beyond the upper tier. Nevertheless, to a large extent, this CSM, and its inherent limitations, guided the initial decisions with respect to the area to be targeted for remediation, injection and extraction well placement, depth of treatment, and the overall geometry of the subsurface elements of the SER system. Not surprisingly, information collected from the installation of the first series of SER wells dictated changes in the CSM, which are described in subsequent chapters.

Chapter 3. General Description of Steam Injection

3.1. NAPL Source Zones and Plume Longevity

The release of man-made chemicals in the form of non-aqueous phase liquids (NAPL) to the subsurface has resulted in persistent ground water contamination. The natural attenuation of NAPL contamination in soil and ground water is slow, resulting in typical plume lives of hundreds to thousands of years. The longevity of NAPL source zones is primarily caused by the environmental stability of the NAPL, its low mobility in soils, slow dissolution rate into moving ground water, and low vaporization rate when located below the ground water table (Hunt et al., 1988a; Mercer and Cohen, 1990; Pankow and Cherry, 1996). This stability in the environment, combined with aqueous solubilities of NAPL constituents, which are typically orders of magnitude higher than the acceptable ground water concentrations, leads to ground water contamination problems that can persist for centuries (Hunt et al., 1988a).

Conventional in-situ remediation techniques applied in unconsolidated media involve fluid injection and extraction at ambient temperature as a means of removing the NAPL from the subsurface environment. However, once NAPL finds its final distribution after the spill occurs it is relatively immobile, and flushing with water and air has limited effect on its mobility. For NAPL found below the water table, remediation approaches employing flushing suffer from mass-transfer limitations due to the characteristically low diffusivities of the constituents in water and the presence of NAPL in regions not in contact with the flowing fluids. The Steam Enhanced Remediation (SER) process was designed to overcome these mass-transfer limitations, and to provide a relatively rapid source removal and aquifer restoration option.

The fractured rock environment creates additional challenges for remediation due to the dual porosity and permeability of the fracture/matrix systems, the potentially limited interconnectivity of fracture networks, and the sequestering of contaminants in the low permeability rock matrix. Currently, no remediation technologies have been proven to be successful in fractured rock, and indeed, few attempts have been made to remediate contaminants in fractured bedrock, despite the fact that a large number of contaminated sites have been identified where at least part of the contamination exists in fractured rock.

3.2. Steam Enhanced Remediation Technology Background

While steam injection for enhanced oil recovery has been practiced for decades by the oil industry (Ramey, 1966; Mandl and Volek, 1969; Volek and Pryor, 1972; Konopnicki et al., 1979), its use for environmental remediation was not considered until the 1980s. The first reported use of steam injection for remediation was a pilot study to remove petroleum hydrocarbons from soils in the Netherlands (Hilberts et al., 1986). The first use of steam to address chlorinated solvent contamination in the subsurface was a pilot study in California in 1988 (Udell and Stewart, 1989). Building on the findings of that second study, additional thermodynamic features of the process were identified and exploited to make the process amenable to the restoration of sites contaminated with volatile and semi-volatile liquid contaminants found above and below the water table, as well as non-volatile compounds in the aqueous phase (Udell et al., 1991; Udell and Stewart, 1992).

The in-situ process using steam injection and aggressive fluids extraction has been called Steam Enhanced Extraction (Udell et al., 1991), Steam Remediation, and Dynamic Underground Stripping. For consistency, the process name “Steam Enhanced Remediation,” or SER, has been adopted in this report.

The mechanisms leading to the mobilization of contaminants in unconsolidated media by steam injection were studied intensively in laboratory experiments and theoretical investigations (Hunt et al., 1988b; Stewart and Udell, 1988; Basel and Udell, 1989; Yuan and Udell, 1993; Sleep and Ma, 1997; Imhoff et al., 1997), and are summarized by Udell (1996) and Davis (1998).

More recently, the co-injection of air during steam injection has been tested and applied both in laboratory studies (Betz et al., 1998; Schmidt et al., 2002; Kaslusky and Udell, 2002) and in the field (IWR, 2003; Earth Tech and SteamTech, 2003; SteamTech, 2003). The injection of air enhances vapor transport between injection and extraction points and reduces the risk of NAPL condensation bank formation that may lead to downward NAPL mobilization. At the recent full-scale remediation at the Young-Rainey STAR Center in Pinellas, Florida, air injection was used to optimize vadose zone remediation by creating a horizontal sweep of vapor, and to assist in venting and controlling cool-down after cessation of steam injection (U.S. DOE, 2003; Heron et al., 2005).

3.3. Thermal Remediation Mechanisms

The steam enhanced extraction process removes volatile and semivolatile contaminants from the subsurface by heating the soil to volatilize them, while displacing mobile liquids (ground water and NAPL) ahead of the advancing steam zone. Liquids displaced by the injected steam are pumped from extraction wells. The vapors containing the volatilized contaminants are captured by vacuum extraction. Once they are above ground, extracted ground water and vapors are cooled and condensed. Liquid hydrocarbons are separated from the aqueous stream for recycling, and process vapors and water are treated before discharge.

Heating the subsurface to temperatures near the boiling point of water leads to dramatic changes in the thermodynamic conditions, and makes NAPL much more mobile. The major effects are:

- The vapor pressure of volatile and semivolatile compounds increases markedly with temperature. As the subsurface is heated from 20°C (68°F) to an average temperature of 100°C (212°F), the vapor pressure of the contaminants will increase by between 10 and 30-fold (Udell, 1996).
- Boiling of co-located NAPL and water phases will occur at temperatures below the boiling point of water (DeVoe and Udell, 1998; Heron, 1998b).
- Adsorption coefficients are reduced by heating, leading to release of contaminants from the soil or rock matrix (Heron et al., 1998a; Sleep and McClure, 2001).
- Viscosity of NAPLs is reduced by heating. The higher the initial viscosity, the greater the reduction. For moderately viscous NAPL, viscosity can be reduced by approximately an order of magnitude by heating from ambient to steam temperature (Davis, 1997). For TCE and other chlorinated solvents, the viscosity typically is reduced by about a factor of two (Heron et al., 1998b).
- DNAPL density is reduced during heating, which improves its flotation and displacement. For chlorinated solvents, the effect is modest, with less than 10 percent swelling of the DNAPL. For DNAPLs such as creosote, the density changes can cause a DNAPL to become less dense than water, aiding in its recovery as an LNAPL (Davis, 2002).
- NAPL-water interfacial tensions for some NAPLs are lowered by as much as two-fold, allowing for improved hydraulic removal of NAPLs (Davis, 1997; She and Sleep, 1998).
- Water solubility increases for organic contaminants at elevated temperatures, while dissolution rates increase by factors of two to five, leading to faster NAPL dissolution and removal (Sleep and Ma, 1997; Imhoff et al., 1997).

These physical effects provide several pathways by which the NAPL is removed from the subsurface:

- Displacement as a NAPL phase and extraction with the ground water (Hunt et al., 1988b; Udell et al., 1997).
- Vaporization and extraction in the vapor phase.
- Volatilization, migration in the steam phase, and condensation in water that is subsequently removed by pumping.
- Dissolution and desorption and removal with the extracted water.

For chlorinated solvents such as PCE, vaporization is believed to be the most important mechanism for recovery, and most of the contaminants are extracted in the vapor phase (typically between 80 and 95 percent). As the contaminants become less volatile, liquid phase recovery becomes more important. For example, approximately 50 percent of the creosote recovered from the Visalia Pole Yard by steam injection was as a NAPL, and approximately equal amounts were recovered in the vapor and aqueous phases (Eaker, 2003).

In addition to the physical removal described above, biological and chemical degradation mechanisms may occur during and after thermal remediation. These mechanisms include:

- Microbial degradation of NAPL components (Newmark and Aines, 1997).
- Abiotic oxidation reactions which occur in water at elevated temperature in the presence of oxygen. These reactions have been called Hydrous Pyrolysis/Oxidation, and may provide some destruction of contaminants such as creosote under certain conditions (Leif et al., 1998; Davis, 2002).
- Hydrolysis at elevated temperature. This is particularly relevant for chemicals with short half-lives such as methylene chloride and 1,1,1-trichloroethane (Jeffers et al., 1989).

Field-scale thermal remediation should be designed to use a combination of the mechanisms listed above. Since contaminants can be effectively mobilized as a liquid NAPL, as a vapor, and as dissolved phases, capture and control of the fluids are essential for successful remediation.

3.4. Steam Injection Demonstrations and Remediations in Unconsolidated Media

Numerous field demonstrations and several full-scale remediations using SER have been completed. The first such demonstration was conducted in 1988 at a solvent recycling facility in San Jose, California (Udell and Stewart, 1989). Steam was injected into the vadose zone in an area containing residual solvents for five days. After heating to near steam temperatures, steam was injected in a cyclic mode in order to induce pressure changes, which is referred to as pressure cycling (Udell et al., 1991; Itamura and Udell, 1995). Pressure cycles were induced by temporarily turning off the steam to the injection wells while continuing to extract ground water and vapors. This led to pressure drops in the formation, which created in-situ boiling and led to extraordinary recovery rates. Typically, 90 percent of the mass in the treatment zone in high permeability regions was removed in that short time frame, although higher solvent concentrations remained in low permeability regions and zones not sufficiently heated.

The second demonstration was conducted at full-scale at the Lawrence Livermore National Laboratory in 1993 (Newmark, 1994; Newmark and Aines, 1997). Nearly 30,000 liters (7,600 gallons) of gasoline were removed from the subsurface, including significant volumes from deep zones 9 meters (30 feet) below the water table. The remediation was conducted over a period of six months, using SER in combination with electrical heating of low permeability zones and electrical resistance tomography (ERT) to monitor steam and hot water movement. The combination of these technologies has been called Dynamic Underground Stripping. In 1996, California regulators confirmed that no further remedial actions were required for the hydrocarbon-contaminated ground water.

The third demonstration was a pilot test at Naval Air Station Lemoore, California, in 1994 (Udell and Itamura, 1995). Almost 300,000 liters (78,300 gallons) of less volatile JP-5 were removed from the subsurface over a period of three months. JP-5 soil concentrations dropped from over 50,000 milligrams per kilogram (mg/kg) to below 10 mg/kg at the location of the water table.

In contrast to these successful demonstrations, other steam injection projects have been completed that did not include the cyclic polishing step, and have been only moderately successful. At the Rainbow Disposal transfer yard in Huntington Beach, California, steam injection was applied to recover diesel fuel with lesser success due to inadequate injection rates and subsurface temperature monitoring (U.S. EPA, 1995). At Hill Air Force Base, Utah, short periods of steady steam injection followed by air injection were applied at a solvent spill site and at an isolated treatment cell containing DNAPL with moderate success (Gildea and Stewart, 1997).

Field demonstrations employing pressure cycling continued in the late 1990's (BERC, 2000; Heron et al., 2000). The Alameda Point demonstration removed about 2,300 liters (600 gallons) of NAPL from a small source area, with overall soil and water VOC concentration reductions in the order of 1,000-fold. The demonstration lasted 70 days, and the results were highly promising for restoration of TCE-rich source zones in shallow unconsolidated soils.

Mass removal of TCE and PCE was demonstrated at the Savannah River Site, South Carolina (IWR, 2002; Oochs et al., 2003). However, post-operational data on soil and ground water quality are not available to assess whether complete aquifer restoration occurred.

Recently, a large, full-scale remediation of a creosote-contaminated site in Visalia, California was completed (Newmark and Aines, 1998; Eaker, 2003). Approximately 590,000 kg (1,300,000 lbs) of wood-treating chemicals were removed from the subsurface during three years of steam injection. Post treatment soil sampling showed significant reductions in creosote concentrations, and ongoing ground water sampling shows aqueous creosote concentrations are continuing to decline. In 2003, ground water samples at the downgradient edge of the property showed pentachlorophenol and benzo(a)pyrene concentrations near or below the cleanup goal.

In 2003, SteamTech completed a full-scale DNAPL site restoration at the Young-Rainey STAR Center, Florida (SteamTech, 2003). This clean-up involved steam and air injection at 36 wells, electrical heating of a bottom clay layer, and fluid extraction from 28 wells. More than 1,360 kg (3,000 lbs) of VOC chemicals were removed in a period of 4.5 months, with post-operational sampling showing that less than 0.5 kg (1 lbs) of VOCs remained in the subsurface. Pressure cycling and air injection were deemed very effective in shortening the remediation time. The highest post-operational ground water concentration in the 48 samples collected was ten times the maximum concentration level (MCL) for TCE; most samples were nondetect. Comparing soil concentrations before and after the remediation showed an average VOC concentration reduction of 99.93 percent (Heron et al., 2005). This result confirmed the assumption that SER can be completely effective for restoring unconsolidated media aquifers contaminated by VOCs to near MCL concentrations.

Overall, SER is now a well-documented technique for NAPL source reduction in unconsolidated media, both above and below the water table. Implemented properly, not only source zone removal, but also restoration – i.e., reduction of contaminants to very low soil and ground water concentrations – are possible.

3.5. Steam Demonstrations in Fractured Rock

NAPL contamination occurring in fractured rock aquifers is common in the United States and in many other areas around the world. In fractured rock, steam migration, and thus the remedial success, is much less predictable. The location of the permeable fractures is typically not accurately known, and connectivity between injection and extraction wells cannot be assumed, as in unconsolidated media. Thus, the design of individual wells and of the overall well-field is a major challenge when transferring steam remediation technology to fractured rock.

The remediation of a TCE source in fractured rock using SER was completed in 2001 at a site near Prague, Czech Republic (Dusilek et al., 2001). The approach was to remove the DNAPL source by vaporization and entrainment of resulting TCE vapors by injecting air, which was recovered by soil gas extraction. The site has three main geologic features: a 6-meter (20-foot) thick permeable near-surface zone comprised of highly fractured sandstone and containing perched water; a 1-meter (3-foot) thick claystone rock aquitard; and a deep, 1.8-meter (6-foot) thick aquifer comprised of highly fractured sandstone. Each unit appeared to be contaminated by NAPL TCE.

Steam and air were first injected into two wells beneath the NAPL source zone, and vapors were extracted from a series of dual-phase extraction wells surrounding the injection wells. After the bottom aquifer was sufficiently heated, steam and air were injected into the upper permeable zone. When both aquifers were heated, air injection was ceased while continuing with pure steam injection. Once the aquifer and aquitard system were heated to the temperature equal to the local boiling point of water, the site was depressurized and then re-pressurized in a cyclical manner to reduce the concentrations of aqueous phase contaminants. Post-steaming ground water analysis in regions treated by SER showed reductions in ground water concentrations from greater than 100 milligrams/liter (mg/l) to less than 0.10 mg/l (Dusilek et al., 2001).

In 2002, SER was field tested at Site 61 at Edwards Air Force Base, California (Earth Tech and SteamTech, 2003). This treatability study used a five-well layout with a single steam injection well surrounded by four extraction wells. The source zone consisted of fractured granite bedrock contaminated with TCE and diesel-range organics. This 45-day field test resulted in the removal of between 900 and 1,800 kg (2,000 and 4,000 lbs) of chemicals, including NAPL. Post-operational sampling showed nondetect soil concentrations in all samples collected above the water table, and reductions of ground water TCE concentrations in the range of 50 to 90 percent. The test was deemed highly successful for the vadose zone source removal. However, the test was not continued long enough to heat the aquifer to near steam temperatures, and thus, no conclusions could be drawn on aquifer restoration efficacy in fractured granite. Pressure cycling and air injection proved beneficial for increasing the chemical mass removal rate by at least a factor of two when compared to continuous steam injection and extraction.

Despite the positive results in unconsolidated media and at the two fractured rock sites addressed prior to this project, the applicability of SER at a site such as the Loring Quarry could not be assured. To the best of our knowledge, no SER demonstration has been completed in such a complex, tight, and sparsely fractured limestone. The depth of DNAPL contamination at Loring Quarry apparently exceeds 21 meters (70 feet), which is at least 17 meters (55 feet) below the water table. At these depths, the limestone fractures are of relatively small apertures (less than 2×10^{-4} meters (6.6×10^{-4} feet)), and very sparse (typically less than one fracture was encountered per meter (3 feet) of core collected). This makes the Loring Quarry much more challenging for SER than the sites treated previously.

Chapter 4. Characterization for Design and Implementation

The pre-operational characterization activities were focused on gathering the information needed to finalize the design of the steam injection and extraction system and the pre-treatment data needed to evaluate its effectiveness. Specific objectives of the characterization activities fell into three general categories: 1) characterization of the fracture system which would control steam movement, 2) characterization of the hydrogeologic system in the target zone for treatment, and 3) determination of the contaminant distribution and concentration in the target area. Characterization of the fracture system was accomplished by obtaining and logging rock cores from the process boreholes and from the three deep wells around the treatment area, and borehole geophysical logging of the process boreholes. Characterization of the hydrogeologic system was accomplished through transmissivity testing and interconnectivity testing between boreholes. Characterization of the contaminant distribution and concentration was accomplished by collecting and analyzing rock chip and ground water samples. Each of these activities is described in detail in the following sections, and the data are presented.

In order to extend the funding that was available for the project, and in an attempt to adhere to the aggressive schedule that was proposed when the project was initiated, the decision was made that boreholes needed for the steam injection, extraction, and monitoring systems would be used to complete all characterization activities. Thus, locations of the boreholes for characterization were driven by the proposed layout of steam injection, extraction, and monitoring wells determined by SteamTech in their preliminary draft work plan (SteamTech, 2001; wells shown in black in Figure 4.0-1), as modified in the field during the team's site visit to accommodate site conditions (wells shown in red). The proposed layout was based on the understanding of the site which was developed from the Phase I and II characterization reports, which is summarized in Chapter 2. The dashed line shows

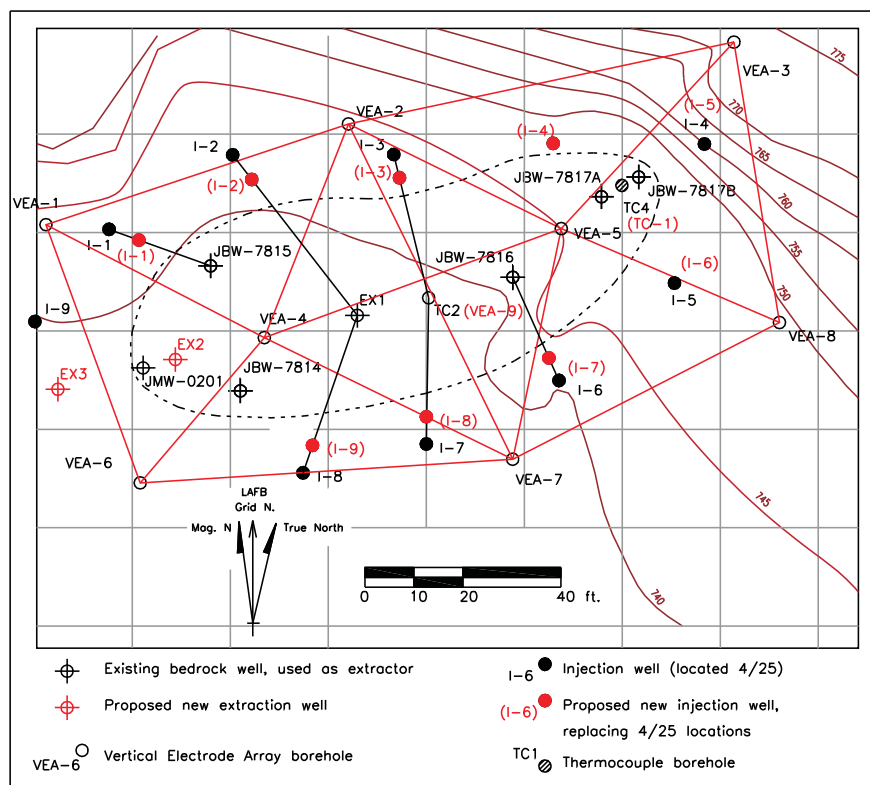


Figure 4.0-1. General site layout developed by SteamTech in April 2001.

the target area chosen for the research project, by agreement between SteamTech and MEDEP. The initial system design included nine injection (I) wells (I-1 to I-9) surrounding the target area on three sides, and four extraction (EX) wells along the centerline of the target area. At the time that Figure 4.0-1 was drawn, it was anticipated that JBW-7816 would be the fourth extraction well; however, it was determined that this well was not adequate for that purpose due to grout contained in many of its fractures, reducing their transmissivity. Thus, it was replaced by extraction well EX-4, located approximately 1.5 meters (5 feet) east of JBW-7816. Six ERT monitoring wells (Vertical Electrode Arrays (VEA), VEA-1 to VEA-3; VEA-6 to VEA-8) surround the injection area, with three additional VEA wells (VEA-4, VEA-5, and VEA-9) along the centerline. In addition, one thermocouple (TC) well (TC-1) was drilled at the eastern end of the target area. Existing boreholes within the target zone were slated to be used for temperature monitoring, or for the borehole radar tomography research conducted by the USGS.

4.1. Characterization Activities

4.1.1. Drilling Program

The initial drilling for the research project was conducted during May and June 2001. A total of 23 boreholes were drilled, ranging in depth from 23 to 46 meters (75 to 150 feet). All of these wells were drilled in the vertical orientation. Figure 4.0-1 shows the locations of the boreholes, and Table 4.1.1-1 provides the drilling details for each well. Boreholes intended to be injection and extraction wells, in addition to the four boreholes within the target area that were intended to be monitoring wells, were diamond cored using HQ (0.10 meter (0.33 feet) diameter) equipment. For those boreholes intended to be injection or extraction wells, the nominal borehole diameter was required to be 0.15 meters (0.5 feet). These boreholes were diamond cored using HQ equipment and then reamed using a reaming shell to 0.15 meters (0.5 feet) after hydraulic testing was complete. Wells were purged after reaming until clear fluid was obtained. Surface casing of 0.15 meters (0.5 feet) diameter was installed in each of these wells using an air rotary rig. The remaining six VEA boreholes were constructed using a 0.10 meter (0.33 feet) air-hammer with 0.15 meters (0.5 feet) surface casing.

Standard HQ double tube methods were used for collecting rock core. Drilling water was obtained from a local fire hydrant which is connected to the base-wide fire protection system. The drilling water was tagged using sodium iodide for later identification in the ground water sampling program. The core was visually inspected for lithological and structural features and boxed for on-site storage. In particular, the presence of open fractures and features of importance to ground water flow were noted. A photoionization detector (PID) was used to screen the core for organic vapors. Appendix B provides the drilling logs for each of the cored boreholes.

4.1.2. Rock Chip Sampling

Rock sampling was first performed during the Phase I characterization activities at the Quarry (HLA, 1998). The objective was to qualitatively evaluate the presence and distribution of contaminants within the rock matrix adjacent to hydraulically active fractures. A sample of rock from a fracture surface was collected with a rock hammer or with the aid of a cold chisel, and placed in a pre-prepared methanol sample jar for extraction. Samples were gently agitated, weighed, then stored at 4°C (40°F). After an extraction period that varied from two days to two weeks, the methanol was transferred to a standard 0.04 liter (0.01 gallon) volatile organics analysis (VOA) vial and analyzed by EPA Method 8260B. This method essentially follows EPA Method 5035 for soil sampling for VOCs, and the samples were referred to as methanol extracted rock chip (MERC) samples. A slightly modified method was used for this research, and the Standard Operating Procedure (SOP) is outlined below:

- An 0.25 liter (0.066 gallon) wide-mouth glass jar containing 0.10 liter (0.026 gallon) reagent grade methanol was pre-weighed to the nearest 1×10^{-5} kg (2.2×10^{-5} lbs) prior to the collection of each sample.
- Immediately following the extrusion of the core from the core tube, rock chips from specific sample locations were obtained by chiseling off chips weighing a total of 0.05 to 0.08 kg (0.11 to 0.18 lbs).
- The chip samples were then immersed in the methanol, and the glass jar weighed again to the nearest 1×10^{-5} kg (2.2×10^{-5} lbs). The sample bottle was marked with the location identification, sample interval, and date and time the sample was collected.
- The glass jar containing methanol and rock chips was then placed in a refrigerator at 4°C (40°F) for seven days.
- Methanol extract was then decanted into a 0.02 liter (0.005 gallon) glass VOA vial using a disposable pipette. The VOA vials containing the extract were capped, labeled, and stored in a refrigerator at 4°C (40°F) until they were shipped in a cooler with ice to the laboratory.
- Methanol extracts were analyzed for volatile organic constituents in accordance with EPA Method 8260B.

Chips were obtained from the fracture surfaces and were generally less than 0.025 meters (0.08 feet) in length and 0.006 meters (0.02 feet) in thickness. During the pre-steam injection characterization phase, rock chip samples were collected from all boreholes that were to be used as injection or extraction wells, as well as the four monitoring well boreholes that were within the target zone for remediation (VEA-4, VEA-5, VEA-9 and TC-1). In addition to the fracture surface samples, a non-fracture control sample (NFCS) was also collected from an intact portion of the core of each borehole. Duplicate samples were collected for every tenth sample. Sand blanks were prepared each day by adding approximately 0.08 kg (0.18 lbs) of sand to a jar with methanol, and these were also submitted for analysis.

Table 4.1.1-1. Well Drilling Details

Well Identification	Core Collected (Y or N)	Total Well Depth (meters bgs)	Total Well Depth (feet bgs)	Top of Casing Elevation (meters msl)	Top of Casing Elevation (feet msl)
I-1	Y	27	90	226.31	742.50
I-2	Y	29	95	225.98	741.39
I-3	Y	30.5	100	226.26	742.32
I-4	Y	33.5	110	227.16	745.29
I-5	Y	36.5	120	227.23	745.50
I-6	Y	33.5	110	227.33	745.84
I-7	Y	30.5	100	226.63	743.53
I-8	Y	27	90	225.94	741.26
I-9	Y	27	90	225.94	741.26
EX-1	Y	24	80	225.88	741.06
EX-2	Y	23	75	226.04	741.61
EX-3	Y	23	75	225.99	741.44
EX-4	Y	30.5	100	226.40	742.79
TC-1	Y	38	125	227.13	745.17
VEA-1	N	32	105	226.25	742.28
VEA-2	N	36.5	120	225.86	741.02
VEA-3	N	45.7	150	237.35	778.70
VEA-4	Y	30.5	100	225.80	740.82
VEA-5	Y	36.5	120	226.85	744.25
VEA-6	N	30.5	100	225.59	740.14
VEA-7	N	35	115	226.13	741.88
VEA-8	N	38	125	225.96	741.35
VEA-9	Y	35	115	226.09	741.77

Analytical results were converted to milligrams VOC per kilogram of rock, and are presented in Table 4.1.2-1. PCE concentrations determined from the MERC samples are also shown in Plate 4.1.2-1. The data show that the shallowest detection of PCE in the MERC samples occurred in EX-3, the western-most borehole of the system, at 7 meters (23 feet) bgs. Moving to the east along the centerline of extraction boreholes, the shallowest detection of PCE in the borehole becomes progressively deeper: 9 meters (30 feet) bgs in EX-2; 10.7 meters (35 feet) bgs in EX-1, and 16.8 meters (55 feet) bgs in EX-4. Visible evidence of contamination was observed in a fracture at 9.4 meters (30.9 feet) bgs in EX-2. VEA-5 and I-5 follow the same trend of deeper contamination, with the shallowest detection at approximately 18.8 meters (62 feet) bgs and 25 meters (82 feet) bgs, respectively. Along the northern line of injection wells, the shallowest detections of PCE are deeper than along the centerline, and again, the shallowest detection of PCE is deeper in the borehole going from west to east. The highest concentrations of PCE in MERC samples were found in I-3, with concentrations of 54 and 72 mg/kg at approximately 29.3 and 29.6 meters (96 and 97 feet) bgs, respectively. I-2 also had high PCE concentrations with 23 mg/kg at 19.8 meters (65 feet) bgs and 38 mg/kg at 27.4 meters (90 feet) bgs. I-4, I-5, and I-6 all have relatively low concentrations of PCE, and all the detections were at depths greater than 21.3 meters (70 feet) bgs. It was noted that the core from I-4 had a slight oily sheen over most of its length, while the core from I-5 had a sheen at depths of 3 to 6 meters (10 to 20 feet) bgs.

Tables 4.1.2-1. Pre-Steam Injection MERC Sample Results

Depth in meters	Depth in feet	Fracture Description	1,1-Dichloroethylene	Benzene	Chlorobenzene	c-1,2-Dichloroethylene	Ethylbenzene	Tetrachloroethylene	trans-1, 2-Dichloroethylene	Toluene	Trichloroethylene	Vinyl Chloride	Xylene (total)
I-1													
4.0	13	P,S,C											
8.2	27	V, S, C											
9.1	30	V, S											
11.9	39	NFCS								0.88J			
12.8	42	V, S, C				0.06J		1.41			0.43		
16.5	54	P, S				0.02J		0.76		1.85	0.44		
16.8	55	B, S				0.03J		1.06			0.22J		
20.7	68	B& V, C Duplicate								0.76			
20.7	68	B & V, C											
23.8	78	B & V, S						0.3					
27.1	89	M											
I-2													
1.5	5	B, C, S											
1.5	5	B, C, S Duplicate											
2.4	8	V, S											
5.5	18	P, S											
6.7	22	B, C											
7.9	26	NFCS											
8.8	29	B, S											
11.0	36	V, C, S											
11.6	38	B, S								0.28J			
14.9	49	B											
15.9	52	B						1.8			0.52		
19.8	65	B, S						23.4			0.59		
19.8	65	B, S Duplicate						22.6			0.55		
24.4	80	B						9.74			0.30J		
27.7	91	M			0.14J			38.2			0.51J		
I-3													
3.0	10	P, S											
3.7	12	B, S											
7.0	23	P&B, S								0.25J			
7.3	24	B, S								0.29J			
7.3	24	B, S Duplicate								0.29J			
7.6	25	Several fractures, S											
10.1	33	P&V, S											
10.4	34	P, S											

Tables 4.1.2-1. Continued

Depth in meters	Depth in feet	Fracture Description	1,1-Dichloroethylene	Benzene	Chlorobenzene	c-1,2-Dichloroethylene	Ethylbenzene	Tetrachloroethylene	trans-1, 2-Dichloroethylene	Toluene	Trichloroethylene	Vinyl Chloride	Xylene (total)
10.7	35	P, S								0.11J			
11.3	37	B, S											
15.2	50	P, S											
15.2	50	P, S Duplicate											
18.6	61	S											
22.9	75	M&V, S						0.54					
23.8	78	NFCS											
24.4	80	B, S						5.39			1.08		
26.8	88	B, M			0.04J	0.05J		41.76	0.04J		1.06		
29.3	96	V, P, O			0.22J			54.35			0.49J		
29.6	97	P, O			0.24J			72.04			0.71		
I-4													
2.4	8	B, S											
5.5	18	B, S, C		0.21			0.7			0.38J			4.24
6.7	22	B, S		0.11J			0.18J						0.58J
7.9	26	B, S											
10.7	35	B&P, S											
10.7	35	B&P, S Duplicate											
11.0	36	B, C, sheen											
13.1	43	V, P, sheen											
15.2	50	M, O, sheen											
18.0	59	V, P, sheen		0.08J									
19.8	65	P, sheen											
21.6	71	B, S, sheen				0.12J		0.53					
23.8	78	V, sheen											
25.6	84	P						0.3					
28.3	93	V, P, C, S											
30.2	99	NFCS, M											
31.1	102	B											
I-5													
4.9	16	P&B, S											
9.1	30	V&B											
9.1	30	V&B Duplicate											
10.4	34	V											
11.3	37	B, S											
11.9	39	P, S											

Tables 4.1.2-1. Continued

Depth in meters	Depth in feet	Fracture Description	1,1-Dichloroethylene	Benzene	Chlorobenzene	c-1,2-Dichloroethylene	Ethylbenzene	Tetrachloroethylene	trans-1, 2-Dichloroethylene	Toluene	Trichloroethylene	Vinyl Chloride	Xylene (total)
12.2	40	B, S											
14.0	46	B, S											
14.6	48	NFCS											
15.2	50	V, S											
17.7	58	M											
19.5	64	P, S											
21.3	70	M, P, S											
23.5	77	M, B, S											
23.8	78	M, B, C											
25.0	82	M, P, S				0.10J		3.13			0.31J		
25.9	85	V, C, S				0.16J		0.72J			0.28J		
25.9	85	V, C, S Duplicate				0.15J		0.68			0.28J		
26.2	86	B, S				0.34		0.53		0.30J			
29.6	97	P											
32.3	106	V, P, S				0.06J		0.27J					
33.8	111	B											
36.3	119	B											
I-6													
3.0	10	B, S, O		0.03J			0.09J						0.64J
4.3	14	B, S		0.03J									0.38J
6.7	22	B, S		0.06J									0.96
7.0	23	B, S		0.08J			0.11J						0.42J
7.9	26	B, S											
8.5	28	B, S		0.03J						0.17J			
11.0	36	B, S											
11.0	36	B, S Duplicate											
11.6	38	B, S											
11.9	39	B, S											
12.5	41	V, C, S											
13.7	45	NFCS											
15.9	52	B											
19.8	65	B, S											
21.9	72	B, S						0.20J					
22.3	73	B, S						0.28J			0.26J		
24.1	79	B, C, S						0.73			0.23J		
27.4	90	M											

Tables 4.1.2-1. Continued

Depth in meters	Depth in feet	Fracture Description	1,1-Dichloroethylene	Benzene	Chlorobenzene	c-1,2-Dichloroethylene	Ethylbenzene	Tetrachloroethylene	trans-1, 2-Dichloroethylene	Toluene	Trichloroethylene	Vinyl Chloride	Xylene (total)
27.4	90	M Duplicate											
28.7	94	B, S						0.19J					
32.6	107	B						0.4					
I-7													
3.4	11	B, S											
5.8	19	B, S						0.37J					
6.4	21	B, S											
7.0	23	B, S											
10.1	33	B, S											
12.8	42	P											
14.3	47	M						1.09					
16.8	55	P, S						5.19			0.39		
16.8	55	P, S Duplicate						4.97			0.39		
18.6	61	B, S				0.35		4.63			1.18		
19.5	64	B, S						2.88					
20.7	68	NFCS						0.71					
21.0	69	M, S		0.03		0.09		4.57			1.07		
22.3	73	V&B, S						1.98					
22.9	75	B, S						1.8			0.24		
24.1	79	P											
27.1	89	M, V											
30.2	99	M											
I-8													
3.0	10	V, S											
3.0	10	V, S Duplicate											
4.0	13	B, S											
7.9	26	B, S											
8.5	28	B, S											
9.1	30	B, S											
10.4	34	P, S								0.33J			
13.1	43	P, S						0.69					
18.6	61	V						2.69			0.37J		
20.4	67	NFCS											
20.7	68	B											

Tables 4.1.2-1. Continued

Depth in meters	Depth in feet	Fracture Description	1,1-Dichloroethylene	Benzene	Chlorobenzene	c-1,2-Dichloroethylene	Ethylbenzene	Tetrachloroethylene	trans-1, 2-Dichloroethylene	Toluene	Trichloroethylene	Vinyl Chloride	Xylene (total)
23.8	78	P, C									0.65J		
27.4	90	V											
I-9													
1.5	5	B, S											
4.9	16	B, S											
7.9	26	B, S											
9.4	31	No fractures											
9.4	31	No fractures Duplicate											
9.8	32	NFCS											
11.6	38	B, S						3.3			0.32		
14.3	47	B											
16.8	55	M											
19.2	63	V, B											
21.9	72	M											
25.9	85	B											
25.9	85	B Duplicate											
26.8	88	B						0.58					
EX-1													
3.0	10	V											
6.1	20	P, S		0.06J						0.49			
6.1	20	P, S Duplicate		0.06J						0.46			
6.7	22	Silt vein								0.44J			
9.4	31	B, S											
11.0	36	B, C, S		0.06J		1.33		2.78		0.59	0.59		
12.5	41	B		0.04J		0.21		3.21		0.23J	0.6		
13.1	43	V, S				0.07J		2.96			0.55		
18.3	60	P, S		0.14J				21.3		0.22J	0.91		0.29J
19.2	63	NFCS											
23.5	77	P						19.1			0.34J		
EX-2													
2.1	7	B&V, S											
3.0	10	V, S											
3.0	10	V, S Duplicate											
4.9	16	B, S		0.02J		0.04J							
5.2	17	B, S											

Tables 4.1.2-1. Continued

Depth in meters	Depth in feet	Fracture Description	1,1-Dichloroethylene	Benzene	Chlorobenzene	c-1,2-Dichloroethylene	Ethylbenzene	Tetrachloroethylene	trans-1, 2-Dichloroethylene	Toluene	Trichloroethylene	Vinyl Chloride	Xylene (total)
5.8	19	B, S		0.019		0.05J				0.19J			
6.7	22	V, S											
9.4	31	V, visible contamination						18.1			0.24J		
13.4	44	NFCS											
16.8	55	B						6.72			0.12J		
17.4	57	V, S, C						1.26					
18.0	59	B, S				0.15J		12			0.58		
21.9	72	V		0.03J	0.04J	1.21		14.3			4.06	0.03J	
EX-3													
2.4	8	BCZ											
3.4	11	B&V, S											
3.4	11	B&V, S Duplicate											
5.2	17	P&B											
5.5	18	P, S				0.03J							
6.7	22	P, S						1.45					
9.1	30	B, C, S			0.02J	0.08J		8.16J			1.72		
9.4	31	B, S						2.48			0.77		
11.9	39	V, P, S			0.02J	0.05J		10.4			1.35		
13.1	43	B, S						5.02			0.29		
17.4	57	B, S											
17.7	58	M											
20.4	67	P						0.31J					
EX-4													
3.4	11	P, S											
4.9	16	B, S											
10.1	33	B, S								0.54			
15.2	50	P											
17.4	57	P, S						5.33			0.36		
17.4	57	P, S Duplicate						5.65			0.37		
19.2	63	NFCS											
21.3	70	B, C, S						4.41			0.38		
25.6	84	M, V, O						7.48					
29.9	98	B, M											
TC-1													
2.7	9	B, S											

Tables 4.1.2-1. Continued

Depth in meters	Depth in feet	Fracture Description	1,1-Dichloroethylene	Benzene	Chlorobenzene	c-1,2-Dichloroethylene	Ethylbenzene	Tetrachloroethylene	trans-1, 2-Dichloroethylene	Toluene	Trichloroethylene	Vinyl Chloride	Xylene (total)
6.1	20	V, S		0.19J			0.20J			0.68			1.07J
7.9	26	B&V, S											
7.9	26	B&V, S Duplicate											
8.2	27	B, S								0.17J			
9.1	30	B, S											
9.8	32	B, S											
11.0	36	B, S											
13.7	45	B, S								0.22J			
13.7	45	B, S Duplicate								0.19J			
15.9	52	M, NFCS											
19.2	63	P, S						0.293					
24.1	79	B&V, S				0.46		2.18		0.32	0.98		
28.7	94	B, S						0.42		0.16J	0.25J		
28.7	94	B, S Duplicate				0.08J		0.30J			0.18J		
35.1	115	V, C											
VEA-4													
1.8	6	B, S											
3.0	10	P, S											
4.0	13	P, S											
5.5	18	B, S											
5.5	18	B, S Duplicate								0.23J			
6.1	20	B, S											
8.5	28	P, S											
9.4	31	B (2), S											
9.8	32	B, S	0.02J	0.03J		1.12		2.84	0.02J	0.20J	1.23		
10.1	33	B, S						0.6					
12.2	40	P, S						1.51					
15.2	50	NFCS											
18.3	60	P, S				0.04J		3.5			0.86		
19.5	64	P, S				0.07J		3.04			1.03		
24.7	81	V						0.56			0.54		
30.5	100	M						8.65			1.73		
VEA-5													
2.7	9	V, C											0.17J
2.7	9	V, C Duplicate		0.02J									0.17J

Tables 4.1.2-1. Continued

Depth in meters	Depth in feet	Fracture Description	1,1-Dichloroethylene	Benzene	Chlorobenzene	c-1,2-Dichloroethylene	Ethylbenzene	Tetrachloroethylene	trans-1, 2-Dichloroethylene	Toluene	Trichloroethylene	Vinyl Chloride	Xylene (total)
5.8	19	B, S											
6.1	20	B, S		0.03J						0.20J			
6.4	21	P, S											0.26J
7.3	24	B, S								0.19J			
8.5	28	B, S											
14.6	48	B											
16.8	55	NFCS											
19.2	63	P						2.51			0.18J		
20.7	68	B, S						7.66			0.99		
22.3	73	B, S						1.84			0.36J		
24.7	81	B, S		0.03J				13.1			1.31		
29.3	96	V		0.03J							0.16J		
29.3	96	V Duplicate		0.03J							0.16J		
34.4	113	M, V		0.04				0.85			0.29		
VEA-9													
4.0	13	B, S											
7.9	26	V, S											
8.8	29	P, S											
9.1	30	B, S											
10.4	34	NFCS											
15.2	50	B, S	0.12J			0.56		6.28	0.12J		2.71		
20.7	68	M, V (2)											
25.0	82	B,M											
25.0	82	B, M Duplicate											
30.2	99	B						1.99			0.16J		
35.1	115	M											

All concentrations are in mg/kg.

Empty cells indicate that the compound was not detected.

P – Fracture perpendicular to bedding

S – Iron oxide staining

V – Vertical fracture

C – Calcite

B – Bedding plane fracture

M – Machine break

O – Odor

Moving to the southern line of injection wells, again the shallowest detections are deeper than along the centerline. I-9 and I-8 also follow the same pattern of the shallowest detections of PCE being deeper going from west to east. I-7, however, does not fit that pattern. I-7 had a small detection of PCE (0.37 mg/kg) at approximately 5.5 meters (18 feet) bgs. Also, the NFCS from I-7 from a depth of 20.7 meters (68 feet) bgs showed a small amount of PCE (0.71 mg/kg). This was the only NFCS obtained during pre-treatment characterization in which PCE was detected. This NFCS was taken from intact rock approximately 0.3 meters (1 foot) from a fracture which contained a moderate amount of PCE. All other NFCS were at least 0.7 m (2 feet) from a fracture that contained contaminants.

In eight of the 23 boreholes, PCE was detected in the deepest fractures sampled, and in boreholes EX-2, I-2 and I-3, the concentrations were greater than 10 mg/kg in the lowest fracture encountered. Thus, it is not likely that the full vertical extent of the PCE has been determined. The very high concentrations in the bottoms of boreholes I-2 and I-3 likely indicate that the contamination continues to the north at these and greater depths.

TCE was the second most commonly detected contaminant in the rock samples. Its concentration was generally around ten percent of the PCE concentration. Other chlorinated compounds detected occasionally in the rock samples include cis-1,2-dichloroethene, trans-1,2-dichloroethene, chlorobenzene, vinyl chloride, and 1,1-dichloroethane.

Fuel components were also detected in many of the rock samples. Benzene and toluene were the most commonly detected, and xylenes were also occasionally detected. Despite the fact that I-4 had an oily sheen over most of its depth, only relatively small concentrations of BTEX were found in samples from 5.5 and 6.7 meters (18 and 22 feet) bgs. The concentration of the fuel components was always low, with all except three detection less than 0.1 mg/kg (toluene in borehole I-1, at 16.5 meters (54 feet) bgs, 1.85 mg/kg; xylenes in I-4 at 5.5 meters (18 feet) bgs, 4.24 mg/kg; and xylenes in TC-1 at 6.1 meters (20 feet) bgs, 1.07 mg/kg).

MERC Data Quality. The most significant quality control (QC) problem with the MERC data was field blank contamination. Nearly all samples, including the sand blanks, contained some amount of 1,2,4-trimethylbenzene, 1,3,5-trimethylbenzene, and n-propylbenzene. Although the source of these contaminants was not determined during the pre-treatment MERC sampling, MERC sampling performed after steam injection established that these hydrocarbons were coming from the waxy coating on the inside of the jar lids. Thus, although a couple of the MERC samples during the Phase II characterization also showed small amounts of trimethylbenzenes, the trimethylbenzenes found in these samples were disregarded as contamination coming from the sample container. Also, some methanol blank samples were found to contain chloroform, chloromethane, styrene, n-propylbenzene, p-isopropyltoluene, and 2-butanone. n-Propylbenzene and isopropyltoluene are fuel components that were also detected in some ground water samples; however, it is likely that the source of the styrene and chloromethane was laboratory contamination, and these results were rejected. Table 4.1.2-1 shows only the VOCs detections determined to be coming from the rock samples.

Duplicate MERC samples were obtained for approximately every tenth sample. Unfortunately, many of these duplicates were from uncontaminated fractures, and thus did not provide useful information of the reproducibility of the sampling. The seven duplicate samples that did provide data on reproducibility generally show very favorable results, with the relative percent difference (RPD) between primary sample and duplicate being less than 10 percent in all samples except one, where the differences were 36 and 37 percent. This shows very good reproducibility in the rock chip samples.

Method detection limits for the analytes in the methanol were generally in the range of 0.01 to 1.5 mg/l (See Appendix C). Since approximately 0.1 liter of methanol were used to extract approximately 0.1 kilograms of rock chips, the detection limits for contaminants in the rock were generally in the range of 0.01 to 1.5 mg/kg. Almost all calibrations were within the QC limits established in the QAPP, as were the matrix spike/matrix spike duplicate (MS/MSD) results and laboratory control sample results.

4.1.3. Borehole Geophysics

Borehole geophysical logs were run on all the new boreholes which were originally planned to be injection (I- series) or extraction (EX- series) wells. Thus, a total of 13 boreholes were logged. The purpose of the geophysical logging was to aid in identifying and characterizing the hydraulically active bedrock fractures encountered in these boreholes. The logging suite included conventional measurements (caliper, fluid temperature, and fluid resistivity), and acoustic televiewer (ATV) imaging. Water-bearing fracture zones were inferred using subjective judgement by correlating numerous geophysical logs. All borehole logs were referenced to depths below the top of the casing, and the geophysical logging winches contained optical depth encoders to maintain depth measurements accurate within approximately +/- 0.06 meters (0.2 feet) throughout the borehole.

Conventional borehole geophysical data was obtained with a Mount Sopris model MGX-II digital logging winch and a Mount Sopris caliper/fluid-temperature/fluid-resistivity sonde. The caliper and fluid logs were recorded at 0.03 meters (0.1 foot) depth increments. Fluid temperature and fluid resistivity logs were recorded during the first logging run at each borehole, using a relatively slow downward logging speed of approximately 0.9 to 1.2 meters (3 or 4 feet) per minute to help identify subtle variations. A sub-assembly on the caliper probe's bottom obtained these fluid measurements. Caliper logging was subsequently performed while pulling the probe upwards through the borehole at approximately 2.4 to 3 meters (8 to 10 feet) per minute. Caliper logs can most confidently detect fractures that cross a borehole at moderate angles, e.g., less than approximately 70 degrees from horizontal, and thus may not accurately detect near vertical fractures.

ATV data were obtained using an Advanced Logic Technologies (ALT) model FAC40 acoustic televiewer probe, with a Mount Sopris model 4MXA logging winch. ATV data were recorded at 0.003 meters (0.01 foot) intervals throughout each borehole, with 1.25 degree arc-segments for each 360 degree scan around the borehole wall, at speeds of approximately 0.76 meters (2.5 feet) per minute. Because water is required to transmit the ATV sonic pulses to the borehole wall, ATV data recording stopped at the water level.

Decontamination between logging runs consisted of an Alconox scrub and tap water rinse of logging cables and probes.

All geophysical logs and summary ATV interpretation tables are included in Appendix D. Summaries of the results for each borehole are given in Table 4.1.3-1. The fluid resistivity plots appeared to show the greatest number of hydraulically active fractures; only occasionally were temperature anomalies noted which were not also shown in the resistivity data. ATV logs are essential for orienting fractures noted in the cores.

Table 4.1.3-1. Summary of the Prominent Fractures as Determined from the Borehole Geophysics

	Caliper Enlargements Depth (meters)	Fluid Resistivity Changes Depth (meters)	Temperature Changes Depth (meters)	ATV- Indicated Open Fractures Depth (meters)	Dip Angles of Open Fractures (Degrees)	Dominant Dip Direction
I-1	3.4, 4.6, 17.4	11.9, 16.8 – 18.9	11.9		30 - 80	West
I-2	2.1, 3.4, 5.8, 7.0	7.0, 10.0 – 10.4	10.0 – 10.4		40 - 80	Southwest
I-3	7.6	7.6, 14.6			40 - 75	Southeast
I-4	2.4 – 4.0	6.1 – 7.6, 10.0			30 - 80	South-southwest
I-5	25.6	7.6, 8.8, 12.2, 15.8, 21.9, 29.0	7.6, 8.8, 12.2, 15.8, 21.9, 29.0		30 - 75	Southeast
I-6		> 9.1	> 9.1		40 - 80	Southeast
I-7	1.5, 3.0, 6.4	6.4	18.6 – 21.3		40 - 80	No preferred direction
I-8		6.1 – 7.3, 8.8 – 12.2, 17.4			30 - 80	Southwest
I-9	2.0, 6.4 – 7.9	6.2, 11.9, 13.1, 14.9, 19.8, 23.2, 24.1	8.2		35 - 80	East-northeast or East-southeast
EX-1	2.1 – 3.0	10.0 – 11.6, 20.4 – 20.7	10.0 – 11.6, 20.4 – 20.7	6.4, 7.3, 12.8 – 13.4, 23.8 – 24.1	35 - 75	Southeast
EX-2	3.0 – 3.7, 5.8 – 6.4	7.0 – 8.2, 11.9			40 - 80	No preferred direction
EX-3	3.4 – 11.9	11.6 – 16.5, 21.3 – 22.2			35 - 70	East
EX-4	3.0, 5.2 – 6.7	5.2 – 6.7, 10.4 – 11.9	5.2 – 6.7, 10.4 – 11.9	5.2 – 6.7	40 - 80	East-southeast

4.1.4. Transmissivity Measurements

4.1.4.1. Method

In order to develop a robust conceptual model and determine the efficiency of steam injection and water withdrawal during the steam injection period, a detailed hydraulic testing program was undertaken during the 2001 field season. The testing was conducted using a straddle packer system designed to isolate specific sections of the borehole. The packer system was coupled to a 0.05 meter (0.17 foot) diameter PVC standpipe to provide access to the isolated section from the ground surface. A 345 kPa (3.4 atm) pressure transducer was used to measure the change in water level in the standpipe during testing. Figure 4.1.4.1-1 illustrates a schematic diagram of the packer and standpipe configuration.

The measurements of transmissivity were obtained using a modified slug test method. This method applies to both 0.1-meter (0.33-foot) and 0.15-meter (0.5-foot) boreholes. Packer positioning was conducted by a wire-line system, and contiguous measurements were obtained in every borehole. Generally, a 3-meter (10-foot) interval was tested; however, to reduce the time to test all boreholes, in some cases larger zones were tested. If the test of the larger zone indicated significant transmissivity, 3-meter (10-foot) intervals within that zone were tested. To conduct a test, the following procedure was employed:

1. Lower the packer assembly to the selected test depth. Test intervals must be contiguous with no overlap or untested gaps. A single packer assembly was used to test the bottom 3 meters (10-feet) or more of the borehole.
2. With the packers deflated, the open hole pressure (hydraulic head) was recorded.
3. The packers were then inflated using nitrogen to the manufacturer's recommendation considering the depth of water.
4. The water level recovery was monitored over a period of 10 minutes (or less, if less than one percent change is noted over one minute). Water level measurements were recorded every 10 to 15 seconds during the pre-test period. When attainment of a static water level required more than 10 minutes, extrapolation to the static water level was conducted. In these cases, the transmissivity of the interval was probably below the measurement capacity of this technique.
5. The slug test was then conducted in the standpipe by quickly adding 5 to 10 liters (1.3 to 2.5 gallons) of water. The recovery was monitored using a data logger over a period of 15 minutes. Water level measurements were recorded every 5 to 10 seconds during the testing period.

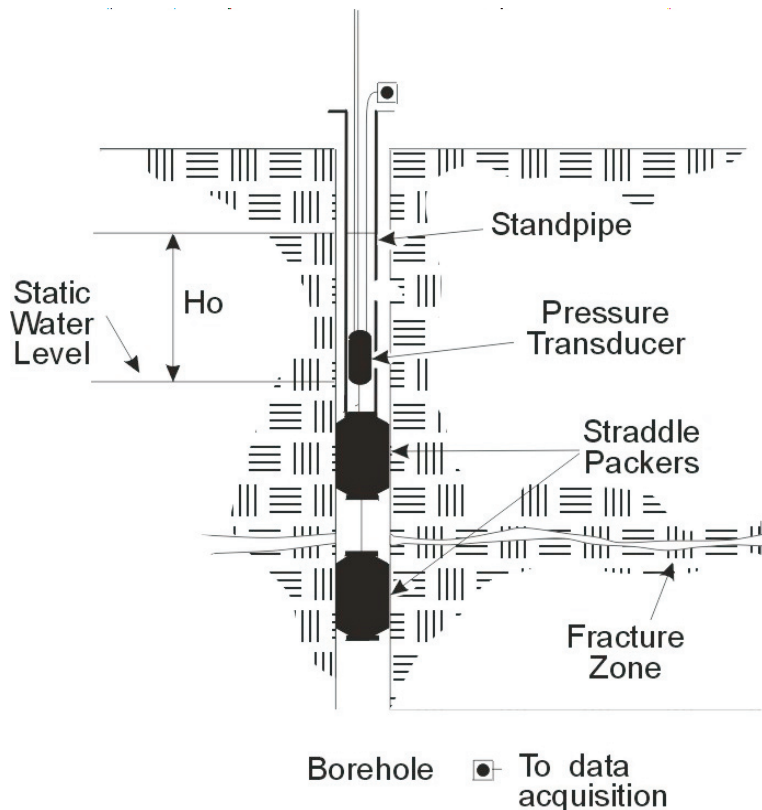


Figure 4.1.4.1-1. Schematic diagram illustrating the packer and standpipe configuration used for measuring transmissivity in the site boreholes.

6. At the end of the 15 minute period, the test was terminated by deflating the packers. Recovery to a stable open-hole pressure was also monitored.
7. For those tests that were conducted to at least 65 percent recovery during the 15 minute recovery period, the results were interpreted using the Hvorslev (1951) and the Cooper et al. (1967) methods. For those tests conducted where less than 65 percent recovery was achieved, the analysis for transmissivity was conducted using the Thiem (1906) equation:

$$h_0 - h_1 = \frac{Q}{2\pi T} \ln \left\{ \frac{R}{r_w} \right\} \quad (4-1)$$

and

$$Q = -\pi r_s^2 \frac{dh}{dt} \quad (4-2)$$

where T is transmissivity, Q is the steady state flow rate (determined from the fall in the water level in the standpipe over all or part of the recovery duration), h_1 is the water level displacement at some time after slug injection, h_0 is the initial water level displacement due to the introduction of the slug, r_s is the standpipe radius, r_w is the well radius, and R is the radius of influence. Combining equations (4-1) and (4-2) and integrating, T is calculated from:

$$T = \frac{r_s^2}{2\Delta t} \ln \left\{ \frac{R}{r_w} \right\} \ln \left\{ \frac{H_0}{H_1} \right\} \quad (4-3)$$

where Δt is the duration between the measurements of hydraulic head H_0 and H_1 . The value of R is determined from $R=2(Tt/S)^{1/2}$ where t is the duration of the water injection (decline) period and S is storativity. The value of storativity was estimated.

8. To provide quality assurance the steps described in Appendix E were undertaken.

During the course of the hydraulic testing program, approximately 123 tests were completed (including duplicates) in boreholes I-1 through I-9, EX-1 through EX-4, JBW-7814 to 7817B, VEA-1 through VEA-9.

4.1.4.2. Discussion of Results

Table 4.1.4.2-1 contains the results from the transmissivity tests. Individual transmissivity measurements for selected wells are plotted against depth to form transmissivity profiles. The locations of individual wells and cross-sections containing profiles are shown in Figure 4.1.4.2-1, and the profiles themselves are presented in Figures 4.1.4.2-2, 4.1.4.2-3, and 4.1.4.2-4. Most of the profiles show the presence of a zone of relatively higher transmissivity in the upper part of the subsurface, typically lying at depths of less than 15 meters (50 feet) bgs. This zone apparently thickens from the east to west across the site, a feature consistent with a relationship to the effects of blasting and excavation within the Quarry. Notable exceptions to this general case are seen in wells I-1, I-5, and JBW-7816, which display transmissivities close to or lower than 1×10^{-6} m²/s (1.1×10^{-5} ft²/s) at shallow depths. Significantly, several of the wells plotted show restricted zones of relatively higher transmissivity (greater than 1×10^{-6} m²/s; 1.1×10^{-5} ft²/s) in the lower portion of the borehole. The presence of such zones in wells I-4 and I-5 at depths of 21.4 to 24.4 meters (70 to 80 feet) bgs and 24.4 to 27.4 meters (80 to 90 feet) bgs, respectively, was of particular interest, as it indicated the possible presence of an interwell connection at depth that corresponded to the location of open fractures sub-parallel to bedding. These open fractures had been identified in cores and by geophysical logging, and provided targets suitable for investigation by subsequent pulse interference testing. Similarly, the recognition of very low transmissivity at depth in wells on the northern edge of the site (I-1, I-2, I-3) provided information that was used to modify the subsequent characterization program and final remediation strategy. These wells had originally been proposed for steam injection; however, the discovery of significant concentrations of PCE at depth, coupled with the low transmissivity of fractured bedrock at the target depths, strongly suggested that these wells were unsuitable for use in the originally intended manner.

Table 4.1.4.2-1. Summary of Individual Well Transmissivity Profiles

Well	Elevation of top of casing (ft msl)	Depth to top seal of isolated zone (ft, BCT)	Depth to top seal of isolated zone (m, BCT)	Depth to bottom seal of isolated zone (ft, BCT)	Depth to bottom seal of isolated zone (m, BCT)	Transmissivity (m²/s)	2b Fracture width (m x 10⁶)
I-1	741.48	29.5	9.0	39.5	12.0	2.E-07	71
I-1	741.48	39.5	12.0	49.5	15.1	7.E-08	48
I-1	741.48	49.5	15.1	59.5	18.1	8.E-06	240
I-1	741.48	59.5	18.1	69.5	21.2	8.E-09	24
I-1	741.48	69.5	21.2	79.5	24.2	1.E-07	62
I-1	741.48	79.5	24.2	92.2	28.1	6.E-08	46
I-2	740.34	15.0	4.6	25.0	7.6	7.E-07	107
I-2	740.34	25.0	7.6	35.0	10.7	8.E-08	52
I-2	740.34	35.0	10.7	45.0	13.7	2.E-06	140
I-2	740.34	25.0	7.6	95.0	29.0	2.E-06	140
I-2	740.34	45.0	13.7	95.0	29.0	7.E-07	107
I-2	740.34	65.0	19.8	95.0	29.0	1.E-06	118
I-2	740.34	85.0	25.9	95.0	29.0	5.E-07	92
I-3	741.27	10.0	3.0	20.0	6.1	2.E-06	152
I-3	741.27	20.0	6.1	30.0	9.1	5.E-06	199
I-3	741.27	30.0	9.1	40.0	12.2	6.E-07	98
I-3	741.27	40.0	12.2	50.0	15.2	9.E-06	251
I-3	741.27	30.0	9.1	100.0	30.5	7.E-06	226
I-3	741.27	50.0	15.2	100.0	30.5	3.E-07	78
I-3	741.27	70.0	21.3	100.0	30.5	2.E-07	68
I-3	741.27	90.0	27.4	100.0	30.5	7.E-08	50
I-4	744.31	10.0	3.0	20.0	6.1	2.E-06	137
I-4	744.31	20.0	6.1	30.0	9.1	5.E-05	451
I-4	744.31	30.0	9.1	40.0	12.2	2.E-06	160
I-4	744.31	40.0	12.2	50.0	15.2	9.E-08	54
I-4	744.31	50.0	15.2	60.0	18.3	2.E-07	65
I-4	744.31	60.0	18.3	70.0	21.3	8.E-08	51
I-4	744.31	70.0	21.3	80.0	24.4	5.E-06	198
I-4	744.31	60.0	18.3	110.0	33.5	3.E-06	180
I-4	744.31	80.0	24.4	110.0	33.5	4.E-07	90
I-4	744.31	100.0	30.5	110.0	33.5	5.E-07	95
I-5	744.42	10.0	3.0	20.0	6.1	9.E-08	54

Table 4.1.4.2-1. Continued

Well	Elevation of top of casing (ft msl)	Depth to top seal of isolated zone (ft, BCT)	Depth to top seal of isolated zone (m, BCT)	Depth to bottom seal of isolated zone (ft, BCT)	Depth to bottom seal of isolated zone (m, BCT)	Transmissivity (m ² /s)	2b Fracture width (m x 10 ⁶)
I-5	744.42	20.0	6.1	30.0	9.1	2.E-07	70
I-5	744.42	30.0	9.1	40.0	12.2	2.E-07	68
I-5	744.42	40.0	12.2	50.0	15.2	8.E-07	111
I-5	744.42	50.0	15.2	60.0	18.3	4.E-06	187
I-5	744.42	60.0	18.3	70.0	21.3	4.E-07	86
I-5	744.42	70.0	21.3	80.0	24.4	2.E-06	145
I-5	744.42	80.0	24.4	90.0	27.4	8.E-06	239
I-5	744.42	70.0	21.3	120.0	36.6	8.E-06	237
I-5	744.42	90.0	27.4	120.0	36.6	5.E-07	94
I-5	744.42	90.0	27.4	120.0	36.6	3.E-07	79
I-5	744.42	110.0	33.5	120.0	36.6	1.E-06	121
I-6	744.79	10.0	3.0	20.0	6.1	4.E-08	42
I-6	744.79	20.0	6.1	30.0	9.1	1.E-07	60
I-6	744.79	30.0	9.1	40.0	12.2	3.E-06	181
I-6	744.79	40.0	12.2	50.0	15.2	8.E-06	243
I-6	744.79	50.0	15.2	60.0	18.3	3.E-08	39
I-6	744.79	50.0	15.2	60.0	18.3	2.E-08	30
I-6	744.79	40.0	12.2	110.0	33.5	9.E-06	251
I-6	744.79	60.0	18.3	110.0	33.5	6.E-07	100
I-6	744.79	80.0	24.4	110.0	33.5	6.E-07	99
I-6	744.79	100.0	30.5	110.0	33.5	5.E-07	95
I-7	742.51	30.0	9.1	100.0	30.5	2.E-07	66
I-7	742.51	50.0	15.2	100.0	30.5	1.E-07	62
I-7	742.51	70.0	21.3	100.0	30.5	7.E-08	48
I-7	742.51	70.0	21.3	100.0	30.5	5.E-08	43
I-7	742.51	90.0	27.4	100.0	30.5	7.E-08	49
I-8	740.21	10.0	3.0	20.0	6.1	6.E-05	468
I-8	740.21	10.0	3.0	20.0	6.1	7.E-05	492
I-8	740.21	20.0	6.1	30.0	9.1	2.E-05	328
I-8	740.21	30.0	9.1	40.0	12.2	1.E-05	262
I-8	740.21	20.0	6.1	90.0	27.4	2.E-05	341

Table 4.1.4.2-1. Continued

Well	Elevation of top of casing (ft msl)	Depth to top seal of isolated zone (ft, BCT)	Depth to top seal of isolated zone (m, BCT)	Depth to bottom seal of isolated zone (ft, BCT)	Depth to bottom seal of isolated zone (m, BCT)	Transmissivity (m ² /s)	2b Fracture width (m x 10 ⁶)
I-8	740.21	40.0	12.2	90.0	27.4	4.E-07	88
I-8	740.21	60.0	18.3	90.0	27.4	2.E-07	74
I-8	740.21	80.0	24.4	90.0	27.4	3.E-07	79
I-9	740.24	10.0	3.0	20.0	6.1	6.E-06	213
I-9	740.24	20.0	6.1	30.0	9.1	5.E-06	209
I-9	740.24	20.0	6.1	30.0	9.1	5.E-06	198
I-9	740.24	30.0	9.1	40.0	12.2	6.E-08	48
I-9	740.24	20.0	6.1	90.0	27.4	3.E-06	168
I-9	740.24	40.0	12.2	90.0	27.4	6.E-07	103
I-9	740.24	60.0	18.3	90.0	27.4	7.E-07	103
I-9	740.24	80.0	24.4	90.0	27.4	2.E-07	73
EX-1	740.11	10.0	3.0	20.0	6.1	1.E-05	270
EX-1	740.11	20.0	6.1	30.0	9.1	3.E-05	383
EX-1	740.11	30.0	9.1	40.0	12.2	3.E-05	357
EX-1	740.11	40.0	12.2	50.0	15.2	7.E-07	106
EX-1	740.11	30.0	9.1	80.0	24.4	2.E-05	348
EX-1	740.11	50.0	15.2	80.0	24.4	5.E-07	98
EX-1	740.11	70.0	21.3	80.0	24.4	8.E-07	110
EX-2	740.63	15.0	4.6	25.0	7.6	2.E-05	295
EX-2	740.63	25.0	7.6	35.0	10.7	2.E-06	137
EX-2	740.63	25.0	7.6	35.0	10.7	1.E-06	135
EX-2	740.63	35.0	10.7	45.0	13.7	3.E-07	84
EX-2	740.63	45.0	13.7	55.0	16.8	2.E-07	69
EX-2	740.63	55.0	16.8	65.0	19.8	2.E-07	74
EX-2	740.63	65.0	19.8	75.0	22.9	3.E-06	171
EX-3	740.42	25.0	7.6	35.0	10.7	3.E-07	82
EX-3	740.42	35.0	10.7	45.0	13.7	1.E-05	256
EX-3	740.42	25.0	7.6	75.0	22.9	1.E-05	273
EX-3	740.42	45.0	13.7	75.0	22.9	6.E-07	101
EX-3	740.42	65.0	19.8	75.0	22.9	6.E-07	98
EX-4	741.77	10.0	3.0	20.0	6.1	2.E-06	153

Table 4.1.4.2-1. Continued

Well	Elevation of top of casing (ft msl)	Depth to top seal of isolated zone (ft, BCT)	Depth to top seal of isolated zone (m, BCT)	Depth to bottom seal of isolated zone (ft, BCT)	Depth to bottom seal of isolated zone (m, BCT)	Transmissivity (m ² /s)	2b Fracture width (m x 10 ⁶)
EX-4	741.77	20.0	6.1	30.0	9.1	4.E-06	193
EX-4	741.77	20.0	6.1	30.0	9.1	4.E-06	193
EX-4	741.77	30.0	9.1	40.0	12.2	9.E-07	115
EX-4	741.77	40.0	12.2	50.0	15.2	5.E-07	93
EX-4	741.77	50.0	15.2	60.0	18.3	4.E-06	183
EX-4	741.77	60.0	18.3	70.0	21.3	4.E-06	185
EX-4	741.77	70.0	21.3	100.0	30.5	1.E-07	61
EX-4	741.77	90.0	27.4	100.0	30.5	2.E-07	64
JBW-7814	739.79	13.0	4.0	56.0	17.1	6.E-07	99
JBW-7814	739.79	26.0	7.9	56.0	17.1	4.E-07	91
JBW-7814	739.79	46.0	14.0	56.0	17.1	2.E-07	69
JBW-7815	739.48	12.0	3.7	22.0	6.7	2.E-06	152
JBW-7815	739.48	18.0	5.5	28.0	8.5	4.E-06	190
JBW-7815	739.48	28.0	8.5	38.0	11.6	4.E-08	41
JBW-7815	739.48	38.0	11.6	48.0	14.6	4.E-08	39
JBW-7816	740.89	15.0	4.6	25.0	7.6	2.E-07	75
JBW-7816	740.89	25.0	7.6	35.0	10.7	7.E-07	108
JBW-7816	740.89	35.0	10.7	45.0	13.7	3.E-07	84
JBW-7816	740.89	45.0	13.7	55.0	16.8	1.E-06	127
JBW-7816	740.89	55.0	16.8	65.0	19.8	7.E-07	108
JBW-7817A	744.30	12.0	3.7	22.0	6.7	2.E-06	162
JBW-7817A	744.30	18.0	5.5	28.0	8.5	8.E-06	237

Table 4.1.4.2-1. Continued

Well	Elevation of top of casing (ft msl)	Depth to top seal of isolated zone (ft, BCT)	Depth to top seal of isolated zone (m, BCT)	Depth to bottom seal of isolated zone (ft, BCT)	Depth to bottom seal of isolated zone (m, BCT)	Transmissivity (m ² /s)	2b Fracture width (m x 10 ⁶)
JBW-7817A	744.30	28.0	8.5	38.0	11.6	9.E-06	249
JBW-7817A	744.30	38.0	11.6	48.0	14.6	7.E-07	104
JBW-7817A	744.30	48.0	14.6	58.0	17.7	3.E-07	84
JBW-7817A	744.30	58.0	17.7	68.0	20.7	1.E-06	125
JBW-7817A	744.30	68.0	20.7	78.0	23.8	1.E-06	129
JBW-7817A	744.30	78.0	23.8	88.0	26.8	3.E-07	84
JBW-7817A	744.30	88.0	26.8	98.0	29.9	2.E-06	139
JBW-7817A	744.30	88.0	26.8	98.0	29.9	6.E-07	98
JBW-7817A	744.30	68.0	20.7	98.0	29.9	3.E-06	173
JBW-7817B	744.19	13.0	4.0	23.0	7.0	8.E-07	111
JBW-7817B	744.19	18.0	5.5	28.0	8.5	1.E-06	123
JBW-7817B	744.19	28.0	8.5	38.0	11.6	3.E-06	166
JBW-7817B	744.19	28.0	8.5	38.0	11.6	3.E-06	162
VEA-1	741.29	28	8.5	38	11.6	3.E-06	178
VEA-1	741.29	35	10.7	45	13.7	1.E-05	285
VEA-1	741.29	45	13.7	55	16.8	5.E-07	96
VEA-1	741.29	55	16.8	65	19.8	5.E-07	98
VEA-1	741.29	65	19.8	75	22.9	7.E-07	104
VEA-1	741.29	55	16.8	105	32.0	5.E-06	199
VEA-1	741.29	55	16.8	105	32.0	5.E-06	200
VEA-1	741.29	75	22.9	105	32.0	4.E-07	85
VEA-1	741.29	95	29.0	105	32.0	6.E-07	98
VEA-2	740.46	15.0	4.6	25.0	7.6	5.E-06	201

Table 4.1.4.2-1. Continued

Well	Elevation of top of casing (ft msl)	Depth to top seal of isolated zone (ft, BCT)	Depth to top seal of isolated zone (m, BCT)	Depth to bottom seal of isolated zone (ft, BCT)	Depth to bottom seal of isolated zone (m, BCT)	Transmissivity (m ² /s)	2b Fracture width (m x 10 ⁶)
VEA-2	740.46	20.0	6.1	30.0	9.1	3.E-07	79
VEA-2	740.46	30.0	9.1	40.0	12.2	6.E-05	463
VEA-2	740.46	40.0	12.2	50.0	15.2	4.E-07	87
VEA-2	740.46	30.0	9.1	120.0	36.6	5.E-05	451
VEA-2	740.46	30.0	9.1	120.0	36.6	7.E-05	500
VEA-2	740.46	50.0	15.2	120.0	36.6	3.E-07	80
VEA-2	740.46	70.0	21.3	120.0	36.6	4.E-07	88
VEA-2	740.46	90.0	27.4	120.0	36.6	8.E-07	109
VEA-2	740.46	110.0	33.5	120.0	36.6	1.E-06	129
VEA-3	775.74	44.0	13.4	54.0	16.5	3.E-05	359
VEA-3	775.74	50.0	15.2	60.0	18.3	4.E-05	400
VEA-3	775.74	60.0	18.3	70.0	21.3	3.E-07	81
VEA-3	775.74	60.0	18.3	70.0	21.3	2.E-07	69
VEA-3	775.74	70.0	21.3	80.0	24.4	9.E-08	53
VEA-3	775.74	80.0	24.4	90.0	27.4	2.E-07	74
VEA-3	775.74	90.0	27.4	100.0	30.5	3.E-07	75
VEA-3	775.74	100.0	30.5	110.0	33.5	4.E-07	85
VEA-3	775.74	110.0	33.5	120.0	36.6	5.E-06	205
VEA-3	775.74	100.0	30.5	150.0	45.7	1.E-05	283
VEA-3	775.74	120.0	36.6	150.0	45.7	8.E-07	112
VEA-3	775.74	140.0	42.7	150.0	45.7	1.E-06	123
VEA-4	739.80	16.0	4.9	26.0	7.9	2.E-05	332
VEA-4	739.80	20.0	6.1	30.0	9.1	1.E-05	279
VEA-4	739.80	16.0	4.9	100.0	30.5	3.E-05	362
VEA-4	739.80	30.0	9.1	100.0	30.5	1.E-06	124
VEA-4	739.80	50.0	15.2	100.0	30.5	8.E-07	109
VEA-4	739.80	70.0	21.3	100.0	30.5	3.E-07	78
VEA-4	739.80	90.0	27.4	100.0	30.5	6.E-07	103
VEA-5	743.26	15.0	4.6	25.0	7.6	3.E-06	172
VEA-5	743.26	20.0	6.1	30.0	9.1	3.E-06	178
VEA-5	743.26	30.0	9.1	40.0	12.2	3.E-06	180

Table 4.1.4.2-1. Continued

Well	Elevation of top of casing (ft msl)	Depth to top seal of isolated zone (ft, BCT)	Depth to top seal of isolated zone (m, BCT)	Depth to bottom seal of isolated zone (ft, BCT)	Depth to bottom seal of isolated zone (m, BCT)	Transmissivity (m ² /s)	2b Fracture width (m x 10 ⁶)
VEA-5	743.26	40.0	12.2	50.0	15.2	4.E-06	193
VEA-5	743.26	50.0	15.2	60.0	18.3	4.E-07	90
VEA-5	743.26	60.0	18.3	70.0	21.3	4.E-06	185
VEA-5	743.26	60.0	18.3	70.0	21.3	4.E-06	192
VEA-5	743.26	70.0	21.3	80.0	24.4	3.E-06	171
VEA-5	743.26	80.0	24.4	90.0	27.4	6.E-08	46
VEA-5	743.26	70.0	21.3	120.0	36.6	4.E-06	187
VEA-5	743.26	90.0	27.4	120.0	36.6	1.E-06	134
VEA-5	743.26	110.0	33.5	120.0	36.6	2.E-06	151
VEA-6	739.82	30.0	9.1	100.0	30.5	7.E-08	50
VEA-6	739.82	50.0	15.2	100.0	30.5	2.E-07	68
VEA-6	739.82	50.0	15.2	100.0	30.5	4.E-07	85
VEA-6	739.82	70.0	21.3	100.0	30.5	1.E-08	29
VEA-6	739.82	90.0	27.4	100.0	30.5	8.E-07	109
VEA-7	740.81	25.0	7.6	35.0	10.7	7.E-06	231
VEA-7	740.81	25.0	7.6	35.0	10.7	1.E-05	257
VEA-7	740.81	35.0	10.7	45.0	13.7	4.E-07	84
VEA-7	740.81	25.0	7.6	115.0	35.1	7.E-06	231
VEA-7	740.81	45.0	13.7	115.0	35.1	9.E-07	116
VEA-7	740.81	65.0	19.8	115.0	35.1	1.E-07	59
VEA-7	740.81	85.0	25.9	115.0	35.1	3.E-07	82
VEA-7	740.81	105.0	32.0	115.0	35.1	1.E-06	120
VEA-8	740.48	10.0	3.0	125.0	38.1	9.E-06	250
VEA-8	740.48	15.0	4.6	125.0	38.1	4.E-08	42
VEA-8	740.48	15.0	4.6	125.0	38.1	4.E-08	42
VEA-8	740.48	35.0	10.7	125.0	38.1	2.E-07	67
VEA-8	740.48	55.0	16.8	125.0	38.1	1.E-07	62
VEA-8	740.48	75.0	22.9	125.0	38.1	1.E-07	58
VEA-8	740.48	95.0	29.0	125.0	38.1	3.E-07	81
VEA-8	740.48	115.0	35.1	125.0	38.1	8.E-07	112
VEA-9	740.81	15.0	4.6	25.0	7.6	4.E-06	196

Table 4.1.4.2-1. Continued

Well	Elevation of top of casing (ft msl)	Depth to top seal of isolated zone (ft, BCT)	Depth to top seal of isolated zone (m, BCT)	Depth to bottom seal of isolated zone (ft, BCT)	Depth to bottom seal of isolated zone (m, BCT)	Transmissivity (m ² /s)	2b Fracture width (m x 10 ⁶)
VEA-9	740.81	25.0	7.6	35.0	10.7	2.E-06	161
VEA-9	740.81	35.0	10.7	45.0	13.7	8.E-08	50
VEA-9	740.81	45.0	13.7	115.0	35.1	2.E-05	302
VEA-9	740.81	45.0	13.7	55.0	16.8	2.E-05	317
VEA-9	740.81	45.0	13.7	55.0	16.8	2.E-05	321
VEA-9	740.81	55.0	16.8	65.0	19.8	2.E-08	31
VEA-9	740.81	65.0	19.8	115.0	35.1	3.E-08	38
VEA-9	740.81	85.0	25.9	115.0	35.1	2.E-08	30
VEA-9	740.81	105.0	32.0	115.0	35.1	2.E-07	73

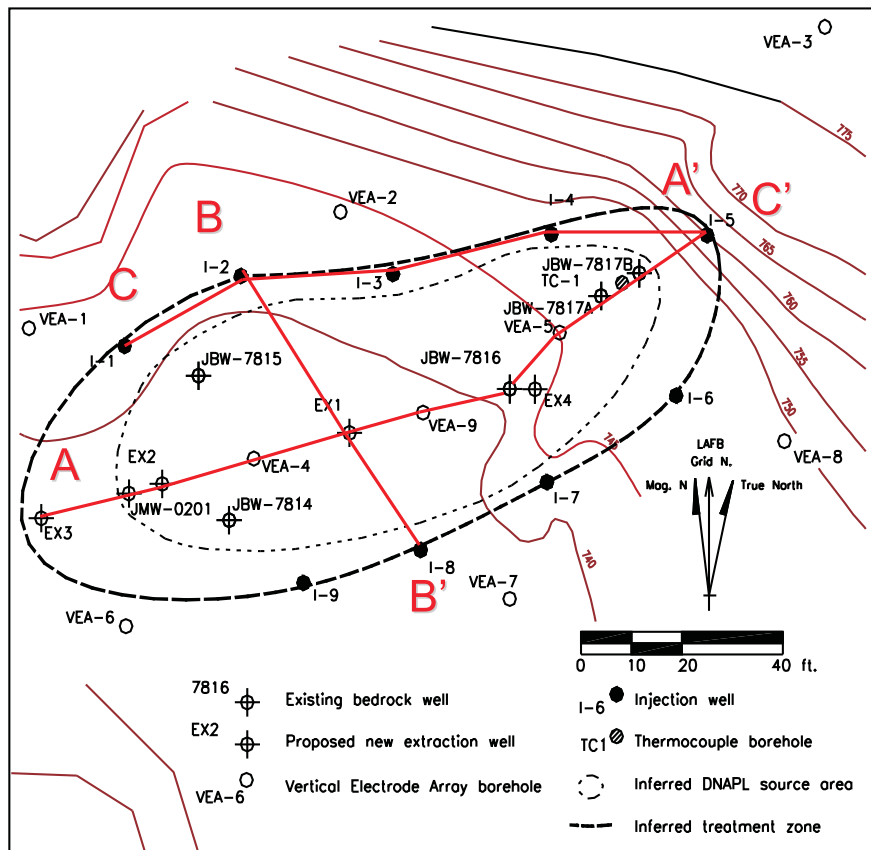
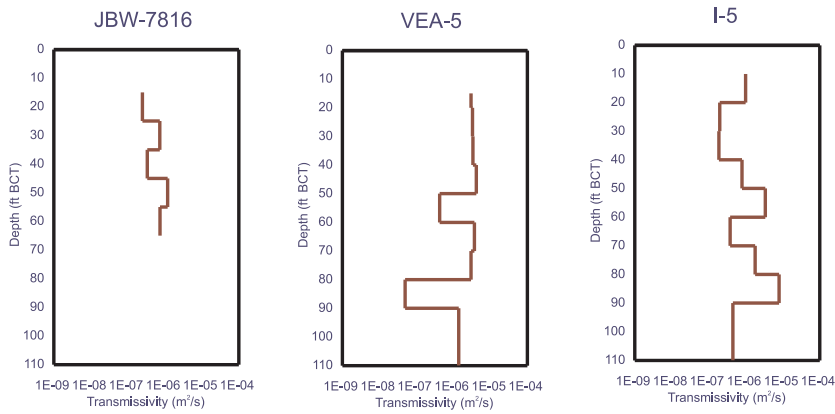
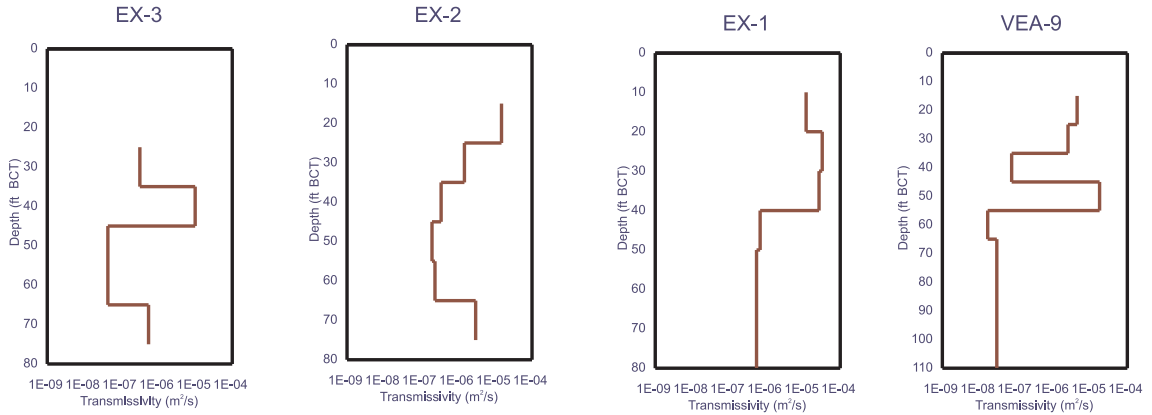


Figure 4.1.4.2-1. Location of wells and cross-section plotted in Figure 4.1.4.2-2 to Figure 4.1.4.2-4.

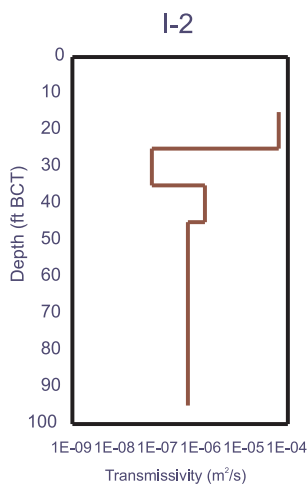
A



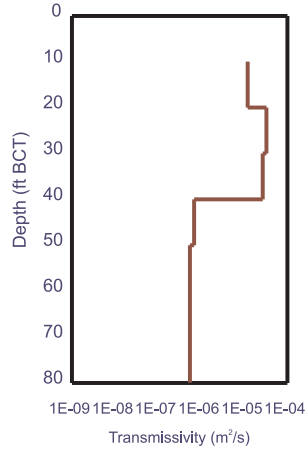
A'

Figure 4.1.4.2-2. Transmissivity versus depth profiles for wells along central axis of site.

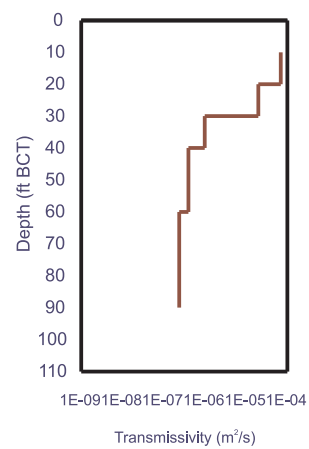
B



EX-1



I-8



B'

Figure 4.1.4.2-3. Transmissivity versus depth profiles for wells in central part of site. These wells lie on a cross-section approximately parallel to the strike of bedding at the site.

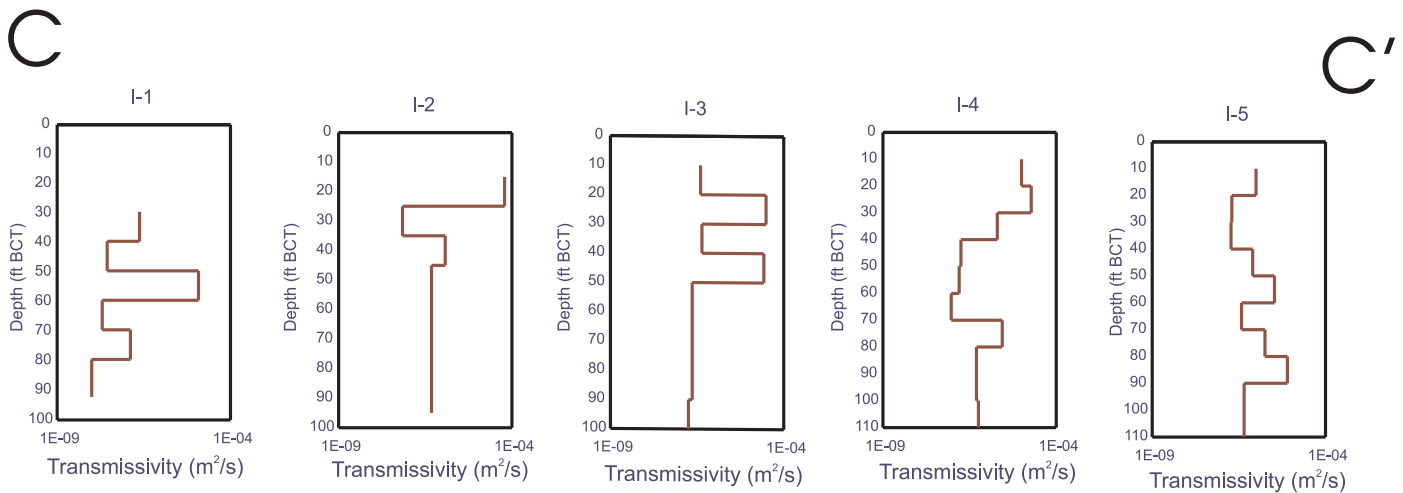


Figure 4.1.4.2-4. Transmissivity versus depth profiles of wells on northern edge of site.

4.1.5. Deep Monitoring Wells

Although detailed on-site information was collected during the initial site characterization for the research project, still very little was known about the off-site migration of aqueous-phase contamination. Very high solvent concentrations are observed in the source area; however, a monitoring well (JBW-7812B) which lies directly south of the target area by approximately 46 meters (150 feet), in what was thought to be the path of the aqueous phase plume, shows only low concentrations.

To assist in the development of a detailed conceptual model and to evaluate the potential for off-site and vertical migration of contaminants or steam, three additional boreholes were drilled in November and December 2001 around the periphery of the proposed steam footprint. The specific objectives of the boreholes are as follows:

1. Detection of vertically-downward and lateral migration of NAPL or aqueous phase contaminants during and after steam injection (Objective S2 of the SITE program).
2. A preliminary estimate of the reduction in off-site aqueous-phase migration (if the downgradient plume was intercepted by one of the wells).

The second objective above was not included in the SITE program evaluation because the lack of an understanding of migration pathways and concentrations prior to the initiation of this research project precluded being able to define changes in offsite migration within the budget and timeframe available. Also, it was recognized that there will be very large uncertainty in any assessment of aqueous-phase migration with the limited number of wells that could be installed with the available funding.

4.1.5.1. Drilling

The boreholes were located in the vicinity of the steam footprint as illustrated in Figure 4.1.5.1-1. The location of each borehole was determined on the basis of proximity to the steam footprint, the potential to intersect bedding plane or axial plane fractures, and the potential to intersect DNAPL or aqueous phase contamination. Two of the boreholes were drilled at 55 degrees from the horizontal (SM-1 and SM-2), and one (SM-3) was drilled in the vertical orientation. The boreholes were drilled using a diamond coring rig with an HQ coring bit, which leaves a borehole 0.1 meters (0.33 feet) in diameter. Double tube retrieval via wireline was used to collect core. Each coring run was 3 meters (10 feet). Drilling water was obtained from the pond in the lower tier (yearly water samples from this pond show that VOCs concentrations are below MCLs). An HW drill collar was used in each borehole. The core was logged immediately following retrieval. The core was logged exclusively for open fractures and features important to ground water flow and contaminant migration. The core logs are included in Appendix B.

In general, weathered open fractures were predominantly found only in the upper 30 meters (100 feet) of each borehole. SM-2 was particularly tight to a depth of 64 meters (210 feet) bgs, as drill water was not lost until drilling had reached a depth of 66.4 meters (218 feet) bgs. Large sections of each of the boreholes were observed to have very few fractures, and this was particularly true in the bottom 30 meters (100 feet) of SM-3. Most of the fractures observed were of bedding plane origin; however, vertical fractures were also observed.

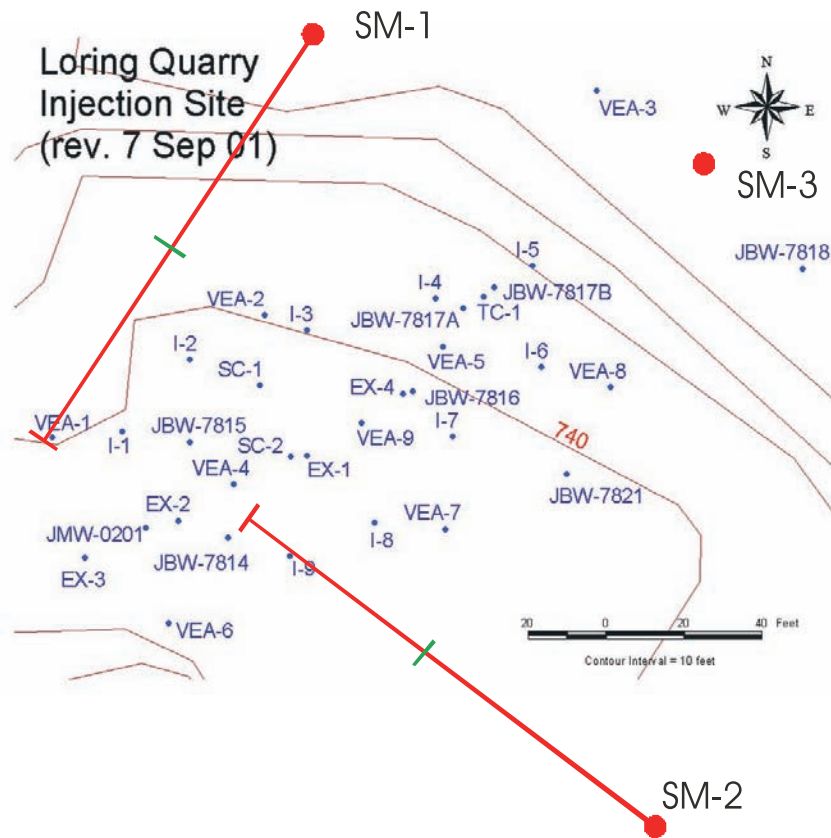


Figure 4.1.5.1-1. Location and orientation of the deeper boreholes constructed around the periphery of the steam footprint. Boreholes SM-1 and SM-2 are inclined at approximately 55 degrees. The tick mark illustrates the point along the borehole projection at which the borehole exceeds the depth of the other boreholes on site.

4.1.5.2. Well Installation and Hydraulic Testing

Immediately following borehole completion (i.e., within 1-3 days), Solinst multi-level casing was installed in each borehole. In each case, the casing design included five isolated intervals of varying lengths. The casing intervals were designed to isolate likely features of significance to the ground water flow system as determined from the core log. The packer elements used to isolate each interval were located over sections of intact, unfractured rock, to provide good seals between intervals. Installation of the casing was conducted manually. Each interval is accessed via 0.016 meters (0.05 feet) outer diameter tubing. A summary of each of the isolated intervals in each of the wells is provided in Table 4.1.5.2-1. The uppermost interval includes the water table.

Water levels were obtained a few weeks after the casing installation, which allowed for seating of the packer elements and equilibration with formation pressures. Figure 4.1.5.2-1 is a plot of hydraulic head versus elevation for each isolated interval. This figure shows that in all cases, vertical flow is downward from the surface. Large vertical gradients exist in each of the wells, indicating zones of low permeability that likely hinder downward movement of ground water and contaminants. The low permeability zone appears to exist at an elevation of approximately 210.3 meters (690 feet) above mean sea level (msl) in SM-2, and around 192 to 198 meters (630 to 650 feet) above msl in SM-1 and SM-3. The very similar hydraulic heads measured at depth in SM-1 and SM-2 indicate good hydraulic connection at this depth in the north-south direction; however, the interconnection to the east at SM-3 is not as strong.

To determine the hydraulic properties of the fractures and fracture zones isolated by the casing intervals, slug tests were conducted in all intervals with the exception of the uppermost in each well. It was assumed (and verified by one test) that the presence of the free surface in the upper interval would limit the ability to measure water flow into the interval (i.e., rendering the hydraulic conductivity too high to measure). The slug tests were conducted by introducing one or more liters of water into the 0.016 meter (0.05 feet) tubing over a period of a minute or less. The recovery of the water level in the tubing was subsequently measured over time. Interpretation of these tests was conducted using the standard Hvorslev method (Butler, 1998). In some cases, the recovery of the water level was too rapid to measure. In this case, an extended slug test was conducted by introducing several liters of water over a period of 4-6 minutes. The response in water level following this procedure was interpreted using the steady-state approximation, where the volume of water injected is interpreted as the volume of water which declines in the tubing over time. This interpretive method is well-accepted and provides estimates of conductivity similar to the Hvorslev method.

Table 4.1.5.2-1. Summary of Casing Intervals for SM-1, SM-2, and SM-3

Well	Port No.	Interval Depth/Length (meters)	Interval Depth/Length (feet)	Elevation (meters msl)	Elevation (feet msl)
SM-1	1	76.2-65.4	250.0-214.5	174.2-183.1	571.6-600.6
	2	64.5-54.6	211.5-179.0	183.8-191.9	603.1-629.7
	3	53.6-36.7	176.0-120.5	192.7-206.6	632.2-677.7
	4	35.8-20.7	117.5-68.0	207.3-219.7	680.1-720.7
	5	19.8-water table	65.0-water table	220.4-221.2	723.1-725.8
SM-2	1	70.1-65.4	230.0-214.5	168.8-142.2	553.7-566.4
	2	64.5-53.6	211.5-176.0	173.4-182.3	568.9-598.0
	3	52.7-36.7	173.0-120.5	183.0-196.1	600.4-643.4
	4	35.8-18.9	117.5-62.0	196.9-210.7	645.9-691.3
	5	18.0-water table	59.0-water table	211.5-223.5	693.8-733.4
SM-3	1	64.6-54.7	212.0-179.5	172.8-182.7	567.0-599.5
	2	53.8-39.3	176.5-129.0	183.6-198.1	602.5-650.0
	3	38.4-23.9	126.0-78.5	199.0-213.5	653.0-700.5
	4	23.0-18.6	75.5-61.0	214.4-218.8	703.5-718.0
	5	17.7-water table	58.0-water table	219.8-224.4	721.0-736.1

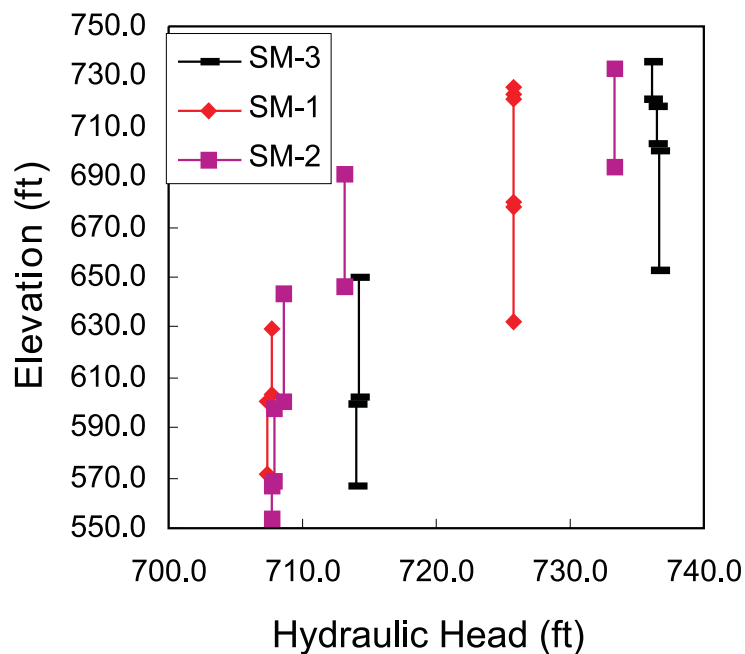


Figure 4.1.5.2-1. Hydraulic head with respect to elevation in each borehole.

The results of the transmissivity testing are shown in Figure 4.1.5.2-2. The variability in transmissivity in these boreholes is similar to the variability found in the process boreholes. It is difficult to relate what is observed in the core logs to the measurements of transmissivity in the boreholes. SM-1 exhibits relatively high transmissivity at shallow depths, and much lower transmissivity in the lower 21.3 meters (70 feet). The decrease in transmissivity at depth coincides with the decrease in hydraulic head. SM-2 exhibits the opposite pattern of transmissivity versus depth, with low transmissivity in the upper 15 meters (50 feet) and higher transmissivity in the lower regions. More uniform transmissivity is observed in SM-3, although there is still a tendency for the transmissivity to decrease with depth. Large sections of the cores for this borehole appeared to be unfractured; however, hydraulic testing shows the borehole to be of moderate-to-high transmissivity. The broken core zone at the bottom of the borehole that appeared to be unweathered and showed no evidence of ground water flow must be the permeable feature that gives rise to the moderately high transmissivity value observed at this depth.

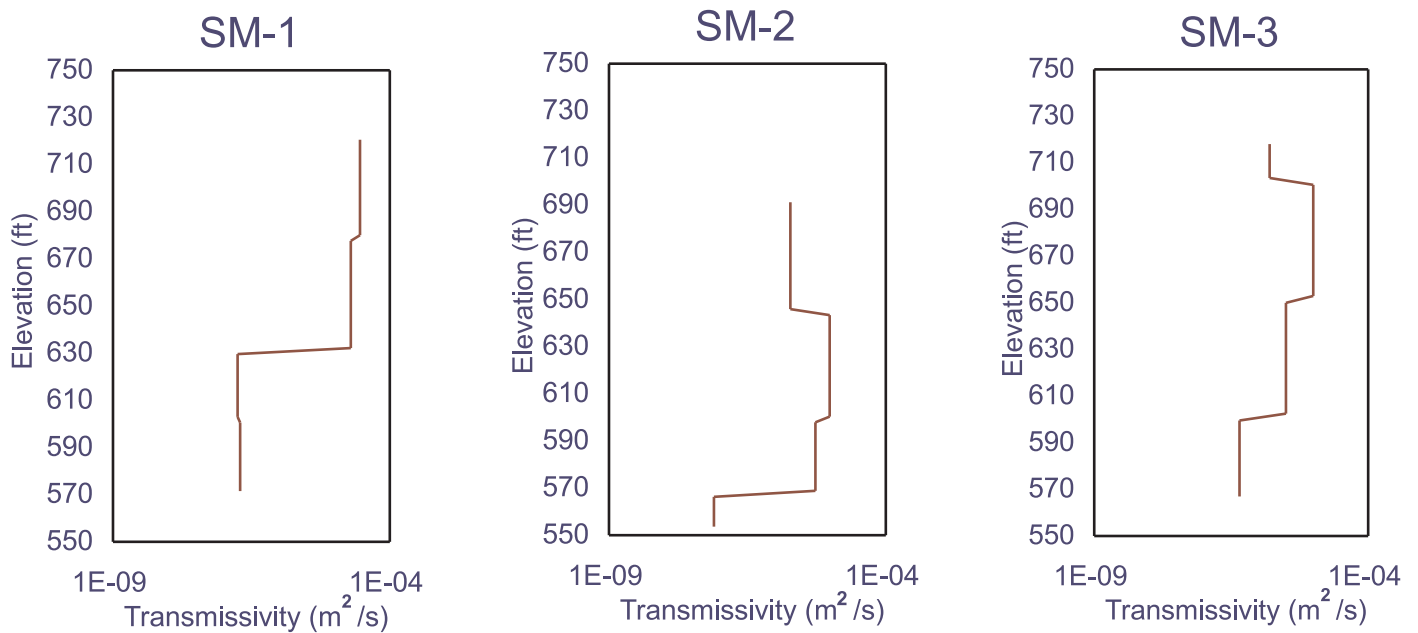


Figure 4.1.5.2-2. Transmissivity with respect to elevation in each deep borehole.

4.1.6. Interconnectivity Testing

The objective of the interconnectivity study is to locate the primary fractures that will carry steam between the proposed injection and extraction wells (and potentially to off-site locations) and to establish the degree of interconnectivity along these fracture pathways. The interconnectivity testing was used to determine if the initial arrangement of injection and extraction wells was viable and if the duration of heating would be sufficient for the purpose of the project. The results when compared to the direct measurement of steam and heat transport would also aid in determining the degree of characterization necessary in the design of injection and extraction well arrays for SER in fractured rock systems. The deep monitoring wells were not included in the interconnectivity testing due to difficulties with installing pressure transducers of sufficient sensitivity in these wells.

4.1.6.1. Methods

To measure fracture interconnectivity and to determine which fractures conduct the majority of the ground water flow, hydraulic measurements were conducted where an isolated interval is pressurized in one borehole, and the response is observed in another. The most efficient means by which to conduct these hydraulic tests is based on the pulse interference test method (Novakowski, 1989). The pulse interference test is conducted by producing a slug test condition or constant pressure test condition in one hole and observing the response in another.

As a result of the unavailability of some equipment at the beginning of the field study, the investigation was conducted in phases where different geometric configurations for the isolated intervals in the source and observation wells were used for each phase. A total of six phases were conducted.

The majority of testing (Phases 1 through 5) was conducted using the slug test method. Figure 4.1.6.1-1 illustrates the configuration that was used for the source and observation wells. The slug was generated by introducing a volume of water sufficient to raise the water level in the standpipe above natural, static levels. A pressure transducer was used to monitor the change in hydraulic head with respect to time in both the source and observation wells. The response was observed in one packer-instrumented borehole (the observation well) during each test. Each test required about 45 minutes to complete. The testing configuration and specific geometry, including interwell separation, are provided in Appendix F for all five phases.

The testing conducted in Phase 6 involved the use of a pressurized source well. In this case, the test section is completely isolated (no standpipe) and water is injected under pressure for a short period of time (2-15 minutes). This generated a larger pulse than the slug source and, in consequence, could be observed over greater distances or through weaker interconnections.

In addition to the method described above, the response to the slug at two other observation points was monitored in open boreholes that were not instrumented with packers for several of the tests. This response was measured using a Telog pressure transducer system.

A Levellogger™ pressure transducer (200 kPa; 2 atm range) was used in the observation well for all tests. The source well was instrumented with a Druck™ pressure transducer (690 kPa; 6.8 atm range) for Phases 1 and 2 of testing and a Microgage™ transducer (345 kPa; 3.4 atm range) for Phases 3 through 6. All transducers were calibrated in the field to ensure the accuracy of results (Appendix F).

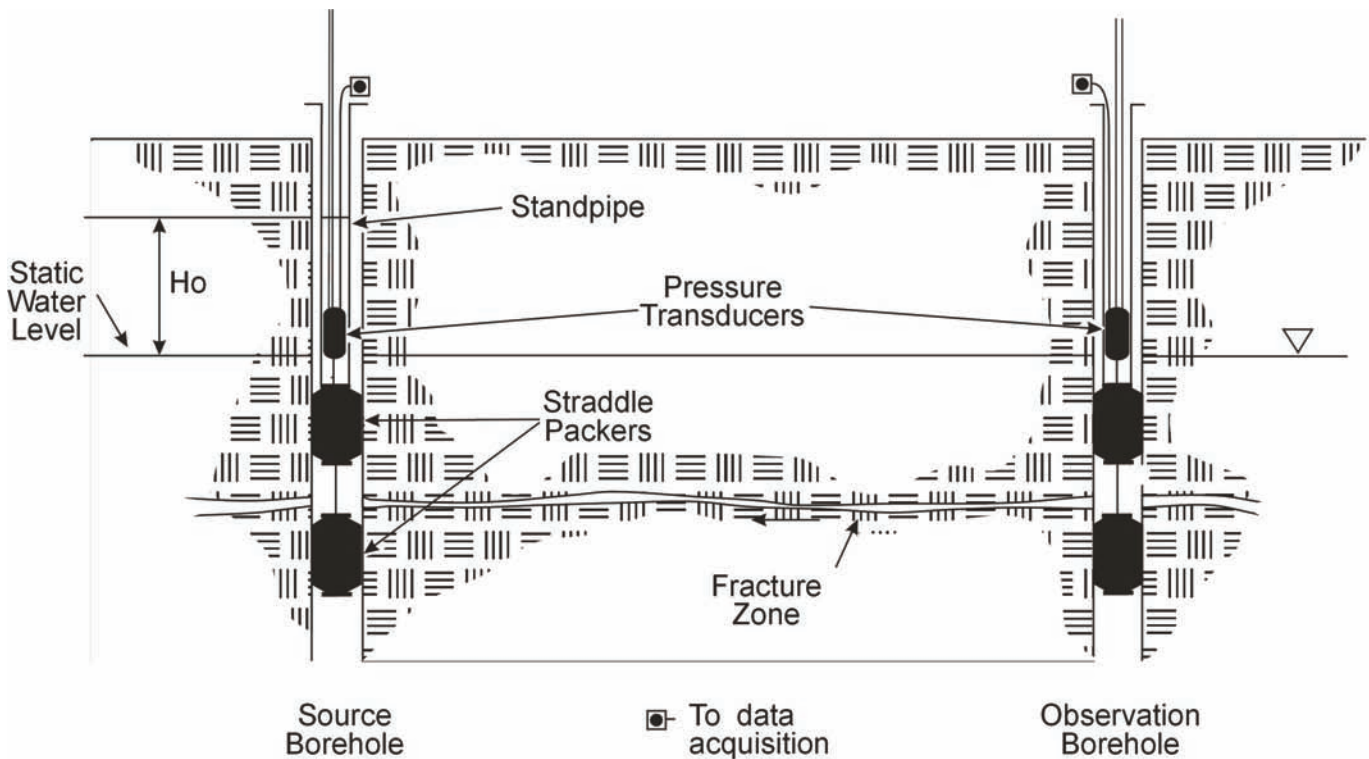


Figure 4.1.6.1-1. Schematic diagram of the apparatus used for the pulse interference tests conducted using the slug test format.

4.1.6.2. Results

Tests conducted using a slug source were interpreted using the graphical method developed by Novakowski (1989), and using a new analytical model developed by Stephenson and Novakowski (2004) (Appendix H). A total of 105 tests were conducted, 25 of which were interpreted using the graphical method while 10 were interpreted with the new model. The estimates of interwell transmissivity are provided in Appendix F (same as for the five phases above) for those test well pairs that showed a measurable response.

The graphical interpretation method requires a precise measurement of the peak value of the response in the observation well and the time lag between the start of the test and the time to the peak response in the observation well. This measurement was obtained using the Levelogger software that was used to operate the Levelogger pressure transducer. Figure 4.1.6.2-1 illustrates the source well and observation well response for a typical test result.

Phase 1 testing identified several interconnections between I-2 and I-3. These interconnections were thought to probably exist downdip along bedding plane fracture features. Some interconnection at greater depth between I-3 and I-4 was also identified. This interconnection was also considered to probably exist downdip along bedding plane fracture features. These tests were completed using a single packer in each well, preventing the determination of the exact depth at which these interconnections were made. Other interconnections were also identified between I-1 and EX-3 and I-2 and JBW-7815, while weak interconnection was found between I-1 and EX-1, and I-2 and EX-2.

Testing completed in Phase 2 identified a connection, considered to be downdip along bedding plane fractures, between I-1 and EX-1 at shallow depths.

Phase 3 testing showed strong connections at shallow depths between I-9 and EX-1, I-8 and EX-1, I-8 and I-9, and EX-1 and I-3. In addition, particularly significant connections were obtained for tests conducted between I-4 and I-5. These wells were found to be connected along a line corresponding to the dip of bedding at both shallow depths (6 to 15 meters; 20 to 50 feet) and at greater depths (15 to 24.4 meters; 50 to 80 feet). Because of these good interconnections, intervals at these depths within these wells were chosen as injection zones in the hope of driving mobilized contaminants up-dip to higher level extraction intervals in adjacent wells. Also, weak responses to testing (yielding non-analyzable data) were observed at depth between I-5 and I-6, I-4 and I-5, EX-1 and I-3, and I-9 and EX-4 in this phase of testing. A weak response, also with non-analyzable data, was observed indicating a connection at shallow depth between I-8 and I-9, and weak responses were also observed between I-9 and EX-4, and I-4 and EX-4.

Two Telog™ pressure transducers were used during this phase of testing to investigate the head response to pulse interference testing in open wells adjacent to the test wells. The results of this additional monitoring are presented in Appendix F.

In Phase 4 of the study, the interconnections between VEA-5 and other wells in the eastern area of the site were investigated. Interconnections between VEA-5 and I-4 at shallow and greater depths and I-5 at greater depths were observed. Based on these interconnections, VEA-5 was first used as an extraction well and then converted to an injection well. Only a weak connection was found to I-6, and no response was observed between VEA-5 and I-7 or EX-4. It should be noted that the location of fractures at depth in VEA-5 with connections to other wells cannot be constrained because the narrow diameter of this well (originally intended to contain an electrode for ERT) prevented use of a straddle packer.

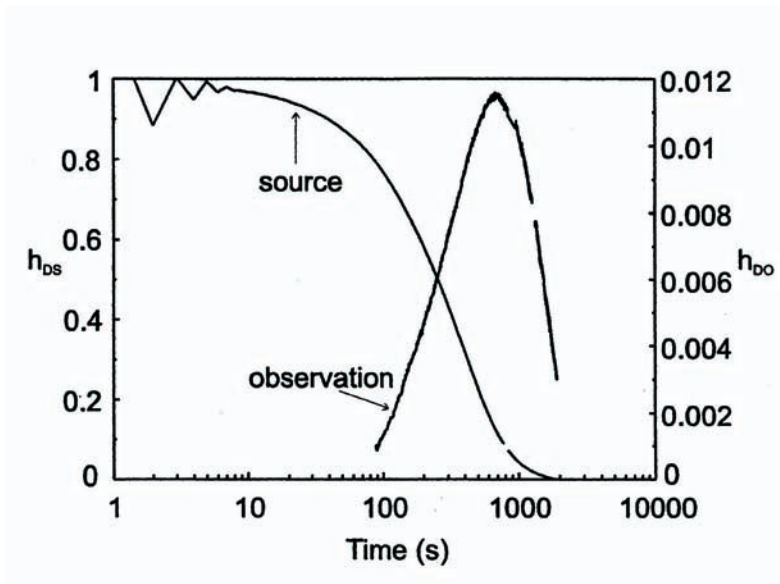


Figure 4.1.6.2-1. The source and observation response for an example pulse interference test. Both the responses are normalized against the initial rise in hydraulic head in the source well.

Phase 5 testing was conducted in order to better understand the nature of the interconnection between I-3 and I-4 that had been identified in Phase 1 testing and by the open-well Telog data collected during Phase 3. While the existence of a connection was confirmed, the location of the interconnected features could not be found and only a weak (non-analyzable) connection was identified between these well pairs. A weak connection was also found between EX-4 and I-6.

The pressurized tests conducted in Phase 6 showed that a possible connection exists between I-4, I-5, and EX-1. The connection is very weak and was found only after extended injection using the constant head apparatus.

During the testing program, open-well water level measurements were made whenever possible, and water levels relative to an arbitrary datum of 225.6 meters (740 feet) above msl have been calculated for wells that were part of the hydraulic testing study. These values are presented in Table 4.1.6.2-1. It was found that the Quarry could be divided into three discrete areas based on internally similar water level (equivalent to the hydraulic head) that stepped down from east to west across the site. Water level values were grouped according to area. The small range of water level elevations within each area indicated the existence of strong interconnection within each area.

Table 4.1.6.2-1. Water Level Measurements Relative to a Datum at 225.6 Meters (740 Feet) Above Mean Sea Level

Wells Lying Within the Western Area		Wells Lying Within the Central Area		Wells Lying Within the Eastern Area	
Borehole	Water Level, Meters Below Datum	Borehole	Water Level, Meters Below Datum	Borehole	Water Level, Meters Below Datum
I-1	9.51	I-2	4.39	EX-4	2.46
EX-3	9.58	I-3	4.35	I-6	2.44
		JBW - 7815	No Elevation Data	I-7	2.45
		EX-1	4.84	VEA - 7	2.46
		VEA-4	4.85	JBW-7817B	No Elevation Data
		JBW - 7814	No Elevation Data	I-4	2.51
		I-9	4.89	I-5	3.66
		I-8	4.89	TC-1	3.13
		EX-2	No Elevation Data	JBW 7817A	No Elevation Data
				VEA - 5	2.54
				JBW - 7816	No Elevation Data

The results of the pulse interference tests tended to define a strong correlation between similar water levels in two open wells and the detection of an interconnection during the pulse testing program. In general terms, it can be stated that more interconnections have been shown between boreholes within each of the areas defined by open-well water levels than between wells in adjacent areas. For the limited number of interconnections found between the eastern and central areas of the footprint, the interconnections were mostly made in the near-surface, highly fractured zone.

It was also apparent that, while some wells within the areas defined by open-well water levels were interconnected, several others showed little or no evidence of interconnection. It is surmised that these apparently hydrologically unconnected wells were located within blocks of rock that were not intersected by the same open bedding plane and vertical fractures that connected the other boreholes. These unconnected wells include EX-4 and I-7 in the eastern area, EX-2 in the central area, and EX-3 in the western area.

4.1.7. Ground Water Sampling

Ground water sampling was performed in boreholes within the treatment zone for evaluating changes in concentrations brought about by the steam injection (SITE Primary Objective P1). Ground water in the deep boreholes was sampled for the purpose of evaluating whether or not contaminants were moved laterally or vertically out of the treatment area by the steam injection (SITE Secondary Objective S2). Two rounds of pre-steam injection sampling were conducted.

4.1.7.1. Sampling of Treatment Area Boreholes

Samples for the purpose of determining changes in ground water quality due to steam injection were obtained only from boreholes that were expected to be used for injection or extraction, since monitoring wells would be grouted with the equipment needed for monitoring (i.e., electrodes and/or thermocouples) and thus, would not be available for sampling after steam injection. A couple of the existing boreholes within the target zone were also included in the sampling program. For the first round of sampling, the intent was to use a dual packer system to obtain ground water samples from 3-meter (10-foot) intervals of the boreholes where the transmissivity had been determined to be greater than $1.7 \times 10^{-6} \text{ m}^2/\text{s}$ ($1.8 \times 10^{-5} \text{ ft}^2/\text{s}$). Intervals with transmissivity less than this are not likely to yield ground water samples in a reasonable time, and thus were not slated for sampling. A few minor changes to this criteria were made to provide better coverage of all the injection and extraction wells. The transmissivity testing did not show any permeable intervals in well I-7; however, it was decided to attempt to obtain a sample from the entire depth of the well. Table 4.1.7.1-1 shows the intervals that were sampled for the first round of pre-treatment ground water sampling.

The approach of determining which intervals to sample based on transmissivity had some limitations, as much of the transmissivity at this site was determined to be at about the water table, while in many of the boreholes, the MERC data had shown that the contaminants were located in deeper fractures that were not necessarily very transmissive. For the second round of pre-steam injection ground water sampling, significant changes were made to provide more meaningful data from the samples obtained. These changes were made based on the results of the MERC sampling, the results of the first round of ground water sampling, and the transmissivity data. Table 4.1.7.1-1 also shows the intervals sampled for the second pre-treatment sampling round. During the second sampling round, a single packer was placed in the center of many of the wells, and a ground water sample was collected from both above and below the packer. In the table, the sampling intervals for these wells are given as “<15 meters” (50 feet) and “>15 meters” (50 feet).

Before the first round of pre-steam injection ground water sampling could be conducted, a few preliminary samples were obtained to determine if the iodine concentrations had returned to background levels, indicating that the drilling water was no longer within the target area. Samples obtained in September 2001 from a few locations were non-detect for iodine (detection limit 0.02 mg/l), thus the first round of samples were obtained in December 2001. Low flow sampling techniques were used to acquire all the samples from the target area wells. Before sampling, the depth to ground water was measured using an electronic water level indicator. The packer assembly (or a single packer) was then lowered into the borehole to the desired depth, and the packers were inflated with nitrogen. A Grundfos Redi Flo 2 (or equivalent) pump was lowered down the riser of the packer assembly to just above the top packer. Ground water was then purged from the isolated interval at a flow of 0.5 liters (0.13 gallons) per minute or less, while monitoring the water level to ensure that the water column did not fall below the top of the isolated interval. Once the drawdown stabilized, the purge water was monitored for pH, specific conductivity, dissolved oxygen, and temperature, and measurements were recorded every three to five minutes. Purging continued until readings stabilized. Ground water samples were then collected in VOA vials which were pre-preserved with hydrochloric acid, and shipped on ice to the laboratory for VOC analysis using EPA Method 8260B.

The results of the ground water sampling are shown in Table 4.1.7.1-2. PCE was the most common ground water contaminant found, and its concentration was greater than the MCL (0.005 mg/l) in all ground water samples from the target area. The highest concentrations of PCE were found in the 10.7 to 13.7 meters (35 to 45 feet) bgs depth of EX-3 (8.8 – 6.3 mg/l). This interval also had the highest TCE concentration (0.84 – 0.28 mg/l). Other intervals that had PCE concentrations greater than 0.1 mg/l during the pre-steam injection sampling were in EX-1, 3 – 6 meters (10 – 20 feet) bgs; EX-1, 6 – 9 meters (20 – 30 feet) bgs; EX-1, 9 – 12 meters (30 – 40 feet) bgs; EX-2, 19.8 – 23 meters (65 – 75 feet) bgs; EX-4, 3 – 6 meters (10 – 20 feet) bgs; and I-3, <15 meters (50 feet) and > 15 meters (50 feet) bgs. However, only the intervals EX-3, 10.7 to 13.7 meters (35 to 45 feet) bgs and EX-2, 19.8 – 23 meters (65 – 75 feet) bgs, had concentrations greater than 0.1 mg/l during both rounds of pre-steam injection sampling.

The concentrations in EX-1 and EX-4 decreased significantly between the December 2001 and April 2002 sampling rounds, and the concentrations in I-3 increased substantially over this same period. Other notable changes in concentration of PCE between the two sampling periods occurred in I-1, 15 – 18 meters (50 – 60 feet) bgs, where the concentration decreased from 0.091 to 0.020 mg/l; I-5, 24.4 – 27.4 meters (80 – 90 feet) bgs, where the concentration increased from 0.018 to 0.075 mg/l; and EX-4, 18 – 21 meters (60 – 70 feet) bgs, where the concentration decreased from 0.096 to 0.021 mg/l.

Table 4.1.7.1-1. Ground Water Sampling Intervals for Treatment Area Wells

	EX-1	EX-2	EX-3	EX-4	I-1	I-2	I-3	I-4	I-5	I-6	I-7	I-8	I-9	JBW-7817A	JBW-7817B	VEA-5
Intervals sampled in December 2001 (meters bgs)	3-6.1 6.1-9.1 9.1-12.2	4.6-7.6 19.8-22.9	10.7-13.7	3-6.1 6.1-9.1 15.2-18.3 18.3-21.3	15.2-18.3	10.7-13.7 12.2-15.2	6.1-9.1 9.1-12.2 21.3-24.4	15.2-18.3 24.4-27.4	9.1-12.2 12.2-15.2	3-30.5	3-6.1 6.1-9.1 9.1-12.2	6.1-9.1	3.7-6.7 26.8-29.9			
Intervals sampled in April 2002 (meters bgs)	<12.2 >12.2	4.6-7.6 19.8-22.9	10.7-13.7	3-6.1 18.3-21.3	15.2-18.3	<13.7 >13.7	<15 >15	21.3-24.4	24.4-27.4	12.2-15.2	3-30.5	<12.2 >12.2	6.1-9.1	26.8-29.9		
Post-treatment sampling intervals (meters bgs)	<12.2 >12.2	4.6-7.6 18.3-21.3	>12.2	3-6.1 6.1-9.1 15.2-18.3 18.3-21.3		<13.7 >13.7	<15 >15	21.3-33.5	21.3-33.5	9.1-15.2	23.5-27.4	14-17.4 17.4-28.3			3-11.1	3-21.3

Table 4.1.7.1-2. Pre-treatment Ground Water Sampling Results from Wells Within the Target Zone

Well I-1		
Interval, meters bgs	15.2-18.3	
Compounds/Date	Dec-01	Apr-02 ^a
Trichloroethylene	0.005J	0.0007J
Tetrachloroethylene	0.091	0.020
Total Xylenes		0.0001

Well I-2			
Interval, meters bgs	10.7-13.7	<13.7	>13.7
Compounds/Date	Dec-01	Apr-02 ^a	Apr-02 ^a
Trichloroethylene	0.002J	0.0017	0.0023J
Tetrachloroethylene	0.048	0.045	0.072

Well I-3			
Interval, meters bgs	12.2-15	<15	>15
Compounds/Date	Dec-01	Apr-02 ^a	Apr-02 ^a
Trichloroethylene	0.006	0.0032J	0.0046
Tetrachloroethylene	0.026	0.130	0.160

Well I-4				
Interval, meters bgs	6.1-9.1	9.1-12.2	21.3-24.4	
Compounds/Date	Dec-01	Dec-01	Dec-01	Apr-02 ^a
Acetone			0.300	
2-Butanone			0.025	
Chloroform				0.0033
Carbon Tetrachloride				0.0018
Benzene				0.0002J
Trichloroethylene	0.032	0.038	0.003J	0.0013
Tetrachloroethylene			0.023	0.0082

Well I-5			
Interval, meters bgs	15-18.3	24.4-27.4	
Compounds/Date	Dec-01	Dec-01	Apr-02 ^a
Chloroform	0.001J	0.001J	
Benzene	0.004J	0.005J	0.0034J
Trichloroethylene	0.002J	0.003J	0.0048J
Tetrachloroethylene	0.018	0.018	0.075
Ethyl Benzene	0.001J	0.001J	
Total Xylenes	0.005		
Styrene	0.003J		

Table 4.1.7.1-2. Continued

Well I-6				
Interval, meters bgs	9.1-12.2		12.2-15.2	
Compounds/Date	Dec-01	Dec-01 ^d	Dec-01	Apr-02 ^a
Methylene Chloride		0.001J		
Chloroform	0.002J	0.002J	0.002J	
Trichloroethylene	0.003J	0.002J	0.002J	0.0021J
Tetrachloroethylene	0.023	0.020	0.021	0.030

Well I-7		
Interval, meters bgs	>30.5 ^b	
Compounds/Date	Dec-01	Apr-02 ^a
cis-1,2-Dichloroethylene		0.0001J
Chloroform	0.003J	0.002
Trichloroethylene	0.004J	0.0017
Tetrachloroethylene	0.016	0.0074

Well I-8					
Interval, meters bgs	3-6.1	6.1-9.1	9.1-12.2	<12.2	>12.2
Compound/Date	Dec-01	Dec-01	Dec-01	Apr-02 ^a	Apr-02 ^a
Acetone	0.014	0.074			
Methylene Chloride		0.001J			
Trichloroethylene	0.004J		0.002J	0.0014	0.002
Toluene					0.0001J
Tetrachloroethylene	0.040	0.010	0.026	0.013	0.024

Well I-9		
Interval, meters bgs	6.1-9.1	
Compound/Date	Dec-01	Apr-02 ^a
Trichloroethylene	0.003	0.0009J
Tetrachloroethylene	0.047	0.013

Well EX-1						
Interval, meters bgs	3-6.1	6.1-9.1	9.1-12.2		<12.2	>12.2
Compound/Date	Dec-01	Dec-01	Dec-01	Dec-01 ^d	Apr-02 ^a	Apr-02 ^a
Chloroform			0.002J	0.002J		
Trichloroethylene	0.008	0.010	0.008	0.007	0.0007J	0.0009J
Tetrachloroethylene	0.100	0.120	0.150	0.140	0.0087J	0.015

Table 4.1.7.1-2. Continued

Well EX-2				
Interval, meters bgs	4.6-7.6		19.8-22.9	
Compound/Date	Dec-01	Apr-02 ^a	Dec-01	Apr-02 ^a
trans-1,2-Dichloroethylene			0.002	
cis-1,2-Dichloroethylene				0.0045J
Chloroform	0.001J		0.003J	
Trichloroethylene	0.004J	0.0011J	0.014	0.014J
Tetrachloroethylene	0.091	0.0235	0.220	0.250

Well EX-3		
Interval, meters bgs	10.7-13.7	
Compound/Date	Dec-01	Apr-02 ^a
trans-1,2-Dichloroethylene	0.045	
Chloroform	0.008	
Benzene	0.017	
Trichloroethylene	0.84	0.28
Tetrachloroethylene	8.80	6.30
Ethyl Benzene	0.001J	
Total Xylenes	0.014	
1,1,2,2-Tetrachloroethane	0.002J	

Well EX-4						
Interval, meters bgs	3-6.1		6.1-9.1	15-18.3	18.3-21.3	
Compound/Date	Dec-01	Apr-02 ^a	Dec-01	Dec-01	Dec-01	Apr-02 ^a
cis-1,2-Dichloroethylene						0.0002J
Chloroform				0.002J	0.003J	0.0037
Carbon Tetrachloride						0.0019
Benzene						0.0001J
Trichloroethylene	0.007	0.0005J	0.006	0.004J	0.005J	0.0019
Tetrachloroethylene	0.10	0.0078	0.067	0.052	0.096	0.021

Well JBW-7817A			
Interval, meters bgs	3.7-6.7	26.8-29.9	
Compound/Date	Dec-01	Dec-01	Apr-02 ^a
Acetone	0.037		
Chloroform	0.009	0.005	
Benzene	0.008	0.003J	0.0027J
Trichloroethylene		0.004J	0.0029J
Tetrachloroethylene	0.025	0.019	0.027

units – mg/l Empty cells indicate not detected.

^a – all equipment blanks for April 2002 sampling round showed acetone (0.046-0.062 mg/l), TCE (0.0002-0.0003 mg/l), toluene (0.0003-0.0004 mg/l), and PCE (0.0046-0.010 mg/l)

^b – Open borehole sampled

^d – duplicate

J – Estimated; Analyte detected between the Method Detection Limit and the Reporting Limit

Other contaminants besides PCE were found during the pre-steam injection ground water sampling. TCE concentrations were typically about 10 percent of the PCE concentration, while smaller concentrations of cis-1,2-DCE were also found in some intervals. Benzene, toluene, ethylbenzene, and xylene (BTEX) were found in EX-3 and I-5, carbon tetrachloride and acetone were detected in well I-4, chloroform and 1,1,2,2-tetrachloroethane were found in well EX-3, and benzene was found in JBW-7817A. Although well VEA-5 was not sampled during the pre-steam injection ground water sampling, it was noted that an LNAPL that appeared to be a fuel was present in this well.

Thus, the highest ground water concentrations of PCE during pre-treatment sampling seemed to generally be along the centerline of the target area, in the extraction wells. This is consistent with the ground water results found during the Phase II characterization (HLA, 1999c). Although the MERC samples had shown most of the PCE contamination to be below a depth of 6 meters (20 feet) bgs, the ground water results showed significant concentrations in some of the shallow intervals of I-3, EX-1, and EX-4. The two sampling rounds show some very significant differences in PCE concentrations in the ground water between the December 2001 and April 2002 sampling events; however, the directions of change are not consistent. Phase II ground water sampling results also showed significant variations in concentration with time in some intervals (HLA, 1999c).

4.1.7.2. Sampling of Deep Wells

Samples to determine whether contaminants were moved laterally or vertically by the steam injection were collected from the three deep boreholes that were installed as part of this research project. These boreholes were outfitted with Solinst multi-level casing. Each well had five isolated intervals selected to isolate likely features of significance to the ground water flow system (See Chapter 4.1.5.). The intervals of each well that was sampled are listed in Table 4.1.7.2-1. The intent of sampling Interval 1 of SM-1 and SM-3 and Interval 2 of SM-2 was to get data below the area to be treated by the steam injection to determine if downward migration of contaminants occurred during the steam injection. Interval 3 of these three wells is approximately at the same elevation as the area targeted for steam injection, and thus these intervals were chosen to provide data on whether lateral migration of contaminants occurred.

These deep wells were first sampled in April 2002, five months after they were installed, and the second sampling round was conducted in June 2002. Grab samples were collected from each of the specified intervals using a Wattera-style foot valve assembly. A 0.0064 or 0.0095 meter (0.021 or 0.031 foot) tube with a foot valve at the bottom was placed inside the 0.016 meter (0.052 foot) standpipe of the appropriate interval, and pumping was done manually by repeatedly lifting and then lowering the foot valve. Samples were collected in VOA vials that were pre-preserved and shipped on ice to the laboratory for analysis by EPA Method 8260B. Purge volumes varied between intervals. For two of the intervals sampled during the first sampling round, two separate samples were taken after purging different volumes and both were submitted for analysis. These results did not show an obvious bias caused by the purge volume. This methodology follows that developed for fractured rock at the Smithville site (Novakowski et al., 1999), and is consistent with published recommendations on ground water sampling in fractured rock (Shapiro, 2002).

Table 4.1.7.2-1. Ground Water Sampling Intervals for Deep Wells

	SM-1	SM-2	SM-3
Intervals sampled in April 2002	Interval 1 Interval 3	Interval 2 Interval 3	Interval 1 Interval 2 Interval 3
Intervals sampled in June 2002 and post treatment	Interval 1 Interval 3	Interval 2 Interval 3	Interval 1 Interval 3

Results from both rounds of samples from the deep wells are given in Table 4.1.7.2-1. Ground water samples from Interval 1 of SM-1, which is below the target area for the steam injection, showed no PCE or TCE contamination. The three contaminants that were detected in this sample (acetone, chloroform, and toluene) are common laboratory contaminants; however, all of these compounds were occasionally detected in ground water samples from the target zone and in effluent samples during the steam injection. Thus, the detection of these contaminants in this sample may indicate a connection between the target zone and this interval. Interval 1 of SM-3, which is located to the east and below the target area for the steam injection, showed a PCE concentration at approximately the detection limit in both pre-steam injection sampling rounds. It is known that the bedding planes dip in this direction; thus it appears that a small amount of dissolved phase PCE followed the bedding planes in this direction. During the Phase II sampling, significant concentrations of PCE (0.57 mg/l) were found at a depth of 42.4 – 45.4 meters (139 – 149 feet) bgs in JBW-7816, which is approximately 30 meters (100 feet) southwest of SM-3 (HLA, 1999c).

Interval 3 of SM-1, which is to the north of the target area and at approximately the same elevation, shows small concentrations of PCE and TCE in both pre-steam injection sampling rounds. Intervals 2 and 3 of SM-2, which are located to the south of and at approximately the same elevation as (or a little below) the target area, show significant contamination. The closest of the process

wells to this borehole, I-7 and I-8, do not contain nearly as much contamination, which leads to a question of whether the area of SM-2 might be another source zone. However, the significant concentrations of TCE, cis-1,2-DCE, and vinyl chloride in this interval may indicate that this is the plume coming from the source zone that is the target for the steam injection, and that dechlorination is occurring in the ground water plume. These intervals also show small levels of BTEX. The three orders of magnitude reduction in PCE concentration in Interval 2 of this well between April and June 2002 is a surprising result that is not consistent with the rest of the data. The presence of high concentrations of contaminants in Interval 2 and 3 of SM-2 means that this well cannot reliably be used for determining if lateral movement of contaminants occurs during the steam injection. The ground water data for Interval 3 of SM-3 show that the fuel-related (LNAPL) plume that is known to exist in the area moved into this well between April and June 2002. This plume is separate from the DNAPL plume.

Table 4.1.7.2-2. Pre-Treatment Ground Water Sampling Results from the Deep Boreholes

Well SM-1				
Interval	Interval 1	Interval 3 ^b	Interval 3 ^c	Interval 3
Compound/Date	Jun-02	Apr-02	Apr-02	Jun-02
Acetone	0.011	0.016		
Chloroform	0.0069	0.029	0.002	0.0083
Trichloroethylene			0.0002J	0.0002J
Toluene	0.0007	0.0009J	0.0008J	0.0007J
Tetrachloroethylene			0.0005J	0.0017
Total Xylenes		0.0001J	0.0001J	

Well SM-2				
Interval	Interval 2		Interval 3	
Compound/Date	Apr-02	Jun-02	Apr-02	Jun-02
Vinyl Chloride	0.0035J	0.0064	0.085	0.073
Acetone		0.005		
1,1-Dichloroethylene			0.025	0.023
Trans-1,2-Dichloroethylene	0.0012J	0.0007J	0.005J	0.0046J
cis 1,2-Dichloroethylene	0.022J	0.034	0.35	0.33
Chloroform		0.011		
Benzene	0.0025J	0.0003J	0.0079J	0.0057J
Trichloroethylene	0.13	0.018	1.20	0.84
1,2-Dichloropropane	0.01J			
Dibromomethane	0.01J			
Bromodichloromethane	0.01J			
Methyl Isobutyl Ketone	0.01J			
2-Chloroethylvinyl Ether	0.05J			
cis 1,3-Dichloropropene	0.01J			
Toluene	0.002J	0.0016		0.0028J
Tetrachloroethylene	0.13	0.0007J	1.20	0.71
Ethyl Benzene				0.0011J
Total Xylenes		0.0001J		0.0048J

Table 4.1.7.2-2. Continued

Well SM-3							
Interval	Interval 1		Interval 2	Interval 3 ^e	Interval 3 ^f	Interval 3	Interval 3 ^d
Compound/Date	Apr-02	Jun-02	Apr-02	Apr-02	Apr-02	Jun-02	Jun-02
Acetone	0.011						
Chloroform		0.0045		0.0013		0.0025	0.001
Benzene						0.001	0.0013
Trichloroethylene						0.0001J	
Toluene	0.0011	0.001	0.0021	0.0022	0.0004J	0.0006	0.0005J
Tetrachloroethylene	0.0002J	0.0002J		0.0002J			
Ethyl Benzene				0.0001J	0.0003J	0.0008J	0.0009J
Total Xylenes		0.0001J	0.0002J	0.0005J	0.0025	0.0052	0.0059
Isopropyl Benzene						0.0027	0.003
n-Propyl Benzene						0.0016	0.0017
1,3,5-Trimethylbenzene						0.004	0.0043
1,2,4-Trimethylbenzene						0.0074	0.0081
Sec-Butyl Benzene						0.0012	0.0013
1,2,3-Trimethyl Benzene						0.0036	0.0039
p-Isopropyl Toluene						0.0011	0.0012

units-mg/l Empty cells indicate the compound was not detected

b – sampled after 0.10 liters purged

c – sampled after 3.5 liters purged

d – represents field duplicate

e – sampled after 0.40 liters purged

f – sampled after 2.1 liters purged

J – Estimate; Analyte detected between the Method Detection Limit and the Reporting Limit

4.1.7.3. Ground Water Data QC Summary

The most significant QC problem with the ground water sampling data was contamination within the equipment blanks. During the December 2001 sampling, equipment blanks contained chloroform at concentrations of 0.001 – 0.002 mg/l, and PCE at concentrations as high as 0.006 mg/l. The low concentrations of PCE detected in the samples from JBW-8717A may have been effected by carryover of PCE within the sampling equipment. During the April 2002 sampling event, equipment blanks contained acetone (0.046 – 0.0062 mg/l), TCE (0.0003 mg/l), toluene (0.0003 – 0.0004 mg/l), and PCE (0.0046 – 0.0010 mg/l). Acetone was never detected in ground water samples obtained using the sampling equipment; however, the low levels of TCE coming from the equipment may have effected most of the ground water sample results. Toluene was only detected in the sample from I-8, and this was likely effected by contamination in the equipment. PCE concentrations in samples from I-1, I-4 (21.3 – 24.4 meters; 70 - 80 feet depth), I-7, I-9, EX-1, and EX-4 should be considered estimates due to possible contamination from the equipment. Because dedicated sampling equipment is used in the deep monitoring wells, these samples are never effected by carryover in sampling equipment. There were no QC problems in the trip blanks.

Duplicate results for the December 2001 and June 2002 sampling events are within QC requirements as set out in the QAPP. Duplicates from the April 2002 sampling event showed large discrepancies in concentrations for chloroform, toluene, ethylbenzene, and total xylenes. TCE and PCE were detected at concentrations close to the detection limits in some samples, but not detected in the duplicate.

4.2. Pre-Operation Conceptual Model of Site

Characterization activities conducted at the site under the auspices of the SITE program in 2001 and 2002, prior to the operation of the steam injection, greatly expanded the understanding of the subsurface environment at the Quarry. In this section, the conceptual model of the site developed from this information, including geological structure, contaminant distribution, and hydrogeology, is discussed.

4.2.1. Geology

Structural information derived from logged cores was integrated with previous geologic mapping and packer testing data to produce cross-sections of the site. A cross-section extending through VEA-1, I-3, and JBW-7819 and summarizing salient features is presented in Figure 4.2.1-1. This exercise allowed some generalizations to be made about the fracture patterns at the Quarry site:

1. Bedding and bedding-parallel fractures: These dip towards the east (azimuth ranging from northeast to southeast), typically at 10-30 degrees, but at up to 45-50 degrees in outcrops at the north, east and west of the site. Subtle variations in lithology, reflecting original sedimentary depositional laminations, are picked out by color variations in weathered, exposed surfaces and in BIPS images. Detailed mapping of the Quarry area (CDM, 1992; HLA, 1999c; Beane et al., 1998) revealed the presence of a gently north-northeast-plunging open fold. The site used for the steam injection lies entirely on the easterly-dipping southeast limb of the fold. While many bedding planes defined by color or lithology changes are not marked by fractures, at least some have apparently served to localize relative displacement of competent beds parallel to the plane of the bedding. These “micro-faults” are commonly marked by mineralization and may retain open fractures.
2. Northeast-striking fractures: These typically dip towards the southeast or northwest at high angles (50-85 degrees). They are predominantly an anastomosing (interlocking) fracture cleavage, which strikes parallel to the axial plane of the regional-scale fold of the northeast-trending Aroostook-Matapedia Anticlinorium, on one limb of which the site lies (Roy, 1987). Variations in bedding orientation around the hinge of third order folds, such as that exposed in the upper tier of the Quarry, cause the strike of the “axial planar” cleavage to cut the strike of bedding at a high angle. This terminology differs from that used in previous descriptions of the site (HLA, 1999c). The observed variability in dip directions from NW to SE may indicate the presence of cleavage fans across the axes of minor folds. Alternatively, this may simply be a product of the anastomosing morphology of the fracture cleavage itself.
3. Northwest-striking fractures: This rather heterogeneous group of fractures typically dips towards the northeast or southwest at a wide range of angles (15-80 degrees). This group contains fractures formed by a variety of causes and probably includes conjugate sets of transverse or oblique fractures generated during folding, unloading, and possibly during blasting operations at the Quarry. Short, irregular or sinuous fractures, commonly lined by clay or micaceous minerals known as stylolites, are also present. These are formed within individual beds as a product of pressure solution early in the burial history of the bedrock and are locally common in the more carbonate-rich beds. Lower angle planar structures associated with mineralization and open fractures having this strike are more problematic, but were suspected to be potentially significant hydraulically (e.g., 25.4 meters; 83.3 feet bgs in I-5). It was suspected that at least some of these structures were minor synthetic and antithetic faults associated with layer-parallel slip between bedding planes during folding. This group of fractures corresponds to those identified as “Axial Planes” by some earlier investigators at the Quarry (HLA, 1999c).
4. Faults: The principal structure is the “CDM” fault (CDM, 1992; Beane et al., 1998), a northwest-trending, easterly-dipping planar structure lying immediately to the west of the steam injection area. It has two strands in the prominent cliff on the north side of the Quarry separated by zones of clay-rich fault gouge, mineral veins, and brecciated bedrock. Smaller faults of both northwest and northeast strike have also been mapped on the upper tier. They are associated with localized brecciation and mineral veining.

4.2.2. Contaminant Distribution

The original concept of COC location, summarized in Chapter 2, envisaged a broadly west-southwest trending dissolved-phase plume extending across the site. This was in accordance with the general hydraulic gradient deduced from earlier characterization (HLA, 1999c). It should be noted, however, that most of the sample points lie in an elongate group of this general trend, rendering it highly likely that a dissolved-phase plume of this orientation would have been deduced. Within that feature, it was apparent from analysis of samples that chlorinated VOCs and petroleum hydrocarbons were concentrated in the eastern part of the site, reaching a maximum concentration for chlorinated VOCs in the vicinity of JBW-7816. Lower, but still elevated, concentrations occur in JBW-7817A, which lies down-dip of bedding from JBW-7816. A second peak in concentration lay at the western end of the site, centered on JMW-0201, where peak historical concentrations in excess of 10 mg/l PCE had been recorded. Drilling of the wellfield for this project unavoidably moved the ground water around, thus the site was left undisturbed after drilling for a period of several weeks in order to allow the aquifer to re-equilibrate. Sampling after this time showed that all of the new wells remained above the action level for PCE of 0.005 mg/l, thereby expanding the area of known contamination from the earlier conceptual model. Overall, dissolved-phase concentrations were significantly lower than the historical peaks in closely adjacent wells, with the exception of EX-3 (adjacent to JMW-0201), which retained PCE concentrations of up to 8.8 mg/l. Over the remainder of the site, dissolved-phase concentrations were in the 0.010-0.150 mg/l range, being locally highest in the center of the site at wells I-3, EX-1, and EX-4.

MERC sampling of weathered fracture rims and rock matrix from recovered core revealed a similar distribution. The maximum concentration of PCE (72 mg/kg) in weathered fracture rims occurred at approximately 29 meters (95 feet) bgs in I-3. High concentrations of PCE were also found in weathered fracture rims in I-2 at 20 meters (65 feet) bgs (23 mg/kg) and 27.4 meters (90 feet) bgs (38 mg/kg). Local peaks in concentration were also found at a range of depths in the west-central parts of the site (e.g., EX-1, EX-2, and EX-3). The shallowest occurrence of PCE in weathered fracture rims was seen to occur at progressively deeper

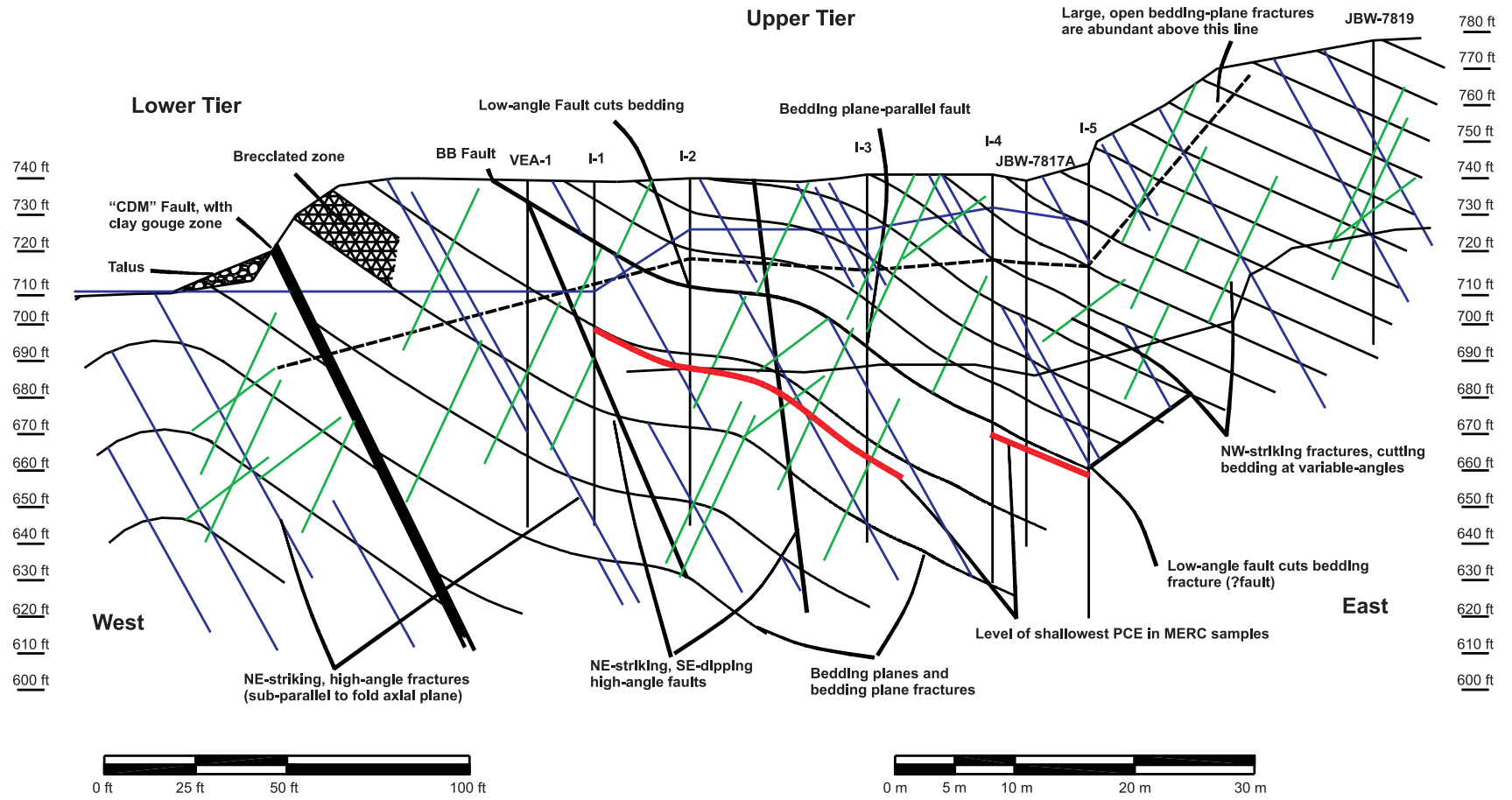


Figure 4.2.1-1. Conceptual model of geological structure at Quarry.

levels from west to east across the site, as described in Chapter 4.1.2. The shallowest occurrence of PCE in MERC samples may be plotted as a surface that dips at 10-15 degrees towards the northeast in the western part of the site and at 30-40 degrees in the eastern part of the site. The orientation of this surface is strikingly similar to the orientation of bedding plane fractures at the site (as summarized in Figure 4.2.1-1). While this may be taken to provide an indication of some degree of structural or stratigraphic control on the location of residual PCE, it should be noted that in at least some cases, the shallowest MERC sample was apparently collected from “axial planar” or other fractures. Below the depth of shallowest occurrence, PCE was only found to occur in matrix samples within approximately 0.3 meters (1 foot) of fractures, suggesting that diffusion of the aqueous phase into the mass of the rock matrix was limited to this extent.

TCE is the second most abundant contaminant in MERC samples and typically occurs at about 10 percent of the concentration of PCE. Other chlorinated compound contaminants detected included cis-1,2-DCE, trans-1,2-DCE, chlorobenzene, vinyl chloride, and 1,1-DCA. All were present at much lower concentrations than PCE and TCE. Fuel components were detected in many samples, all of which were at low concentrations.

While this mass of contaminant may have been effectively immobile, it corresponded to the general location of highest dissolved-phase concentrations for PCE. These data altered the conceptual model of the site in that the original concept of a source of all contaminant from a surface spill in the eastern part of the site, where storage drums had been removed from the vicinity of JBW-7817A and B, entering the aquifer by percolation and subsequent dispersion in solution, could no longer be sustained. The presence of peaks in concentration of dissolved-phase and adsorbed PCE in the subsurface in areas removed from known surface spills suggested that complex flow paths involving migration along strike of bedding-plane fractures towards the northwest and southeast, and across bedding on axial planar and on other high-angle fractures, may have been followed.

4.2.3. Hydrogeology

Taking into consideration the fracture network model developed via outcrop data, geophysical testing results, and the results of this hydraulic testing study, an improved conceptual fracture network model was developed.

Bedding plane fracture features (striking to the north and dipping to the east at 10 to 30 degrees but up to 45 degrees at the eastern and western ends of the site) appeared to dominate flow at this site. Many vertical and sub-vertical fracture features were also identified, and these features were expected to play a major role in the ground water flow system.

The results and interpretation of pulse interference testing (as well as previous single-well hydraulic testing data, ATV results, and borehole core logging data) indicated that the upper (near-surface) zones of most boreholes were highly fractured and of relatively high permeability. The shallow zones of many wells, from the ground surface to 9 – 12 meters (30 – 40 feet) bgs, were shown to be interconnected through intersections of fractures within this heavily fractured zone.

Fewer interconnections were found between the deeper intervals. These interconnections, however, play the largest role in providing a pathway for the steam injected at depth. Accordingly, those interconnections identified by pulse interference testing were used to locate specific injection and extraction wells and intervals used in the final design for SER at the eastern end of the site.

In general, the results of the pulse interference tests identified three separate areas of interconnection within the proposed steam footprint. These zones of interconnection also coincided with very distinct groups of water levels observed under open-hole conditions. For the purpose of this discussion, these interconnected areas will be called the Western, Central, and Eastern areas. The list of wells lying within each of these areas is given in Table 4.2.3-1.

Table 4.2.3-1. Wells Within Interconnected Areas

Wells Within Western Area	Wells Within Central Area	Wells Within Eastern Area
VEA-1	I-2	I-4
I-1	VEA-2	I-5
EX-3	I-3	JBW-7817B
VEA-6	JBW-7815	TC-1
	EX-1	JBW-7817A
	VEA-9	VEA-5
	EX-2	JBW-7816
	VEA-4	EX-4
	JBW-7814	I-6
	I-9	I-7
	I-8	VEA-7

The lack of pulse interference testing response between the areas suggests that they are effectively isolated from each other, most probably because sparsely fractured zones of low permeability rock separate them. Considering the dip of the bedding, it is likely that large blocks of inclined rock are pervasive at this site. The eastward dip of the dominant open fractures in these blocks of rock was expected to strongly diminish the east to west component of ground water flow, resulting in a very large hydraulic gradient between the blocks in this direction. By contrast, the hydraulic gradients developed along strike of bedding within these blocks was expected to be much smaller.

Figure 4.2.3-1 shows the identified interconnections in plan view. Each of the interconnections illustrated exists only for the pair shown. Thus, connections shown along a specific vector such as I-9, to EX-1, to I-3 are only between well pairs, and no direct connection between I-9 and I-3 may exist. To determine connections amongst multiple boreholes, fracture features that define the connections must be identified and correlated.

Note that interconnections between the eastern and central areas of the site are limited to a connection between I-3 and I-4 along the northern perimeter. This connection was explored in some detail during the interconnectivity testing (test numbers 15, 93-98; see Appendix F), and the best connection was identified between a fracture feature at 12 meters (40 feet) depth in I-3 and the deepest fracture feature in I-4.

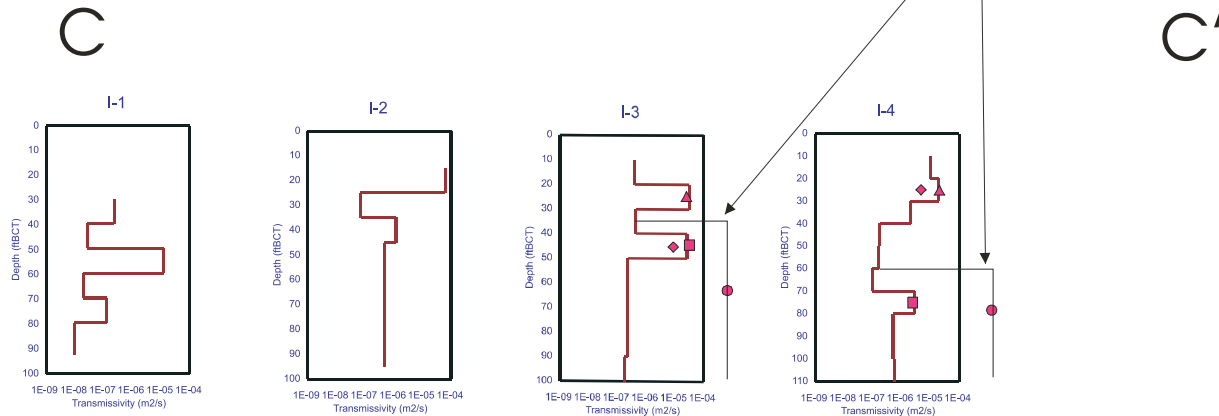
To help illustrate the connections in the east-west direction, a number of cross-sections are constructed in the following figures. The key to the cross sections is given in Figure 4.2.3-2 where each letter pair represents a cross section for a series of wells along the illustrated line.

Figure 4.2.3-3 illustrates the complexity of the interconnection between I-3 and I-4 using the distribution of single-well transmissivity for each of the boreholes. Thus, as described above, only a weak response was observed between the lowermost fracture feature in I-3 and the lowermost fracture feature in I-4.

The interconnections observed between I-4 and I-5, illustrated in Figure 4.2.3-4, are better established than those between I-3 and I-4. In this case, two approximately parallel bedding plane features dipping to the east are identified. The continuity along these features is highly transmissive, and it is believed that these features would provide excellent pathways for steam and ground water flow. The lower connection occurs at a dip of not more than 30 degrees, less than that of the overlying feature, but comparable to the dip of the bedding at this location. Thus, it was thought to be highly probable that this feature is a low-angle fault of high permeability. This interconnection, defined by hydrological testing, corresponds closely in location and orientation to a group of features marked by geophysical anomalies, bedding-parallel veining and fracturing, and PCE-contamination in I-3, I-4, I-5, and JBW-7817A. This had previously been identified as a zone of potentially high permeability on the basis of core-logging, down-hole geophysical profiling, and rock sampling.

This cross section displays interconnections between I-3 and I-4

I-3 and I-4 were isolated with a single packer below the depth of the horizontal line for this test

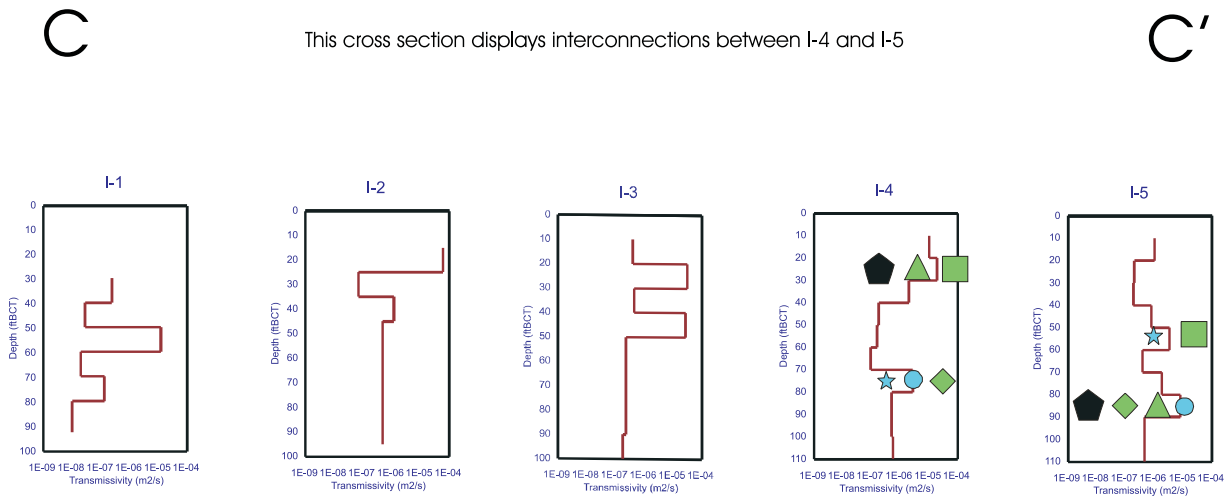


Interconnections between wells are indicated by like symbols placed at the depths where an interconnection was discovered
 Symbols are sized to convey the value of Transmissivity (in m2/s) for the specific interconnection
 An example of the sizing protocol is shown below

- = Weak Response / Non - Analyzable Data Set
- = $1 \times 10^{-6} \leq$ Transmissivity $< 1 \times 10^{-5}$
- = $1 \times 10^{-5} \leq$ Transmissivity $< 1 \times 10^{-4}$

Figure 4.2.3-3. Interconnection along the northern perimeter of the site.

This cross section displays interconnections between I-4 and I-5



Interconnections between wells are indicated by like symbols placed at the depths where an interconnection was discovered
 Symbols are sized to convey the value of Transmissivity (in m2/s) for the specific interconnection
 An example of the sizing protocol is shown below

- = Weak Response / Non - Analyzable Data Set
- = $1 \times 10^{-6} \leq$ Transmissivity $< 1 \times 10^{-5}$
- = $1 \times 10^{-5} \leq$ Transmissivity $< 1 \times 10^{-4}$
- = $1 \times 10^{-4} \leq$ Transmissivity

Figure 4.2.3-4. Interconnections between I-4 and I-5.

To aid in the visualization of the fracture network structure at the site, a number of three-dimensional figures were constructed using FRACMAN (Golder, 1998) and CAD-based software (Surfer) (from Stephenson & Novakowski, 2003) and are presented below as Figures 4.2.3-5 thru 4.2.3-9. The planes depicted in these figures represent an observed connection between pairs of wells. Fracture planes are mapped for all connections that displayed at least a “weak response” (See Appendix F). Fracture connection planes are shaded to improve differentiation between the fracture features. The width of the fracture plane has been chosen arbitrarily and does not necessarily convey an inferred width of the feature. Also, the pathway (or pathways) that allows interconnection between well pairs may be more complex than the interconnection shown in these figures. However, these figures serve to summarize the general location and orientation of structures that would control the flow system and provide the steam migration pathways at the Quarry. Figures 4.2.3-5 through 4.2.3-9 each display all fracture interconnections discovered during the hydraulic testing study. White lines indicate locations of wells and two or three wells are identified in each diagram in order to give the reader a quick bearing reference. Appendix F should be consulted for exact depths and locations of interconnections. These diagrams are designed to display typical trends that were discovered at the site.

Figure 4.2.3-5 shows the fracture interconnections in profile looking almost due east. From the vantage point depicted in this figure, it is clear that connections along the strike of bedding planes are prevalent at this site. Interconnections between I-8 and EX-1 and I-9 and EX-1 are among these “along strike” interconnections.

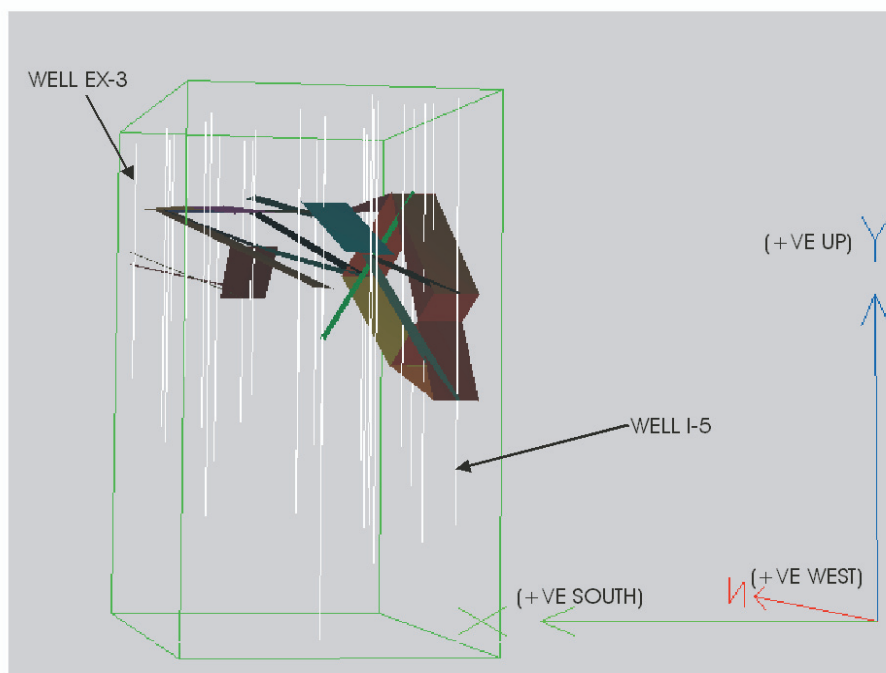


Figure 4.2.3-5. Profile view of fracture interconnections looking east.

Figure 4.2.3-6 shows the fracture interconnections looking towards the northeast. This figure shows interconnections that occurred along strike as well as along the dip of the bedding plane features.

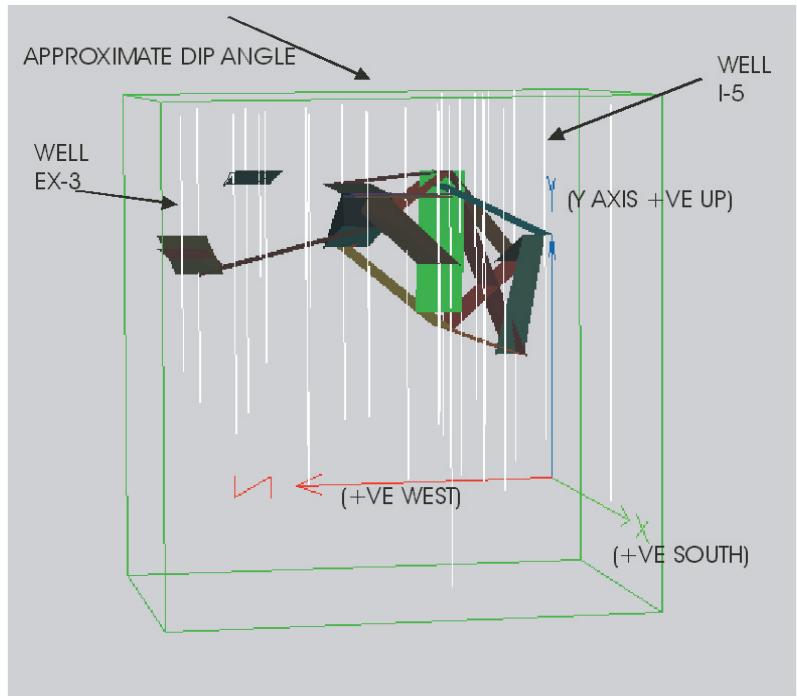


Figure 4.2.3-6. Fracture interconnections looking towards the northeast.

Figure 4.2.3-7 displays fracture interconnections that likely occur along the dip of bedding plane features. The perspective of this figure is a profile view from the south looking north across the site.

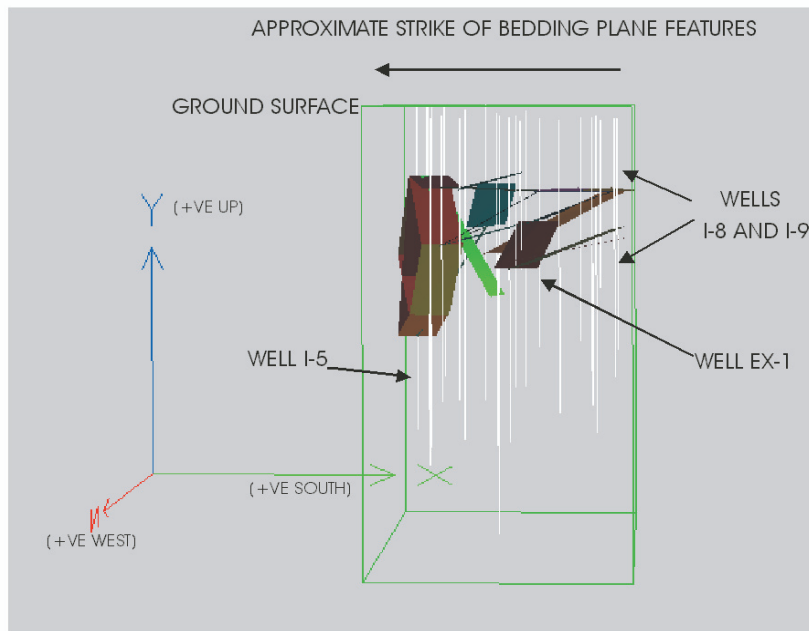


Figure 4.2.3-7. Profile view of fracture interconnections looking north.

Figure 4.2.3-8 is a view of the fracture interconnections from above looking to the northeast. This figure again illustrates the interconnections that exist between well pairs located in an orientation parallel to strike and those located in an orientation parallel to dip.

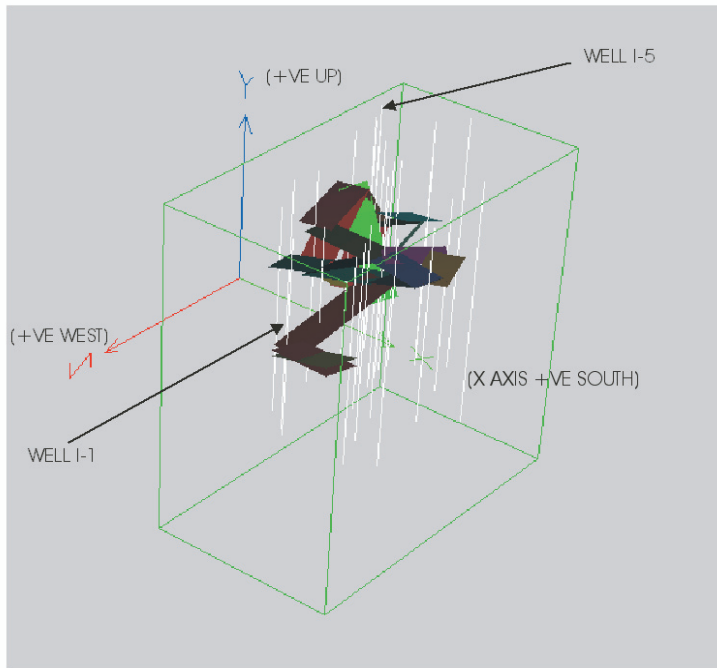


Figure 4.2.3-8. Fracture interconnections looking down and towards north-northeast.

Figure 4.2.3-9 displays fracture interconnections looking downwards towards the northeast and shows the concentration of interconnections found in the northeast quadrant of the site. It is also evident from this figure that interconnections are prevalent between well pairs located along strike and down dip.

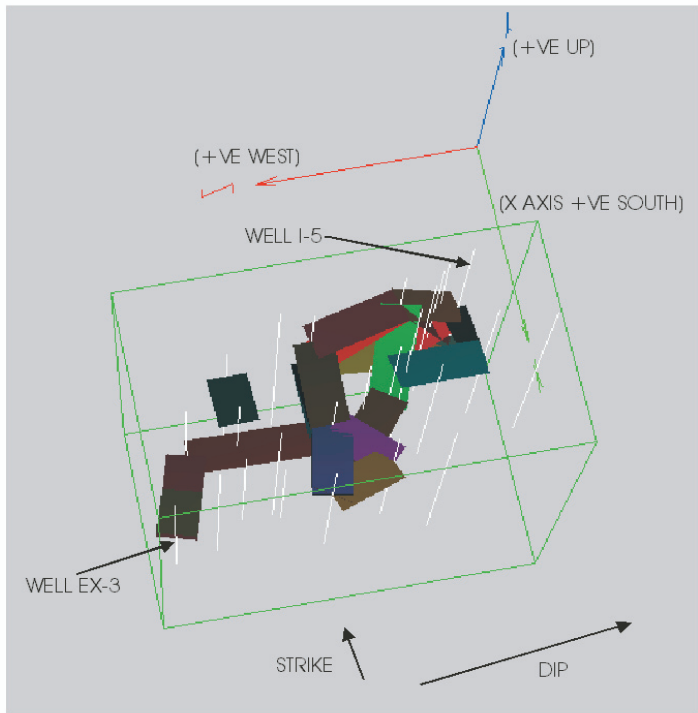


Figure 4.2.3-9. Profile view of fracture interconnections looking downwards towards the northeast.

Chapter 5. Well Field, Process, and Subsurface Monitoring Design

5.1. Injection and Extraction System (As-Built)

The steam remediation system consisted of a network of vertical wells and borings. The layout of the well field is summarized in Figure 5.1-1.

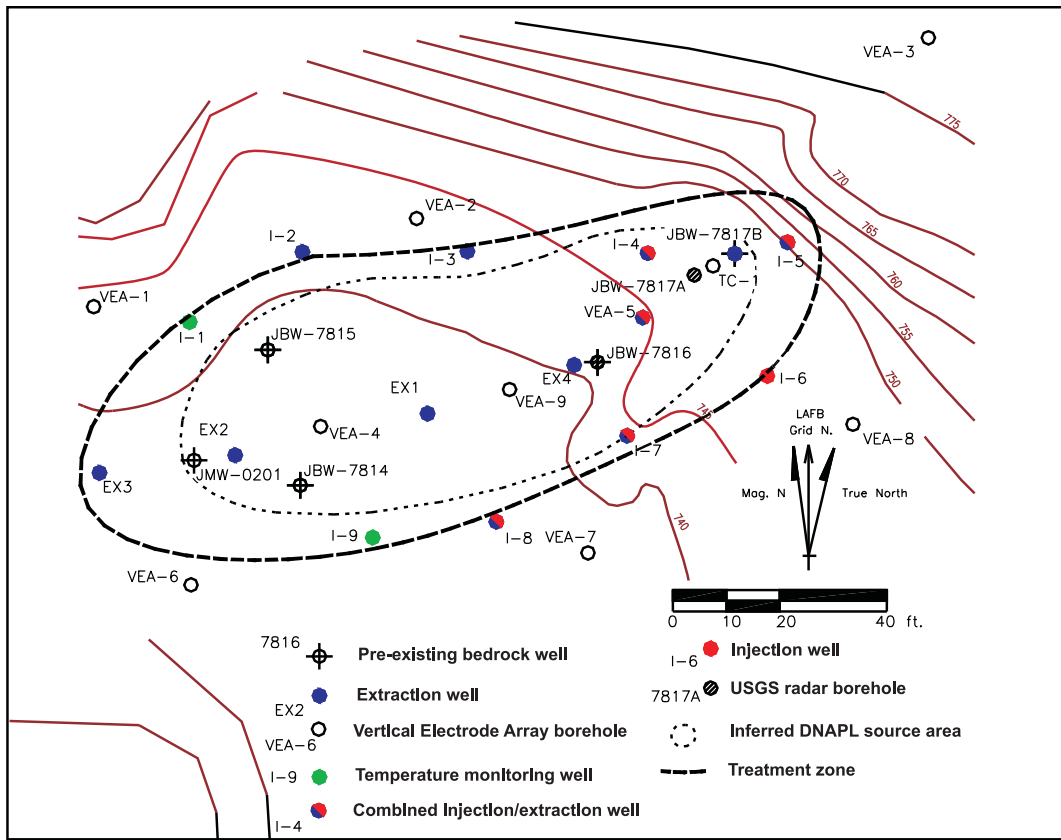


Figure 5.1-1. Well field layout. Legend shows how the wells were used at the initiation of steam injection.

The network consisted of 13 boreholes of 0.15 meter (0.5 foot) diameter, intended for use as injection or extraction wells, and 10 boreholes at 0.10 meter (0.33 foot) diameter, intended for use as geophysical (ERT) and/or temperature monitoring locations. An additional six pre-existing monitoring wells of 0.15 meter (0.5 foot) diameter were also intended for use as monitoring points. The newly drilled borings extended in total depth from 23 to 36.6 meters (75 to 120 feet) bgs (see Table 4.1.1-1), stepping down to greater depths from west to east across the target area. The intention of the eastward increase in total depth was to allow each of the wells to access the eastward-dipping planar structure that was suspected, on the basis of previous site characterization data, to have controlled the migration of DNAPL.

The original design concept shown in Figure 4.0-1, consisting of a well field in which a perimeter of steam injection wells would drive mobilized contaminants towards a line of centrally-located dual-phase extraction wells, was modified in response to contaminant distribution and hydrogeological data collected during drilling of the process borings and subsequent characterization activities. Rock chip data indicated that significant contamination was present in borings I-2 and I-3 that had been intended for use as steam injectors, while aquifer testing revealed that the area of optimum interwell connection was located in the eastern part of the site. In response to this information, the decision was made to focus steam injection and heating at the eastern end of the site in

wells I-4, I-5, and I-6, at the lowest part of the suspected migration-controlling structure, and in the zone of greatest permeability and best interwell hydraulic connections. Wells lying up-dip of this structure that showed both contamination and potentially useful hydraulically conductive features were used as dual-phase extraction wells.

The electrical resistivity and temperature monitoring boreholes were used essentially as intended in the original design, consisting of a perimeter of six borings surrounding a central axis of three borings completed with Vertical Electrode Arrays (VEAs) and digital thermocouples, augmented by boreholes completed with temperature monitoring equipment only. Details on the monitoring design are presented in Chapter 5.3.

Steam was produced in an above-ground steam generating unit (Chapter 5.2.1), from which steam was transferred using a steam header at 690 kPa (6.8 atm) gage pressure (corresponding to a temperature of about 170°C; 340°F) to the well field through steel pipes. A steam manifold and schedule 40, black steel pipes were used to deliver the steam to the well heads. At the injection well heads, the pressure was reduced to the desired injection pressures, which had been estimated before construction to lie between 200 and 620 kPa (2 and 6 atm), dependent on injection depth. The steam injection pressure was controlled to an accuracy of within 7 kPa (0.07 atm) using Taylor steam pressure regulators. The corresponding injection temperatures were 135 to 155°C (275 to 330°F).

The injection wells were completed with multiple screened intervals and sandpacks separated by grout plugs, in order to enable the injection pressure to be varied at several different target depths. Well I-6 was completed with three discrete injection intervals, while wells I-4 and I-5 were completed with deep and intermediate injection intervals. The shallowest intervals of I-4 and I-5 were used for dual-phase extraction. Wells I-7, I-8, and VEA-5, which were initially completed for extraction, were subsequently retrofitted with deep (all three wells) and intermediate (I-7 and I-8) steam injection intervals. Well design features are summarized in Figure 5.1-2a and Figure 5.1-2b.

Extraction wells were completed as open borings with sealed well heads connected to the dual-phase extraction system. Pneumatic positive-displacement top-loading 0.10 meter (0.33 foot) Clean Environment Equipment AP-4 and bottom-loading 0.10 meter (0.33 foot) QED Environmental Systems Hammerhead H4 pumps were used for liquid extraction. Wells I-3, I-7, and EX-4 were completed with both top-loading and bottom-loading pumps because the presence of both LNAPL and DNAPL was suspected in the vicinity of these boreholes, as evidenced during drilling and pre-operational sampling. The relatively shallower wells at the western (up-dip) end of the site were completed with single, bottom-loading pumps. All other wells were completed with single top-loading pumps, as there was no indication of DNAPL presence near these boreholes. Wells I-4 and I-5, in which steam was injected in lower and intermediate depths, were completed with top-loading pumps in their upper parts, which remained open and unlined. Wells I-7, I-8, and VEA-5, which were initially completed as extraction only wells, retained top-loading pumps in the upper part after the wells were retrofitted for steam injection at depth.

Ground water and dissolved-phase contaminants extracted from the extraction wells were combined in the main liquid line before being transferred to the effluent treatment system. The design of the liquid effluent treatment system is discussed in greater detail in Chapter 5.2.3. An “as-built” layout and plot plan for the equipment used is shown in Figure 5.1-3.

Vapors were extracted from all extraction wells. The extracted vapors were transported under a vacuum to the treatment system through a system of surface piping carried on pipe racks. Upon reaching the treatment system, condensed liquid and vapor phases were separated and cooled, and the vapor was then dried. Remaining organic contaminants in the dry, heated vapors were removed by carbon adsorption before the vapor was emitted to the atmosphere. The design of the vapor treatment system is discussed in greater detail in Chapter 5.2.2.

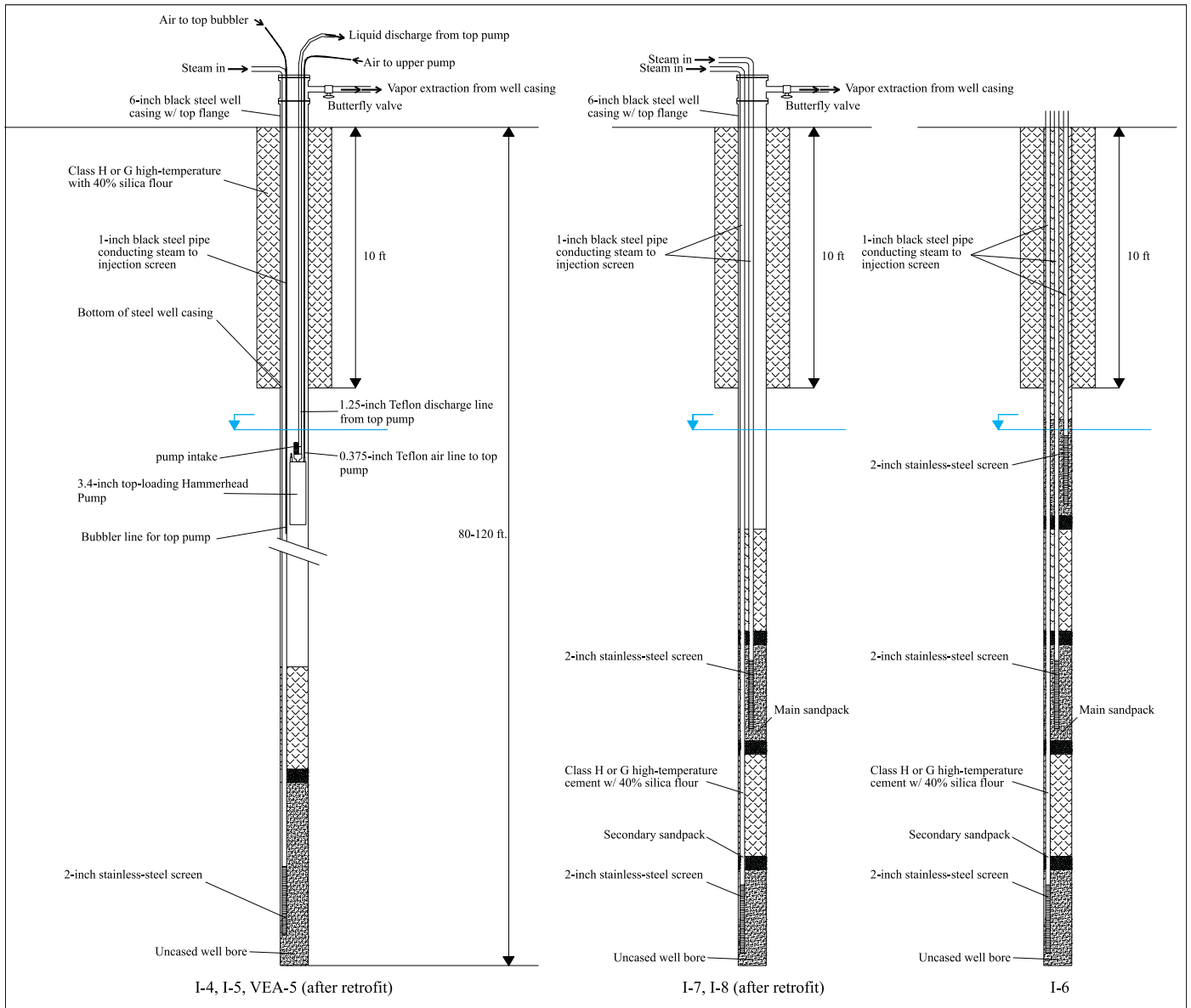


Figure 5.1-2a. Injection well design summary.

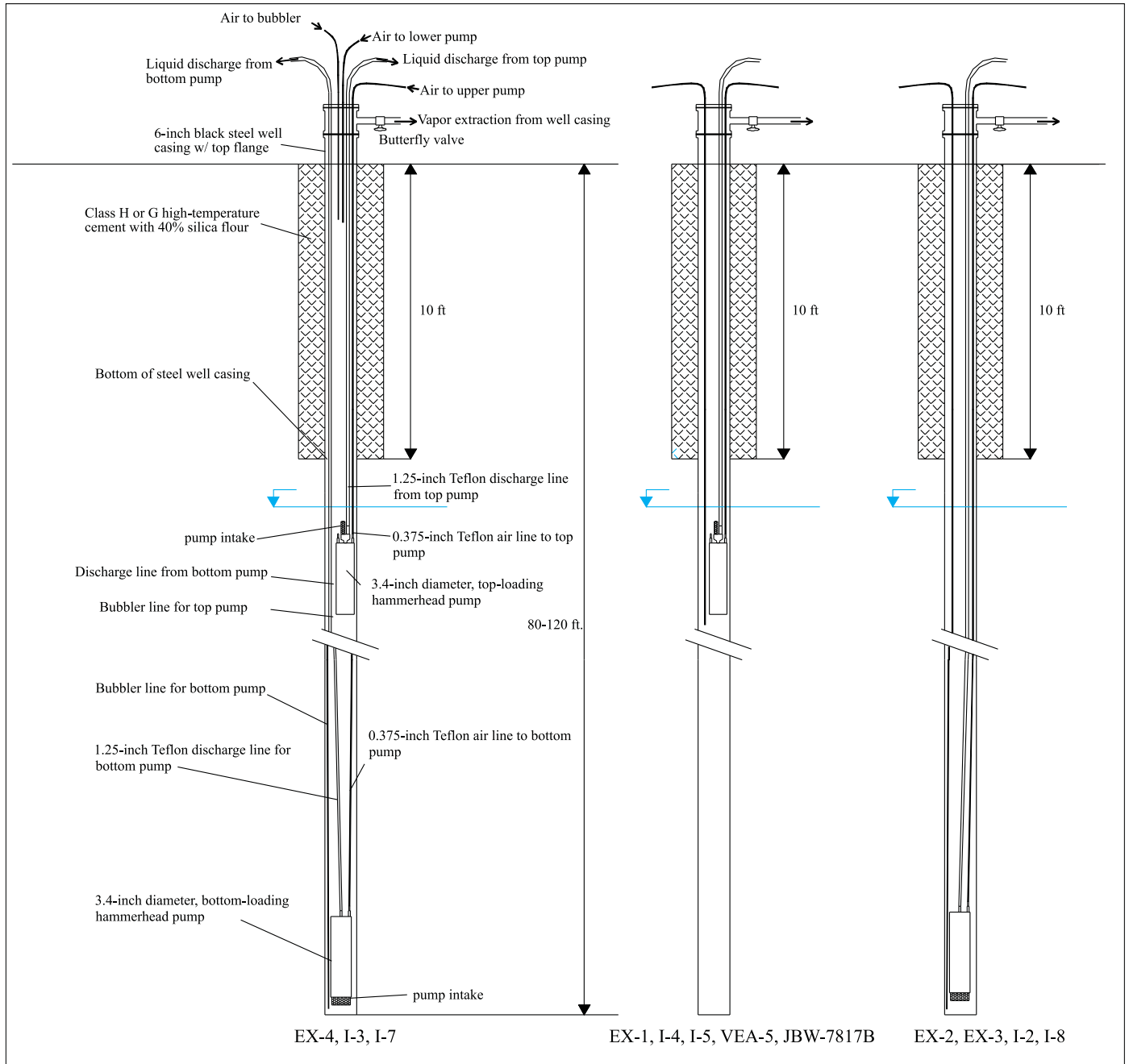


Figure 5.1-2b. Extraction well design summary.

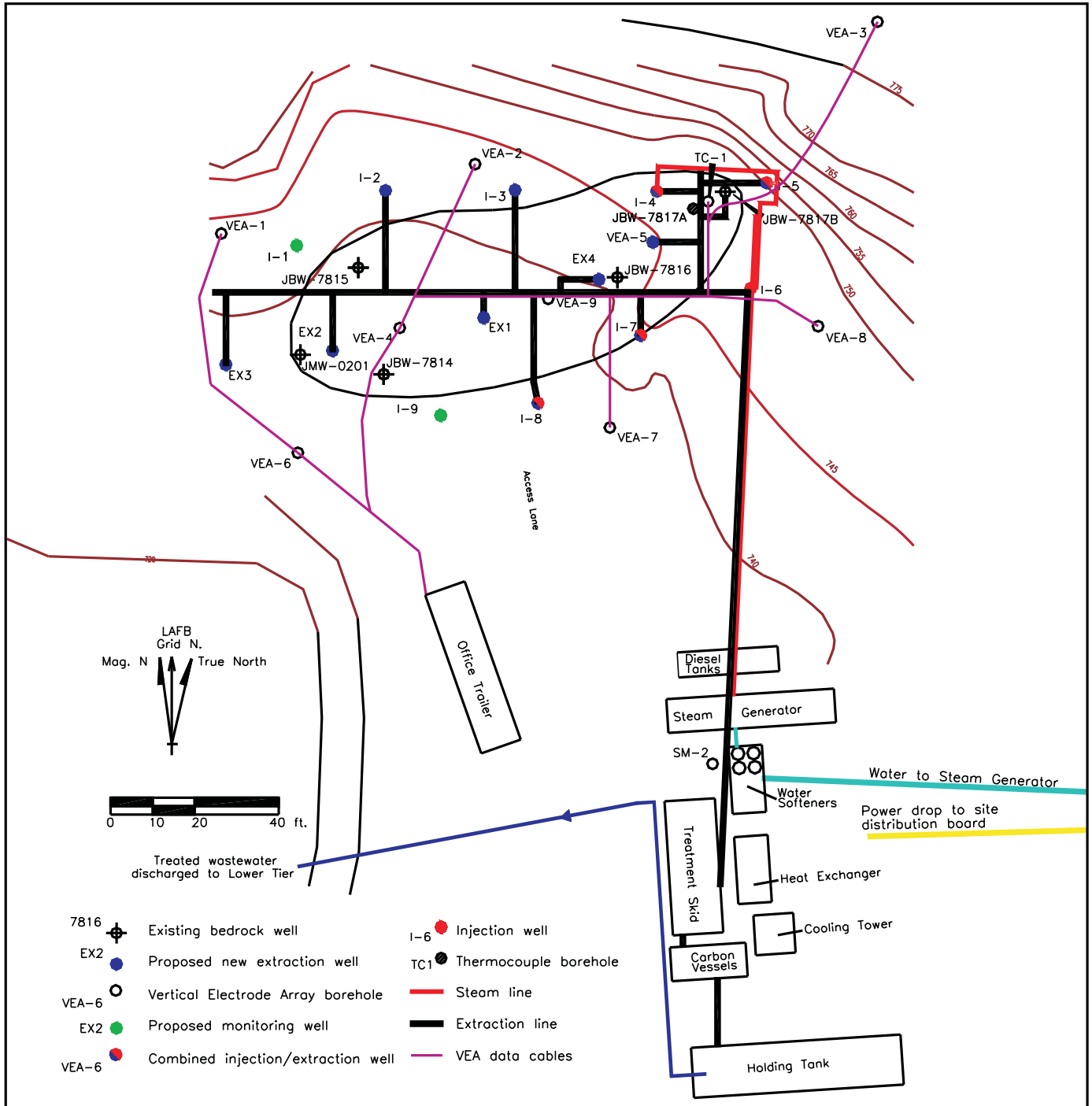


Figure 5.1-3. Site layout, as-built.

5.2. Above-Ground Systems

5.2.1. Steam Generation

The components used in the steam generation system and their specifications are summarized in Figure 5.2.1-1 and listed in Table 5.2.1-1.

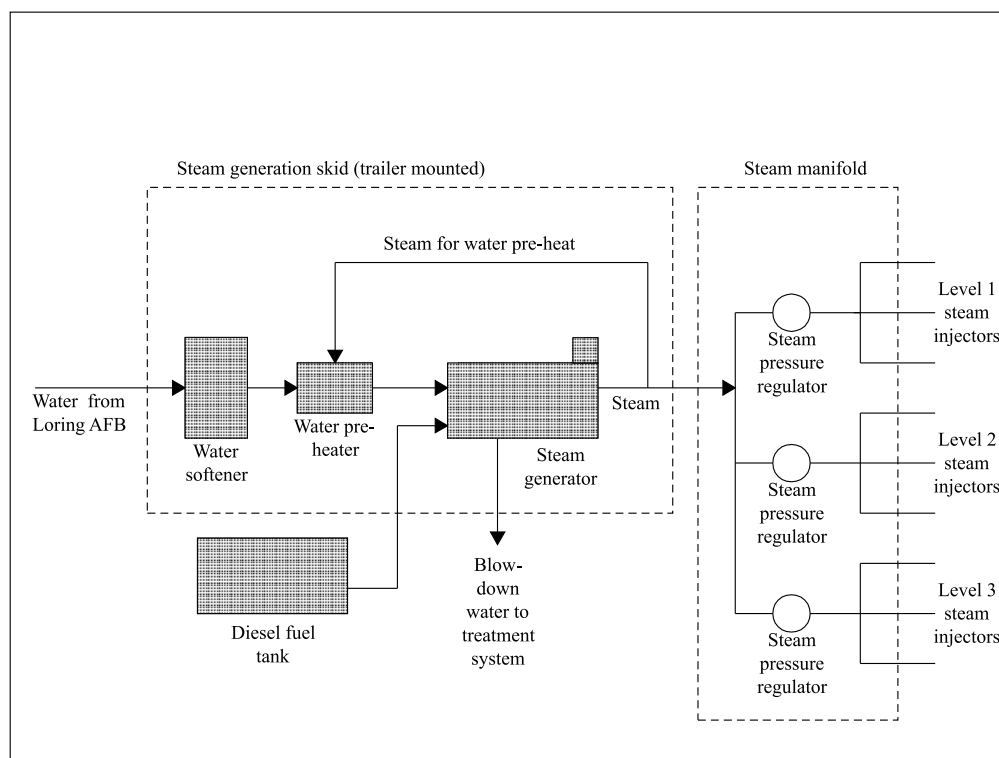


Figure 5.2.1-1. Steam generation and distribution system schematic.

Table 5.2.1-1. Major Design Parameters and Process Equipment Specifications

Equipment description	Function	Design rating/specifications	Comments
Power supply	Power to equipment	300 A, 480 V, 3-phase	Average load 50-150 A, from Loring AFB power line
Power panel	Breakers, meter and distribution	300 A, 480 V in, 480 V/240 V/110 V out	No backup power planned
Water supply	Water to steam and treatment system	Max 150 lpm (40 gpm) briefly, 76 lpm (20 gpm) continuous at 414 kPa (4 atm)	Average water usage was below 38 lpm (10 gpm)
Water pre-treatment unit	Supply soft, low oxygen water to steam generator	95 lpm (25 gpm), TDS < 250 mg/l, DO < 0.5 mg/l	Sulfite added to reduce DO levels, pH and TDS adjusted to prevent scale buildup
Diesel fuel tank	Fuel for steam generator	11,400 liters (3,000 gallons)	
Steam generator	Supply steam to injection well system	8.4 Million kJ/hr (8 Million Btu/hr), ~ 3,600 kg/hr (8,000 lb/hr), 135°C (275°F), 200 kPa (2 atm)	Steam quality at injection points should be >80%

Table 5.2.1-1. Continued

Equipment description	Function	Design rating/specifications	Comments
Steam pressure regulator and manifold	Reduce pressure to injection pressure and split steam into separate lines to injection wells	Steam regulator valves, 0.05 meter (0.17 foot) steam pipe manifold with orifice plates for steam flow measurement	Orifice plates sized for 45-225 kg/hr (100-500 lbs/hr) of steam flow in each injection line
Vapor line condenser/heat exchanger	Cool vapors to ~ 30-40°C (86-104°F) and condense out condensable gases	Maximum cooling capacity 880 kW (3 Million Btu/hr), max condensate flow 23 lpm (6 gpm), effluent temperature <40°C (104°F) (vapor & liquids)	Ran at much less than full capacity most of the time. Designed for peak performance at time of steam breakthrough, which never occurred
Liquid-vapor separator, KO-2	Knock out liquid component and condensate after cooling	23 lpm (6 gpm) liquid, 7.6 scmm (250 scfm) non-condensable vapor	Removed condensate from vapor stream
Vacuum pump, liquid ring with associated cooling system	Apply vacuum to vapor extraction line	2 pumps each 7.6 scmm (250 scfm), inlet side vacuum 50 kPa (0.5 atm), Outlet side pressure between 100 & 150 kPa (1.0 & 1.5 atm) absolute	Used dual pumps for a total rate of about 11 scmm (400 scfm)
Liquid-vapor separator, KO-3	Knock out liquid component after vacuum pump	0.53 lpm (2 gpm) liquid, 11 scmm (400 scfm) non-condensable vapor	Also serves to recover seal water for re-circulation to vacuum pumps
Air drying unit	Remove moisture from vapor stream	Reduce humidity to below 80% for 7.6 scmm (250 scfm) stream	Heat exchangers and liquid knockout in packaged unit
Vapor phase carbon canister system	Adsorb organics from vapor stream	Inlet 11 scmm (400 scfm), 100-150 kPa (1.0-1.5 atm) absolute pressure, <50°C (122°F), Max organic load 23 kg/hr (50 lb/hr), 2 units each containing 227 kg (500 lbs) of carbon	Two canisters in series, where the upstream canister removes the bulk of the mass. The primary unit was a dual bank steam regeneration unit
Liquid line heat exchanger	Cool pumped water and NAPL to ~ 30-40°C (86-104°F)	Maximum cooling capacity 300 kW (1x10 ⁶ Btu/hr), max liquid inlet flow 95 lpm (25 gpm)	
Gravity liquid separator	Separate LNAPL-water-DNAPL liquids	Total inlet 95 lpm (25 gpm) (99-100% water, 0-1% NAPL)	Both LNAPL and DNAPL could be present, but no NAPL was separated
NAPL tanks	Store recovered product	Max 950 liter (250 gallon) capacity	Placed on secondary containment
Water carbon canister system	Remove dissolved organics from liquid effluent stream	95 lpm (25 gpm), 2 canisters in series, 227 kg (500 lbs) each	Breakthrough never happened
Water holding tank	Store clean water for discharge	80,000 liters (21,000 gallons)	

The steam was generated on-site in a diesel-fired steam generator rated at a maximum of 3,650 kg/hour (8,000 lbs/hour), equivalent to an energy input of 8,500,000 kJ/hour (8,000,000 Btu/hour). The maximum water supply requirement of up to 150 lpm (40 gpm) (instantaneous) of potable water was obtained from a fire hydrant immediately adjacent to a former storage building at the edge of the taxiway system. Water was supplied from the hydrant to the steam generator on a demand basis. Average water usage was below 40 lpm (10 gpm). The water supplied to the steam generator was pre-treated to adjust pH, dissolved oxygen, and total dissolved solids (TDS) levels to an acceptable standard, using an ion-exchange water softener and pre-heater (standards are defined in Table 5.2.1-1). The steam injection pressure was controlled to an accuracy of within 7 kPa (0.07 atm) using air-powered oil-field type pressure regulators. A steam manifold and schedule 40, black steel pipes were used to deliver the steam to the well heads. Molded fiberglass insulation was fitted to all steam pipes to minimize heat losses and reduce the burn hazard for personnel.

5.2.2. Effluent Extraction and Treatment Systems

The effluent treatment systems were designed to treat: (1) all vapors extracted from the subsurface by the vacuum extraction system, and (2) liquids (NAPL and water) extracted from the subsurface by the liquid recovery system. The components of the vapor and liquid treatment systems are summarized in Figure 5.2.2-1. Table 5.2.1-1 contains specifications for the process units.

5.2.2.1. Vapor Extraction and Treatment System

The extracted vapors were transported under a vacuum (typically 3 – 30 kPa; 0.03 – 0.3 atm) to the treatment system through above-ground steel pipes carried on pipe racks. Upon reaching the treatment system, the vapor was passed through a heat exchanger/condenser, where the temperature was reduced to below 50°C (120°F). Cooling to this temperature caused condensation of water vapor and some contaminants (the condensable gases). The condensate was then removed from the vapor stream in a liquid-vapor separator (KO-2), and the non-condensable gases were carried to the vacuum pump. The effluent vapors from the vacuum pump were passed through a liquid-vapor separator (KO-3), and then dried in an air drier to form dry vapor of less than 80 percent humidity. The dry, heated vapors were treated by carbon adsorption, passing through two canisters in series, before clean vapor was emitted from the stack to the atmosphere. Sampling ports were located in front of the carbon adsorption system (V-1) and at the emission point (V-4).

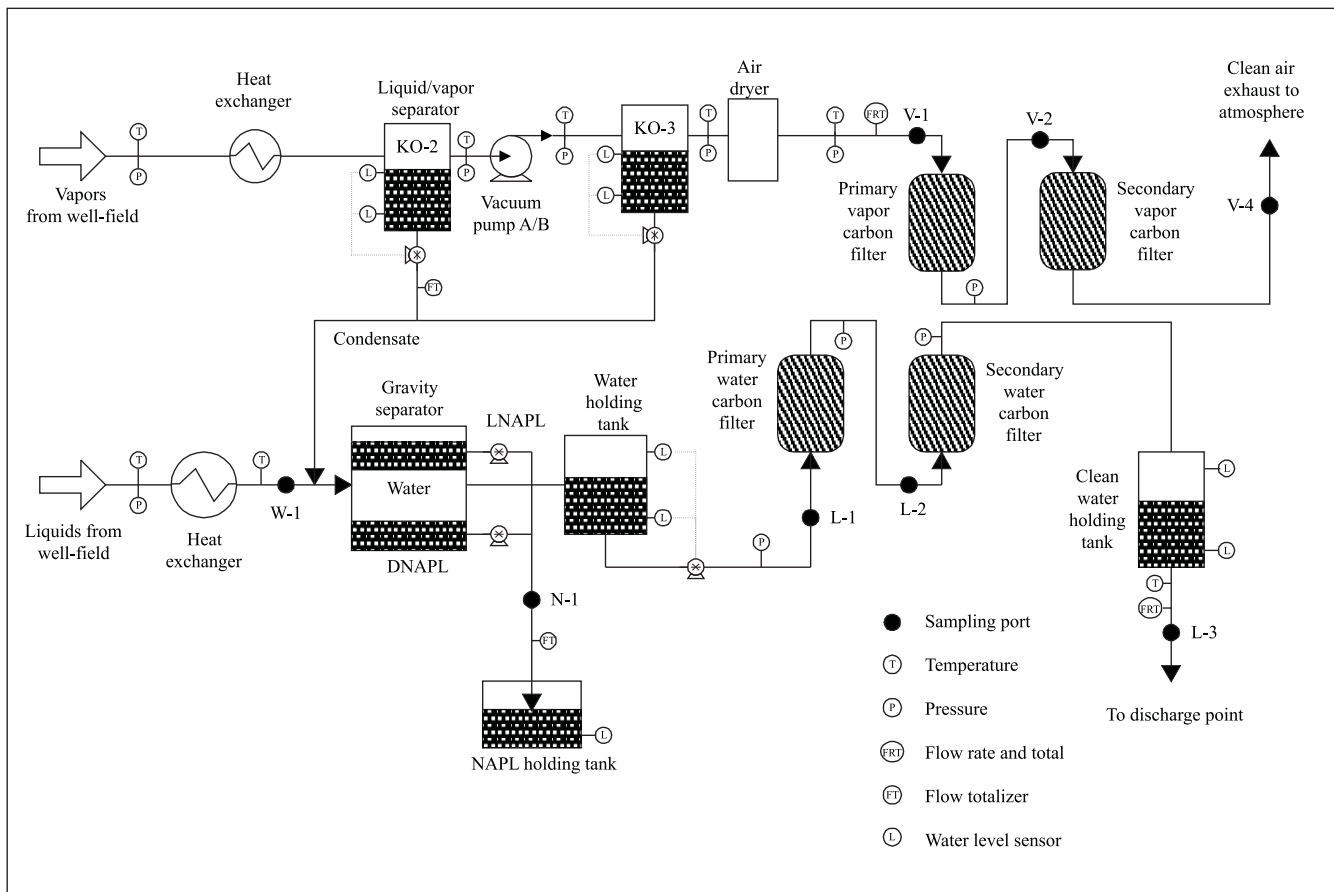


Figure 5.2.2-1. Extracted vapor and liquid treatment system schematic.

5.2.2.2. Water Extraction and Treatment System

The components of the liquid treatment system are summarized in Figure 5.2.2-1. Specifications for individual process equipment units are provided in Table 5.2.1-1. The liquids extracted from each of the extraction wells were routed through a main liquid line for transportation to the treatment system. At the treatment system, they were combined with the condensate from each of the liquid-vapor separators in the vapor treatment system. The combined liquids were passed through a heat exchanger in order to dissipate some of the heat transported from the well field. The cooled liquids were then passed through a gravity separator, in which any NAPL present would be removed. If present, DNAPL and coarser solids would have been removed from the bottom of the tank and stored in a holding tank on-site. LNAPL, if present, would have formed a floating layer in the gravity separator and been transferred to the LNAPL holding tank on-site. The clear water from the separator was temporarily stored in a holding tank before being passed through two canisters of granular activated carbon (GAC) to remove organic contaminants. Treated water was stored in a large holding tank on-site, from which it was periodically discharged to the lower, flooded level of the Quarry through a flexible hose.

It was intended that any recovered NAPL would be disposed of at the conclusion of the research project by shipping it to a recycler or alternatively to a hazardous waste disposal facility. As insignificant quantities of NAPL were recovered, carbon filtration of the liquid and vapor streams removed all of the organic contaminants mobilized during operations.

5.3. Subsurface Monitoring

Physical conditions present in the subsurface volume of the study area were frequently monitored using direct and indirect methods. These methods were:

- Temperature within wells and borings was measured directly using DigiTAM™ digital thermocouple strings.
- Formation resistivity in the inter-well rock mass was measured using electrical resistance tomography (ERT). This method permits temperature and saturation to be approximated.

The design of the temperature and ERT monitoring are described below, and the results are presented and discussed in Chapter 7. In addition to these two types of subsurface monitoring, which are commonly used with steam injection remediation, the USGS undertook a borehole radar tomography research project concurrent with this project to determine if radar tomography could detect the movement of steam and/or heat during steam injection into fractured limestone. A brief description of Borehole Radar Tomography technology and the results achieved during this research project are provided in Appendix G.

5.3.1. DigiTAM™ Temperature Monitoring System

Dedicated temperature monitoring equipment, consisting of strings of digital thermocouples (DigiTAMs), were installed at locations shown on Figure 5.1-1. DigiTAMs were installed in all new boreholes (VEA, I, EX, and TC wells) and in six pre-existing monitoring boreholes (JBW-7814, JBW-7815, JBW-7816, JBW-7817A, JBW-7817B, and JMW-0201). In those boreholes or wells in which grout plugs or seals were set, the DigiTAM string was housed in 0.025 meter (0.08 foot) diameter high-temperature resistant fiberglass pipe. This was necessary to ensure that the sensors remained dry at all times for maximum reliability. DigiTAM sensors were spaced at 1.5 meter (5 feet) intervals from the bottom of the borehole to within 3 meters (10 feet) of the surface.

The temperature was read from each sensor automatically using a computer-controlled logging system supplied by McMillan-McGee. The temperature data were stored on a hard drive at the site trailer and uploaded to an off-site server three times daily.

5.3.2. ERT System

Electrical Resistance Tomography (ERT) was used to indirectly monitor the migration of heated fluid and steam at the study site. Cross-borehole ERT using Vertical Electrode Arrays (VEAs) allows for mapping of the interpolated resistivity distribution in the subsurface within the volume contained by the VEAs. Resistivity within this volume in a thermal remediation environment is primarily sensitive to temperature and saturation and is influenced by heating and fluid or steam migration processes. This technique has been used in thermal remediation monitoring programs at a number of sites in unconsolidated media (e.g. LaBrecque et al., 1996).

In the context of steam injection within fractured rock, ERT senses changes in resistivity that reflect saturation changes, that are in turn caused by temperature and phase changes in pore fluids and by temperature increases in the rock matrix. Rock porosity remains constant before and during steam injection. According to Archie's Law, bulk resistivity is an inverse power function of both porosity and saturation (Archie, 1942):

$$\rho_t = F \cdot \frac{\rho_w}{S_w^2} = \frac{0.62}{\phi^{2.15}} \cdot \frac{\rho_w}{S_w^2}$$

where:

- 0.62 is a constant;
- ρ_t is the bulk resistivity of partially-saturated clay-free sediments;

- F is the formation factor which is the function of porosity ϕ ;
- ρ_w is the pore fluid resistivity; and
- S_w is saturation

A medium having greater than 80 percent saturation at any porosity may show more than an order of magnitude increase in resistivity if its saturation is reduced to below 20 percent.

Resistivity of saturated rock is an exponential function of the reciprocal of temperature (Llera et al., 1990). Many physical properties of media and pore fluid affect the bulk resistivity. A simplified relation is given by:

$$\rho_t = \frac{\alpha}{\phi^{2.15}} \cdot e^{k/T}$$

where:

- α is a complicated function of water resistivity, viscosity, hydration ionic radius, concentration, elementary charge, Faraday's constant, and valency;
- k is a function of Boltzmann's constant and activation energy of viscous flow; and
- T is absolute temperature.

Llera et al. (1990) measured the resistivity of lithified limestone of 0.26 percent porosity at 12,930 Ohm-meter (ohm-m). The ratio of resistivity at 30°C (86°F) to that at 120°C (248°F) is 14.3. This indicates that steam injection in lithified limestone with less than one percent porosity can produce more than an order of magnitude resistivity decrease in response to the elevated temperature.

VEAs were installed into nine dedicated boreholes (Figure 5.1-1) ranging in total depth from 30 meters (100 feet) to 46 meters (150 feet) bgs, becoming deeper from west to east across the site in order to parallel the dip of the dominant bedding planes. Electrode spacing was set at 1.5 meter (5 feet) centers from total depth to 3 meters (10 feet) bgs, with the exception of VEA-3, in which the topmost electrode was set at 10 meters (30 feet) bgs, as this borehole was drilled from a topographically higher location than the others. In consequence, individual VEAs contained from 19 to 25 electrodes dependent on total depth, and a total of 197 electrodes comprised the ERT system.

Resistivity data were collected using a SYSCAL R1 Plus™ earth resistivity meter and 240-electrode switch box manufactured by IRIS Instruments. Individual Teflon-insulated, silver coated copper wires extended from each electrode on the VEA to the ground surface where they were connected to a multi-conductor cable within a junction box. The multiconductor cable extended from the junction box to the operations trailer, where the data collection and processing equipment were housed. The 197 wires from each electrode in the field installation (19 to 25 electrodes per VEA) were connected to the IRIS switch box and SYSCAL R1 Plus.

Data were collected and processed for ten two-dimensional planes connecting pairs or groups of VEA boreholes. Individual data planes are listed in Table 5.3.2-1. During field characterization activities in Summer 2002 it was found that VEA-5 contained a floating fuel product. Thus, this borehole was made an extraction well initially, and borehole TC-1 was completed as a VEA. Command files were developed to collect data from all ten data planes using both dipole-dipole and bipole-bipole arrays. This approach allowed for an adequate density of data while reducing the overall time needed for data collection (within 24 hours). The SYSCAL R1 Plus meter was connected to a personal computer, on which the IRIS remote control option had been installed. Raw data were then collected and stored directly on the PC hard drive using Microsoft Task Manager.

Table 5.3.2-1. List of ERT Profiles

VEAs used	Profile Name
VEA-3/VEA-2/VEA-1	3-2-1
VEA-3/VEA-8	3-8
TC-1/VEA-9/VEA-4	TC1-9-4
VEA-6/VEA-1	6-1
VEA-6/VEA-4/VEA-2	6-4-2
VEA-7/VEA-4/VEA-1	7-4-1
VEA-7/TC-1/VEA-3	7-TC1-3
VEA-7/VEA-9/VEA-2	7-9-2
VEA-8/TC-1/VEA-2	8-TC1-2
VEA-8/VEA-7/VEA-6	8-7-6

5.4. Modifications Made During Operations

During operations, the innovative nature of this application, some equipment failures, and unanticipated difficulties in steam delivery and heat-up effectiveness compelled the replacement or modification of both individual equipment components and also of the operation strategy. These changes are discussed below.

Concern about the slow rate of heating of the subsurface led to a decision to convert three wells that had initially been used for extraction (VEA-5, I-7, and I-8) to injection wells. Approximately 50 days after steam injection was initiated, these wells were retrofitted with one or two deep steam injection intervals, and top-loading pumps were retained in the upper parts of the retrofitted wells (see Figure 5.1-2). VEA-5 was chosen to be converted to an injection well because it was known to be interconnected to the other wells in the eastern portion of the site. I-8 was chosen to be converted to an injection well because it was known to have significant permeability. I-7 was thought to have low permeability based on the results of the transmissivity tests done in Summer 2001; however, it was decided to try to inject into this borehole in an effort to get as much steam into the ground as possible.

In a related attempt to increase the rate of heating in the subsurface, a decision was also made in early September 2002 to increase the steam injection pressure. In unconsolidated media applications of steam injection, such as ground water remediation or enhanced oil recovery, a common rule for establishing safe injection pressures is to set the maximum pressure at 11.3 kPa/meter (0.034 atm/foot) of overburden (Davis, 1998). As had been observed at the Edwards AFB Site 61 steam pilot earlier in 2002 (Earth Tech and SteamTech, 2003), the mechanical strength of lithified rock is such that this rule provides a large margin of safety against potential rock failure and escape of steam. The steam injection pressure was incrementally increased to the maximum pressure sustainable by the steam generator (930 kPa; 9.2 atm, corresponding to about 180°C; 356°F). Particular attention was paid to frequent visual monitoring of wellhead conditions while the system operated at higher pressure. No incidents or steam short-circuiting to the surface were observed.

As the start date of operation was changed to late August, and operations were expected to last approximately three months, it became apparent that the process equipment was not sufficiently protected against low temperatures. Several flowmeters at various points were replaced because of frost damage, which became particularly problematic in November, by which time the local daily temperature was continuously below 0°C (32°F). Steam heat trace was added to all fluid lines in early November. In recognition of the continued risk of equipment failure because of freezing or of heavy snowfall, a protective temporary weather shelter was constructed to house the process equipment in mid-November.

Early in operations, modest vacuum (less than 3.4 kPa; 0.03 atm) was observed at the well heads even during periods with significant vapor flow from the formation (more than 6 scmm; 200 scfm). It was suspected that the highly broken rock and fill occupying the vadose zone immediately below ground surface in the study area was permitting convenient pathways for atmospheric air to be drawn into the extraction wells, thereby preventing maintenance of a strong vacuum. In order to test this hypothesis, and to minimize the effect of the suspected vadose zone connections to the atmosphere, a thin concrete layer was spread on the ground surface within the study area in mid-October to act as a vapor cap. The area covered by the cap is shown in Figure 5.4-1. The vapor cap led to only slightly higher vacuums. It is suspected that near horizontal fractures which are exposed at the western extent of the target area where the upper tier drops to the lower tier were causing vapor leakage into the area. Therefore, the vapor cap did not have the desired effect.



Figure 5.4-1. Location of the concrete seal placed over the eastern part of the site in mid-October.

Chapter 6. Injection-Extraction Rates and Water-Energy Balances

6.1. Injection Rates

6.1.1. Steam Injection Rate

Steam was distributed to the injection well heads using a steam header at about 690 kPa (6.8 atm) pressure (temperature of about 170°C ; 340°F). At the injection well heads, the pressure was reduced to the desired injection pressures, which had been estimated before construction to be between 200 and 620 kPa (2 and 6 atm) (temperature of about 135 to 155°C; 275 to 330°F), dependent on injection depth. Steam injection rates are summarized in Figure 6.1.1-1. The energy injected into each well is shown on Figure 6.1.1-2.

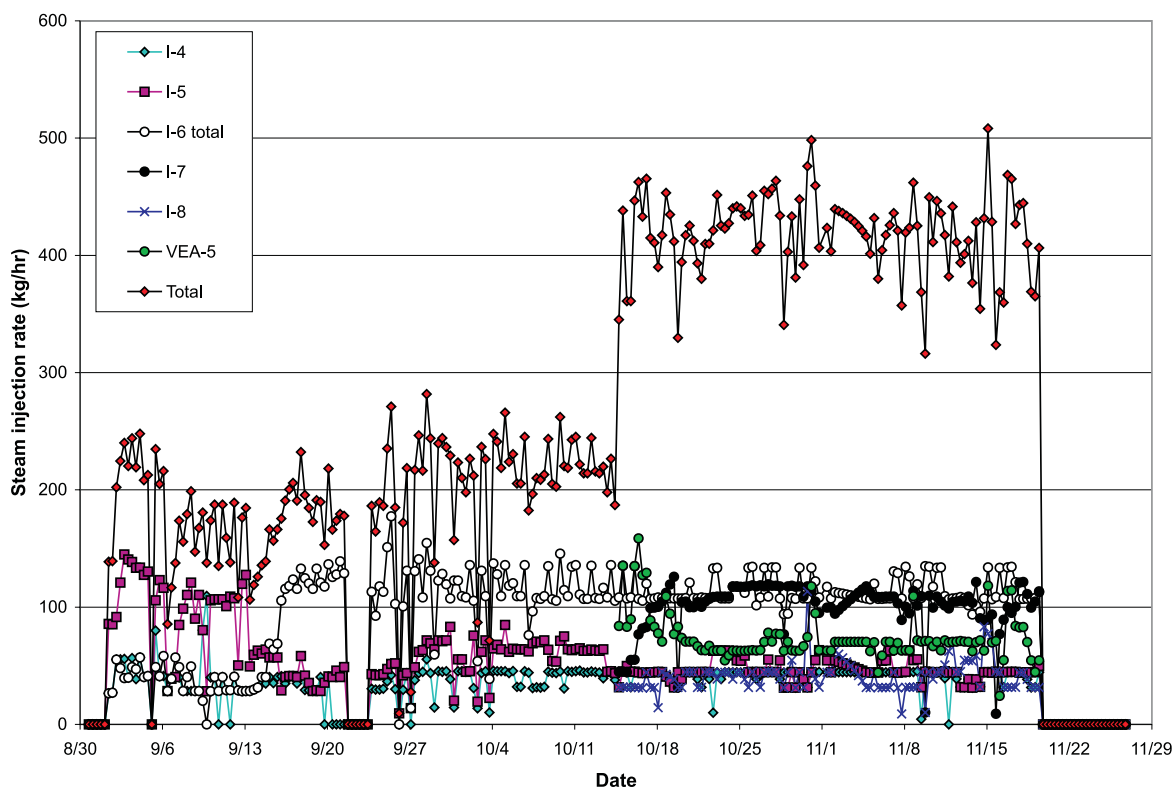


Figure 6.1.1-1. Injection rate for each of the injection wells.

Steam was initially injected in wells I-4 and I-5 (single deep injection interval) and at the deepest screen in well I-6. In wells I-4 and I-6 (deep), an injection rate of 27 – 59 kg/hr (60 – 130 lbs/hr) could be maintained, with periodic fluctuations. On September 14-15, the middle and shallow injection intervals of I-6 were brought on line. Flow rates into these intervals were in the range of 27 – 41 kg/hr (60 – 90 lbs/hr) normally, increasing the total flow into I-6 to approximately 113 – 136 kg/hr (250 – 300 lbs/hr). I-5, which had slightly higher hydraulic conductivity than the other wells, initially reached an injection rate of 145 kg/hr (319 lbs/hr). The injection pressure in this interval was reduced from 345 to 200 kPa (3.4 to 2 atm), and the injection rate correspondingly declined to about 100 kg/hr (220 lbs/hr). The sharp increase in injection rate apparent between September 12 and 13 (Figure 6.1.1-1) corresponds to a 100 percent increase in injection pressure to 410 kPa (4 atm). This increase was immediately followed on September 13 by a rapid, large decrease in injection rate to about 59 kg/hr (130 lbs/hr), which was then maintained with minor fluctuations until the temporary cessation of steam injection on September 21. This decrease in injection rate corresponds to the beginning of air injection in well I-5. During this period, air in the well was maintained at the same pressure as the steam. The apparent consequence of this was to prevent steam from entering the formation.

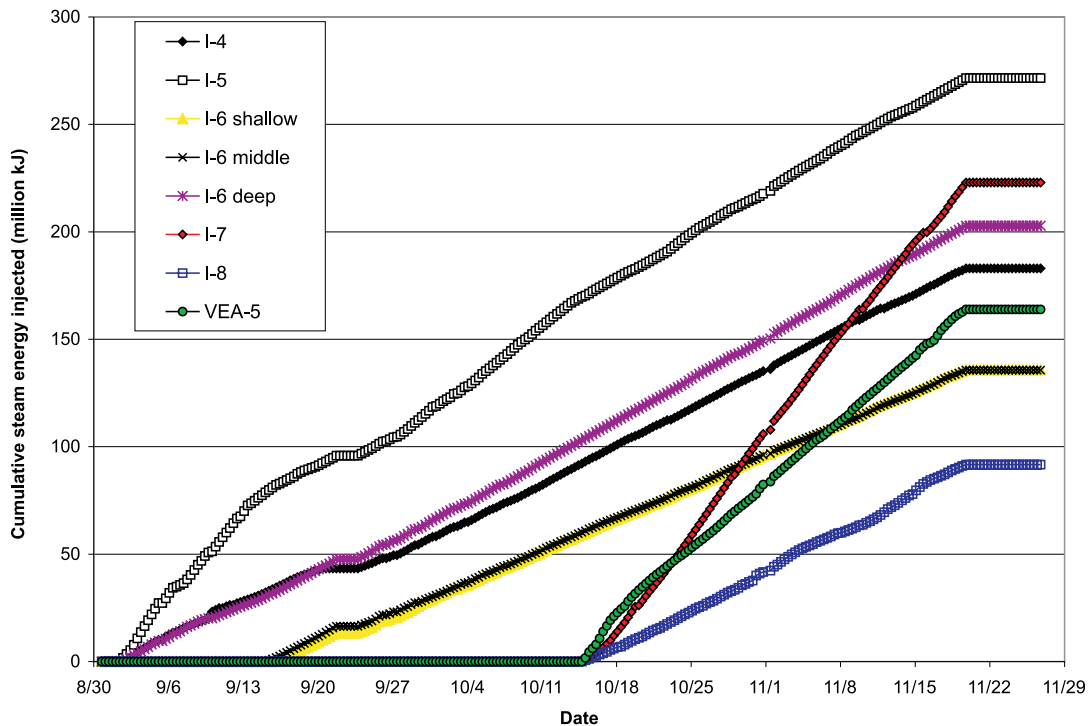


Figure 6.1.1-2. Cumulative energy amounts injected into each injection well.

Steam injection in all wells was halted for a short period between September 21 and 22 for modifications to the steam generator. On resumption of steam injection on September 22, steam injection pressures were maintained at a level slightly lower than the air pressure in the same well. This had little discernable impact on injection rate in wells I-6 (all levels) and I-4, in which the total range extended from about 14-64 kg/hr (30-140 lbs/hr). Steam injection rates in well I-5, which had earlier been shown to have the highest formation permeability to steam and which continued to permit air to enter the formation, were maintained at a generally higher, but more variable rate of 9-85 kg/hr (20-187 lbs/hr). These injection rates were maintained, with only minor fluctuations, until the end of steam injection on November 19.

As discussed in Chapter 5, wells I-7, I-8, and VEA-5 were retrofitted for steam injection in mid-October. The design features of these wells are summarized in Figure 5.1-2. Steam injection began in these wells on October 14. VEA-5, which was the only retrofit well to be completed with a single injection interval, was initially brought up to a pressure of 825 kPa (8.2 atm) by October 18, which was maintained with minor fluctuations until the end of steam injection on November 19. This pressure allowed an initial injection rate of up to 159 kg/hr (350 lbs/hr), which rapidly declined to a rate of around 64 kg/hr (140 lbs/hr) by October 21. This rate was maintained, with periodic fluctuations within the 23-113 kg/hr (50-250 lbs/hr) range, until the end of steam injection on November 19.

Steam injection rates were not separately recorded for the two screened intervals in wells I-7 and I-8. The total injection rate for each well, representing the sum injected through the mid-level and deep screens, is summarized in Figure 6.1.1-1. The total steam injection to well I-8 underwent an initial rapid rise to about 45 kg/hr (100 lbs/hr). The injection rate through the two screened intervals in this well remained within the 32-45 kg/hr (70-100 lbs/hr) range, with minor fluctuations, until November 1. After that date the injection rate varied more widely, ranging between 9 and 83 kg/hr (20 and 184 lbs/hr) before final shut down on November 19.

Well I-7 underwent an initial rapid rise in injection rate from October 14-19 after which it remained at 91-118 kg/hr (200-260 lbs/hr) with fluctuations until the end of steam injection in this well. The most notable excursion from relatively steady injection rates was seen on November 15, when it dropped to 9 kg/hr (20 lbs/hr). An incipient failure of the steam delivery line on the morning of November 9 forced a halt to steam injection to the mid-level screened interval in well I-7. The low steam injection rate recorded on November 9 occurred several hours later and was presumably unrelated to the end of steam injection to the mid-level interval. There is no immediate cause of the sudden drop in injection rate that can be attributed to operations of the steam generation and injection system, hence, an unknown hydrogeological cause must be assumed. Note that after the mid-level interval was shut off, injection pressure at the deep interval remained effectively constant, while the total injection rate for the well remained comparable to that observed while both intervals were active. This suggests that relatively little steam had been entering the formation through the middle interval.

The onset of steam injection into the retrofit wells is marked by a large increase in the total rate of steam injection to the subsurface from 181-272 kg/hr (400-600 lbs/hr) prior to October 14 to 317-508 kg/hr (700-1,120 lbs/hr) in the period afterwards, consequent on the introduction of an additional five injection intervals. The total amount of energy injected will be discussed further in Chapter 6.4 in conjunction with the energy balance.

6.1.2. Air Injection Rates

Air was injected in order to help develop fractures for improved steam injection rates, to create a buoyant vapor phase to force vaporized contaminants to migrate upward through fractures into the unsaturated zone, and to assist in vadose zone flushing after initial heat-up was achieved. Air injection rates are summarized in Figure 6.1.2-1 and 6.1.2-2.

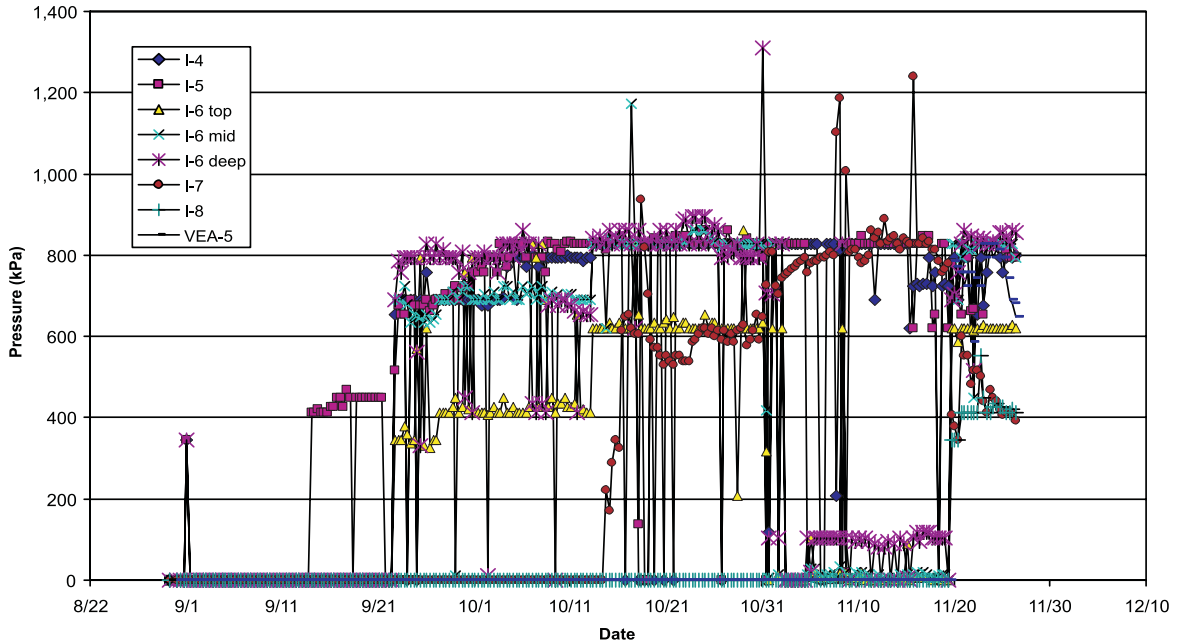


Figure 6.1.2-1. Air injection pressure versus time.

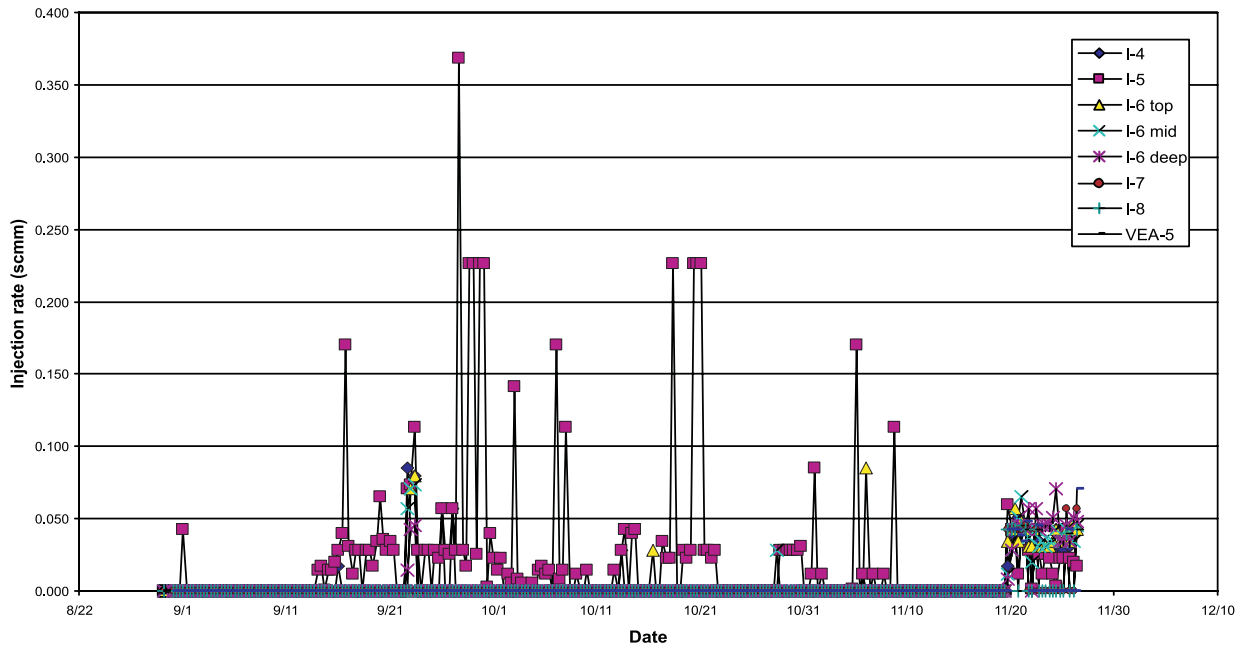


Figure 6.1.2-2. Air injection rate versus time.

Air injection began on August 31 in wells I-4, I-5, and through the deepest screen in I-6. It was discovered that air could not enter the formation at pressures that could be sustained over extended periods using the available equipment. Only well I-5 accepted air at a pressure of less than 345 kPa (3.4 atm), permitting an injection rate of about 0.042 scmm (1.5 scfm) to be maintained. In so doing, the high air pressure prevented the co-injection of steam, thus air injection was stopped in all wells after a short initial period.

Air injection was resumed in well I-5 alone on September 14 at a pressure of 410-550 kPa (4-5.4 atm), allowing an injection rate of up to 0.17 scmm (6 scfm) to be maintained for short periods, with 0.014-0.042 scmm (0.5-1.5 scfm) being more typical. An equipment failure forced the boiler to be shut down on September 21, allowing aggressive air injection to be resumed in all wells at high pressure. At this time, injection pressures in wells I-4, I-5, and the middle interval in I-6 were initially maintained at about 690 kPa (6.8 atm). The deep injection interval in I-6 was set at a pressure of about 790 kPa (7.8 atm), while the shallow interval in I-6 was set at about 415 kPa (4.1 atm). At these pressures, air injection was sustainable at rates ranging from 0.057-0.085 scmm (2.0-3.0 scfm) in the mid and shallow depth intervals and at 0.014-0.045 scmm (0.5-1.6 scfm) in the deep interval of I-6. These pressures were set at a level slightly lower than the steam pressure in the same injection interval, in order to minimize the potential for high air pressure to block entry of steam to the formation. Despite this, in all wells except I-5, air injection rates diminished to zero within one day of the resumption of steam injection on September 22 (Figure 6.1.2-2). Isolated periods of active air injection occurred in well I-4 on September 26 and 27, while steam injection was stopped. The possible causes of these and similar short spikes in injection rate in well I-6 are unknown at present. The supply of compressed air to the injection wells continued after resumption of steam injection on September 22 until the end of steam injection on November 19.

Air injection pressures were stepped up to their final levels of 825 kPa (8.2 atm) for I-4, I-5, and the deep and mid levels of I-6 and 620 kPa (6.1 atm) for the shallow interval in I-6 between October 4 and 14. In well I-5, air continued to be injected at low rates (typically 0.028 scmm (1.0 scfm) or less) throughout the period of operation. In all other wells, although they remained pressurized throughout, air did not enter the formation at a measurable rate.

After the end of steam injection on November 19, air injection was resumed, and air entered the formation through all screened intervals at rates of up to 0.071 scmm (2.5 scfm). In each well, the sustainable injection rate after prolonged steam injection was somewhat lower than in the early period of aggressive air injection on September 22-23.

Air injection in the retrofit wells VEA-5, I-7, and I-8 (deep screened intervals only) was started on November 19, immediately after cessation of steam injection, and continued until the last day of operations at the site on November 26 (Figure 6.1.2-2). Injection pressures of 585-825 kPa (5.8-8.2 atm) were maintained in VEA-5 and I-7, corresponding to injection rates of 0.034-0.071 scmm (1.2-2.5 scfm). In well I-8, a lower injection pressure of 345-550 kPa (3.4-5.4 atm), corresponding to an injection rate of about 0.042 scmm (1.5 scfm), could be maintained. As discussed in Chapter 8, this period led to large increases in the PID headspace readings on the extracted water as well as increased contaminant concentrations in the vapor phase effluent.

6.2. Extraction Rates

6.2.1. Vapor Extraction Rates

Vapor flow rates (total from all the extraction wells) were measured immediately upstream from the V-1 sample port just after the final liquid-vapor separator and the air drier (See Figure 5.2.2-1) using a pitot tube, and are summarized in Figure 6.2.1-1.

Flow rates from individual wells were measured using pitot tubes inserted in the 0.05 meter (0.17 foot) vapor pipe from each extraction well, and used to balance the applied vacuum between the wells (data not shown). Typical well head vacuums observed were in the 1.7 to 10.2 kPa (0.017 to 0.100 atm) range. The pitot tube readings were corrected for the vacuum using a standard equation supplied by the manufacturer.

Total vapor extraction rates in the initial period of operations were variable, ranging from 7.25 scmm (256 scfm) to a high of 10.3 scmm (363 scfm) on September 3. The failure of one of the two vacuum pumps on that day caused a drop in extraction rate to about 5.66 scmm (200 scfm), which continued until September 4, at which time the second vacuum pump failed, and vapor extraction was stopped. The extraction of vapor was restarted using a single vacuum pump on September 5 at an initial rate of 5.9 scmm (209 scfm). Extraction continued at a rate of 5.1-7.9 scmm (180-280 scfm) until October 1. On this date, the second vacuum pump was brought back on-line, allowing the vapor extraction rate to be increased to 8.3 scmm (292 scfm). Extraction was continued at 7.1-8.5 scmm (250-300 scfm) until frost damage on November 2 caused one of the vacuum pumps to fail for a second time. The extraction rate then rapidly decreased to 5.1 scmm (179 scfm) on November 3, at which time a mechanical failure in the remaining vacuum pump ended vapor extraction. Vapor extraction was resumed using a single vacuum pump on November 5. The initial extraction rate was set at less than 5.7 scmm (200 scfm) and was gradually increased to 6.2 scmm (219 scfm) by November 9. Extraction was continued at 5.7-6.6 scmm (200-233 scfm) until November 26, when it was reduced to 3.6 scmm (127 scfm) briefly before final shut down at the end of field operations.

During operations, a total of 824,000 cubic meters (29.1 million cubic feet) of non-condensable vapor was extracted from the formation.

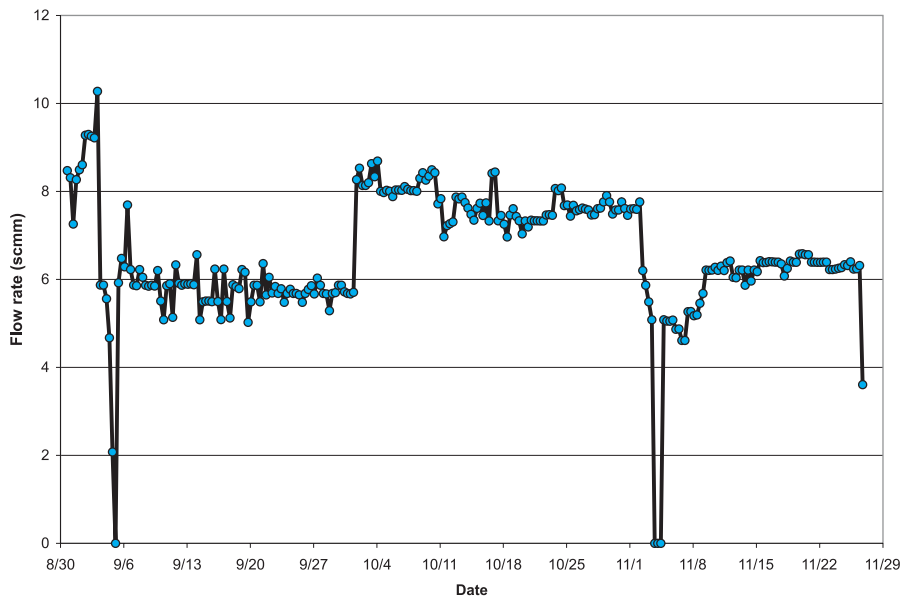


Figure 6.2.1-1. Extracted vapor flow rates.

6.2.2. Ground Water Extraction Rates

The cumulative volume of liquid from individual pumps was monitored at each well head using pump stroke counters. In addition, the combined liquid volume pumped from the wellfield was monitored at W-1 (See Figure 5.2.2-1.). The volume of condensate transferred from the liquid-vapor separators in the vapor treatment system was monitored upstream from its point of entry to the main liquid treatment system. As a further means of assessing liquid flow rates, the output volume of the liquid treatment system to the GAC canisters was monitored at point L-1. Three days after the start of pumping from the wellfield (September 3), imperfect seals in the check valves of several of the deep pumps were found to have contributed to discrepancies in the individual well volume totals. In addition, the introduction of air to the liquid lines had led to an overestimation of the total wellfield pumped liquid volume. The faulty seals in the deep pumps were replaced during the course of operations. However, as a result of the initial problem, the total wellfield liquid volume was calculated as the difference between the total treatment system output (location L-1) and the condensate input (location KO-2) for the remainder of operations at the site. The average flow rate from the wellfield for each 8-hour period during operations is summarized in Figure 6.2.2-1.

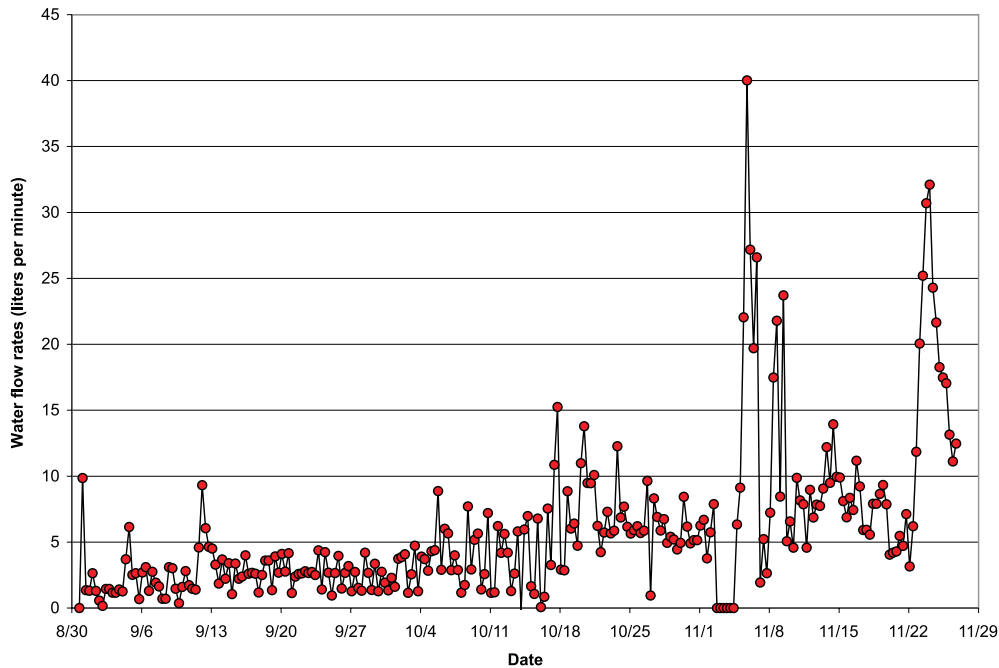


Figure 6.2.2-1. Extracted liquid flow rates for wellfield (calculated for point W-1 based on L-1 and KO-2 data).

During the first month of operation, the total liquid extraction rate was typically below 7.6 lpm (2 gpm). Later, the extraction rate increased to between 7.6 and 15 lpm (2 and 4 gpm), and peaked at 40 lpm (11 gpm) for a short period when the system was re-started after a shut-down period in the first week of November. The extraction rate peaked again at about 32 lpm (8 gpm) later in November, during an aggressive extraction period after steam injection had been ceased on November 19.

Over the course of this field test, a total of 739,000 liters (195,200 gallons) of water was extracted as a liquid phase. Figure 6.2.2-2 shows the cumulative water amounts extracted from each well.

It is evident that some of the extraction wells produced significantly more water than others. The wells that produced the most water were EX-1, EX-3, EX-4, I-2, and I-3 (all located either on the north or middle row of boreholes). It should be noted that well I-7 produced the most water of all the wells prior to its conversion to steam injection on October 15. It can also be seen that many of the wells had a sharp increase in their extraction rates at different times, particularly just after steam injection was terminated. The increased pumping rates were used to lower the water level in the boreholes to increase the pressure drop between injection and extraction wells, as part of the pressure cycling in the subsurface.

6.3. Water Balance

6.3.1. Methods

The water mass balance is calculated as follows:

$$M_{\text{net extraction}} = M_{\text{out, liquid}} + M_{\text{out, vapor}} - M_{\text{in, steam}}$$

The steam injection rate was estimated for each of the injection wells based on steam flow measurements:

$$M_{\text{in, steam}} = \sum (m_{\text{in, steam}} \times dt)$$

where $m_{\text{in, steam}}$ is the flow rate, and t is time. Each value of m was calculated based on an orifice plate pressure drop reading and the temperature of the steam. Average values for each day of injection were used.

The data from the steam measurements were compared to two additional lines of data used to document the actual steam production rates:

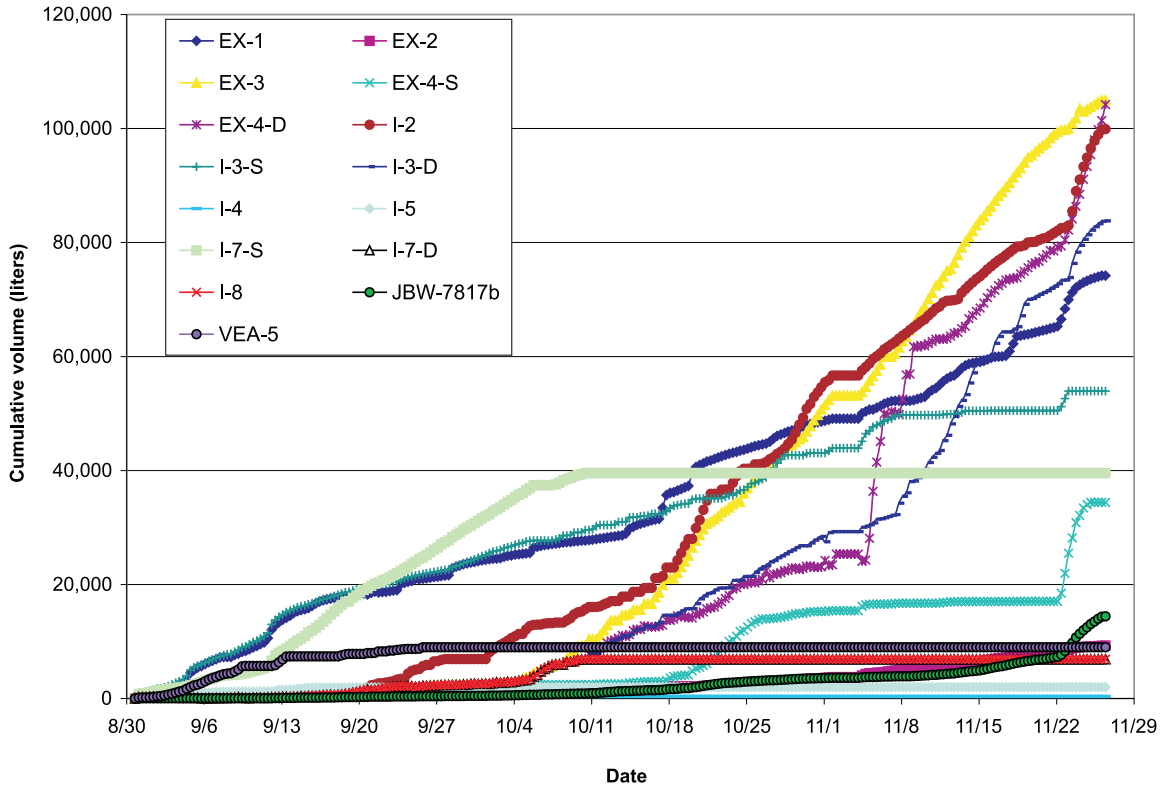


Figure 6.2.2-2. Cumulative water extraction from each of the extraction wells, based on corrected stroke counter measurements.

1. The diesel usage was converted to an equivalent steam production rate, assuming a boiler efficiency of 85 percent, and a diesel energy content of 39,000 kJ per liter (140,000 Btu per gallon). This was done during the first month of steam injection, and the numbers matched relatively well (data not shown).
2. The water used by the boiler (minus the amount of blow-down water which was metered separately) was converted to equivalent steam injection rates. The total rates were compared and found to match relatively nicely (data not shown).

Overall, the data from orifice plate measurements, diesel usage, and water usage matched within 10 to 20 percent. This was taken as evidence that the boiler was operating as designed, and that a steam quality of at least 80 percent was achieved. Since the water usage data were recorded most frequently, and appeared to have the best resolution (the meter reading would also capture fluctuations between readings), these data were used for the mass and energy balance calculations.

The mass removal in the liquid form is a simple summation of the measurements from each of the extraction pumps:

$$M_{\text{out, liquid}} = \Sigma (m_{\text{liquid}} \times dt)$$

where the values for m_{liquid} were derived from a pump stroke counter installed for each pump.

The mass removal in the form of vapor (steam, water vapor) ideally is calculated by the liquid production rate in the condenser:

$$M_{\text{out, vapor}} = \Sigma (m_{\text{condensate}} \times dt)$$

where $m_{\text{condensate}}$ is the flow rate of condensate, measured by a flow meter.

The net extraction was estimated based on the water balance equation presented in the beginning of this section. Similarly, net water extraction rates were estimated by the difference of the measured flows:

$$m_{\text{net extraction}} = m_{\text{liquid}} + m_{\text{vapor}} - m_{\text{in, steam}}$$

The liquid mass was determined by the flow meter at location W-1, or the difference between L-1 and KO-2 readings at times when air in the liquid lines made W-1 readings unreliable. The mass corresponding to the vapor flow was determined from the KO-2 flow-meter, which measured the amount of condensate produced by cooling the extracted vapors.

6.3.2. Results

Both flow rates (in lpm) and cumulative masses (in liters) were calculated for the appropriate streams (Figures 6.3.2-1 and 6.3.2-2).

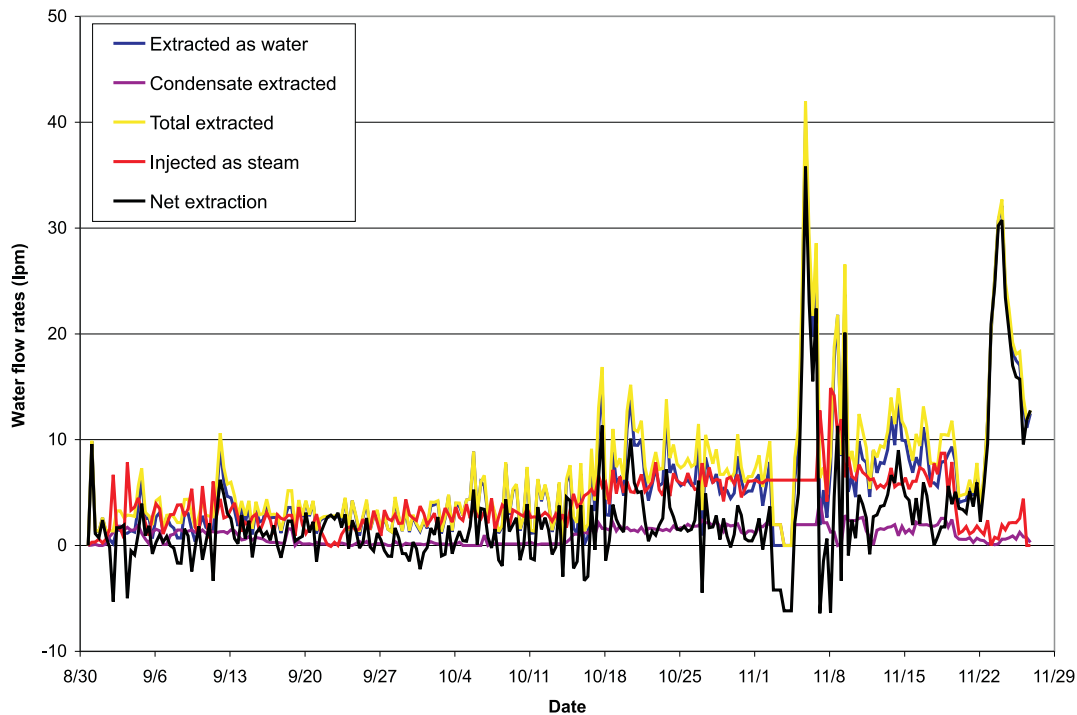


Figure 6.3.2-1. Water flow rates for the various injection and extraction streams. The steam was converted to equivalent liquid flow.

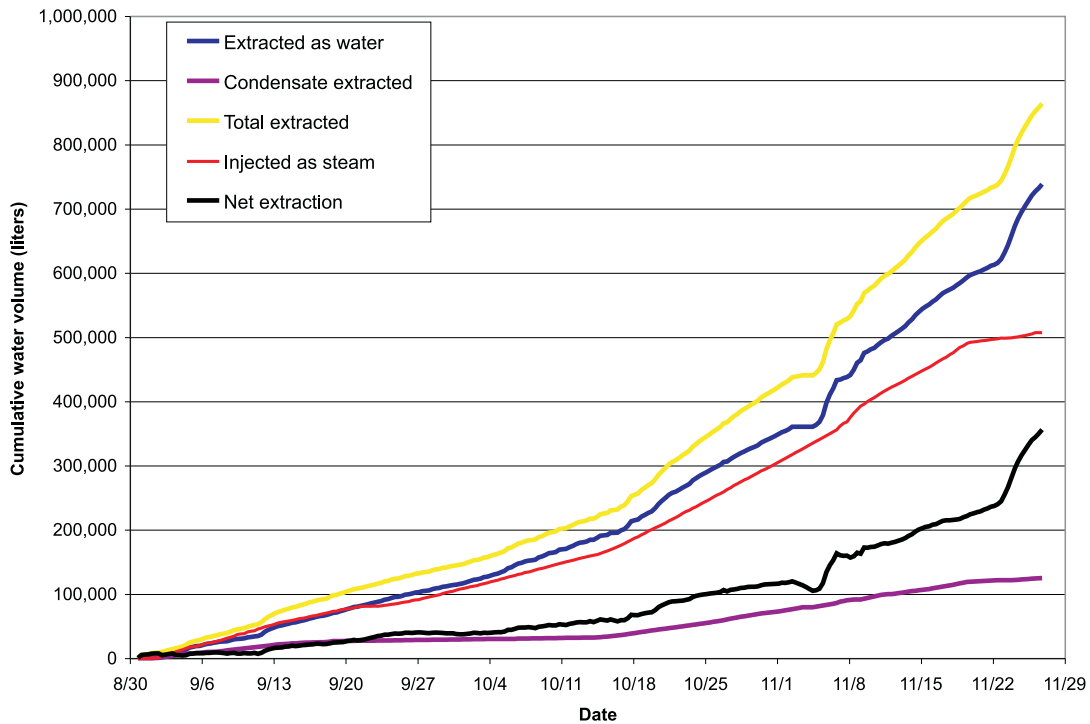


Figure 6.3.2-2. Cumulative water volumes and balance. The steam volume was converted to equivalent water volume.

The mass balance shows 507,000 liters (134,000 gallons) injected as steam and 844,000 liters (223,000 gallons) extracted, for an overall net extraction of about 337,000 liters (89,000 gallons) during operations. This is likely significantly more than a pore volume of the target area. Extracted steam condensate accounted for approximately 125,000 liters (33,000 gallons), or about 15 percent of the recovered water, and about 25 percent of the steam injected. However, it is likely that a large part of this steam migrated from injection to extraction intervals within the same borehole (I-4, I-5, I-7, I-8). This steam would not have contributed significantly to overall site heating.

Water flow rates were very modest for a site of this size. Liquid extraction rates generally were in the 2 to 15 lpm (0.5 to 4 gpm) range for all the extraction wells combined. Similarly, steam injection rates were modest, ranging from a typical 2 to 7.6 lpm (0.5 to 2 gpm), which is equal to 115 – 454 kg/hr (250 – 1,000 lbs/hr) total for the injection wells combined, despite the relatively high injection pressure used. It was only after a shut-down (on November 5) and during aggressive pressure cycling (November 23-24) that water extraction rates exceeded 26 lpm (7 gpm) for all the wells combined. When it occurred, the duration was short. These observations support the geologic interpretation and the slug-test results which indicated that fractures are sparse and have limited permeability, and that the resulting rock has overall low hydraulic conductivity.

The mass flow rates reveal that while overall net extraction was assured by always maintaining a net cumulative water extraction for the site, there were short periods where the injection rate exceeded the extraction rate (where the black line falls below the zero line on Figure 6.3.2-1). Since these periods were short, and interspersed with longer periods of net extraction, the mass balance shows that overall, more water was entering than leaving the target volume during the test.

This large volume of water that was pulled into the site was partially caused by the less-than-optimal design for the injection and extraction system that was used here. With the original design, which would have surrounded the target area with injection wells while extracting from the center of the area (See Figure 4.0-1), the amount of water extracted from outside the target zone would have been limited. However, the design was altered due to contaminant distribution and interconnectivity considerations, and extraction only took place at the western side of the site. This allowed large amounts of water to be pulled towards and into the extraction system. Some of the water might have been moved long distances. Figure 6.2.2-2 shows that EX-3 and I-2 were two of the largest producers of water; these wells were also two of the wells that were the furthest from the injection wells. They could have pulled in water from the west and north of the target area. Well I-7 was also producing a significant amount of water before it was converted to an injection well, and this well could have pulled in water from the south. Thus, it is likely that water moved into the site laterally from at least three directions.

6.4. Energy Balance

6.4.1. Methods

Cumulative energy (E) is calculated as a summation of enthalpy fluxes (Q):

$$E = \Sigma (Q \times dt)$$

An estimated energy balance was maintained for the site:

$$E_{in, steam} = E_{out} + E_{net}$$

where $E_{in, steam}$ represents the cumulative energy delivered by steam injection, E_{out} is the cumulative removal of energy by the extraction wells, and E_{net} is the net addition of energy to the site. The latter value is used later to estimate the heated volume of rock, based on the measured quantities of injected and extracted energy.

The energy fluxes are related for each time step as follows:

$$Q_{in, steam} = Q_{out} + Q_{net}$$

where Q denotes enthalpy flux (in kJ/hr; Btu/hr). Energy increments are estimated as follows:

$$Q_{in, steam} = \Delta m_{in, steam} \times \Delta H_{steam-ambient}$$

where m is mass of steam. This calculation was done for each of the injection wells, and average daily values were used for the steam flow rates. The enthalpy of the steam was calculated from steam tables, using a steam pressure of 550 kPa (5.4 atm), and an ambient temperature of 15°C (59°F):

$$\begin{aligned} \Delta H_{steam-ambient} &= (2756 - 58) \text{ kJ/kg} = 2698 \text{ kJ/kg} \\ &= (1,185 - 25) \text{ Btu/lb} = 1,160 \text{ Btu/lb} \end{aligned}$$

The enthalpy flux was calculated for the joint liquid stream to the treatment system:

$$Q_{liq} = \Delta m_{water} \times c_{p, water} \times (T - T_0)$$

For the extracted vapor stream, the energy flux in vapor and steam was calculated based on treatment system data:

$$Q_{non cond. gas} = \Delta m_{air} \times c_{p, air} \times (T - T_0)$$

$$Q_{steam out} = \Delta m_{condensate} \times \Delta H_{steam-ambient}$$

where m is mass, H is specific enthalpy (in kJ/kg; Btu/lb), c_p is heat capacity (in kJ/kg/C; Btu/lb/F), T_0 is background temperature, and T is temperature.

The total energy removal from the test volume was estimated as follows:

$$Q_{out, total} = Q_{liq} + Q_{non cond. gas} + Q_{steam out}$$

The temperatures achieved and measured using the temperature sensors were compared to the temperatures estimated based on the calculated energy balance. The stored energy is related to the target area heat capacity, and the measured average temperature as follows:

$$E_{storage} = C_{p,site} \times (T_{avg} - T_0) + m_{steam} \times \Delta H_{steam-ambient}$$

where $C_{p,site}$ is the overall heat capacity of the target area, estimated from the volume (V) and specific heat capacity of the rock and water:

$$C_{p,site} = V_{rock} \times c_{p, rock} + V_{water} \times c_{p, water}$$

The steam energy stored as a vapor at any given time is relatively small, and was neglected in the calculations. For comparison with the measured temperatures, the energy balance was used to estimate the average temperature ($T_{energybal}$) of the target area volume:

$$T_{energybal} = T_0 + E_{storage}/C_{p,site} = T_0 + (E_{in, steam} - E_{out} - E_{loss})/C_{p,site}$$

where T_0 is set as the average background temperature (10°C; 50°F).

6.4.2. Results

Figure 6.4.2-1 shows the enthalpy fluxes in and out of the site. Figure 6.4.2-2 shows the cumulative energy balance.

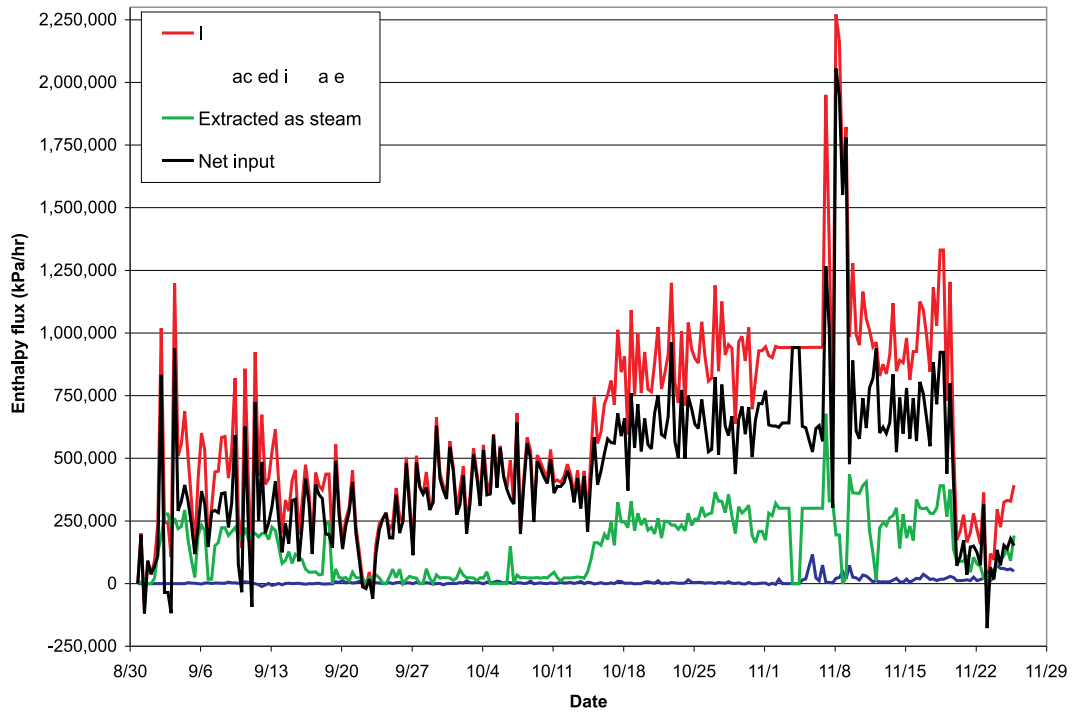


Figure 6.4.2-1. Enthalpy fluxes for the various streams during operations.

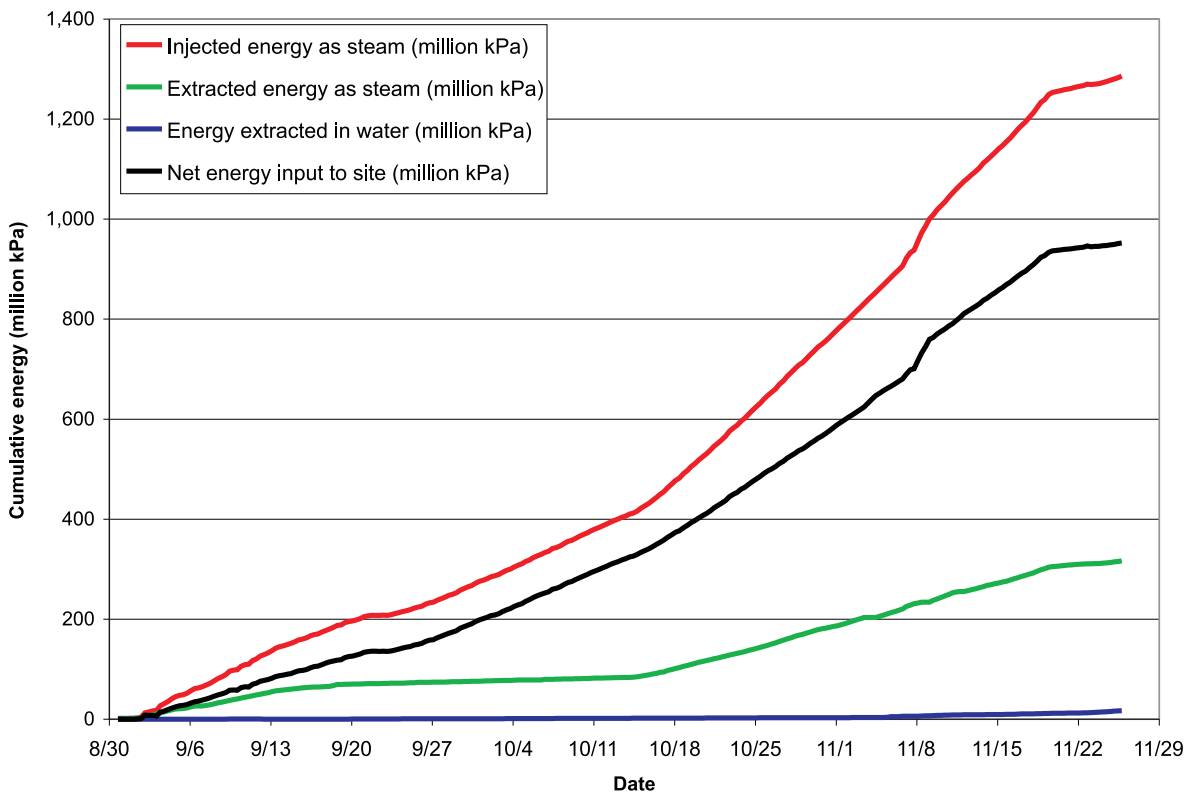


Figure 6.4.2-2. Energy balance with cumulative energies for the various streams during operations.

Overall, 1,286 million kJ (1,219 million Btu) of steam energy were injected, and 316 million kJ (300 million Btu) were extracted as steam. Since the pumped water remained relatively cool, only about 17 million kJ (16 million Btu) were extracted with the water. This is a very unusual result when compared to other sites, where the water typically accounts for a large fraction of the removed energy. This reflects the fact that the site was not adequately heated during the period available for steam injection. A net energy addition of about 950 million kJ (900 million Btu) was achieved, with the net energy increasing throughout operation.

Until the addition of three steam injection wells on October 14, the enthalpy flux of the injected steam remained in the 263,000 to 791,000 kJ/hr (250,000 to 750,000 Btu/hr) range. After addition of the three other wells, the total enthalpy flux increased to between 791,000 and 1,319,000 kJ/hr (750,000 and 1,250,000 Btu/hr). During aggressive pressure cycling from November 7 to 9, enthalpy fluxes were increased to the 2,110,000 kJ/hr (2,000,000 Btu/hr) range (Figure 6.4.2-1).

The enthalpy removal in the form of extracted steam generally followed the steam injection rates (green curve shown in Figure 6.4.2-1). This energy removal began as soon as the steam injection began, indicating that at least a part of the extracted steam migrated within or near the injection boreholes to the upper extraction intervals. It is impossible to say whether this steam migrated through fractures and then returned to the boreholes through other fractures, or whether the steam penetrated the grout seals in the boreholes. However, the overall effect was to reduce the energy delivery to the bulk of the target area volume, while allowing the entire injection boreholes to be at steam temperature. The hot borehole then led to heating by thermal conduction away from the boreholes.

It is expected that steam heating will be highly heterogeneous in a fractured rock setting. Despite this fact, energy calculations that provide estimates of average heating rates, or the volume of rock that could be heated to a certain temperature, may be of interest. Figure 6.4.2-3 presents such a calculation.

Based on the energy balance (yielding the overall net energy addition to the site), an average temperature can be estimated for a given volume assumed to be impacted by the operations. Using a heat capacity value of 0.879 kJ/kg/K (0.21 Btu/lb/F) for limestone, an area of 15 meters (50 feet) by 45.7 meters (150 feet), an average depth of 27.4 meters (90 feet), and a porosity of 1 percent, the estimated energy needed to raise the whole site to boiling is about 4,010 million kJ (3,800 million Btu). Since only a net amount of 950 million kJ (900 million Btu) was deposited (Figure 6.4.2-2), the calculated average site temperature is relatively low, and remains below 32°C (88°F) (Figure 6.4.2-3). The average temperature increase that can be expected is in the 20°C (68°F) range.

Using the energy balance, the volume that could have been brought to the co-boiling temperature (87°C; 189°F) and to 100°C (212°F) can be estimated. These volumes increase steadily during operation, as the net energy did. An estimated volume of 4,500 cubic meters (159,000 cubic feet) can be heated to boiling (100°C; 212°F) by the energy deposited during operation (Figure 6.1.1-2). This is about 22 percent of the target area volume. The volume that could be heated to the co-boiling temperature was estimated as 7,000 cubic meters (246,000 cubic feet), which is approximately 27 percent of the target area volume.

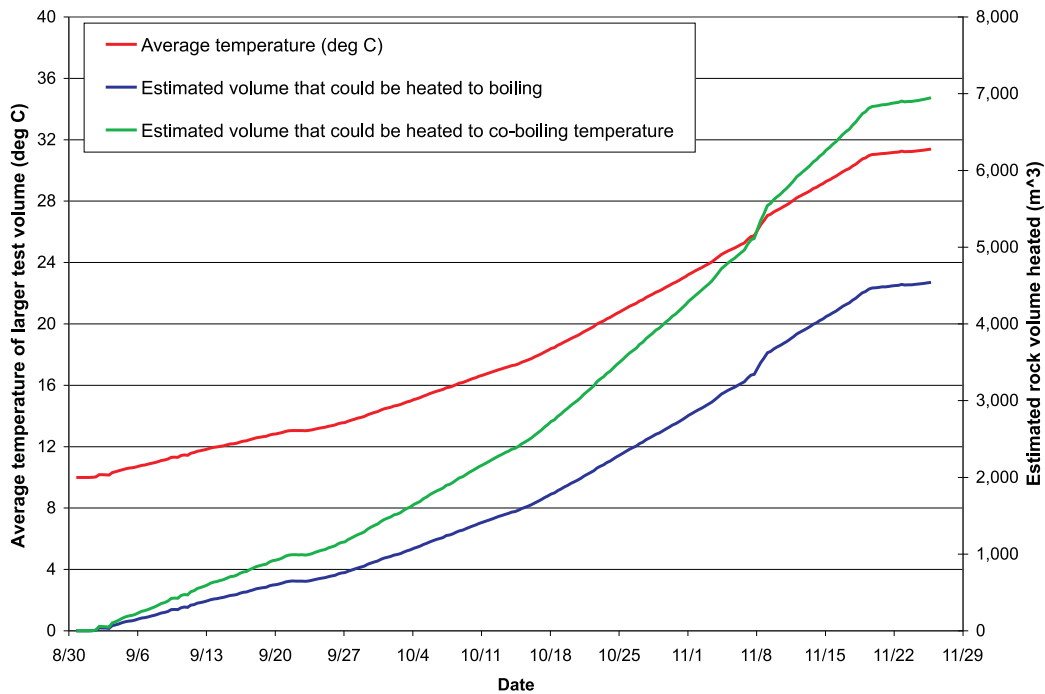


Figure 6.4.2-3. Calculation of average subsurface temperature in the test volume and estimated rock volumes that could be heated to 87 and 100°C (189 and 212°F). Calculations were based on the net energy addition to the site from Figure 6.4.2-2.



Chapter 7. Subsurface Temperature and ERT Monitoring Results

7.1. Temperature Monitoring

Temperature monitoring was carried out using Digital Thermocouples (DigiTAMs), which were read using a prototype digital thermocouple recorder. Summary charts of temperature versus time for all borings on dates when data were collected and temperature versus depth profiles for selected dates are contained in Appendix I.

7.1.1. General Trends in Heating

The background temperature profile of each well and boring was collected immediately before the beginning of steam injection in August 2002. All of the profiles had a similar outline, with a temperature at the bottom of the wellhead casing of 13-18°C (55-64°F). The temperature rapidly declined through the vadose zone to reach 6-8°C (43-46°F) at the water table (Figure 7.1.1-1). The background temperature in the saturated zone remained within this range to the total depth in all borings and wells. The fixed position and wide spacing (1.5 meters; 5 feet) of the thermocouples prevented their use to locate discrete fractures where temperature anomalies might indicate entry or exit of ground water from the wellbores.

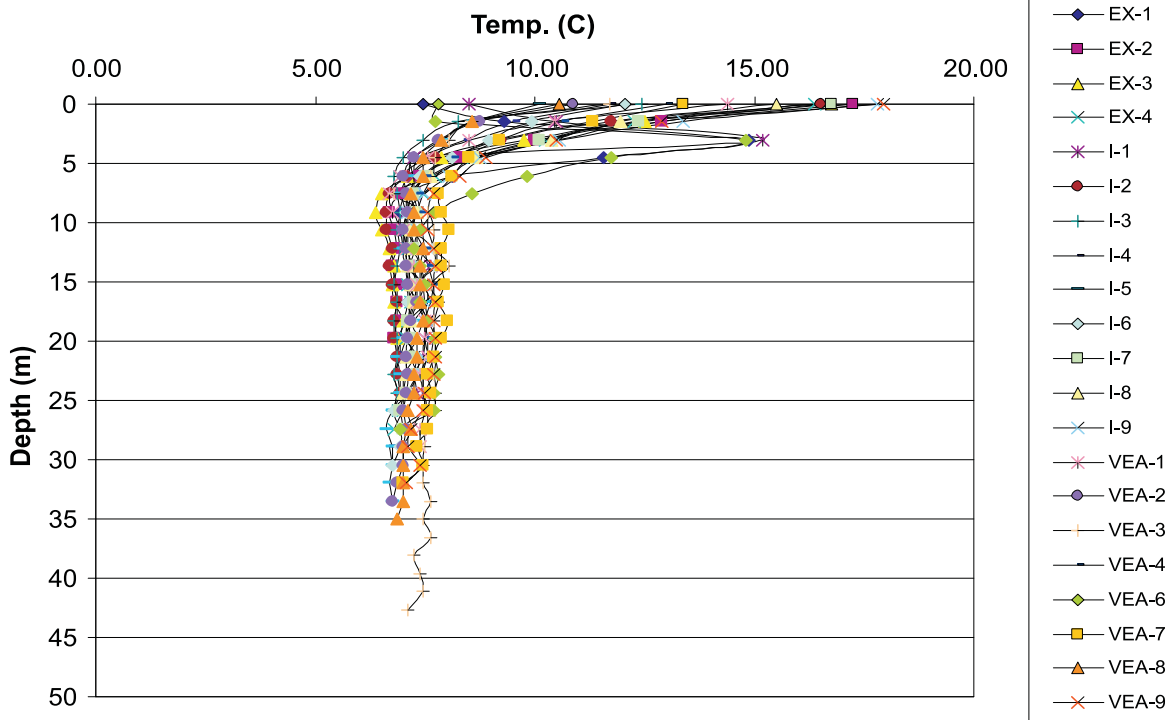


Figure 7.1.1-1. Background temperature profiles in site wells.

Steam injection began on September 1 in wells I-4 and I-5 at depths greater than 21 meters (70 feet) and in three separate intervals in I-6 at depths of 10-15 meters (30-50 feet), 18-24 meters (60-80 feet), and 27-34 meters (90-110 feet). Sparse data from the steam injection wells (Plate 7.1.1-1) show a very rapid increase to around 100°C (212°F) in all three injection wells. Areas adjacent to the grout plugs are typically somewhat cooler than the open wellbores, while the deepest measurements in wells I-5 and I-6 show no immediate significant rise in temperature in the first few days of injection. Plotting the first appearance of heating in temperature versus time plots (defined as a temperature increase of greater than 1°C (2°F) degree in the saturated zone) allows the progressive heating of the site to be seen in three phases (Figure 7.1.1-2):

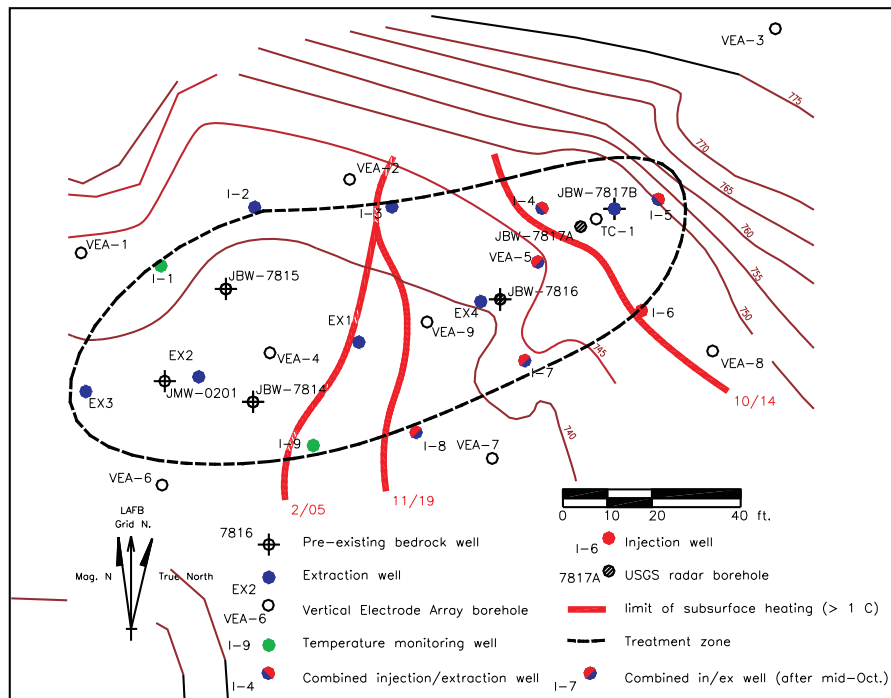


Figure 7.1.1-2. Interpreted progression of heating across site.

- Phase 1 extended from September 1 until October 14, during which time the original three injection wells were in use, and heating was restricted to the eastern area of the site.
- Phase 2 extended from October 14, when the retrofitted steam injection wells (I-7, I-8, and VEA-5) were brought into use, until the end of steam injection on November 19, during which time heating extended into the central area of the site.
- Phase 3 extended from the end of steam injection until the last temperature measurements in early February 2003, during which time heat up continued and expanded in the western and central areas of the site, and cool down began at the eastern and southern boundaries of the site after a short period of continued temperature increase in the eastern area.

During the first phase, heating was apparently restricted to the eastern region. The group of wells consisting of JBW-7817A, TC-1, and JBW-7817B show a similar pattern of heating, although data are only available from shallow depth for JBW-7817B (Figure 7.1.1-3).

Boring VEA-8 also records a slight heat up during this period. The lower temperature increase at this location may be a reflection of the greater distance that heated water would necessarily travel from the closest steam injection well at I-6. The relatively modest temperature increase during this period (17°C (31°F) in JBW-7817A; 30°C (54°F) in TC-1; 4°C (7°F) in VEA-8) indicates that no steam connection had been made between the adjacent steam wells and the monitoring wells. However, heated water was being circulated by indirect routes between these wells. The lack of heating in well VEA-5, which is closely adjacent to steam well I-4, strongly suggests that hot water movement is essentially restricted to NW-SE movement. This lies parallel to the strike of bedding and of the NW-trending joint sets. The restriction of circulation of heated water to the eastern area of the site is in accordance with predictions of connectivity made after extensive aquifer testing at the site (Stephenson and Novakowski, 2004; see Appendix H).

The limited area and intensity of heat up in the first month of steam injection led to the retrofitting of extraction wells I-7, I-8, and VEA-5 for steam injection. This introduced heat sources to the central area of the site, an area which previous aquifer testing had indicated to have a limited connection to the eastern area. A rapid increase in temperature was apparent in wells EX-4 and JBW-7816 (Figure 7.1.1-4), in which a response was first apparent within four days of steam injection in the retrofit wells. These wells saw a maximum rise of 14-16°C (25-29°F) within the saturated zone by the end of steam injection on November 19. Well VEA-7, which was about 6 meters (20 feet) from the closest steam well, saw a temperature rise of about 6°C (11°F) in November, while VEA-9 and I-3 saw slight (greater than 1°C; 2°F) rises in temperature in November also. The very limited heating observed during November in I-3 and VEA-7 suggested that the movement of heated water along strike of bedding from the new steam injection wells was less significant in this part of the site than had been the case in the eastern area. Similarly, the limited heating observed in VEA-9, despite the fact that it lies a short distance up-dip from EX-4 (which had undergone rapid heating), suggests that up-dip migration of heated water in this part of the site was more limited than had been the case in the eastern area.

The site continued to show temperature increases in some areas for a period after cessation of steam injection on November 19 (see Plate 7.1.1-2). The impact of this continued circulation of heated water is most apparent in the eastern part of the central area, where rises in temperature of 1-3°C (2-5°F) were seen in EX-1 and I-9 (Figure 7.1.1-5). In those areas of the site adjacent to steam injection wells, heating was seen to reach a peak within a month of the end of steam injection, after which time the maximum temperatures began to decline. A migration of the peak temperature southwards and westwards from the steam wells is apparent, notably in the eastern area and around the southern boundary of the site. Also, by early February 2003, steam well I-8 had cooled to a lower temperature than the adjacent monitoring point VEA-7 (Figure 7.1.1-6), suggesting the migration of a “pulse” of heated water away from the site in a broadly southerly direction. Temperature monitoring was not continued in all wells after late December, so the true extent of continued temperature rise in the area of VEA-9 in February 2003 cannot be determined.

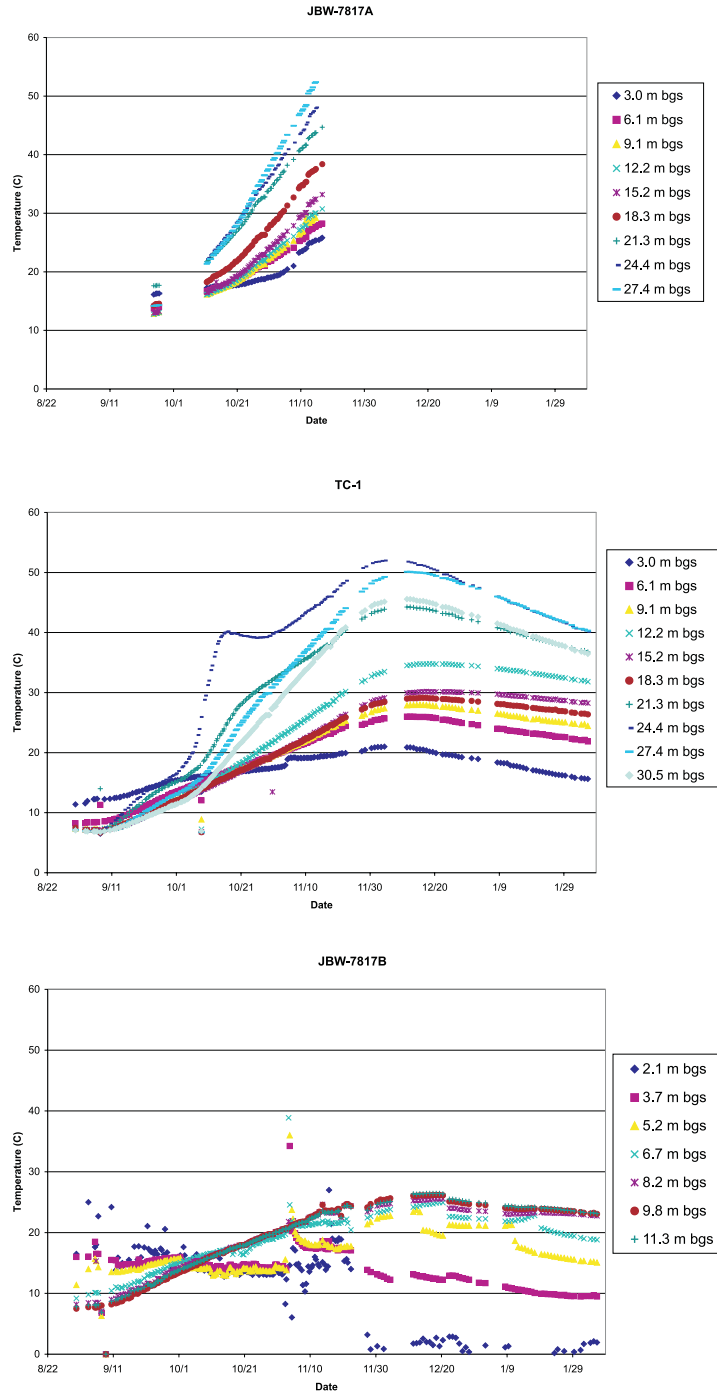


Figure 7.1.1-3. Temperature profiles of wells in the eastern area.

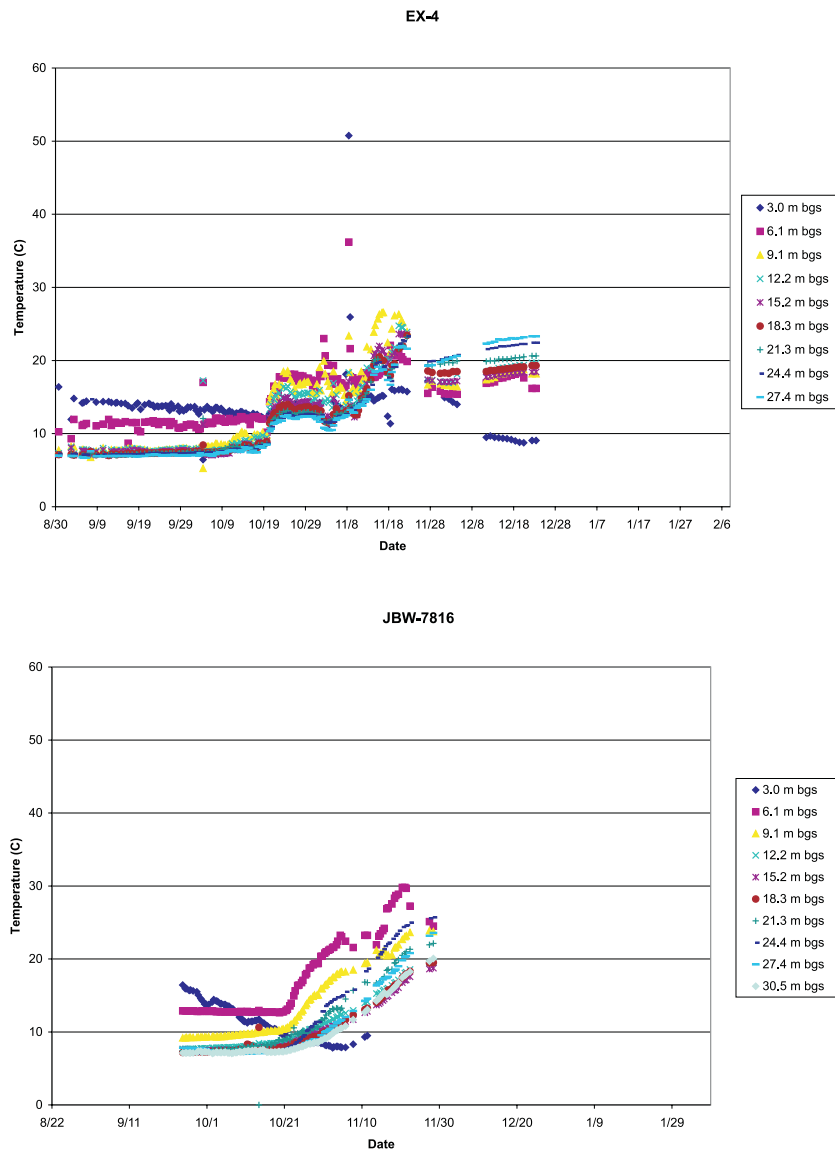


Figure 7.1.1-4. Temperature profiles of wells in central area showing heat up after October 14.

7.1.2. Temperature Data Supporting Interconnectivity Testing

When profiles of temperature versus depth are plotted using data from selected “milestone” dates, a time sequence can be constructed. The earliest profile plotted shows the conditions immediately prior to commencement of steam injection at the site, the second profile shows the temperature profile after approximately six weeks of steam injection and just before the conversion of VEA-5, I-7, and I-8 from extraction wells to steam injection wells, the third shows conditions when all of the steam injection wells were in operation, and the fourth shows the temperatures on the day that the steam injection ceased. The existence of a significant rise in temperature between the second and third profiles indicates that the retrofit and subsequent steam injection in the new wells had created steam/heat/hot water migration pathways that were previously not accessed. The fourth profile does not always correspond to the highest temperatures achieved in a monitoring well, as heat continued to migrate after the injection of steam had ceased, due to conduction and ground water flow.

The temperature profiles can be grouped into four categories:

- Profiles showing a constant temperature increase throughout steam injection.
- Profiles showing a temperature rise occurring after addition of new steam wells.
- Profiles showing a response that may suggest vertical migration of heat.
- Profiles showing temperature increase at a distance from the injection wells.

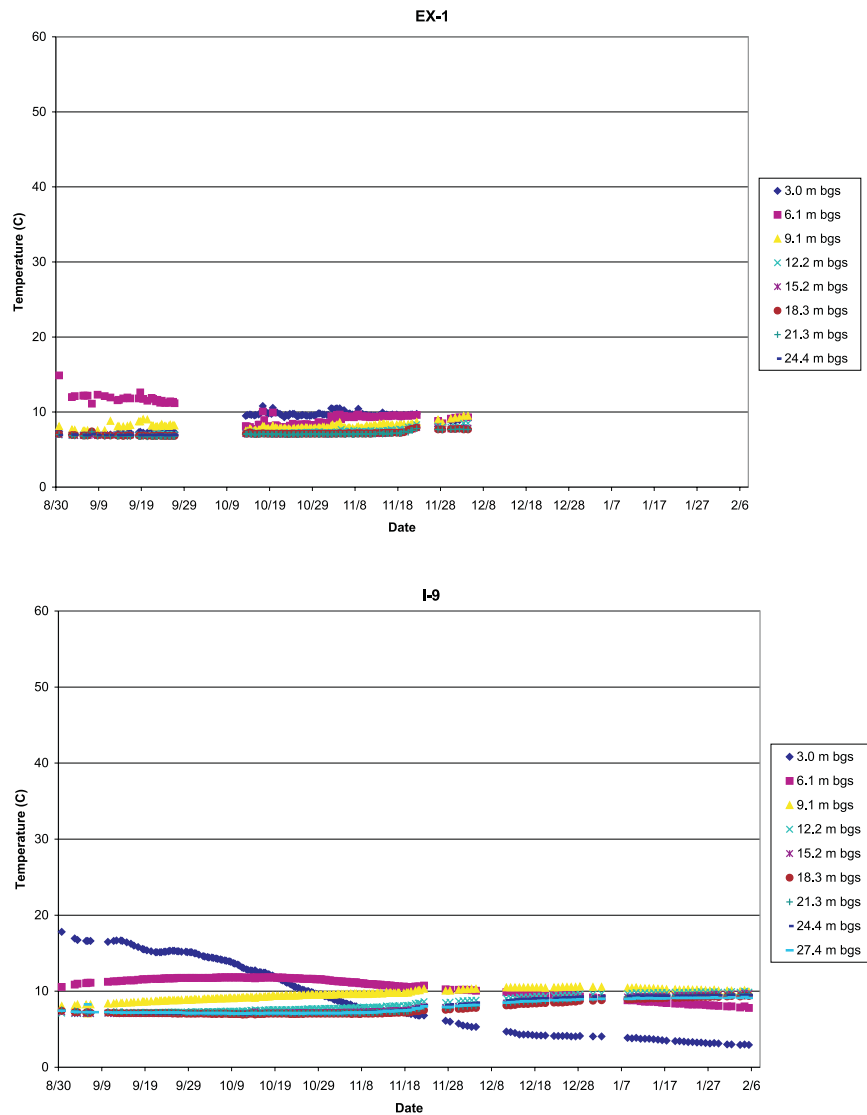


Figure 7.1.1-5. Temperature profiles of wells in western area showing heat up after November 19.

7.1.2.1. Profiles Showing a Constant Temperature Increase

Several temperature monitoring locations showed a significant and constant temperature increase from the beginning of steam injection through to the time when injection ceased. Within the area of the original steam injection wells in the eastern portion of the site, a steady temperature increase was seen in wells EX-4 and TC-1 at depths of approximately 20 and 24 meters (65 and 80 feet), respectively. This anomaly was considered to probably be associated with a single bedding-parallel fracture, perhaps correlating with the open, partly mineralized bedding-parallel fractures at 21.3 and 24 meters (69.9 and 80 feet) in core from these wells. In these wells, increases in temperature were also observed at depths ranging from 9 to 15 meters (30 to 50 feet). These shallower peaks in the temperature profile suggested the presence of heat migration through two distinct features in EX-4 and through a single, or two closely-spaced, fractures in TC-1. In both wells, bedding plane fractures showing staining or weathering are present at these depths in recovered core. An additional peak in the temperature profiles, interpreted as indicating heat migration, occurs at greater depths in both wells. In both wells these temperature peaks lack any obvious correlation with fractures logged in core. The presence of a “vertical” fracture with a “strong diesel odor” at 25.6 meters (84 feet) bgs in EX-4 may represent the source of heating at 26-27 meters (85-90 feet) bgs in the temperature profile for that well.

The location of the temperature anomalies are indicated on the temperature versus depth profiles in Figures 7.1.2.1-1 through 7.1.2.1-5. Significant temperature increases in an individual well can often be related to heat migration along bedding plane features. Vertical fractures also likely play a role in many cases, for example, the temperature peaks at 20 and 27 meters (65 and 90 feet) bgs in EX-4 probably correspond to high-angle northeast and northwest striking fractures logged in core. However, these features probably serve to connect bedding plane features that extend across the site.

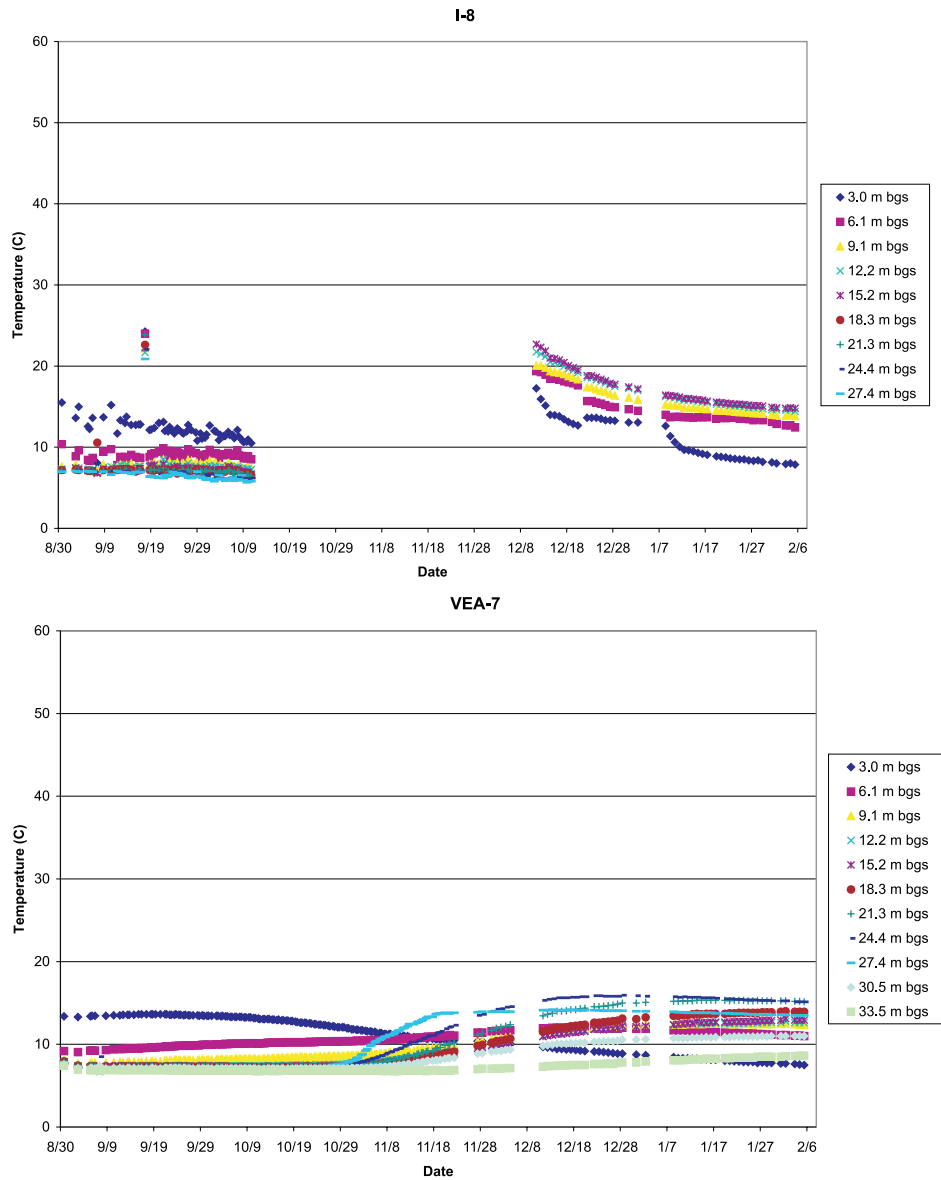


Figure 7.1.1-6. Temperature profiles of well I-8 and boring VEA-7 on southern boundary of site, showing rise in temperature of peripheral boring VEA-7 while adjacent steam injection well I-8 cools.

Figure 7.1.2.1-1A shows the temperature versus depth profile for well TC-1. A large temperature increase is evident at a depth of 24 meters (80 feet). The depth of the temperature increase corresponds to the prominent bedding plane features logged in core at this depth and to the location of a strongly interconnected zone identified during pulse interference testing (See Figures 4.2-6 – 4.2-10.). A temperature increase was also observed in TC-1 at depths of 12 and 17 meters (40 and 55 feet). These increases were considered to be the result of upward migration of steam entering shallower open bedding plane fractures, or perhaps the product of lateral migration of steam along strike of bedding plane fractures from the shallow injection interval in I-6. These shallow features in TC-1 were also identified during hydraulic testing. Precise correlation of temperature anomalies with fractures logged in core, or ATV imagery, is rendered problematic due, in part, to the 1.5-meters (5-feet) resolution on temperature readings in the grouted thermocouple monitoring boreholes, and possibly also to the effect of mixing in the open wells in which the thermocouple arrays were installed. Temperature spikes associated with shallower features also were seen in EX-4, VEA-7, JBW-7816, and VEA-3. A small temperature increase in TC-1 was observed at a depth of 29-30.5 meters (95-100 feet), which may correspond to a prominent bedding plane fracture logged in core at a depth of 28.5 meters (93.5 feet). The use of deep steam injection intervals in I-4, I-5, and I-6 is considered to have allowed this deeper bedding plane feature to be accessed.

Figure 7.1.2.1-1B shows the temperature response in monitoring well VEA-8. A temperature increase is evident at a depth of 32 meters (105 feet). This feature was considered by Stephenson et al. (2003) (See Appendix H) to be associated with the same

fracture observed in TC-1 at 24 meters (80 feet) bgs (Figure 7.1.2.1-1A). Although pulse testing was not completed between any of the injection wells and VEA-8, it is thought that the features mentioned above extend to VEA-8 and that they played a major role in heat migration during operations. Evidence of the effect of heat migration in shallower features is also visible within the temperature profile of VEA-8. The temperature rises observed in this well are the largest of any of the monitoring wells with the exception of TC-1, which lies in the center of the injection well group (I-4, I-5, I-6 and VEA-5). This suggests that considerable off-site migration of heat occurred along-strike of northwest-striking fractures (most probably bedding fractures) towards the southeast.

It is particularly noteworthy that there is evidence of a major fracture pathway for heated water occurring at this depth in VEA-8, as transmissivity profiling of this boring (summarized in Chapter 4.1.4) indicated very low transmissivity throughout the borehole. A similar situation was present in the retrofit steam well I-7, which showed comparably low transmissivity in its initial profile based on water injection studies, yet ultimately had a higher ground water extraction rate and then steam injection rate than wells with higher measured transmissivity. This apparent paradox may in part be a product of the different behavior of water at ambient temperature used during transmissivity and interference testing compared to the use of a hot vapor at elevated pressure during steam injection. However, these observations may also indicate the limitation of carrying out short duration injection testing of the type used in transmissivity profiling and pulse interference testing at this site. In low permeability, fractured bedrock such as is present at the Loring Quarry, long-term drawdown tests would potentially enable more subtle interwell connections to be identified, while allowing the wider zone of influence of hydraulic perturbation during steam injection and extraction to be established. In addition, the existence of several wells that performed somewhat better than initial transmissivity profiling would have suggested underscores the importance of using a range of types of measurements and observations, including transmissivity profiling, pulse interference testing, detailed head mapping and monitoring, temperature monitoring, core logging, and integration with regional mapping to develop a better understanding of fracture systems in the subsurface.

Some evidence of down-dip heat migration was also observed towards the northeast, in VEA-3 (Figure 7.1.2.1-5D). This well lies at some distance down-dip and is approximately twice as distant from the main injection wells as VEA-8. A significant temperature increase was only observed in this well at depths of 36 and 39 meters (120 and 130 feet) bgs, about one month after the end of steam injection. The temperature continued to increase at a slow rate until the last temperature measurement was taken in February 2003.

Figure 7.1.2.1-1C shows the temperature profile of well JBW-7817A. A strong temperature anomaly was present at a depth of 23 meters (75 feet) that is probably the product of heat migration in an open, partly mineralized bedding plane fracture logged in BIPS imagery at 22.2 meters (72.8 feet) bgs. This well had an open-hole thermocouple string configuration, and the effects of mixing are apparent from the smooth temperature profile (in contrast to the profiles with distinct “spikes” displayed in wells where the thermocouples were grouted into place).

The temperature anomalies detected in the depth profiles are so commonly associated with bedding plane-parallel fractures that heat migration appeared to have largely occurred within bedding-plane parallel features, with steeper bedding-crossing fractures having acted as connections between bedding plane fractures. Stephenson et al. (2003) further suggested that the groups of temperature increases seen in all wells and borings were associated with features (identified as BP1, BP2, BP3, and BP4) that could be correlated across the site. These features crossed the boundaries of the supposed isolated hydrogeological areas identified by hydraulic head measurements. It was thought that hot water was able to cross these boundaries under steam injection conditions because of the continuous injection at high rates for extended periods into the dominant open bedding plane fracture features. A “pinching off” of bedding plane features or a decrease in fracture aperture at the perimeter of an area defined by a “plateau” in hydraulic head would not stop heat migration even though hydraulic testing at low pressures over short periods and hydraulic head measurements indicated the boundaries to be largely impermeable.

The temperature versus depth profile of TC-1 offers the clearest picture of the prominent heat migration pathways at the site. When the location of those pathways was considered in combination with the location of hydraulically connected features identified by pulse interference testing, a conceptual model for heat migration and ground water flow can be developed. If the location of these features is extended across the site using the bedding plane dip and considering the varying surface elevations, their presence is indicated in several wells. The features that are shown in TC-1 will appear at a higher elevation in the up-dip (south-westerly) direction and a lower elevation in the down-dip (north-easterly) direction. Assuming a bedding plane dip of 25 degrees in the eastern part of the site, this can be expressed as an approximate gain or loss of 1.4 meters (4.7 feet) in feature elevation for every 3 meters (10 feet) traveled in the up- or down-dip direction. For example, the four heat migration features observed in TC-1 at 12, 17, 24, and 30 meters (40, 55, 80, and 100 feet), would all be predicted to appear 9.8 meters (32 feet) away in an up-dip direction in EX-4 at depths of 7.6, 12, 20, and 26 meters (25, 40, 65, and 85 feet) bgs, respectively. The temperature versus depth profile for EX-4 (Figure 7.1.2.1-2B) shows temperature anomalies at 7.6, 10.7, 13.7, 20, and 27.4 meters (25, 35, 45, 65, and 90 feet) bgs. This can be interpreted as a result of the coalesced BP2,3 feature in TC-1 having diverged into separate features in EX-4 at 10.7 and 13.7 meters (35 and 45 feet) bgs. The individual contributions from BP2 and BP3 may be indistinguishable in TC-1 due to the close spacing of the features relative to the thermocouple spacing or because at least one of the features in EX-4 corresponds to an east-dipping bedding crossing fracture. Several BIPS, ATV, and geophysical logs recorded low-angle (less than 15 degrees) fractures of this orientation. While this interpretation is effective for the eastern part of the site, attempts to correlate structures associated with individual temperature increases across the entire site in a manner consistent with the mapped variations in bedding plane

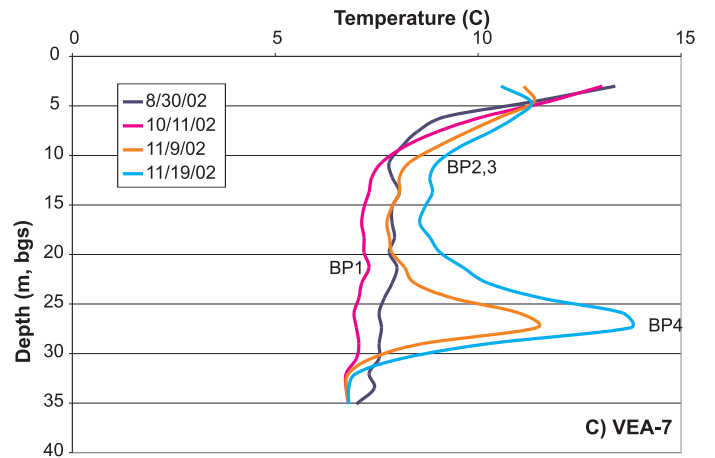
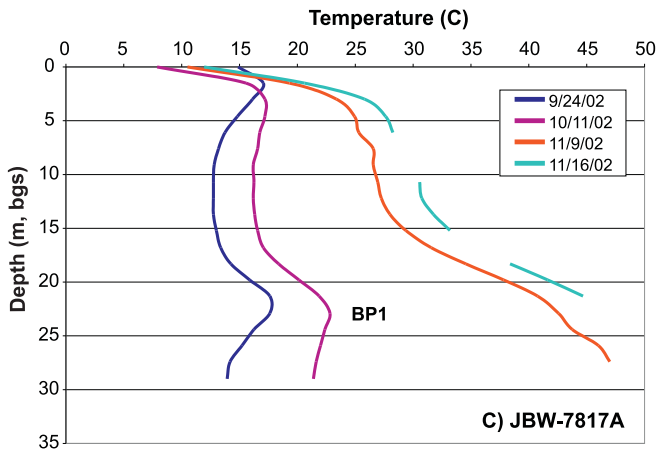
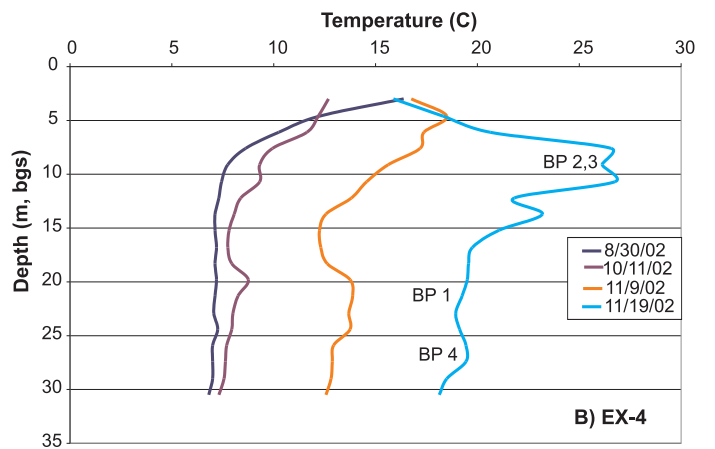
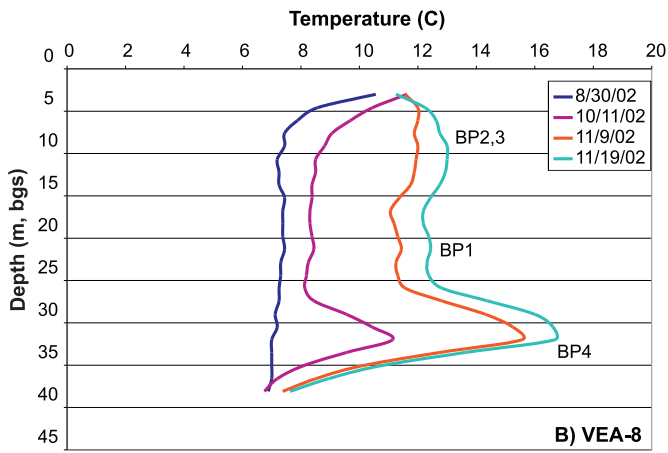
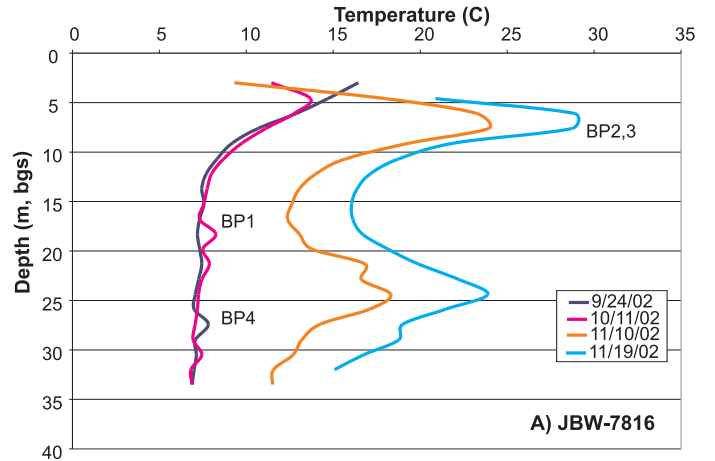
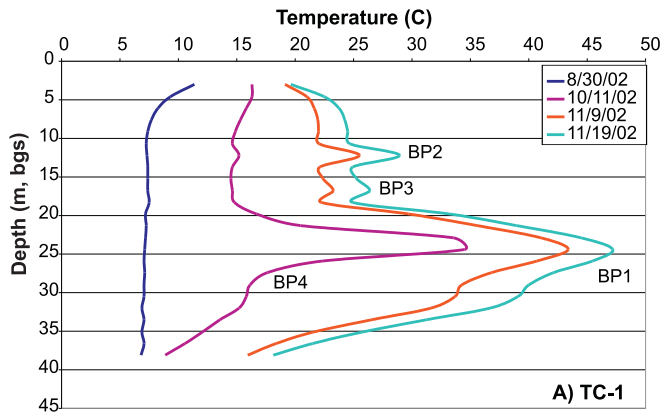


Figure 7.1.2.1-1. Wells exhibiting constant temperature increase.

Figure 7.1.2.1-2. Wells exhibiting post-retrofit temperature increase.

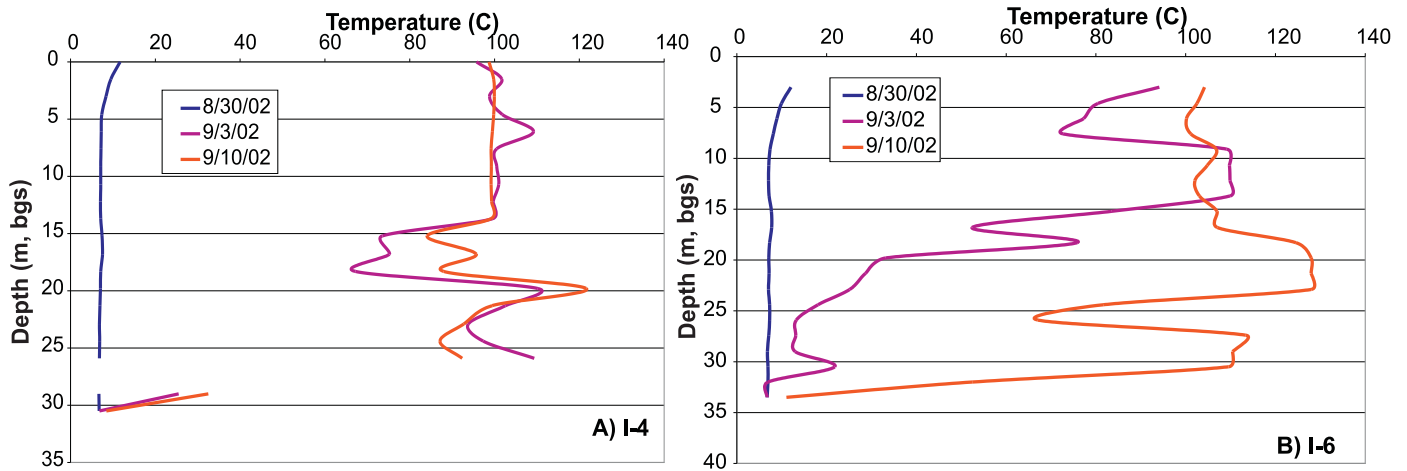


Figure 7.1.2.1-3. Wells exhibiting evidence of vertical heat migration.

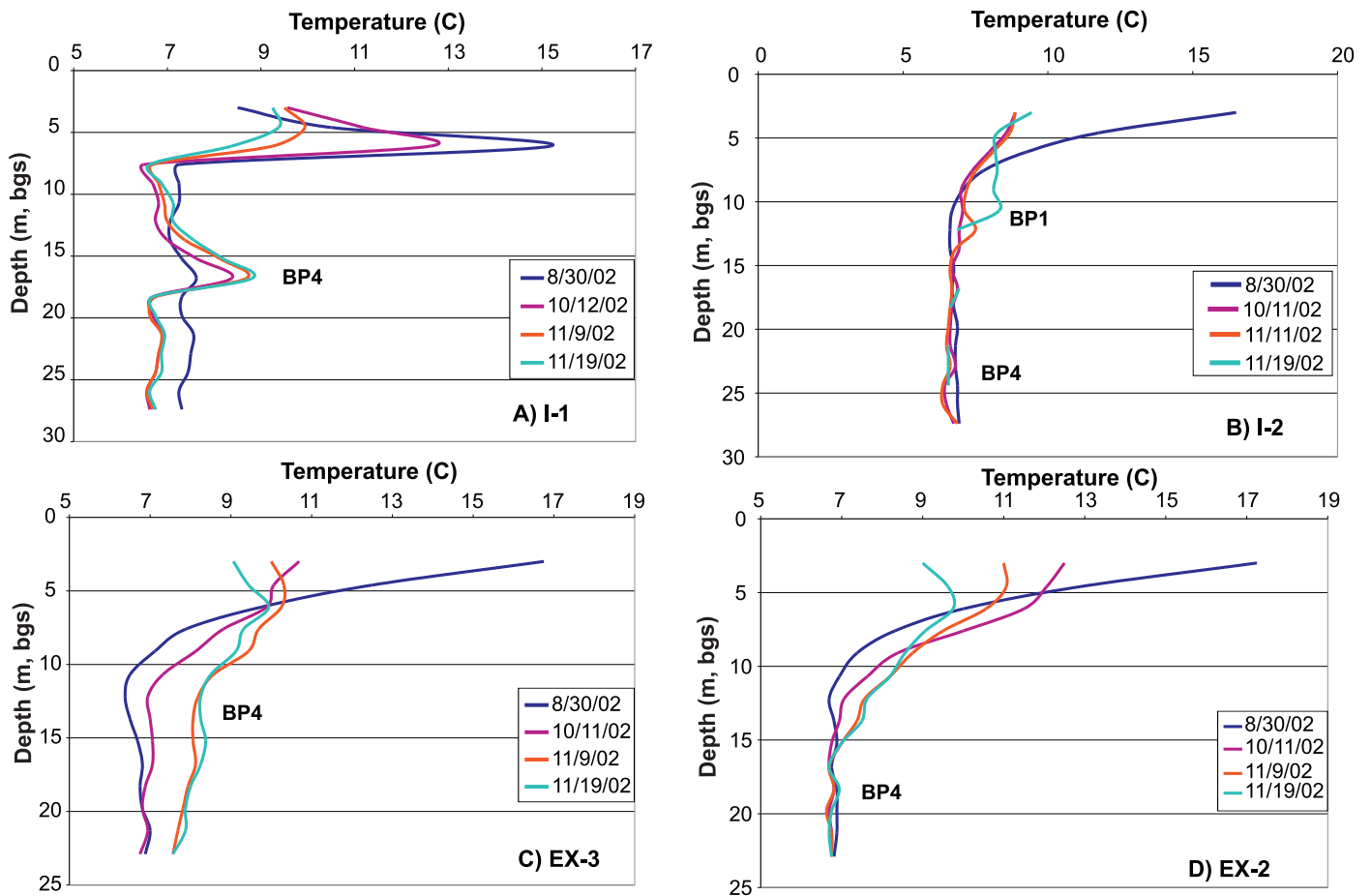


Figure 7.1.2.1-4. Wells exhibiting long distance temperature response.

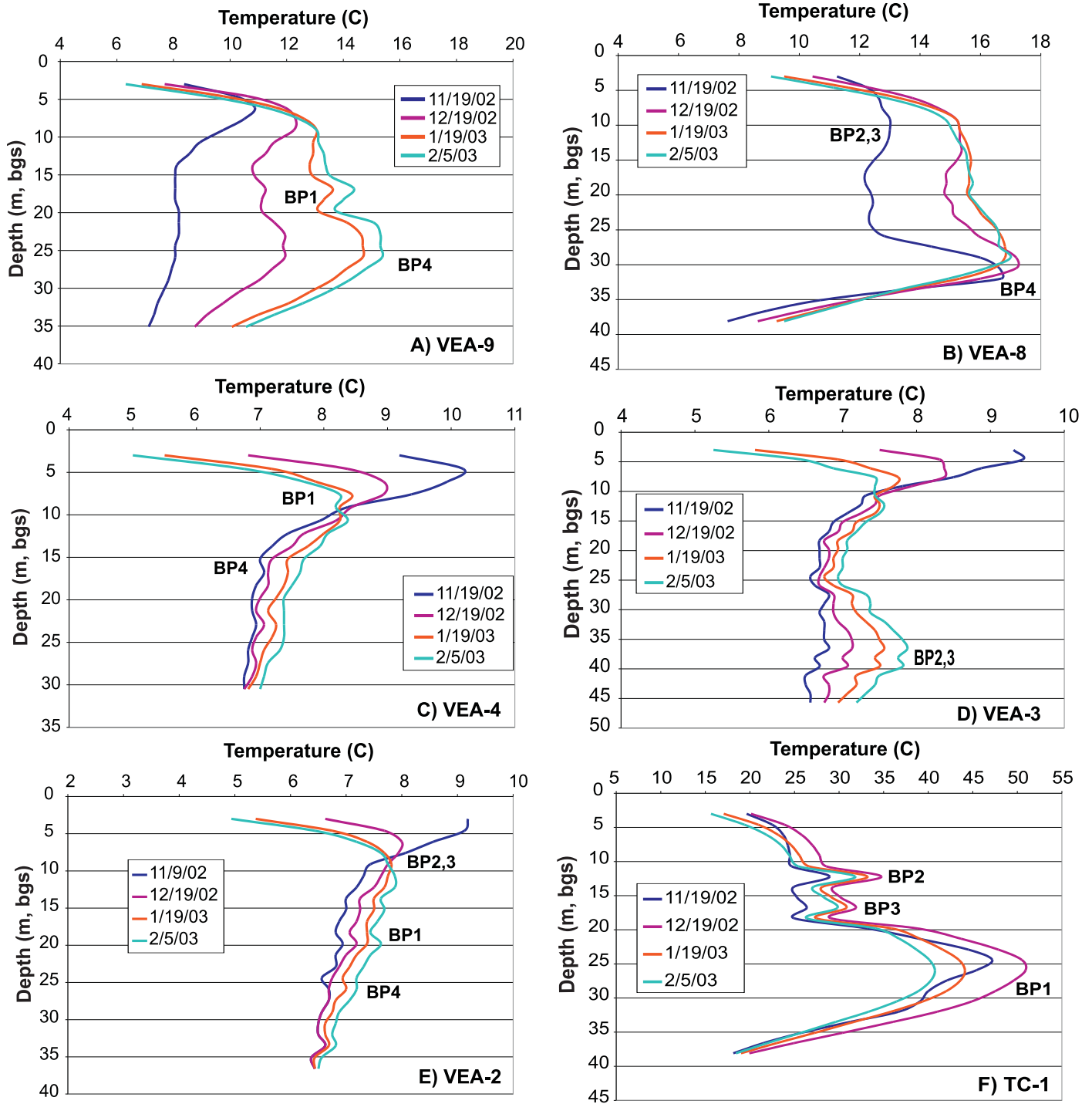


Figure 7.1.2.1-5. Post-injection temperature monitoring profiles.

orientation have proved to be problematic. While there are reasons to assume that bedding plane fractures probably control and localize fluid flow and heat migration over distances of up to ten or so meters locally, there is no basis for assuming that individual bedding fractures form significant fluid conduits over greater distances. It seems probable that high-angle structures, including small faults, joints, and fracture cleavage, may all serve to link areas of fluid flow within closely spaced and parallel groups of bedding plane fractures.

7.1.2.2. Profiles Showing a Post-Retrofit Temperature Increase

Some monitoring well temperature profiles indicate a significant increase only after wells I-7, I-8, and VEA-5 were converted into injection wells. Well I-8 lies within the central area delineated during the interconnectivity testing and hydraulic head measurements. Injection into this well was probably the cause of the significant thermal migration observed in the monitoring wells lying within the central area after the retrofitting of wells. Although steam injection into the eastern area did cross the boundary between the eastern and central areas, steam injection directly into the central area allowed more heat to be injected and to be delivered to interconnected wells in this area along higher aperture features.

The thermal response in JBW-7816 is shown in Figure 7.1.2.1-2A. This response clearly displays the effect of the presence of two viable fracture feature interconnections. The second deepest feature, at a depth of 18 meters (60 feet), probably corresponds to the open, partly mineralized bedding plane fractures seen at 18.2-18.3 meters (59.7-60 feet) bgs in BIPS imagery. It is correlated with a similar feature in JBW-7817A at 22.2 meters (72.8 feet). A deeper feature is also present in this temperature profile and occurs initially at a depth of 27 meters (90 feet) and subsequently becomes more pronounced at 29 meters (95 feet) bgs. This may correspond to an open fracture identified in BIPS imagery at 29.3 meters (96.1 feet) bgs. The significant post-retrofit temperature increase in JBW-7816 over the total depth of the well could be the result of heat conduction due to the close proximity of the monitoring well to the new injection wells, particularly I-7 and VEA-5.

Figure 7.1.2.1-2B shows the temperature profile increase in EX-4 after the retrofit. Heat migration at shallower depth is thought to have occurred between the mid-depth or bottom injection interval in I-7 to the monitoring and extraction well EX-4, at a depth of 7.6-10.7 meters (25-35 feet). This well is very close to JBW-7816 and similar trends are present within the two temperature profiles. Figure 7.1.2.1-2C shows the response in VEA-7. This well is in close proximity to injection well I-8 and shows a large temperature increase at a depth of 27 meters (90 feet) bgs.

It is difficult to assess the cumulative effects of injection wells in order to confirm that three separate areas occur across the site based on the thermal migration data alone. Hydraulic head measurements suggest that this is the case, and the temperature profile displayed in JBW-7816 (Figure 7.1.2.1-2A) does not contradict this evidence.

7.1.2.3. Profiles Showing a Response that Suggests Vertical Heat Migration

Evidence that may indicate vertical heat migration through vertical fractures is visible in temperature data collected from early time temperature data in wells I-4 and I-6. Figures 7.1.2.1-3A and 7.1.2.1-3B show the temperature profiles in these wells early in operations, when all steam injection was through the deepest screens (i.e., below 21 meters; 70 feet). The presence of features BP1 and BP4 is evident in both wells. Upwards vertical migration of heat into features BP2 and BP3 most probably resulted in the temperature increase observed in these shallower features. Stephenson et al. (2003) present evidence to demonstrate that a temperature increase of the magnitude observed in these wells could not have occurred by conduction through unfractured rock rapidly enough to have produced the response seen in I-4 and I-6. It should be noted that no vertical fractures of any extent were logged in core recovered from these wells. The rapid increase in temperature seen in these wells may also be a consequence of heat migration within fractures at the contact between the wellbore and the grout plugs in these wells. Temperature data from the other wells used for steam injection are insufficient to test this possibility.

Several other monitoring wells exhibit a temperature increase of less than 2°C (4°F) in the upper 12-20 meters (40-65 feet) intervals. These wells include JBW-7814, VEA-2, VEA-6, JMW-0201, VEA-1, VEA-4, and EX-1. These modest increases can be attributed to the overall heating of the site. It is probable that heat migration in the shallow, permeable zone and vertical heat migration through deeper vertical fractures combined to cause these temperature increases.

7.1.2.4. Profiles Showing Evidence of Long-Distance Thermal Migration

Hydraulic testing data and hydraulic head measurements across the site suggest separated areas of interconnectivity, with areas showing some connection across boundaries at depth. These boundaries are probably zones of lower fracture aperture that only small quantities of water could penetrate. The modeling exercises conducted by Stephenson et al. (2003) show that very small fracture apertures combined with high injection rates, such as those used at this site, can result in thermal migration over long distances.

Figure 7.1.2.1-4A shows the temperature profile of I-1. The temperature increase shown in this profile occurs at a distance of about 30 meters (100 feet) from the nearest injection well, and it occurs within the first few weeks of operation. The temperature increase occurs at a depth of 16.7 meters (55 feet), which may correspond to an open, partly mineralized fracture with associated weathering logged at 16.8 meters (55.3 feet) depth in core. This feature cannot be readily correlated with any other temperature anomaly by projection down-dip towards the east using the observed variation in bedding orientation along this path. However, it is considered unlikely that such a marked, yet localized, temperature excursion was unrelated to the injection of steam at the site. Stephenson

et al. (2003) speculated that the high steam injection rates into this feature from both I-4 and I-5 and possibly other injection wells produced a velocity in a single structural feature, or more probably a group of linked, bedding-parallel features, of such magnitude that heat was able to migrate a distance of almost 30 meters (100 feet) without dissipation to the surrounding matrix. A smaller matrix thermal diffusivity than was assumed for modeling purposes may have also contributed to this transport process.

The existence of a connection between the eastern end of the site and I-1 in the western end was suggested by the pulse interference testing data, in which a single connection between wells I-4 and I-3 was apparent. Testing also indicated a connection between wells I-2 and I-3. While the connections between wells I-2 and I-1 were not investigated during the pulse interference testing, the existence of a connection between these wells is considered to be likely due to similarities in hydraulic head in the two wells and the short interwell distance.

Similar temperature increases, however slight, are also observed at large distances in Figures 7.1.2.1-4B, C and D. These figures show the response in wells I-2, EX-3, and EX-2 respectively. These wells are all located at distances greater than 9 meters (30 feet) from the nearest injection well, and all show an increase in temperature significantly earlier than the analysis presented by Stephenson et al. (2003) predicted for injection from one depth interval (or well) only. Possible fracture features are identified in these figures; however, the same ambiguity arises in the analysis of these wells as in the case of I-1 due to possible bedding plane orientation changes over larger distances.

In sedimentary formations, the importance of open bedding plane fractures for ground water flow has been well documented (e.g., Mackie, 2000; Michalski and Klepp, 1990; Morin et al., 2000; Novakowski and Lapcevic, 1988). Where this type of feature was located at the Loring Quarry, it was found to play a large role in the delivery of heat across the site. Off-site migration may have occurred along the primary features discussed in this Chapter, as the boundaries identified by head measurements apparently inhibited, but did not prevent, the radial heat migration initiated at the injection wells. Heat migration and contaminant mobilization may have occurred away from the injection wells if not limited by areas of low permeability or extraction wells.

7.1.3. Post-Steam Injection Temperature Monitoring

The wells described in the previous section were monitored for a three-month period after the steam injection ceased (from November 19, 2002 through February 17, 2003). The extraction wells were taken off line approximately one week after the end of steam injection. It is evident that the extraction had some effect on thermal migration; however, it is difficult to assess this effect due to the number of extraction points distributed across the site and the lack of thermal and hydraulic monitoring locations beyond the limits of the treatment area. In addition, thermal distributions were never measured at a time when extraction wells were not in operation while injection was underway. This action would have provided more information on the influence that extraction wells have on steam and heat migration. Several wells (VEA-9, VEA-8, VEA-4, VEA-3, VEA-2, and TC-1) gave evidence of further heat migration after steam injection had ceased (See Figure 7.1.2.1-5A-F). The locations of these features have been indicated beside temperature profiles presented in Figure 7.1.2.1-5A-F.

7.1.4. Post-SER Borehole Investigation

During July 2003, eight boreholes were completed within the area treated by the SER system (See Chapter 9.1.). In addition to the recovery of rock chip samples for assessment of contaminant distribution, the fracture features that were thought to play a major role in the SER system were observed in some of the boreholes. For example, a drill-back borehole completed in close proximity to TC-1 (BD I-5-6; see Plate 4.1.2-1) revealed the presence of a fracture feature at a depth where the projection of the 24.4 meter (80 feet) bgs fracture feature in TC-1 would be predicted to lie. The fracture, shown in Figure 7.1.4-1, showed staining and stress fracturing had occurred above and below the fracture, probably due to high injection pressures. It appeared that this fracture carried the majority of steam/hot water and possibly distributed steam/hot water to other bedding plane fractures via connections made through vertical fractures.

In conclusion, it can be stated that, while monitoring data collected during the operation of the steam remediation pilot test tended to confirm the validity of the pre-operational conceptual model, the injection of steam at high pressures over an extended period of time allowed certain fracture connections and fluid pathways to be identified that could not have been identified using only the aquifer test methods employed.

7.2. Subsurface ERT Monitoring

In order to provide a resistivity standard against which changes generated during the demonstration could be evaluated, two sets of background ERT data were collected on August 29 and 30. The background data were used as a resistivity baseline for the calculation of difference values used in developing time-lapse images of the change in subsurface resistivity and conductivity over time.

The earth resistivity meter suffered a hardware failure immediately after the background data had been collected. Troubleshooting and modification of the meter prevented the collection of any further data during the initial period of operations from September 1-10. Data collection resumed on September 11 and continued on a daily basis throughout steam operations, then on a lesser frequency during the cooling phase until January 2003.



Figure 7.1.4-1. Fracture at 23.4 meters (76.9 feet) bgs in BD I-5-6.

The raw ERT data binary files were processed using PROSYS® software, produced by IRIS Instruments, to generate data files prior to inversion. These data were then subjected to resistivity inversion processing using EarthImager® software, produced by Advanced Geosciences, Inc. (AGI). EarthImager® software was used to produce two-dimensional electrical resistance tomography models for multiple boreholes. It was also used to produce percentage difference time-lapse images by comparing background model data to subsequently collected model data to obtain the percentage difference in resistivity and conductivity.

The resolution of the ERT data was equal to approximately one half the electrode spacing (i.e., 0.76 meters; 2.5 feet). Modeling conducted by SteamTech and by sub-contractors indicated that the ERT profiles produced could be expected to detect linear conductive features of as little as 1 meter (3 feet) in length, having a diameter less than 0.01 meter (0.03 feet) – a feature comparable in scale to a fluid-filled, or steam-filled, fracture.

The processed and inverted data were used to generate two-dimensional images that were exported as jpg files in which resistivity was represented as a continuum on a color scale. All images were generated using the same color scale to allow easy comparison of time-sequences. Images produced from each data set were of measured resistivity, change in resistivity relative to background data (expressed as a percentage), and change in conductivity relative to background data. Plots of change in conductivity (the reciprocal of resistivity) have been found to produce images of sharper contrast in fractured rock settings, allowing narrow linear features to be more easily discerned. Images of relative change in conductivity for all planes on dates when data were collected are contained in Appendix I. Plotting of changes in conductivity (as the reciprocal of resistivity) revealed increases of up to 600 percent in the central area of the site. Predictions of the relationship between bulk resistivity and temperature presented in the work plan (SteamTech, 2002) required a temperature increase of the order of 15°C (27°F) for this magnitude of change in conductivity to occur (Figure 7.2-1). This is clearly not supported by direct temperature measurement by thermocouples in wells placed along the line of the ERT profiles, such as EX-1 and EX-4 in profile TC1-9-4 (See Figure 7.2-6). The relationship between bulk resistivity and temperature must be investigated further, while the sensitivity must also be tested by the application of forward modeling. An investigation of these relationships warrants additional research, and forms part of a future research project proposed by some of the authors. The implication is that the 300-600 percent increases in conductivity seen in the profiles were generated by temperature increases of no more than a few degrees, and that the conductivity changes produced by areas adjacent to steam wells (such as VEA-5) are much greater and have merely been truncated to prevent the pre-set color scale of the images from being strongly skewed towards small regions of relatively very high conductivity. This possibility raises the question of what practical purpose ERT might serve as a monitoring tool in a fractured rock setting. Setting a limited and fixed range of values is useful in determining the location of structures through which hot water is moving, although it necessarily limits the ability to map true temperature in the subsurface, making the images semi-quantitative only. Mapping the true extent of conductivity changes will tend to obscure the role of discrete structures in controlling fluid movement, but will allow mapping of local peaks in temperature, indicating where the hottest water lies within any profile. The location of steam should not be effected by the limited, fixed range of conductivity,

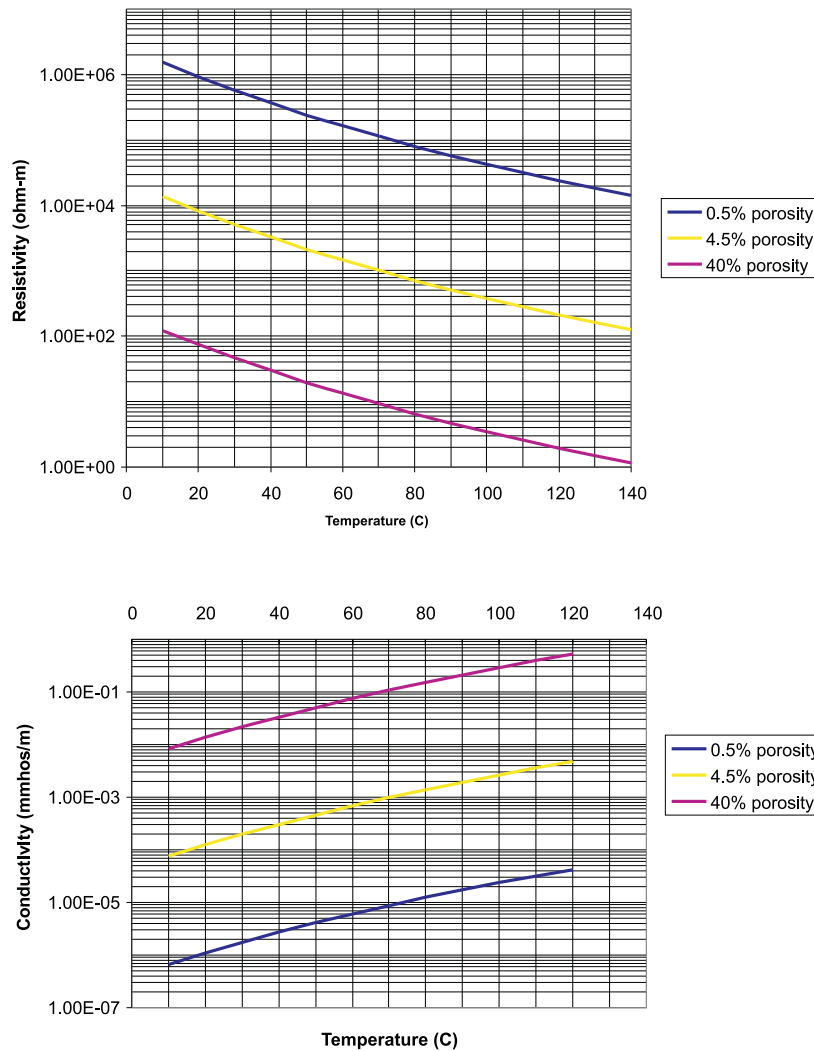


Figure 7.2-1. Relationship of bulk resistivity to temperature (top) and bulk conductivity to temperature (bottom).

as the very low resistivity anomaly associated with the presence of dry steam would be expected to stand out in a sequence of progressively lowered resistivity while ground water was being heated to boiling temperature within an open fracture. The question of resolution remains important, however, as the behavior of boiling fluids in a narrow fracture remains uncertain. Experimentation and modeling are necessary in order to develop a greater understanding of the dimensions of steam cells in narrow fractures and to determine the limits of fracture width in which ERT techniques can image very narrow zones of boiling. These factors also warrant future research.

While noting these limitations, it is possible to make some general observations regarding the ERT monitoring data from the Loring Quarry. The grid of planes imaged during the study is shown in Figure 7.2-2. The perimeter profiles (1-2-3, 3-8, 1-6, and 8-7-6, see Figure 7.2-3) show essentially no change in conductivity over much of their length, suggesting they remained cool (probably close to ambient temperatures) throughout steam injection and the cool-down period. The notable exceptions to this are in the vicinity of VEA-8, in planes 3-8 and 8-7-6. A small conductivity anomaly, apparently located in a high-angle structural feature, is located between 23-27 meters (75-90 feet) depth in both planes. This first becomes apparent on October 4, reaches a maximum intensity in profiles 3-8 and 7-8 in early November, and ultimately persists in images of these planes until the final data set collection (Figure 7.2-4). A second conductivity anomaly is present at a depth of about 15 meters (50 feet) in profile 6-7, adjacent to the upper steam injection interval in well I-8. This first becomes apparent on October 30 and extends downwards to connect with a linear horizontal anomaly by November 11. As noted above, the temperature at these conductivity anomalies cannot currently be calculated from the available data; however, VEA-8 is known to have increased in temperature by 8-9°C (14-16°F) above ambient temperatures in this time period. The significance of these anomalies is that they provide evidence of the passage of heated ground water within a limited cross-sectional area across the southern boundary of the study site. This observation confirms, in part, the southward migration of heated water suggested by thermocouple data and the conceptual model based on pulse interference testing of the aquifer, that predicted ground water flowpaths parallel to strike of easterly-dipping open fractures.

The presence of zones of slightly elevated conductivity, which are apparent as linear, vertical anomalies parallel to many of the VEAs (e.g., VEA-2, VEA-3, and VEA-8, shown in Figure 7.2-5) is problematic. In some cases, these are probably artifacts of impaired data collection or processing. This is most probably so in TC-1 and VEA-7, where the narrow parallel anomalies are not present in intersecting planes using data collected on the same dates. In other cases, where low intensity anomalies persisted throughout the project, they were initially thought to represent roughly cylindrical zones of enhanced fracture permeability induced by drilling of the VEA borings. Down-the-hole hammer techniques employed in the relatively brittle bedrock may have enhanced fracture permeability immediately adjacent to the boring, but beyond the subsequent influence of the grout with which the borings were sealed. However, infiltration of mud during rock drilling more commonly causes reduction of formation permeability around wells if subsequent development fails to recover the bulk of the injected mud. It may be that the presence of relatively conductive (bentonite-based) drilling mud in fractures around the borings that was injected into fractures under pressure during drilling or subsequent reaming-out of borings to completion diameter may also account for this feature.

The bulk of the intense (>300 percent conductivity increase) conductivity anomalies lie within the perimeter defined by the outermost VEAs. Examples using data collected on November 30 are shown in Figure 7.2-6. These linear conductivity anomalies are considered to correspond to the intersection of planar, structurally-controlled zones of higher permeability, which form pathways for movement of heated water. The majority of these features have high apparent dips (typically greater than 40 degrees), suggesting that the dominant structural features influencing fluid flow are not bedding-parallel fractures, which typically dip at 30 degrees or less. Individual linear anomalies cannot be reliably correlated between ERT profiles at present; however, some broad groupings are apparent.

The presence of several strong, apparently westerly-dipping linear features in the western part of the site (e.g., plane 6-4-2 in Figure 7.2-6), and rather less clearly-defined apparently steeply northwesterly-dipping linear features (e.g., planes TC1-3 and 8-TC1-2 in Figure 7.2-6), and apparently steeply northeasterly-dipping linear features (e.g., plane TC1-9-4 in Figures 7.2-6 and 7.2-7) in the eastern part of the site is most easily reconciled with a structural model in which NW-striking, SW-dipping features are predominant in the western part of the site, while NE-striking features, dipping towards both the NW and SE, are predominant in the eastern part of the site. The intersection of high-angle planes of these orientations with the vertical planes of the images would be expected to produce the range of apparent dip angles and directions seen in the images.

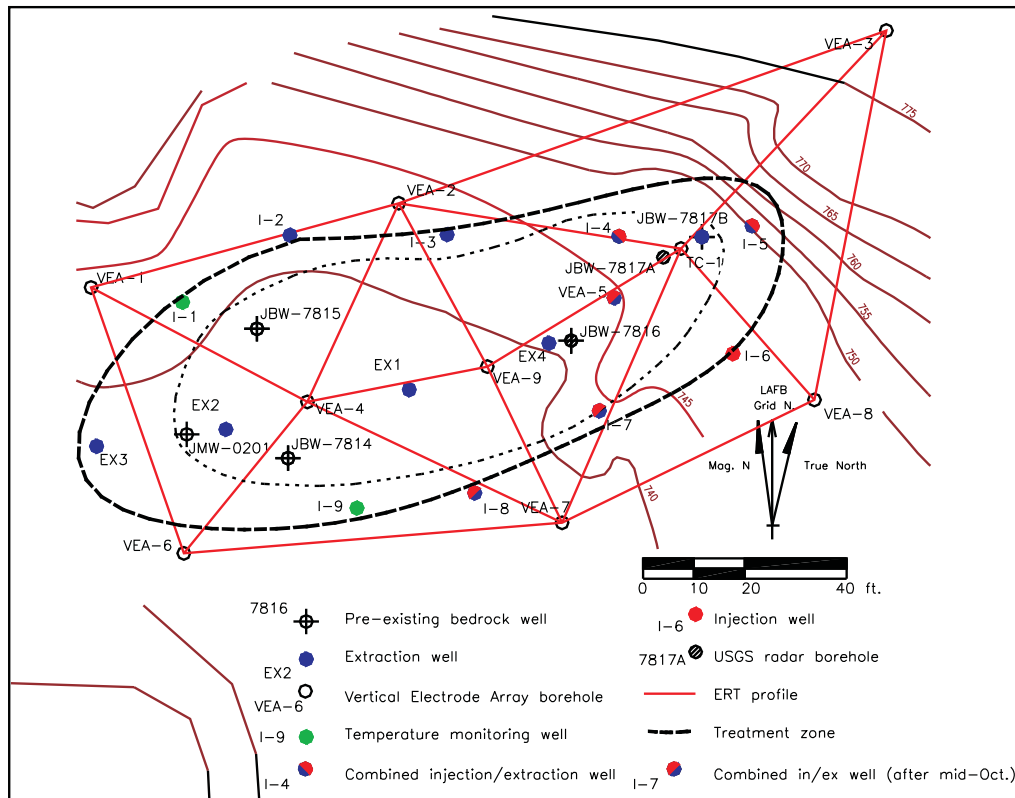


Figure 7.2-2. Site map, showing location of ERT profiles listed in Table 5.3.2-1.

The problems associated with correlation of these anomalies with the observed geology and aquifer properties are illustrated by consideration of plane TC1-9-4 (a time sequence is shown in Figure 4.2-7). The apparently westerly-dipping (from VEA-9 towards TC-1) planar features seen in the TC1-9 plane progressively develop in intensity from October 4 to November 19. These anomalies have a consistent orientation over this period, with an apparent dip of about 45 degrees. The plane TC1-9 contains the former monitoring well JBW-7816, which was logged using optical televiewer. Prominent open “axial planar” fractures dipping towards the ESE at 60-70 degrees are recorded at depths of about 16 and 22 meters (52 and 72 feet) bgs. Fractures of this orientation would produce lineations of an apparent dip about 45 degrees where they intersected the plane of the ERT image. It is striking that the southerly-dipping interwell connection crossing well EX-4, interpreted from aquifer testing data by Stephenson and Novakowski (2004) and shown in Figures 4.2.3-5 – 4.2.3-9 in this report, is close in location and orientation to these fractures and a reasonable interpretation of the ERT images. It is readily apparent, however, that the apparently flat-lying conductivity anomalies present throughout the project in the 9-4 plane (Figure 7.2-7) cannot be reconciled with structures logged in core or with interconnected fracture orientations deduced from aquifer testing. Similarly, the coalescence of the early planar conductivity anomalies in the plane TC1-4 after November 19 (Figure 7.2-7) cannot be accounted for by any changes in temperature or saturation without further field and bench-scale investigation to quantify the ERT expression and sensitivity of real fractured rock structures.

There seems little doubt that ERT does provide an effective means for monitoring heatup of the subsurface during thermal remediation, as indicated by the apparently consistent structural orientation of anomalies and correlation of increased conductivity in anomalies during heating of the site, followed by a decline during cooling.

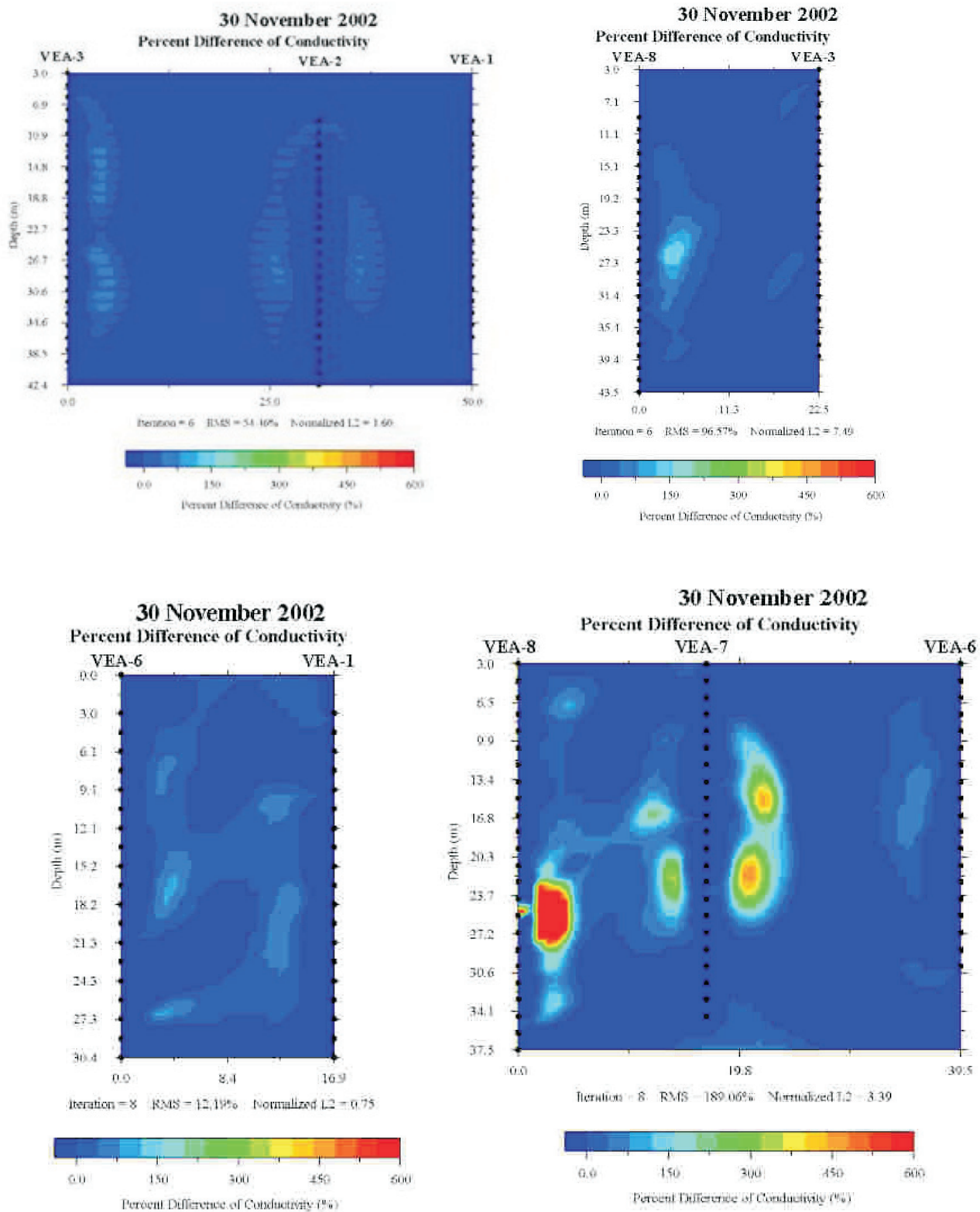


Figure 7.2-3. Conductivity profiles of perimeter planes, November 30.

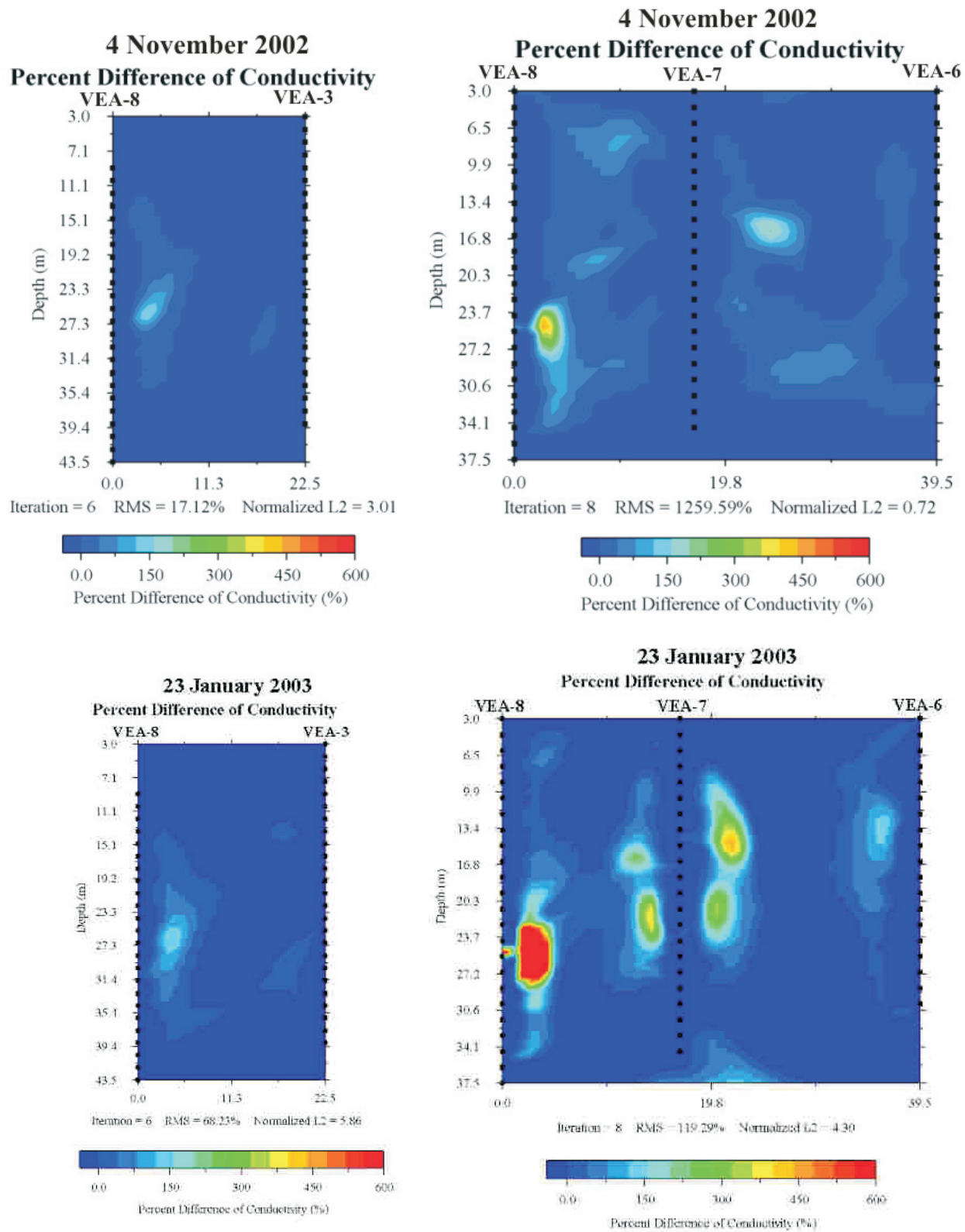


Figure 7.2-4. Resistivity anomalies interpreted as indicating the passage of heated water across the perimeter of the treatment area.

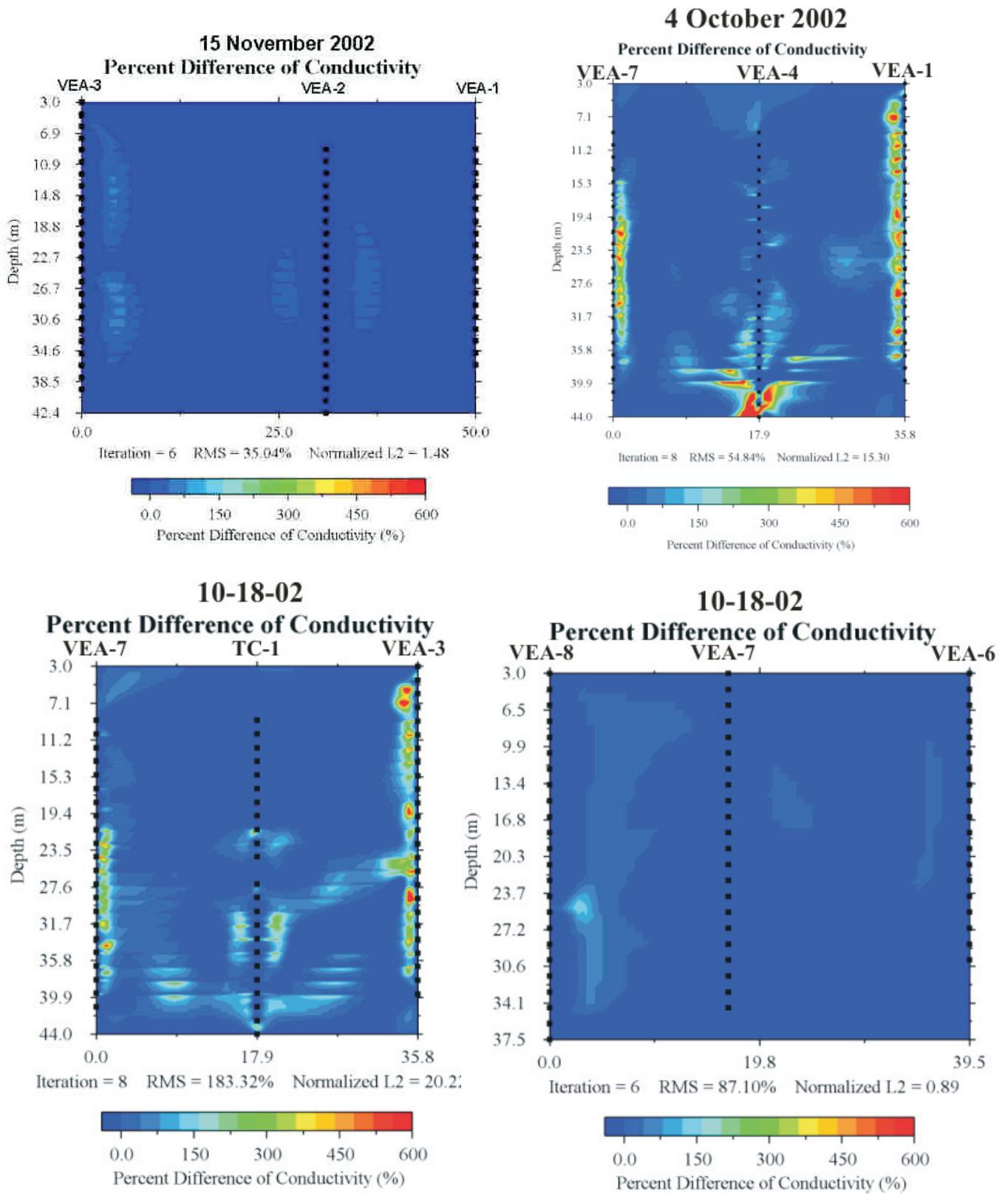


Figure 7.2-5. Examples of high conductivity anomalies parallel to VEA borings.

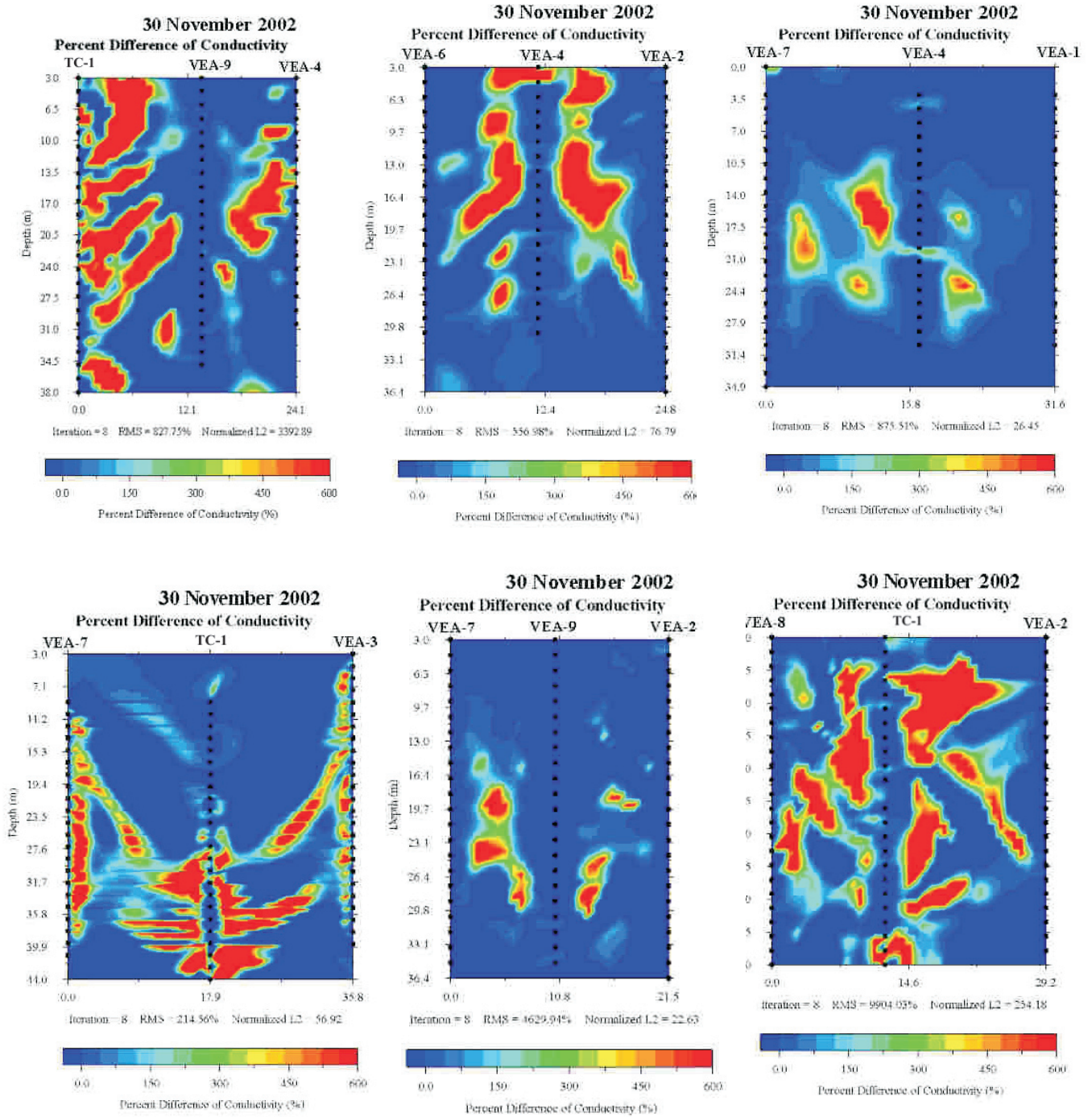


Figure 7.2-6. Conductivity profiles of interior planes, November 30.

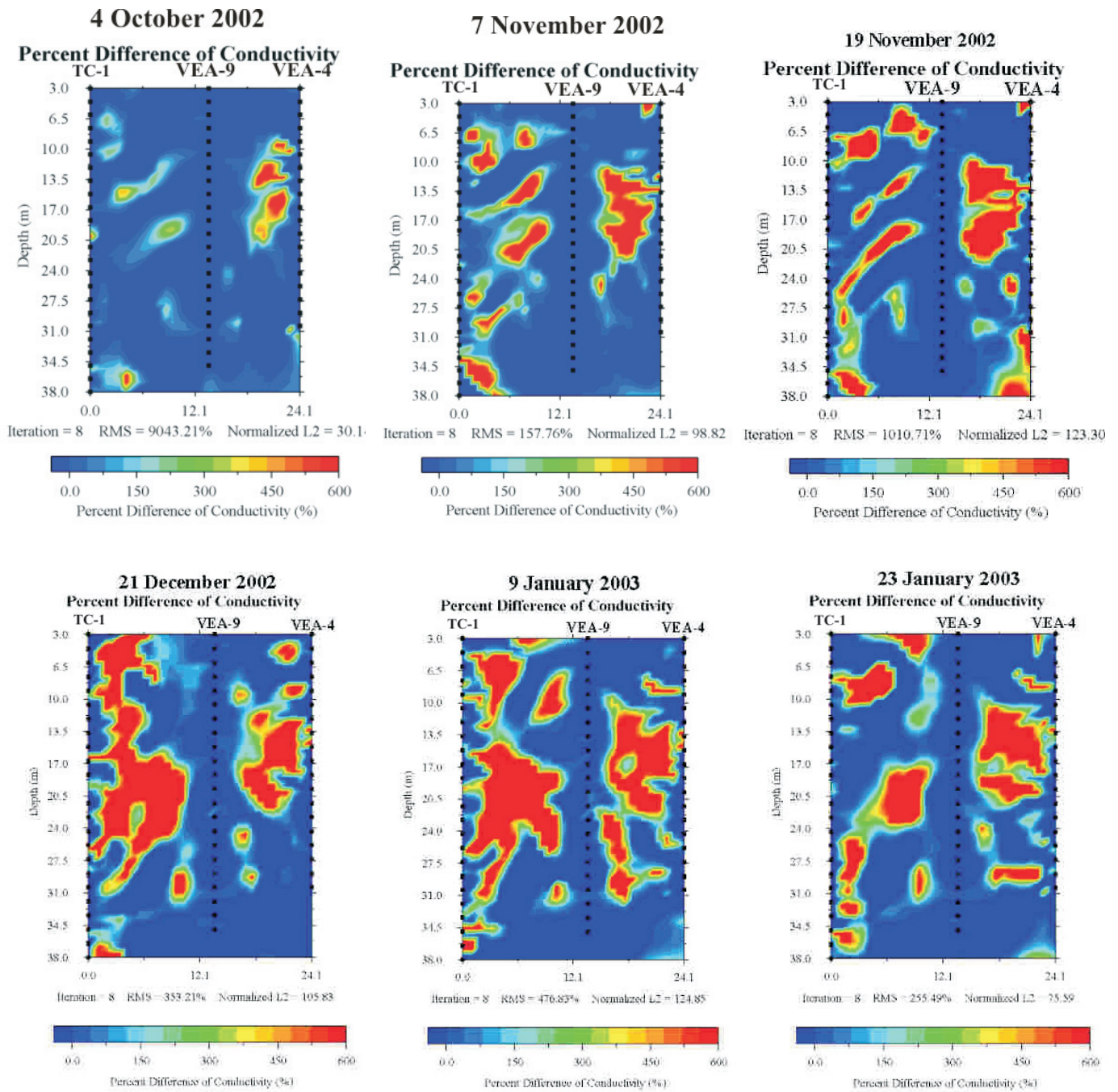


Figure 7.2-7. Plane TC1-9-4, showing development of conductivity anomalies over time.



Chapter 8. Effluent Sampling Results

A variety of effluent samples were obtained during SER operations to meet several different objectives. The objectives were to:

1. monitor the performance of the technology during operations;
2. evaluate the ability of SER to enhance the recovery of VOCs from fractured limestone;
3. document the amount of contaminants recovered;
4. document that discharge criteria for vapors and water were met.

Sampling to monitor the performance of the extraction system was performed by SteamTech and consisted of screening ground water samples from each of the extraction wells using a Photo-Ionization Detector (PID) headspace method (described in Chapter 8.1.1) three times a week, and weekly collection of samples from each of the wells. These samples were submitted for analysis using EPA Method 8260. In addition, three process streams (W-1, KO-2, and L-1; see Figure 5.2.2-1) within the effluent treatment system were also screened using the PID headspace method, and continuous flame ionization detector (FID) readings were taken of the vapor stream just before it entered the carbon vessels. These results are presented in Chapter 8.1.

Ground water and vapor samples were obtained throughout the extraction operations by EPA for the purposes of monitoring the rate of contaminant recovery over time and to document the amount of contaminants recovered. Sampling consisted of daily collection of samples of the vapor stream (from sampling point V-1; see Figure 5.2.2-1) and combined water flows (from sampling point L-1, see Figure 5.2.2-1) that were submitted for analysis using EPA Methods TO-15 and 8260, respectively. These results are presented in Chapter 8.2.

Compliance monitoring was performed by SteamTech, and consisted of weekly collection of samples of the vapor and water effluent streams, obtained from sample ports V-4 and L-3, respectively (See Figure 5.2.2-1). These samples were submitted for analysis via EPA Methods TO-14 and 8260, respectively. These results are presented in Chapter 8.3.

8.1. Ground Water and Process Stream Results

8.1.1. Extraction Well PID Screening

Water samples were screened for volatile contaminants on the basis of a headspace PID reading on a 0.5 liter (0.13 gallon) sample in a 1-liter (0.26-gallon) bottle. The PID screening was performed after the sample had equilibrated to room temperature for at least one hour. The cap was removed from the sample container, and the PID tip inserted about 0.05 meters (0.17 feet) into the sample container. The signal would peak after about 3-5 seconds, and the highest PID reading was recorded. After that, dilution air would make the signal decrease.

PID screening was done using a handheld PID (MiniRae 2000) calibrated to a 100 ppmv isobutylene standard gas. Extraction well PID screening sample results are shown on Figures 8.1.1-1 and 8.1.1-2.

During the first three weeks of operation, all sample headspace readings (except the water from VEA-5) were relatively low (below 100 ppmv). VEA-5 had readings between 200 and 600 ppmv until liquid extraction was discontinued from this well on September 26 (the well was converted to a steam well and began injecting on October 14).

Several of the extraction wells started showing elevated PID screening levels after about three weeks of operation. The wells with the most dramatic increases in the months of September and October were the following:

- EX-1 (steadily increased to about 400 ppmv by late October).
- EX-2 (spiked at 2,600 ppmv on October 13-14, and stayed around 2,000 ppmv through October).
- EX-3 (increased to between 600 and 1,500 ppmv in October).
- I-2 (increased to a peak of 9,100 ppmv on October 14, then declined to below 1,000 ppmv by the end of October).
- JBW-7817B (increased to 180 ppmv in late September, averaged around 70 ppmv in October).
- I-3 deep (increased to 228 ppmv on October 24, averaged around 100 ppmv in late October).

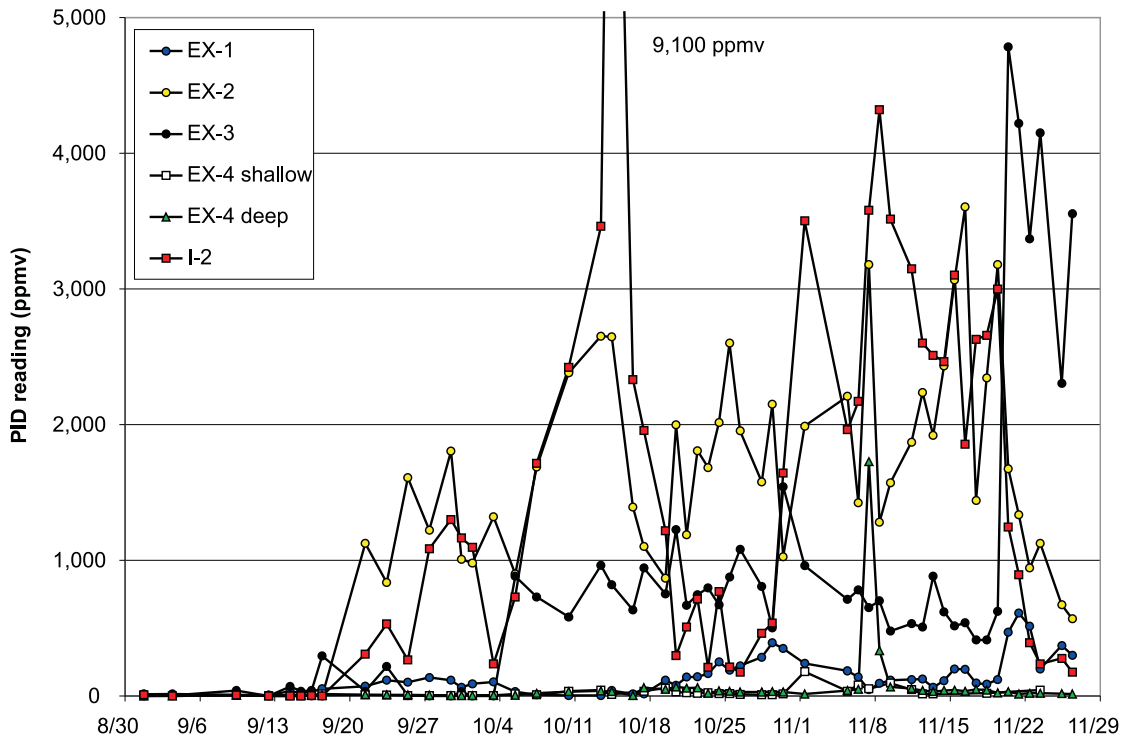


Figure 8.1.1-1. Headspace PID screening data for the first subset of extraction wells.

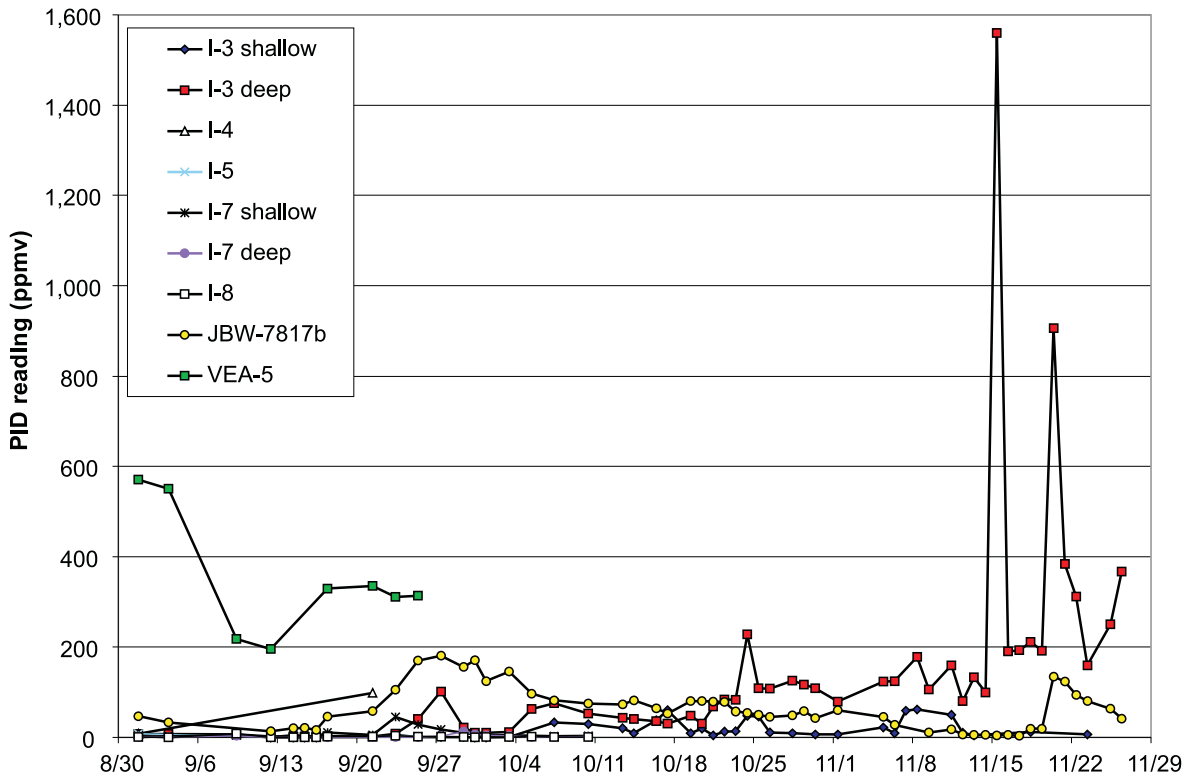


Figure 8.1.1-2. Headspace PID screening data for the second subset of extraction wells.

During the last four weeks of operation, several wells had more dramatic increases in the PID headspace readings:

- EX-1 (peaked at 611 ppmv on November 21).
- EX-2 (four readings above 3,000 ppmv).
- EX-3 (peaked at 4,800 ppmv on November 20 and remained above 2,000 ppmv).
- EX-4 Deep (a single high reading of 1,720 ppmv on November 7, otherwise below 100 ppmv).
- I-2 (peaked at 4,320 ppmv and then declined steadily to less than 500 ppmv).
- JBW-7817B (peaked at 134 ppmv and then declined steadily to less than 50 ppmv).
- I-3 Deep (peaked at 1,560 ppmv on November 15, then declined to around 500 ppmv).

Note that steam injection ceased on November 19. Several wells had a large PID headspace increase right after this date. These wells were:

- EX-1.
- EX-3.
- I-3 Deep.
- JBW-7817B.

These wells are located across most of the target area, and not in a certain area of the site.

Overall, these PID screening data indicated that effluent water concentrations varied considerably between individual extraction wells, and over time. However, one overall trend is that very low levels were recorded for the first three weeks of operation, and that substantial increases were seen in most wells. Also, the PID screening results indicate that the extracted water was at its highest VOC concentrations during the last two weeks of operation.

8.1.2. Extraction Well VOC Samples

Ground water samples from individual wells were collected weekly from sample points using standard techniques (three VOA vials filled to capacity without headspace). The samples were analyzed for VOCs by EPA Method 8260B.

The results of the VOC analyses for the four most abundant contaminants (PCE, TCE, naphthalene, and 1,2,4-trimethylbenzene) are shown on Figures 8.1.2-1, 8.1.2-2, 8.1.2-3, and 8.1.2-4, respectively.

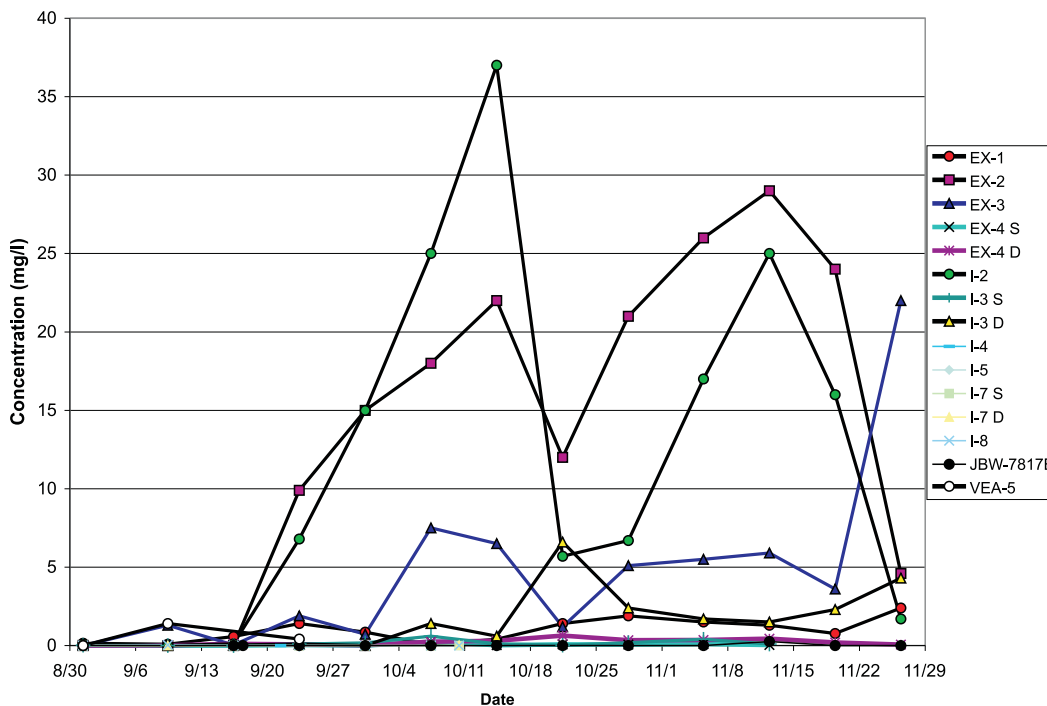


Figure 8.1.2-1. PCE concentrations in the VOC grab samples from the extraction wells.

The concentration of PCE in the extracted water was relatively modest (below 1.4 mg/l) during the first three weeks of operation for all wells. During late September and October, large increases were observed, particularly in the following wells:

- EX-2 increased to 22 mg/l on October 14, and 29 mg/l on November 12.
- EX-3 increased to between 5 and 7.5 mg/l in October and November, but reached its maximum concentration of 22 mg/l at the last day of sampling, November 26.
- I-2 peaked at 37 mg/l on October 14, and at 25 mg/l on November 12. The first peak corresponded to the highest PID screening value recorded on that day (Figure 8.1.1-1).
- I-3 Deep peaked at 6.6 mg/l on October 22, then stayed between 1.5 and 5 mg/l through the last sampling round.

The other extraction well PCE concentrations remained below 2.5 mg/l throughout.

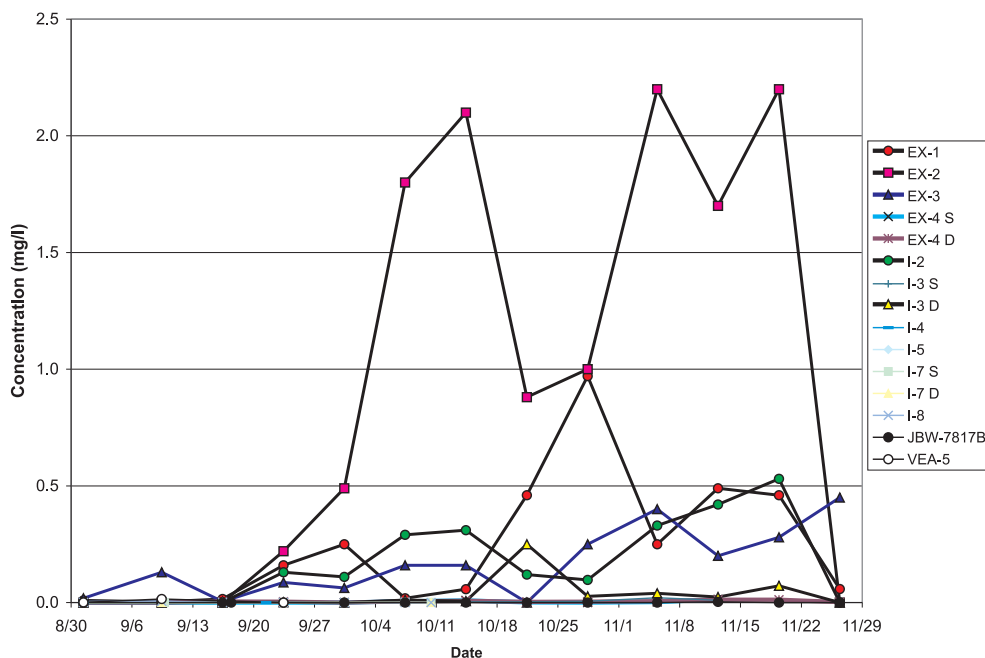


Figure 8.1.2-2. TCE concentrations in the VOC grab samples from the extraction wells.

The concentration of TCE in the extracted water was relatively modest (below 0.13 mg/l) during the first three weeks of operation for all wells. During late September and October, large increases were observed, particularly in the following wells:

- EX-1 peaked at 0.97 mg/l on October 26.
- EX-2 increased to 2.1 mg/l on October 14, and 2.2 mg/l on November 5 and November 19.
- EX-3 increased in October and November, and reached its maximum concentration of 0.45 mg/l at the last day of sampling, November 26.
- I-2 peaked at 0.31 mg/l on October 14, and at 0.53 mg/l on November 18.
- I-3 Deep increased to 0.25 mg/l on October 21, then declined again.

The other extraction well TCE concentrations remained below 0.05 mg/l throughout. Thus, TCE concentrations were generally 10 percent or less of the PCE concentration throughout the operational period.

The concentration of naphthalene in the extracted water was relatively modest (below 0.02 mg/l) during the first three weeks of operation for all wells. During late September and October, significant increases were observed, particularly in the following wells:

- EX-1 increased to 0.054 mg/l on October 28, and remained above detection limits except for the sampling event on November 19.
- EX-2 increased to the 0.30-0.80 mg/l range, and peaked at 1.30 mg/l at the last sampling event on November 26. Note that the PCE and TCE concentrations decreased between the last two sampling rounds, the opposite trend that the naphthalene exhibited.

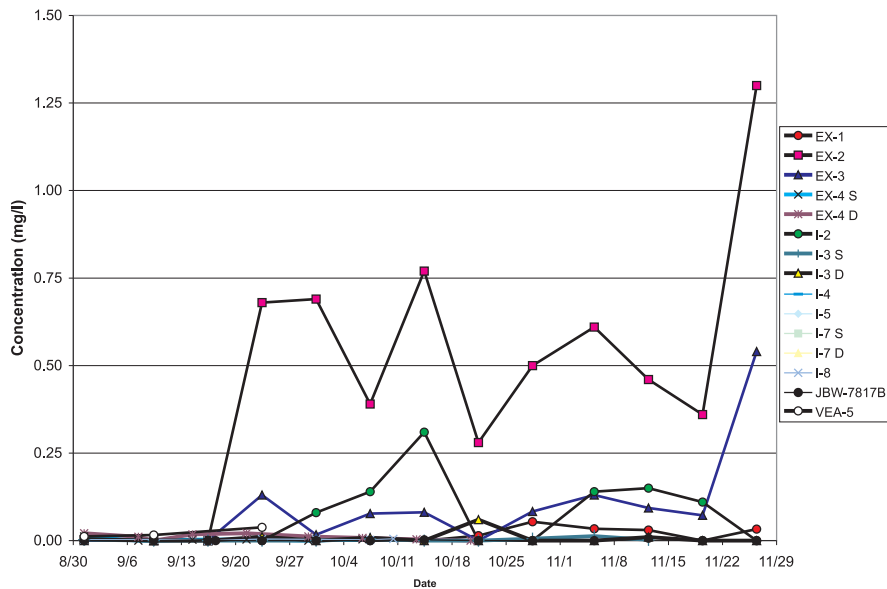


Figure 8.1.2-3. Naphthalene concentrations in the VOC grab samples from the extraction wells.

- EX-3 increased to the 0.05-0.13 mg/l range in October and November, and reached its maximum concentration of 0.54 mg/l at the last day of sampling, November 26.
- I-2 peaked at 0.31 mg/l on October 14, and at 0.15 mg/l on November 12. At the last sampling event, the concentration was below the detection limit of 0.10 mg/l.
- I-3 Deep increased to 0.06 mg/l on October 21, then declined again.

The other extraction well naphthalene concentrations remained below 0.04 mg/l throughout. Note that VEA-5 had naphthalene concentrations in the 0.012-0.038 mg/l range while it was extracting, however, this well was taken off-line on September 24, and converted to steam injection on October 14.

The concentration of 1,2,4-trimethylbenzene in the extracted water was significant in the water from VEA-5 during the first three sampling events. For the other wells, concentrations consistently were below 0.02 mg/l during the first three weeks of operation. During late September and October, some increases were observed, particularly in the following wells:

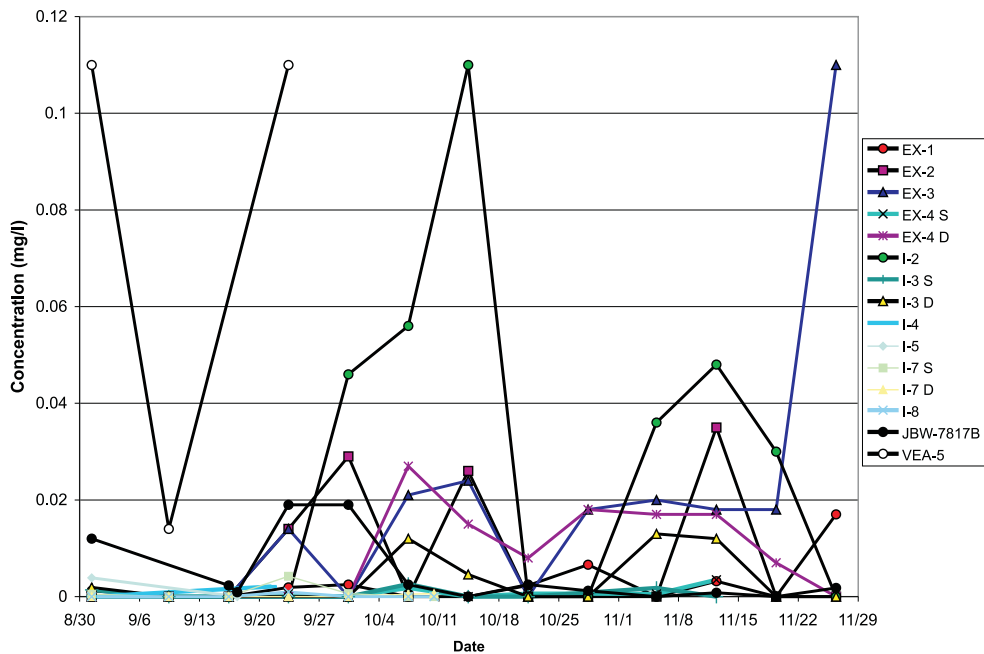


Figure 8.1.2-4. 1,2,4-Trimethylbenzene concentrations in the VOC grab samples from the extraction wells.

- I-2 increased to 0.110 mg/l on October 14, then declined again, and later increased to 0.048 mg/l on November 12.
- EX-2 had three samples in the 0.026 to 0.035 mg/l range, with several non-detects in between. It should be noted that the detection limits for the EX-2 samples were relatively high (0.025-0.050 mg/l), presumably due to high concentrations of other VOCs in these samples (PCE, TCE, and naphthalene were all at elevated concentrations in these samples).
- EX-3 started increasing to the 0.010-0.025 mg/l range in late October and November, and peaked at 0.110 mg/l at the last sampling event on November 26.

The remaining extraction wells generally had concentrations below 0.02 mg/l.

8.1.3. PID Screening of Process Streams

Figure 8.1.3-1 Shows the PID screening results for three selected process water streams:

- W-1 is the water from the extraction wells.
- KO-2 is condensate from the vapor extraction line.
- L-1 is the combined, cooled water stream prior to carbon filtration.

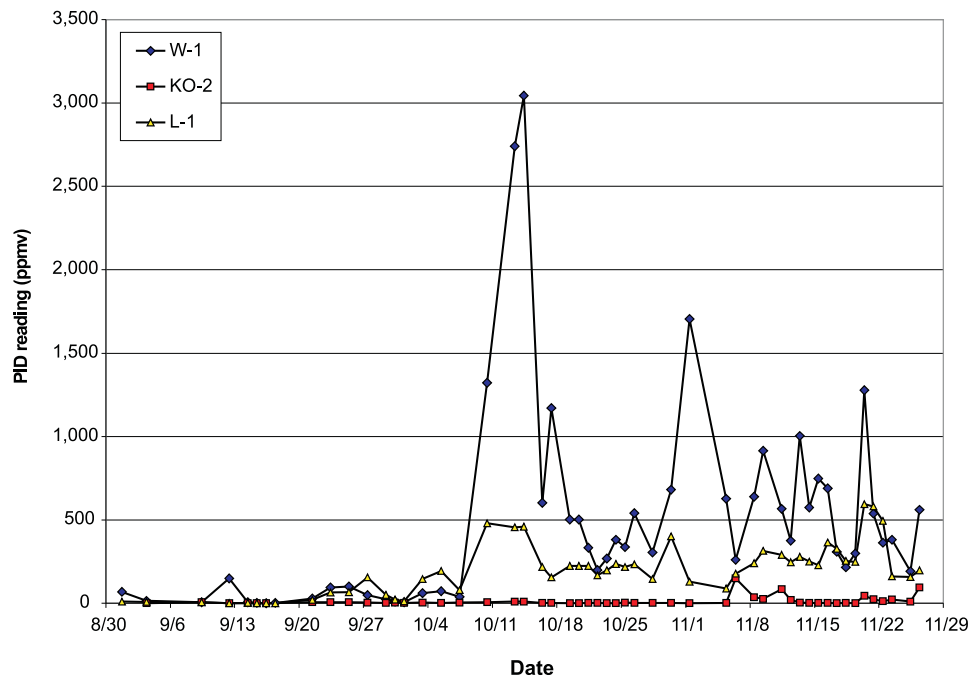


Figure 8.1.3-1. Results of PID headspace screening of process water samples. W-1 is the water from the extraction wells, KO-2 represents condensate from the vapor extraction lines, and L-1 is the combined, cooled water stream prior to carbon filtration.

The W-1 water samples stayed below 200 ppmv until October 10, then increased to above 3,000 ppmv on October 14, which coincided with the extremely high PID readings on the water from I-2 and EX-2. After this peak, a relatively steady decline to around 400 ppmv by the end of October was observed. In November, the readings fluctuated between 200 and 1,700 ppmv, without any clear trend being apparent.

The KO-2 condensate remained relatively clean, with PID readings remaining below 100 ppmv, except for a peak value of 150 ppmv on November 6. This indicates that the steam extracted from the wells and condensed in the pipes and the heat exchanger was relatively low in VOCs. As stated in the discussion of the energy balance (see Chapter 6.4), other operational data suggest that the majority (if not all) of the extracted steam was extracted from the upper intervals of the wells equipped with steam injection intervals below an extraction interval (I-4, I-5, I-7, I-8, VEA-5). Thus, the steam would be expected to remain relatively clean even as increased contaminant concentrations were observed in other process streams.

The combined and cooled water stream sampled at L-1 showed a similar trend to W-1, but had generally lower PID readings. This can be explained by mixing of the extracted water with relatively clean water from KO-2, and by evaporative VOC losses in surge tanks such as the gravity separator, GS-1. The vapors were recovered by the vacuum system (an odor control system extracted vapors from the headspace in the vessels), and treated in the vapor phase carbon system.

8.1.4. Vapor Screening Results (FID)

SteamTech performed vapor screening using an automated FID. Since the VOC data are far more accurate, no mass estimates were made based on the V-1 screening data. The results of the continuous FID screening are shown in Figure 8.1.4-1.

After a short initial period with readings in the 1 to 10 ppmv range, the FID readings were consistently low (below 0.010 ppmv) until late September, with a few exceptions. On September 27, a spike occurred (7.5 ppmv), followed by a long period where the readings varied between zero and 3 ppmv, with no clear trend being apparent. After November 19, the reading increased to 44.1 ppmv, and remained elevated until the end of operations on November 26. The increases in FID readings during these last seven days of operation were very significant. These increases started immediately after steam injection was ceased on November 19, and air injection was initiated an hour later the same day.

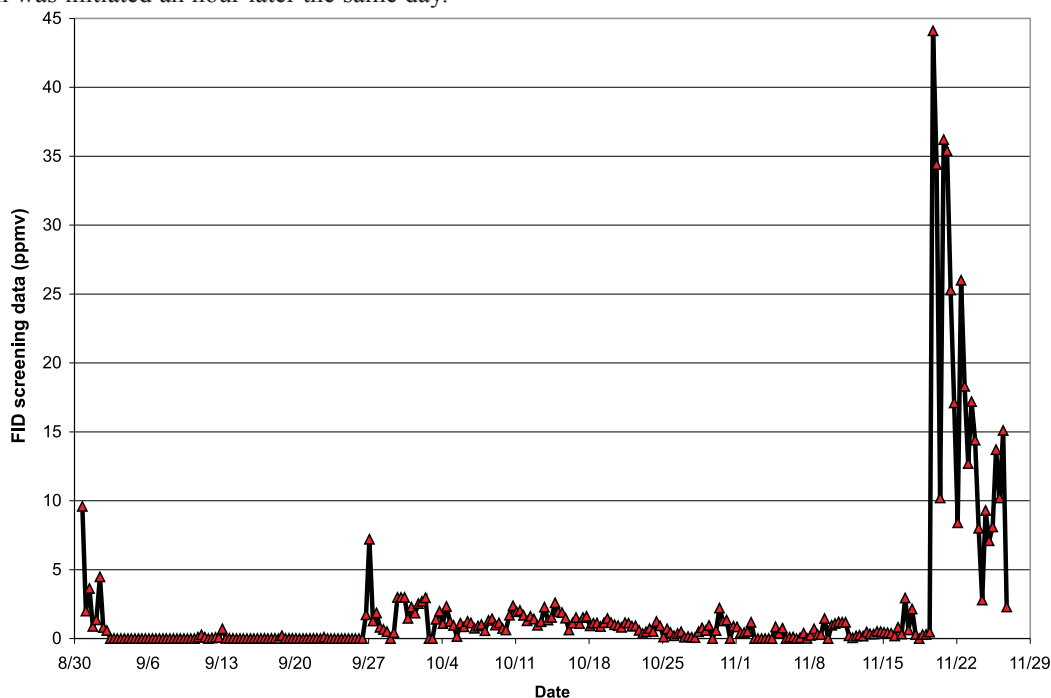


Figure 8.1.4-1. Results of continuous FID screening of vapors at location V-1 (untreated vapor).

8.2. Contaminant Recovery Rates and Total Contaminants Recovered

Primary objective P2 of the SITE program called for determining recovery rates as a function of time as well as the total mass of contaminants recovered by SER in each of the effluent streams. To meet this objective, EPA collected flow rate and contaminant concentration data on a daily basis for the effluent vapor and water streams. Provisions were made also to determine the quantity and composition of any NAPLs collected; however, NAPL was not recovered during this project.

8.2.1. Vapor Phase Recovery

In order to track vapor recovery rates and to determine the mass of contaminants recovered in the vapor phase, vapor samples were collected from sampling port V-1, located after the air dryer and just before the vapor stream entered the primary vapor carbon filter (Figure 5.2.2-1). The port consists of a 0.006 meter (0.02 foot) stainless steel tube connected to the main vapor line through a ball valve. Samples were collected on a time integrated basis over a 24-hour period. A critical flow orifice flow meter was used to collect vapors from the main vapor line at a rate of approximately 0.003 lpm (8×10^{-5} gpm). The vapor passed through a 7×10^{-6} meter (2.1×10^{-6} foot) filter and was collected in a 6 liter (1.6 gallon) summa canister. The vapors were analyzed by EPA Method TO-15. Table 8.2.1-1 contains the analytical results. Figure 8.2.1-1 shows the concentrations of various components in the vapor phase over the life of the project.

Vapor phase concentrations were generally low initially, in the range of 0.10 ppmv total VOCs. Concentrations began to slowly increase after approximately two weeks of steam injection, with concentrations generally in the range of 0.2 to 0.5 ppmv, and occasional spikes to concentrations of greater than 1 ppmv. The increased concentrations observed on September 23 correspond to the time when the steam injection system was shut down temporarily for maintenance, and air injection rates into the top interval of I-6 and into I-4 were significantly increased. The extremely high concentrations during the last week of extraction correspond to when the steam injection ceased, and significant amounts of air were injected into all of the in injection wells.

PCE was the most common contaminant detected in the vapor samples, while TCE was the second most commonly detected contaminant. Other chlorinated hydrocarbons detected in the vapor samples included carbon tetrachloride, acetone, and chloroform. Fuel components accounted for a significant proportion (typically 10 to 35 percent) of the vapor samples during September, and the commonly detected fuel components include xylenes, toluene, heptane, hexane, cyclohexane, ethylbenzene, benzene, and trimethylbenzenes. The composition of the vapor stream changed over time, with fuel components concentrations decreasing while the concentration of solvents increased. After approximately a month of steam injection, the concentration of fuel components in the effluent vapors was almost zero, and it remained low for the remainder of the project.

For the purpose of calculating recovered mass, vapor flow rate in the main vapor line was measured daily as the summa canister was changed. A pitot tube was used for the measurement, and corrections were made for temperature and pressure in the line. SteamTech also collected vapor phase flow rate data every 8 hours, and these data are shown in Figure 6.2.1-1. The lower flow rates of around 6 scmm during the early and latter part of the project are due to one of the blowers being down. When both blowers were operational, flow rates ranged from 7 to 8 scmm.

Daily recoveries and the cumulative recovery of VOCs in the vapor stream are shown in Figure 8.2.1-2. This graph shows a small increase in recovery rates in late September. At this time, there was no significant increase in temperature in any of the extraction wells; although, wells in the eastern part of the site (close to the initial steam injection wells) were showing small temperature increases. Extraction rates remained at approximately this level (with a couple spikes) throughout the remainder of the steam injection. A very significant increase in recovery rate during the last week of extraction, after the steam injection was ended, is also shown. The amount of contaminants recovered in the vapor phase during the last week of operations was greater than the amount collected during the previous 2.5 months of operations. The total mass of contaminants recovered in the vapor phase was estimated to be 3.33 kg (7.34 lbs). An estimated 2.55 kg (5.62 lbs) of PCE were recovered in the vapor stream, comprising approximately 77 percent of the total mass recovered in this phase. TCE was the next most abundant component of the vapor stream, with 0.24 kg (0.54 lbs) recovered. Other compounds of significant quantity in the vapor stream were: carbon tetrachloride, 0.194 kg (0.42 lbs); acetone, 0.098 kg (0.22 lbs); tetrahydrofuran, 0.088 kg (0.19 lbs); and hexane, 0.043 kg (0.095 lbs).

QC Summary. In general, the vapor phase data met the quality assurance criteria set out in the QAPP, and the data can be used for the project objectives. Many laboratory blanks contain acetone, but the concentration never exceeded 0.00011 ppmv, and this did not cause any of the data to be qualified. Benzene was detected in one blank sample at a low concentration. Duplicate sample results showed RPDs generally below 40 percent, with only three results exceeding the acceptance criteria of 50 percent. Approximately 10 percent of the data was validated, and as a result of the validation, some of the data was qualified as estimates. An “L” qualifier was used when the estimated value was below the calibration range, and a “J” qualifier was used when the analytical holding time was not met, or when other minor calibration problems were identified.

Table 8.2.1-1. Analytical Results for Vapor Samples from Sample Point V-1

Finish Date	31-Aug	1-Sep	2-Sep	3-Sep	4-Sep	5-Sep	6-Sep	7-Sep	8-Sep	9-Sep	10-Sep	11-Sep	12-Sep
compound													
1,1,1-Trichloroethane													
1,1,2-Trichloroethane													
1,1-Dichloroethane													
1,2,4-Trimethylbenzene	0.001	0.0018	0.0018	0.0021	0.0015	0.0024	0.0011	0.00097	0.00081	0.00083	0.0012	0.0033	0.0013
1,2-Dibromoethane													
1,3,5-Trimethylbenzene		0.00064	0.00066	0.00082	0.00062	0.0018	0.00046	0.00042				0.0014	0.00052
1,3-Butadiene													
2-Hexanone						0.0027							
4-Ethyltoluene	0.00051	0.00088	0.001	0.0013	0.00096	0.0015	0.00069	0.0005	0.00043	0.00046	0.00072	0.0021	0.00077
Acetone	0.0077	0.01	0.055	0.0097	0.013	0.032	0.0089	0.0082	0.0074	0.0091	0.0077	0.0097	0.009
Benzene	0.00071	0.0009	0.0014	0.00098	0.00096	0.0019	0.00048	0.00066	0.00058	0.00055	0.00055	0.0007	0.0005
Bromoform													
Carbon Disulfide			0.0024	0.00054		0.0057	0.00068	0.00057	0.00078	0.00092	0.0013	0.0011	0.00092
Carbon Tetrachloride			0.0027	0.012	0.02	0.1	0.014	0.0091	0.013	0.018	0.02	0.02	0.019
Chloroform	0.0039	0.0025	0.0047	0.005	0.0077	0.038	0.0068	0.0053	0.0074	0.01	0.01	0.01	0.0099
Cyclohexane	0.0036	0.006	0.0036	0.0052	0.0033	0.0028	0.0022	0.0021	0.0011	0.0022	0.0018	0.0093	0.0021
Dichlorodifluoromethane	0.00056	0.00068	0.00026	0.00076	0.0005		0.00044	0.00068		0.0008	0.00085	0.00088	0.00082
Ethylbenzene	0.0034	0.003	0.0011	0.00084	0.0011	0.0014	0.0005	0.00044	0.0004		0.00047	0.0011	
Heptane	0.0072	0.011	0.0036	0.0036	0.0035	0.0035	0.0021	0.0016	0.0011	0.0011	0.0016	0.0046	
Hexane	0.0041	0.007	0.0079	0.0061	0.0048	0.006	0.0031	0.003	0.0017	0.0026	0.003	0.0089	0.0029
Methyl Ethyl Ketone	0.0021	0.0039	0.015		0.0078	0.029	0.0024	0.0024	0.0021	0.0059	0.0064	0.0064	0.0073
Methyl Isobutyl Ketone													
Methyl-t-Butyl Ether				0.00044									
Methylene Chloride				0.00074	0.00058	0.0019	0.00048	0.00042	0.00051				
Styrene				0.002									
Tetrachloroethylene	0.028	0.08	0.036	0.029	0.031	0.044	0.029	0.023	0.023	0.033	0.03	0.044	0.032
Tetrahydrofuran	0.016	0.024	0.02	0.019	0.014	0.018	0.0096	0.0089	0.0058	0.0092	0.0093	0.042	0.009
Toluene	0.00069	0.016	0.0029	0.0088	0.0054	0.001	0.00041	0.00044	0.00051	0.00045			
Trichloroethylene	0.0091	0.0064	0.0056	0.0056	0.0068	0.017	0.0065	0.0054	0.0061	0.0074	0.0077	0.01	0.0081
Trichlorofluoromethane				0.00041					0.00021				
cis-1,2-Dichloroethylene	0.00062	0.00055	0.00052	0.00044	0.00047	0.00078	0.00052	0.00053	0.00052	0.00065	0.00066	0.001	0.00072
m/p-xylenes	0.012	0.015	0.0067	0.0031	0.0035	0.004	0.0015	0.0013	0.0011	0.0012	0.0016	0.0039	0.0017
o-Xylene	0.0016	0.0028	0.0015	0.0009	0.0013	0.00093		0.00032				0.00081	

All results are in ppmv.
Empty cell indicates not detected.

Table 8.2.1-1. Continued

Finish Date	13-Sep	14-Sep	15-Sep	16-Sep	17-Sep	18-Sep	19-Sep	20-Sep	21-Sep	22-Sep	23-Sep	24-Sep	25-Sep
compound													
1,1,1-Trichloroethane							0.005						
1,1,2-Trichloroethane													
1,1-Dichloroethane							0.0043						
1,2,4-Trimethylbenzene	0.0062	0.0021	0.0052	0.0033	0.0018	0.0049			0.0055	0.0088	0.025		
1,2-Dibromoethane							0.0044						
1,3,5-Trimethylbenzene	0.0028		0.0027	0.0017		0.0025							
1,3-Butadiene													
2-Hexanone							0.0044						
4-Ethyltoluene	0.0041		0.0039	0.0027		0.0036				0.0079	0.022		
Acetone	0.019	0.0043	0.018	0.017	0.056	0.019	0.058	0.026	0.048	0.027	0.063	0.028	0.018
Benzene	0.00093						0.0095						
Bromoform							0.0056						
Carbon Disulfide	0.0018		0.0022				0.0071						
Carbon Tetrachloride	0.029	0.0043	0.012	0.0085	0.0079	0.032	0.047	0.066	0.056	0.047	0.14	0.13	0.1
Chloroform	0.013	0.0025	0.0086	0.0039	0.002	0.0041	0.0095						0.0046
Cyclohexane	0.023	0.0073	0.022	0.015	0.0075	0.018	0.012	0.0074	0.0069	0.087	0.12	0.01	0.0084
Dichlorodifluoromethane	0.0012		0.0013										
Ethylbenzene	0.0019		0.0017							0.0065			
Heptane	0.014	0.0072	0.014	0.013	0.0067	0.014	0.0075	0.027	0.026	0.28			0.0081
Hexane	0.026	0.011	0.025	0.023	0.012	0.022	0.02	0.014	0.014	0.13	0.17	0.018	0.011
Methyl Ethyl Ketone	0.012				0.0077		0.016		0.0078				
Methyl Isobutyl Ketone	0.021		0.023					0.01		0.088	0.15	0.016	
Methyl-t-Butyl Ether													
Methylene Chloride							0.0062						
Styrene													
Tetrachloroethylene	0.2	0.12	0.22	0.24	0.16	0.19	0.2	0.2	0.24	0.28	1.2	0.28	0.18
Tetrahydrofuran	0.074	0.029	0.077	0.065	0.03	0.067	0.036	0.029	0.026	0.34	0.43	0.047	0.034
Toluene				0.0011	0.0016		0.0096						
Trichloroethylene	0.011	0.0034	0.013	0.0072	0.0053	0.014	0.015	0.01	0.012	0.017	0.32	0.042	0.016
Trichlorofluoromethane							0.0048						
cis-1,2-Dichloroethylene	0.00094		0.0015				0.005						
m/p-xylenes	0.0069	0.0031	0.0076	0.0054	0.0051	0.006	0.0083			0.023	0.056	0.0068	0.0052
o-Xylene	0.0011		0.0012										

All results are in ppmv.
 t cell i cates t etecte .

Table 8.2.1-1. Continued

Finish Date	26-Sep	27-Sep	28-Sep	29-Sep	30-Sep	1-Oct	2-Oct	3-Oct	4-Oct	5-Oct	6-Oct	7-Oct	8-Oct
compound													
1,1,1-Trichloroethane													
1,1,2-Trichloroethane													
1,1-Dichloroethane													
1,2,4-Trimethylbenzene													
1,2-Dibromoethane													
1,3,5-Trimethylbenzene													
1,3-Butadiene													
2-Hexanone													
4-Ethyltoluene													
Acetone	0.015	0.018	0.02	0.026	0.025	0.025	0.021	0.034	0.023	0.013	0.02	0.015	0.02
Benzene													
Bromoform													
Carbon Disulfide													
Carbon Tetrachloride	0.16	0.2	0.017	0.035	0.0088	0.022	0.011						
Chloroform	0.0043		0.0061	0.0042									
Cyclohexane	0.0041		0.0053	0.0041			0.0048	0.0042					0.0048
Dichlorodifluoromethane													
Ethylbenzene													
Heptane	0.0046												
Hexane	0.0068	0.0074	0.0085	0.0073	0.0079	0.0066	0.0081	0.008	0.009	0.008	0.0086	0.0082	0.009
Methyl Ethyl Ketone								0.0086					
Methyl Isobutyl Ketone		0.0067	0.0075	0.006			0.0063	0.0056		0.007	0.0063	0.0066	
Methyl-t-Butyl Ether													
Methylene Chloride													
Styrene													
Tetrachloroethylene	0.13	0.18	0.13	0.091	0.056	0.16	0.22	0.15	0.079	0.15	0.11	0.14	0.077
Tetrahydrofuran	0.018		0.019				0.016	0.013					
Toluene													
Trichloroethylene	0.015	0.029	0.034	0.013	0.0093	0.014	0.021	0.01		0.0067		0.0064	0.0057
Trichlorofluoromethane													
cis-1,2-Dichloroethylene													
m/p-xylenes	0.0046		0.0035					0.0034					0.0052
o-Xylene													

All results are in ppmv.
 t cell i icates t etecte .

Table 8.2.1-1. Continued

Finish Date	9-Oct	10-Oct	11-Oct	12-Oct	13-Oct	14-Oct	15-Oct	16-Oct	17-Oct	18-Oct	19-Oct	20-Oct	21-Oct
compound													
1,1,1-Trichloroethane													
1,1,2-Trichloroethane				0.0015									
1,1-Dichloroethane													
1,2,4-Trimethylbenzene													
1,2-Dibromoethane													
1,3,5-Trimethylbenzene													
1,3-Butadiene													
2-Hexanone													
4-Ethyltoluene													
Acetone	0.029	0.011	0.027	0.021	0.03	0.021	0.021	0.021	0.022	0.066	0.059	0.034	0.028
Benzene										0.0096			
Bromoform													
Carbon Disulfide										0.0047			
Carbon Tetrachloride						0.005	0.0092		0.0056	0.0085	0.021	0.028	
Chloroform							0.0043	0.0034	0.0032	0.0048	0.0043	0.0041	0.0041
Cyclohexane	0.0052	0.005	0.0068	0.0057	0.0047	0.0049	0.0048	0.0029	0.0029				
Dichlorodifluoromethane													
Ethylbenzene													
Heptane													
Hexane	0.0099	0.0086	0.012	0.0098	0.0099	0.0082	0.0086	0.0056	0.0058	0.014	0.0073	0.0056	0.0039
Methyl Ethyl Ketone			0.0074	0.0057	0.0079	0.0087				0.017	0.014	0.0079	0.0077
Methyl Isobutyl Ketone	0.0068	0.0067											
Methyl-t-Butyl Ether													
Methylene Chloride										0.0047			
Styrene													
Tetrachloroethylene	0.12	0.09	0.091	0.13	0.16	0.27	0.17	0.12	0.19	0.17	0.25	0.21	0.23
Tetrahydrofuran			0.019	0.017	0.017	0.016	0.019	0.011	0.012	0.013	0.012	0.012	0.0078
Toluene										0.013			
Trichloroethylene	0.005	0.0042	0.0041	0.0045	0.0049	0.0067	0.011	0.0067	0.0062	0.0083	0.012	0.011	0.011
Trichlorofluoromethane													
cis-1,2-Dichloroethylene													
m/p-xylenes			0.0044	0.0031		0.0031	0.0041	0.0027		0.0073			
o-Xylene													

All results are in ppmv.
 t cell i icates t etecte .

Table 8.2.1-1. Continued

Finish Date	22-Oct	23-Oct	24-Oct	25-Oct	26-Oct	27-Oct	28-Oct	29-Oct	30-Oct	31-Oct	1-Nov	2-Nov	3-Nov
compound													
1,1,1-Trichloroethane													
1,1,2-Trichloroethane													
1,1-Dichloroethane													
1,2,4-Trimethylbenzene													0.0018
1,2-Dibromoethane													
1,3,5-Trimethylbenzene													0.0011
1,3-Butadiene													0.00021
2-Hexanone													0.0016
4-Ethyltoluene													0.0015
Acetone	0.027	0.031	0.019	0.037	0.023	0.037	0.025	0.026	0.053	0.035	0.035	0.079	0.0013
Benzene													0.00046
Bromoform													
Carbon Disulfide													0.00066
Carbon Tetrachloride	0.033	0.0076	0.0035	0.0073	0.0039	0.0054	0.0037	0.0086	0.031	0.0089			0.003
Chloroform	0.0046			0.0034	0.0027	0.0041	0.0042	0.0045	0.011	0.0042	0.0031	0.0059	0.0078
Cyclohexane										0.003			0.0018
Dichlorodifluoromethane													0.0004
Ethylbenzene													0.00047
Heptane													0.0078
Hexane	0.0041				0.0035			0.005	0.0058	0.0065	0.004	0.0047	0.003
Methyl Ethyl Ketone	0.0083											0.016	0.0043
Methyl Isobutyl Ketone									0.0079				
Methyl-t-Butyl Ether													
Methylene Chloride													
Styrene													
Tetrachloroethylene	0.27	0.21	0.18	0.25	0.12	0.091	0.1	0.16	0.38	0.052	0.19	0.13	0.0028
Tetrahydrofuran	0.0074												0.0052
Toluene					0.0059								0.00047
Trichloroethylene	0.02	0.013	0.0085	0.012	0.01	0.0087	0.0082	0.016	0.027	0.014	0.013	0.013	0.00096
Trichlorofluoromethane													0.00023
cis-1,2-Dichloroethylene													
m/p-xylenes													0.002
o-Xylene													0.00026

All results are in ppmv.
 t cell i cates t etecte .

Table 8.2.1-1. Continued

Finish Date	5-Nov	6-Nov	7-Nov	8-Nov	9-Nov	10-Nov	11-Nov	12-Nov	13-Nov	14-Nov	15-Nov	16-Nov	17-Nov
compound													
1,1,1-Trichloroethane													
1,1,2-Trichloroethane													
1,1-Dichloroethane													
1,2,4-Trimethylbenzene													
1,2-Dibromoethane													
1,3,5-Trimethylbenzene													
1,3-Butadiene													
2-Hexanone													
4-Ethyltoluene													
Acetone	0.041	0.043	0.049	0.21	0.061	0.046	0.051	0.049	0.045	0.036	0.026	0.035	0.023
Benzene													
Bromoform													
Carbon Disulfide													
Carbon Tetrachloride	0.0032	0.0051	0.006							0.0057	0.014		0.0047
Chloroform	0.1	0.071	0.011	0.025	0.026	0.0044	0.0055	0.0036		0.0041	0.0037	0.0036	0.0033
Cyclohexane													
Dichlorodifluoromethane													
Ethylbenzene													
Heptane													
Hexane		0.0037			0.0036			0.0037			0.0047		
Methyl Ethyl Ketone		0.013			0.018			0.013					
Methyl Isobutyl Ketone													
Methyl-t-Butyl Ether													
Methylene Chloride													
Styrene													
Tetrachloroethylene	0.16	0.16	0.2		0.16	0.16	0.16	0.1	0.12	0.11	0.22	0.1	0.11
Tetrahydrofuran													
Toluene													
Trichloroethylene	0.0075	0.007	0.0084	0.032	0.0068	0.0075	0.0072	0.006	0.0071	0.0072	0.022	0.0065	0.0064
Trichlorofluoromethane													
cis-1,2-Dichloroethylene													
m/p-xylenes													
o-Xylene													

All results are in ppmv.
 t cell i icates t etecte .

Table 8.2.1-1. Continued

Finish Date	18-Nov	19-Nov	20-Nov	21-Nov	22-Nov	23-Nov	24-Nov	25-Nov	26-Nov
compound									
1,1,1-Trichloroethane									
1,1,2-Trichloroethane									
1,1-Dichloroethane									
1,2,4-Trimethylbenzene									
1,2-Dibromoethane									
1,3,5-Trimethylbenzene									
1,3-Butadiene									
2-Hexanone									
4-Ethyltoluene									
Acetone	0.042	0.025	0.081	0.52	0.25	0.24	0.2	0.21	0.17
Benzene									
Bromoform									
Carbon Disulfide									
Carbon Tetrachloride		0.0059		0.28	0.52	0.26	0.42		0.15
Chloroform									
Cyclohexane									
Dichlorodifluoromethane									
Ethylbenzene									
Heptane									
Hexane	0.0036	0.0095	0.099	0.17	0.09				0.066
Methyl Ethyl Ketone									
Methyl Isobutyl Ketone			0.04				0.038		
Methyl-t-Butyl Ether									
Methylene Chloride	0.022								
Styrene									
Tetrachloroethylene	0.074	0.1	0.93	5.2	5.3	3.2	3.4		4.5
Tetrahydrofuran		0.026	0.22	0.38	0.242	0.23	0.17		0.14
Toluene	0.0072								
Trichloroethylene	0.0043	0.0082	0.28	0.8	0.81	0.45	0.36	0.37	0.46
Trichlorofluoromethane									
cis-1,2-Dichloroethylene									
m/p-xylenes									
o-Xylene									

All results are in ppmv.

t c e l l i c a t e s t e c t e .

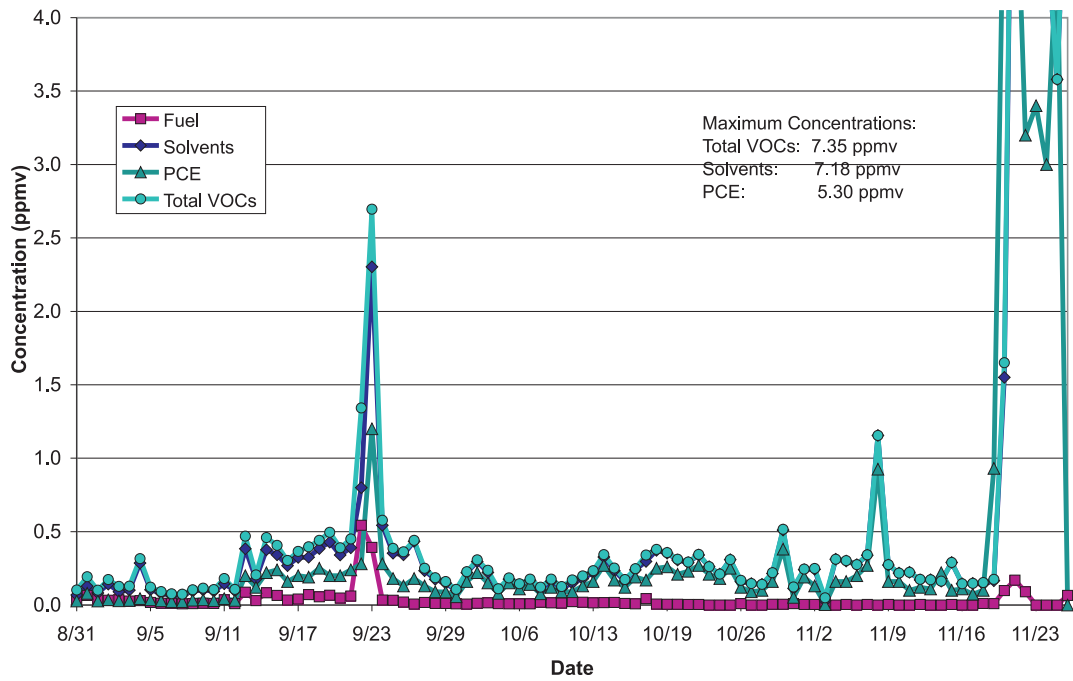


Figure 8.2.1-1. Vapor phase effluent concentrations over time.

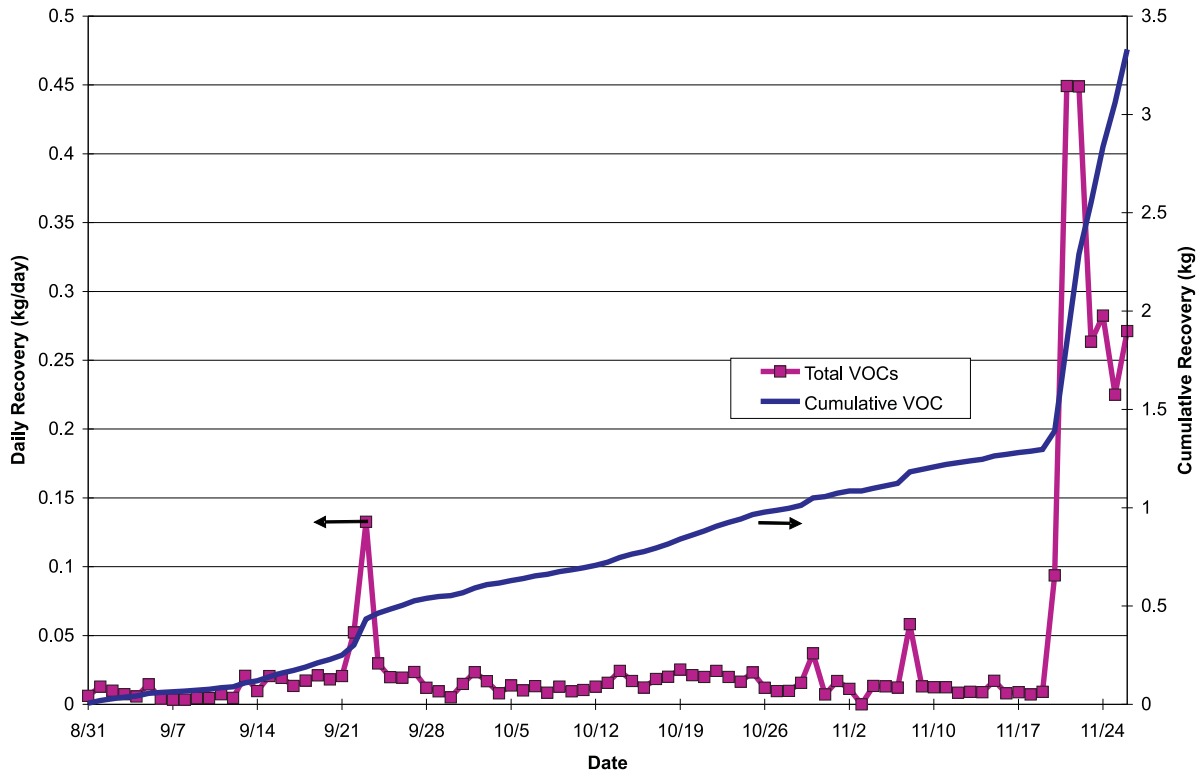


Figure 8.2.1-2. Vapor phase total VOC daily and cumulative recoveries.

8.2.2. Aqueous Phase Recovery

Aqueous phase samples were collected from port L-1, located after the gravity separator and before the primary liquid carbon filter (Figure 5.2.2-1). Thus, this liquid stream included any condensate from the knockout tanks and air dryer, but would not include NAPL (had any been collected). Samples were collected once a day through a 0.0064 meter (0.02 foot) stainless steel tube connected to the pipe through a ball valve. These samples were analyzed by EPA Method 8260B for VOCs, and by Maine Health and Environmental Testing Laboratory Method 4.2.17 for Gasoline Range Organics (GRO), and Method 4.1.25 for Diesel Range Organics (DRO). Table 8.2.2-1 and Figure 8.2.2-1 show the concentrations of VOCs, DRO, and GRO in the effluent as a function of time.

The initial VOC concentration in the effluent was low (around 0.075 mg/l), and during the first three weeks of steam injection, concentrations declined to less than 0.020 mg/l. Approximately three weeks after steam injection was initiated, effluent VOC concentrations started to increase dramatically, with concentrations jumping two orders of magnitude in a ten-day period. Concentrations continued to increase over the rest of the steam injection. The highest concentration of solvents in the effluent (9.54 mg/l) occurred on October 31. PCE was the most commonly detected VOC in the effluent, and in most samples, comprised 90 percent or more of the VOCs detected. Early in the project, significant acetone concentrations were detected in the liquid effluent samples; however, acetone was not detected after about the first three weeks of steam injection. TCE was the second most commonly detected VOC, and comprised about five percent of the total mass of VOCs. Other VOCs detected in the liquid phase in the early stages of the project were BTEX, trimethylbenzenes, cis- and trans-1,2-dichloroethylene, and trichlorobenzenes; however, after the first month or so of operations, PCE was generally the only VOC detected in the aqueous phase samples. Generally the detection limits for the other target analytes were high (See Appendix C), which would mask small concentrations of other compounds present.

GRO concentrations in the effluent were also low initially, and decreased further to undetectable levels during the first three weeks of the steam injection (See Appendix C for detection limits.). GRO concentrations in the effluent increased sharply at that time, and were generally in the range of 0.5 to 2.0 mg/l through the rest of the project. GRO concentrations in the effluent were at their highest concentration on October 31, the same day that VOC concentrations peaked.

DRO in the effluent initially was fairly high, with a concentration in the first effluent sample of about 5.5 mg/l. During the first three weeks of steam injection, the DRO concentration also decreased, to less than 1.0 mg/l. DRO concentrations then increased, along with the VOC and GRO concentrations. DRO concentrations remained in the 1.0 to 5.0 mg/l range throughout most of the project. The final sample collected showed a jump in the concentration to 17.6 mg/l, which was the highest concentration measured during the project. This high concentration may indicate that DRO NAPL was about to be recovered in the effluent.

Thus, the aqueous effluent concentrations versus time show that initially the system performed as might be expected in a pump-and-treat system, with concentrations declining to an asymptotic level. However, as heat was added to the system, the aqueous phase concentrations of VOCs, GRO, and DRO simultaneously began to increase, and continued to increase through the rest of the project.

In order to determine the volume of liquid effluent collected, the cumulative flow in the liquid line was noted via a totalizing flowmeter at the time the samples were collected. The liquid flow rates are shown in Figure 6.2.2-1. These flow rate data were used along with the concentrations given in Table 8.2.2-1 to calculate the recovery of VOCs, GRO, and DRO in the effluent. Fuel components detected by EPA Method 8260B were not included in this calculation, as they would be included in the GRO analysis. Concentrations as a function of time as well as cumulative recoveries are shown in Figures 8.2.2-2, 8.2.2-3, and 8.2.2-4 for VOCs, GRO, and DRO, respectively. PCE accounted for approximately 90 percent of the solvents recovered. The total mass of solvents recovered in the liquid phase was 1.71 kg (3.8 lbs). The total amount of GRO recovered was 0.55 kg (1.22 lbs), and 1.768 kg (3.90 lbs) of DRO were recovered.

QC Summary. Essentially all of the aqueous phase effluent data were determined to meet the acceptance criteria contained in the QAPP, and thus, could be used for the project objectives. Relative percent differences for field duplicates for volatile samples never exceeded 10 percent. Acetone was detected in many of the trip blanks, but the concentration never exceeded 0.01 mg/l. The trip blank for November 7 showed a potential problem with a PCE concentration of 0.12 mg/l, TCE detected at 0.0079 mg/l, and cis-1,2-DCE at 0.0003 mg/l. This PCE concentration is approximately 3 percent of the sample result that day, but TCE and cis-1,2-DCE were below detection limits in the sample. MS/MSD results showed recoveries for a few compounds slightly outside the acceptance criteria; however, TCE was the only one of these compounds that was also detected in the corresponding sample. Validation of approximately 10 percent of the data revealed only minor quality problems that did not adversely effect the usability of the data. The most common problems were low response factors or low laboratory control sample recoveries which resulted in the rejection of the nondetect results for some compounds in the affected samples. Of the affected compounds, only acetone, methyl ethyl ketone, 2-hexanone, and 1,2,3-trimethylbenzene were detected in some samples from the site.

For the GRO analysis, RPDs of duplicate samples never exceeded four percent. Trip blanks generally showed no contamination; although, MTBE was detected in a few at low concentrations. One trip blank had a GRO concentration of 0.038 mg/l, which was 2.5 percent of the concentration in the corresponding sample, and thus should not effect the results. One trip blank arrived broken and could not be analyzed. A complete set of MS/MSD data could not be analyzed due to equipment problems in the laboratory

Table 8.2.2-1. Analytical Results for Aqueous Phase Samples from Sample Location L-1

Date	30-Aug	31-Aug	1-Sep	2-Sep	3-Sep	4-Sep	5-Sep	6-Sep	7-Sep	8-Sep	9-Sep	10-Sep	11-Sep	12-Sep	13-Sep	14-Sep
Acetone		0.02400	0.01300	0.07800	0.03800	0.01800	0.02300	0.02000	0.02100	0.02000	0.02600	0.01100	0.01200	0.02000	0.01500	0.00900
t-1,2-Dichloroethylene														0.00020		
cis-1,2-Dichloroethylene		0.00080												0.00030		
Chloroform		0.00640	0.00110													
Benzene		0.00040														
Trichloroethylene	0.00420	0.00870	0.00100	0.00150	0.00090	0.00050	0.00050	0.00030	0.00030	0.00020				0.00110	0.00070	0.00040
Toluene	0.00160															
Tetrachloroethylene	0.07000	0.03600	0.02100	0.07500	0.02800	0.02100	0.01430	0.01000	0.00920	0.00670	0.00420	0.00180	0.00190	0.04100	0.04000	0.01600
Ethyl Benzene	0.00190	0.00070	0.00060											0.00030		
Total Xylenes	0.00390	0.00190	0.00130											0.00090		
1,3,5-Trimethylbenzene			0.00110													
1,2,4-Trimethylbenzene	0.00610	0.00240	0.00440											0.00280	0.00180	
1,2,3-Trimethylbenzene			0.00180											0.00130		
1,2,4-Trichlorobenzene					0.00120	0.00100	0.00100	0.00120						0.00200	0.00460	
Naphthalene														0.00210	0.00300	
1,2,3-Trichlorobenzene															0.00160	
Gasoline Range Organics	0.02500	0.13100	0.05900	0.07000		0.01000								0.06800	0.08200	
Diesel Range Organics	5.57000	0.90700	1.16000	2.08000	1.15000	0.63000	1.38000	0.76500	1.04000	1.05000	0.61000	0.69500	0.37900	0.89300	1.05000	0.43700

Date	15-Sep	16-Sep	17-Sep	18-Sep	19-Sep	20-Sep	21-Sep	22-Sep	23-Sep	24-Sep	25-Sep	26-Sep	27-Sep	28-Sep	29-Sep	30-Sep
Acetone	0.00620	0.00540	0.00720													
t-1,2-Dichloroethylene																
cis-1,2-Dichloroethylene															0.00170	
Chloroform																
Benzene																
Trichloroethylene	0.00070	0.00050	0.00070	0.01700	0.04500	0.02300	0.03300	0.03900	0.04300	0.03400	0.03300	0.02600	0.03300	0.02400	0.03400	0.02200
Toluene																
Tetrachloroethylene	0.00750	0.00590	0.00820	0.12000	0.86000	0.44000	0.40000	0.51000	0.51000	0.58000	0.56000	0.69000	1.50000	0.18000	0.15000	0.10000
Ethyl Benzene																
Total Xylenes																
1,3,5-Trimethylbenzene																
1,2,4-Trimethylbenzene																
1,2,3-Trimethylbenzene																
1,2,4-Trichlorobenzene				0.02000												
Naphthalene																
1,2,3-Trichlorobenzene																
Gasoline Range Organics				0.21600	0.39500	0.30300	0.19700	0.24000	0.24400	0.28300	0.28700	0.42800	0.65800	0.10400		0.06200
Diesel Range Organics	0.51900	0.26500	0.77300	2.67000	1.92000	0.97300	0.50900	0.74700	1.17000	0.80700	0.78900	1.60000	1.82000	0.72400	0.93000	0.77900

Table 8.2.2-1. Continued

Date	1-Oct	2-Oct	3-Oct	4-Oct	5-Oct	6-Oct	7-Oct	8-Oct	9-Oct	10-Oct	11-Oct	12-Oct	13-Oct	14-Oct	15-Oct	16-Oct
Acetone																
t-1,2-Dichloroethylene																
cis-1,2-Dichloroethylene																
Chloroform																
Benzene																
Trichloroethylene	0.02900	0.04200	0.04300		0.06600		0.01900			0.05800						
Toluene																
Tetrachloroethylene	0.30000	3.80000	1.50000	0.81000	1.70000	0.43000	0.62000	3.00000	2.50000	2.90000	4.70000	4.50000	6.40000	5.30000	4.80000	4.00000
Ethyl Benzene																
Total Xylenes																
1,3,5-Trimethylbenzene																
1,2,4-Trimethylbenzene																
1,2,3-Trimethylbenzene																
1,2,4-Trichlorobenzene																
Naphthalene																
1,2,3-Trichlorobenzene																
Gasoline Range Organics	0.28700	1.04000	0.70500	0.54500	0.49800	0.34800	0.40100	0.83300	0.66800	1.23800	1.51400	1.23400	1.78900	1.41900	1.27000	1.25400
Diesel Range Organics	1.55000	2.21000	2.82000	2.15000	1.13000	1.27000	1.42250	2.45000	1.89000	2.40000	4.43000	1.93000	3.20000	2.28000	3.53000	3.34000

Date	17-Oct	18-Oct	19-Oct	20-Oct	21-Oct	22-Oct	23-Oct	24-Oct	25-Oct	26-Oct	27-Oct	28-Oct	29-Oct	30-Oct	31-Oct	1-Nov
Acetone																
t-1,2-Dichloroethylene																
cis-1,2-Dichloroethylene																
Chloroform										0.92000	0.96000					
Benzene																
Trichloroethylene							0.03200		0.16000	0.34000		0.11000	0.10000	0.13000	0.24000	0.14000
Toluene																
Tetrachloroethylene	2.50000	2.10000	2.90000	1.50000	2.20000	2.80000	0.31000	0.40000	2.30000	2.40000	1.40000	1.50000	1.40000	4.00000	9.30000	3.00000
Ethyl Benzene																
Total Xylenes																
1,3,5-Trimethylbenzene																
1,2,4-Trimethylbenzene																
1,2,3-Trimethylbenzene																
1,2,4-Trichlorobenzene																
Naphthalene																
1,2,3-Trichlorobenzene																
Gasoline Range Organics	0.99100	1.11400	1.33600	0.64500	0.91300	1.14400	0.14300	0.56600	0.96600	0.60400	0.39500	0.51000	0.38200	1.70000	2.20000	1.20000
Diesel Range Organics	2.39000	2.32000	2.49000	1.56000	1.75000	3.76000	1.45000	1.10000	2.01000	1.07000	0.63300	0.83900	0.93800	4.88000	4.98000	2.35000

Table 8.2.2-1. Continued

Date	2-Nov	5-Nov	6-Nov	7-Nov	8-Nov	9-Nov	10-Nov	11-Nov	12-Nov	13-Nov	14-Nov	15-Nov	16-Nov	17-Nov	18-Nov	19-Nov
Acetone																
t-1,2-Dichloroethylene																
cis-1,2-Dichloroethylene																
Chloroform	0.12000															
Benzene																
Trichloroethylene		0.01800	0.04300		0.05000	0.13000	0.09300	0.10000					0.08500		0.14000	0.12000
Toluene																
Tetrachloroethylene	0.13000	0.67000	1.40000	4.60000	1.70000	4.00000	2.30000	2.40000	0.87000	2.60000	1.60000	1.60000	2.50000	2.90000	3.00000	3.80000
Ethyl Benzene																
Total Xylenes																
1,3,5-Trimethylbenzene																
1,2,4-Trimethylbenzene																
1,2,3-Trimethylbenzene																
1,2,4-Trichlorobenzene																
Naphthalene																
1,2,3-Trichlorobenzene																
Gasoline Range Organics	0.11900	0.26000	0.41900	1.54300	0.45100	0.74500	0.55100	0.46900	0.28400	0.55300	0.38700	0.41100	0.41700	0.55100	0.48100	0.64900
Diesel Range Organics	1.95000	0.56300	0.59000	1.96000	0.73500	1.38000	0.94900	0.89800	0.64300	1.20000	2.08000	0.80900	0.79900	1.18000	0.93200	1.24000

136

Date	20-Nov	21-Nov	22-Nov	23-Nov	24-Nov	25-Nov	26-Nov
Acetone							
t-1,2-Dichloroethylene							
cis-1,2-Dichloroethylene							
Chloroform							
Benzene							
Trichloroethylene	0.08500	0.09200	0.06300				
Toluene							
Tetrachloroethylene	4.80000	4.40000	3.10000	2.00000	1.70000	1.10000	4.20000
Ethyl Benzene							
Total Xylenes							
1,3,5-Trimethylbenzene							
1,2,4-Trimethylbenzene							
1,2,3-Trimethylbenzene							
1,2,4-Trichlorobenzene							
Naphthalene							
1,2,3-Trichlorobenzene							
Gasoline Range Organics	1.40800	1.82900	1.72200	1.22600	0.75500	0.50700	1.43100
Diesel Range Organics	1.86000	4.07000	4.50000	4.04000	3.71000	1.89000	17.60000

All concentrations in mg/l.
Empty cell indicates not detected.

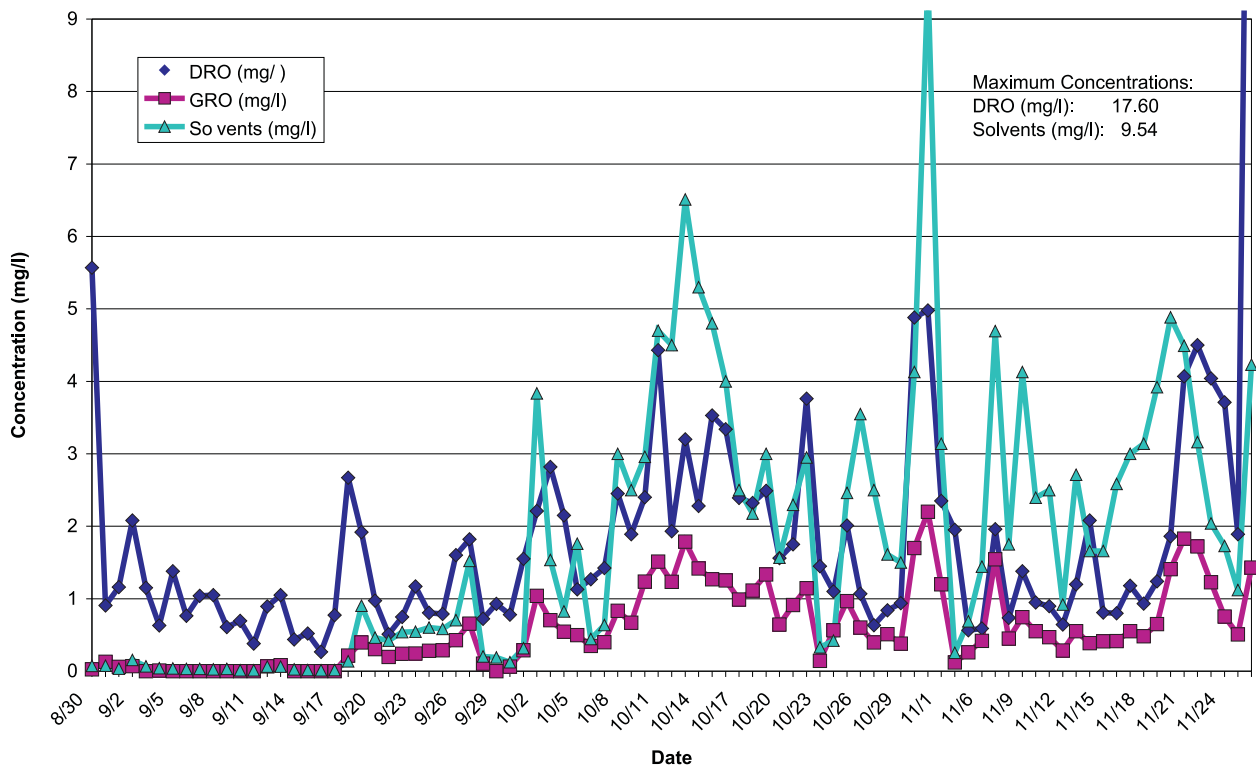


Figure 8.2.2-1. Aqueous phase effluent concentrations of total solvents, GRO, and DRO.

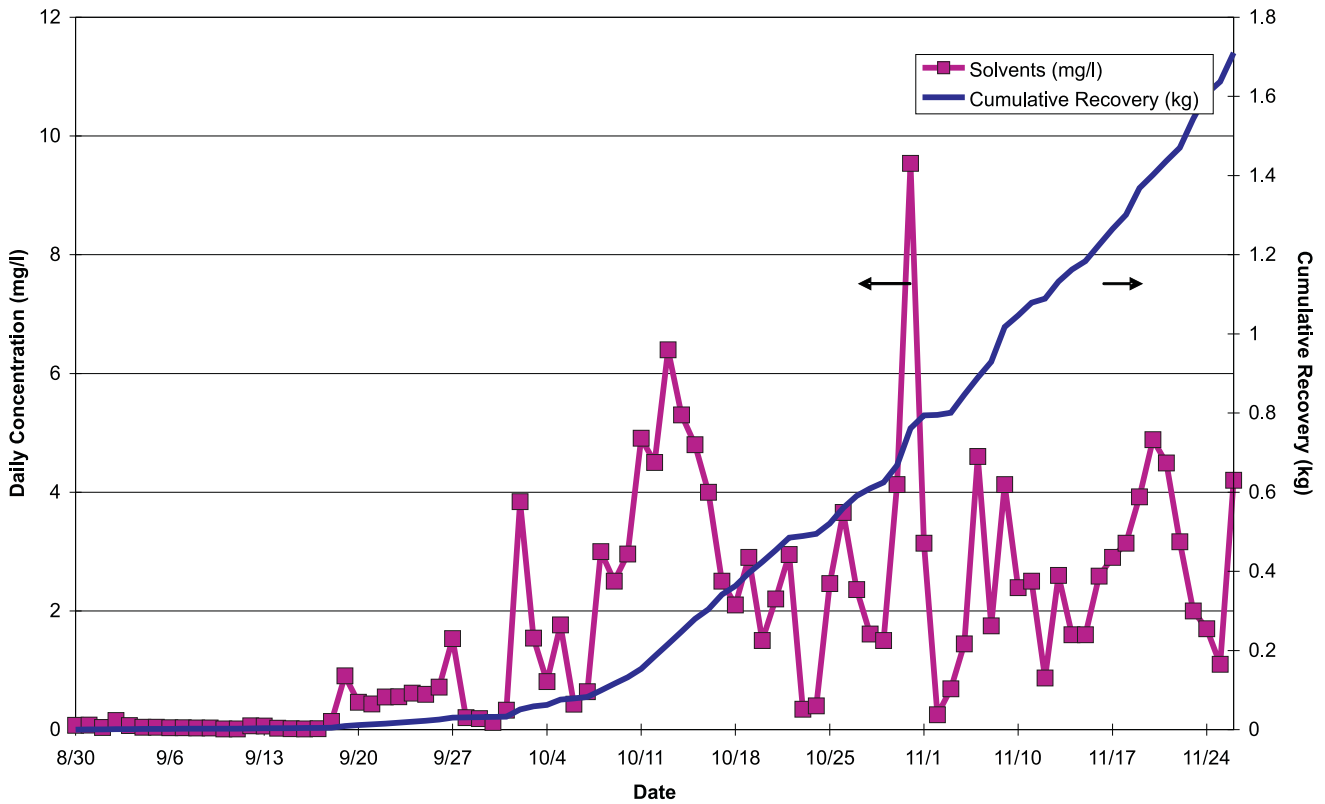


Figure 8.2.2-2. Solvent concentrations in the aqueous phase and cumulative recoveries.

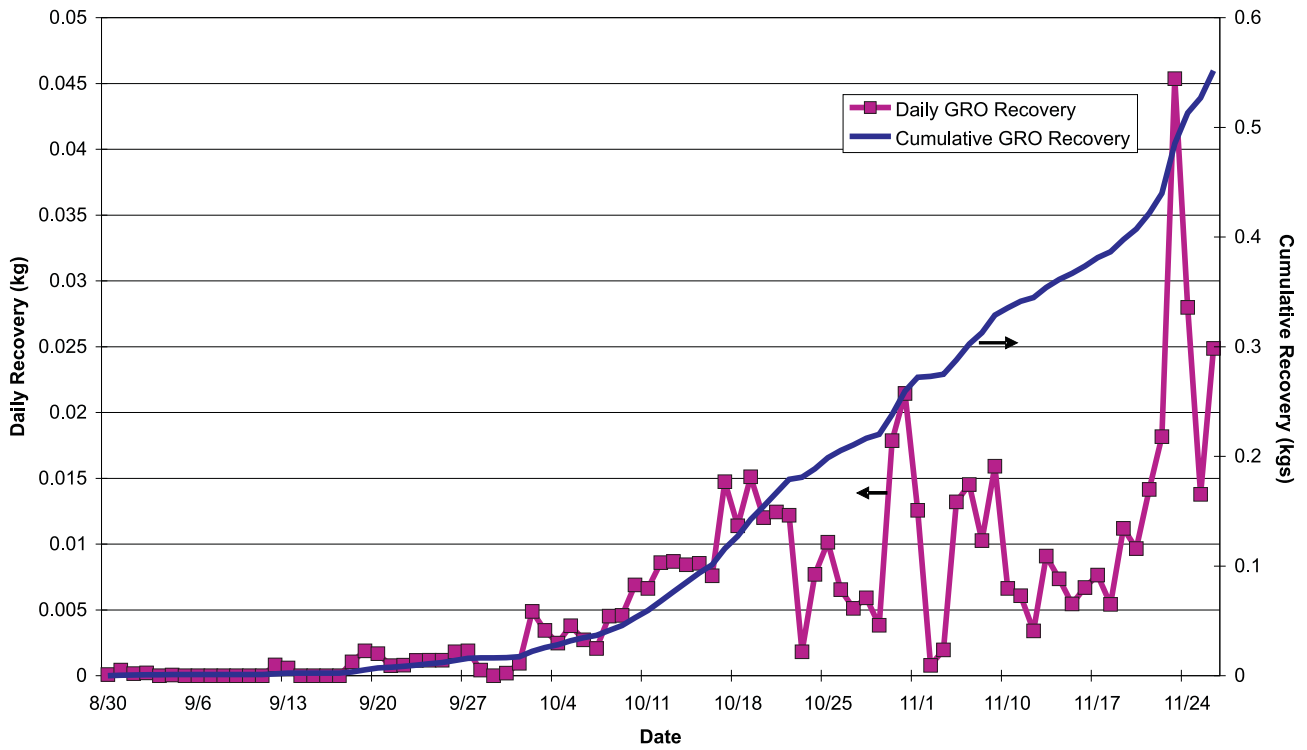


Figure 8.2.2-3. GRO daily and cumulative recovery in the aqueous phase.

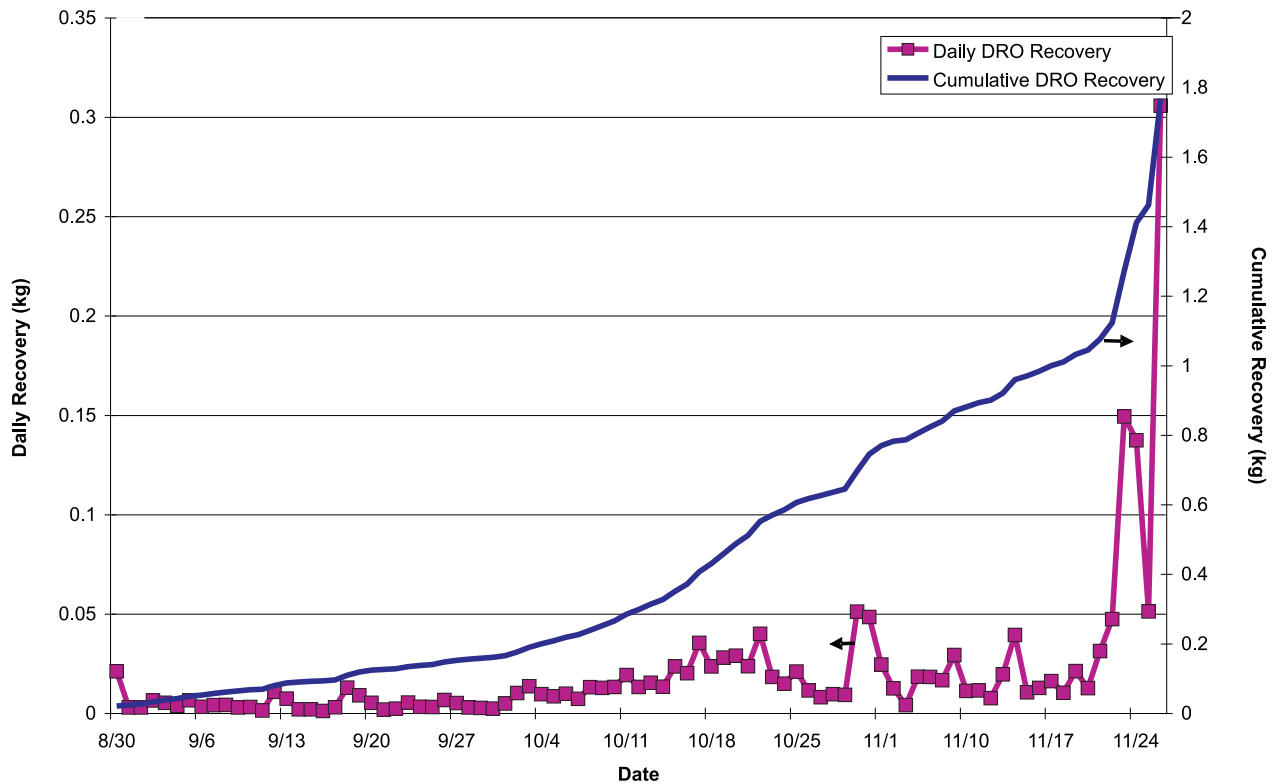


Figure 8.2.2-4. DRO daily and cumulative recovery in the aqueous phase.

or problems with inadequate spike levels. When MS/MSD results were obtained, they met the acceptance criteria set out in the QAPP. Validation of approximately 10 percent of the results showed that sampling and analysis quality control met the acceptance criteria set out in the QAPP and concluded that the data can be used for the project objectives. The only problem noted during the validation was some laboratory blank contamination due to high levels of late-eluting compounds in the samples.

For the DRO field and laboratory duplicates, most RPDs of duplicate samples were within 10 percent; only two were significantly outside the acceptance criteria of 20 percent (35 percent and 58 percent). A few samples were received at temperatures outside the temperature limitations. All MS/MSD results met acceptance criteria set up in the QAPP. Validation results showed that some methylene chloride blanks were outside the acceptance criteria, but they were still significantly lower than the sample results. Generally, the data quality met the acceptance criteria.

8.2.3. Total Mass Recovered

The total mass of contaminants recovered during this project was estimated to be 7.36 kg (16.2 lbs). The types of contaminants recovered in each phase are summarized in Table 8.2.3-1. Forty-five percent of the total mass recovered was in the vapor phase, while the remainder was recovered in the aqueous phase. Although some fuel components were on the target analyte list for the vapor samples, other fuel components could have been present in the vapor phase that were not on the list of analytes. Thus, the estimate of gasoline components recovered is likely low. DRO also was not quantified in the vapor phase; however, due to the high boiling points of these compounds (approximately 170 to 430°C; 338°F to 806°F) it is not likely that DRO components were present in the vapor phase at significant concentrations. Approximately 57 percent of the contaminant recovered was PCE, while 24 percent was DRO, and the remainder was GRO and other solvents.

Table 8.2.3-1. Summary of Contaminant Mass Recovered in Each Phase

	Vapor	Liquid	Total
PCE	2.55 kg (5.62 lbs)	1.65 kg (3.64 lbs)	4.20 kg (9.26 lbs)
TCE	0.245 kg (0.54 lbs)	0.033 kg (0.07 lbs)	0.278 kg (0.62 lbs)
Other VOCs	0.536 kg (1.18 lbs)	0.026 kg (0.06 lbs)	0.562 kg (1.24 lbs)
GRO	NA	0.552 kg (1.22 lbs)	>0.552 kg (1.22 lbs)
DRO	NA	1.768 kg (3.90 lbs)	>1.768 kg (3.90 lbs)
Total contaminants recovered	>3.30 kg (7.28 lbs)	4.030 kg (8.88 lbs)	>7.360 kg (16.23 lbs)

NA- Not Analyzed

8.3. Compliance Monitoring

Secondary objective S4 of the SITE program called for documentation of the ability of the ground water and vapor treatment system to treat the effluent streams to meet discharge limits. SteamTech collected samples of the treated vapors and liquids before discharge to determine the effectiveness of their treatment systems. These samples were collected on a weekly basis, and were compared to applicable discharge limits. Based on these results, it can be concluded that the vapor and water treatment systems used by SteamTech were effective for treating the effluent streams to meet discharge criteria. More details on the results of the compliance monitoring are given below.

8.3.1. Emitted Vapor Concentrations

Vapor samples were collected from sample point V-4, the air emissions point. Analysis was performed using EPA Method 8260B. The results of the analyses of V-4 samples are shown in Table 8.3.1-1.

Only two samples contained VOC above the reporting limits. The sample from November 12 contained PCE at 0.021 ppmv, and the sample from November 26 had a PCE concentration of 0.12 ppmv. Thus, only extremely small quantities of PCE were emitted to the atmosphere. Due to the low concentrations measured, and the dominance of nondetect concentrations, a cumulative mass calculation was not made.

8.3.2. Discharged Water Samples

The treated water discharged to the lower tier was sampled for VOCs weekly during operations (location L-3). The results are shown in Table 8.3.2-1.

Three compounds were detected in the water:

- Isopropylbenzene at 0.00064 mg/l on September 23.
- Carbon tetrachloride at levels of 0.0010 and 0.0022 mg/l on October 21 and November 12, respectively.
- PCE at levels of 0.0047, 0.00077, and 0.00077 mg/L at the three last sampling rounds on November 12, 19, and 26.

The mass of chemicals discharged to the lower tier is extremely low (significantly below one kilogram). Cumulative mass estimates were omitted due to the low concentrations.

Chapter 9. Post-Treatment Rock and Ground Water Sampling

Post-treatment ground water and rock chip samples were obtained for comparison to pre-treatment samples to fulfill SITE objectives P1 and S1, respectively.

9.1. Rock Chip Sampling Results

Post-treatment rock chip samples were acquired in July 2003. Eight locations adjacent to where pre-treatment rock chips had been acquired were chosen for sampling. Core locations were chosen to give a wide range of treatment extent, and these locations are shown on Plate 4.1.2-1. At the eastern side of the site, where most of the steam was injected, a core was obtained that was centrally located between I-5 and I-6 (BD-I-5-6). Cores were also obtained adjacent to VEA-5 and I-7, which were originally used as extraction wells but were converted to injection wells approximately five weeks after steam injection was initiated. Each of the extraction wells through the center of the treatment area, EX-1 to EX-4, were also chosen for post-treatment sampling, as these cores had some of the highest concentrations in the pre-treatment sampling, and these were some of the locations to which contaminants were being moved in order to be extracted from the subsurface. I-3 was also chosen as a drill back location for the same reasoning. Cores 0.05 meter (0.17 foot) in diameter were obtained for the post-treatment sampling using the triple tube drilling technique, and again rock chip samples were acquired using a hammer and a cold chisel. The extraction protocol outlined in Chapter 4.1.2 was followed, except that the methanol was removed from the sample at the laboratory rather than in the field. Sampling was concentrated in the depths of the boreholes where contamination had been detected during pre-treatment characterization, or where there was visible evidence of contamination.

Post-treatment MERC sampling results for PCE are shown on Plate 4.1.2-1 adjacent to the pre-treatment results, and Table 9.1-1 presents the results for all of the post-treatment MERC samples. The figures on Plate 4.1.2-1 clearly show that PCE concentrations in the rock were lower in the post-treatment samples than in the corresponding location during pre-treatment sampling. The smaller core size used for the drillback meant that less fracture surface was available for sampling, and more of the matrix further from the fracture was, of necessity, included in the sample. It is speculated that this might have had some effect on relative concentrations of pre- and post-treatment samples; however, it cannot be determined at this time if the smaller core size used for the drillback may have caused overall lower concentrations to be measured in these samples.

BD-I-5-6 was approximately 4.6 meters (15 feet) southwest of I-5 and 4.6 meters (15 feet) northwest of I-6. Thus, it was in the center of the area where most of the steam was injected. While steam likely reached this area at depth, the upper portion of the borehole would be expected to experience only modest temperature increases due to heat conduction from the nearby steam injection wells. It was noted that fractures to a depth of approximately 6 meters (20 feet) bgs in this borehole had a sheen and petroleum hydrocarbon odor. The MERC analysis showed the presence of small concentrations of BTEX and isopropylbenzene, compounds had been found in the shallow portion of I-6 prior to treatment, and these compounds persist in the fractures down to a depth of at least 5 meters (16.4 feet) bgs after treatment. PCE was first detected in this borehole at a depth of 22.1 meters (72.6 feet); however, the concentrations were low, ranging from 0.05 to 1.44 mg/kg, with the highest concentration detected in the lowest fracture sampled. These concentrations are generally similar to the concentrations found in I-5, and somewhat less than the concentrations found in I-6, with the exception of the sample from a vertical fracture at 28.9 meters (94.8 feet), which is somewhat higher than might be expected based on pre-treatment sampling results. TCE was also detected in the same fractures with PCE in concentrations ranging from 0.03 to 0.28 mg/kg. Other chlorinated compounds detected are cis- and trans-1,2-DCE and chloroform.

BD-VEA-5 was 1.4 meters (4.5 feet) north of VEA-5, which had been used for steam injection, and thus this location likely saw a small but measurable increase in temperature over its length due to heat conduction from VEA-5. This borehole also had small concentrations of BTEX compounds at approximately the depth of the water table. PCE was detected in this borehole only in fractures deeper than 19.1 meters (62.8 feet) bgs, and concentrations ranged from 0.10 to 3.38 mg/kg. The highest concentration was found in a bedding plane fracture with significant staining, indicating that it had been active in the ground water flow system. This appears to be a significant reduction from concentrations that were as high as 13.1 mg/kg in the pretreatment samples.

BD-I-7 was located approximately 1.8 meters (6 feet) northeast of I-7, and thus also was likely heated somewhat by heat conduction. PCE concentrations in this core ranged from 0.23 to 0.71 mg/kg, which may be a significant reduction from the concentrations that went as high as 5 mg/kg in I-7. Small amounts of TCE were also detected in this core, ranging from 0.09 to 0.22 mg/kg. The

Table 9.1-1. Post-Treatment Rock Chip Sampling Results

Depth in meters	Depth in feet	Fracture Description	1,2,3-trichlorobenzene	1,2,4-trichlorobenzene	1,3-dichlorobenzene	benzene	chlorobenzene	chloroform	cis-1,2-dichloroethylene	ethylbenzene	naphthalene	trans-1,2-dichloroethylene	tetrachloroethylene	trichloroethylene	toluene	total xylenes
BD-VEA-5																
4.4	14.4	V&H, S				0.06				0.11					0.23	0.69
4.4	14.4 Duplicate	V&H, S				0.09				0.16					0.22	0.89
5.6	18.5	V,S														0.17
5.6	18.5 Re-extract															
18.7	61.4	NFCS														
19.1	62.8	H,S				0.04							0.1			
20.4	66.8	BCZ, S														
21.9	72	B,S											3.38	0.16		
25.2	82.7	V, S, C, M											0.18			
BD-EX-1																
6.2	20.5	V, S													0.18	
11.1	36.5	B, C, S														
12.1	39.7	V, S, Sheen	0.12	0.32		0.07			0.04		0.08		0.77	0.06	0.06	0.02
12.1	39.7 Duplicate	V, S, Sheen	0.11	0.29		0.09			0.04		0.08		0.89	0.09	0.07	0.03
14.2	46.7	NFCS														
17.9	58.8	S, not open				0.04					0.11		5.14	0.14	0.04	
25.0	81.9	V, S							0.1				2.58	0.23		
BD-EX-2																
9.7	31.7	NFCS			0.03										0.56	
13.4	44	V, S											2.46	0.1		
14.3	46.8	B, S											0.78			
16.8	55.2	MB														
19.1	62.8	V, S											0.5			
19.1	62.8 Re-extract												0.15			

Table 9.1-1. Continued

Depth in meters	Depth in feet	Fracture Description	1,2,3-trichlorobenzene	1,2,4-trichlorobenzene	1,3-dichlorobenzene	benzene	chlorobenzene	chloroform	cis-1,2-dichloroethylene	ethylbenzene	naphthalene	trans-1,2-dichloroethylene	tetrachloroethylene	trichloroethylene	toluene	total xylenes
BD-EX-3																
6.1	20.1								0.1				1.01	0.9	0.04	
6.1	20.1 Duplicate								0.09				0.96	0.73	0.05	
9.0	29.5	V, C											1.89	0.07		
12.7	41.7	B											1.24	0.1	0.02	
12.7	41.7 Re-extract												0.44	0.05		
14.0	45.9	B, C, S							0.08				3.34	0.47		
14.6	48	NFCS														
16.8	55	B, S, C							0.14				1.32	0.49		
BD-EX-4																
5.5	18	B, S, Sheen													0.08	0.07
7.5	24.7	B, S													0.04	0.06
9.9	32.5	V, S														0.04
9.9	32.5 Duplicate	V, S										0.02			0.03	0.05
14.8	48.7	B, S											0.07			0.04
16.4	53.9	H, S														
18.4	60.4	B, C, S										0.02	0.65	0.32		0.02
20.1	66	NFCS														
20.7	67.9	V, S											0.34	0.32	0.03	
24.5	80.4	B														
BD-I-3																
23.2	76.2	B, S, C											0.4	0.11		
23.2	76.2 Re-extract												0.08			
23.7	77.8	NFCS											0.73	0.11		
26.0	85.4	H, S, B											2.75	0.1		
26.3	86.4	V, C, S				0.05			0.03				1.34	0.33		

Table 9.1-1. Continued

Depth in meters	Depth in feet	Fracture Description	1,2,3-trichlorobenzene	1,2,4-trichlorobenzene	1,3-dichlorobenzene	benzene	chlorobenzene	chloroform	cis-1,2-dichloroethylene	ethylbenzene	naphthalene	trans-1,2-dichloroethylene	tetrachloroethylene	trichloroethylene	toluene	total xylenes
26.3	86.4 Duplicate	V, C, S							0.03				1.82	0.46		0.05
30.1	98.6	B, C, S				0.02	0.05		0.03		0.06	0.03	15.78	0.4		0.05
30.3	99.5	H, S											7.02	0.31		0.05
30.3	99.5 Re-extract												1.74	0.07		
BD-I-5-6																
2.7	8.9	V&B, S, O, Sheen				0.1				0.04					0.08	0.2
2.7	8.9 Re-extract					0.03									0.03	0.03
2.7	8.9 Duplicate					0.15				0.07					0.15	0.39
5.0	16.4	V, S, O				0.25				0.24		0.04			0.29	1.09
5.0	16.4 Re-extract					0.06				0.04					0.08	0.16
15.0	49.3	NFCS														
18.1	59.3	B, C, S														
18.1	59.3 Duplicate															
22.1	72.6	V, S						0.1					0.16	0.08		0.03
23.4	76.9	B, S						0.03	0.22			0.03	0.23	0.28		
23.4	76.9 Re-extract								0.09				0.12	0.16		0.03
25.4	83.3	B														
25.8	84.6	V, S											0.05			
28.9	94.8	V, S											1.44	0.21		
BD-I-7																
15.0	49.1	V, S														
15.5	50.7	V, S											0.71	0.15		
15.5	50.7 Duplicate	V, S											0.37	0.09		
20.5	67.3	NFCS							0.15				0.23	0.21	0.04	
21.3	70	V, S											0.45	0.22		

nonfractured core sample (NFCS) collected from a depth of 20.1 meters (68 feet) bgs in I-7 had shown a small concentration of PCE (0.71 mg/kg). A sample from a broken core zone at a depth of 20.5 meters (67.3 feet) bgs in BD-I-7 showed a small concentration of PCE, as well as small concentrations of TCE, cis-1,2-DCE, and toluene.

BD-EX-4 was located approximately 1.4 meters (4.5 feet) north of EX-4. EX-4 showed a temperature increase along its length due to heat conduction from a nearby injection well, and also showed a small temperature increase at a depth of about 6 to 12 meters (20 to 40 feet) bgs that appears to be steam/hot water flow in a fracture. PCE concentrations found in EX-4 prior to treatment ranged from 4.41 to 7.48 mg/kg. Samples obtained from the same depth range in BD-EX-4 had PCE concentrations ranging from nondetect to 0.65 mg/kg. TCE concentrations ranged from nondetect to 0.32 mg/kg. Very low concentrations of trans-1,2 DCE were also detected in the post-treatment core. A fracture at 5.5 meters (18 feet) bgs in BD-EX-4 contained an oil sheen and significant staining, and the rock chip analysis detected small amounts of toluene and xylene in this fracture. Fractures at this depth in EX-4 had been nondetect during the pre-treatment sampling, thus, the small amount fuel components detected post-treatment may indicate that contaminants were being displaced toward EX-4 for recovery.

BD-EX-1 was located approximately 1.2 meters (3.8 feet) south of EX-1. EX-1 had shown a small temperature increase (to 20°C; 68°F) at a depth of 6.1 meters (20 feet) bgs during the later part of the steam injection. Pre-treatment rock chips in this area had shown PCE concentrations as high as 19 and 21 mg/kg at the bottom of the borehole. PCE concentrations in the bottom of BD-EX-1 were 5.14 and 2.58 mg/kg. The highest concentration was detected in a fracture that was not thought to be open based on visual observation of the core in the field. Detections of TCE were as high as 0.23 mg/kg. Small amounts of BTEX compounds were detected in the central portion of this borehole, as well as 1,2,3-trichlorobenzene, 1,2,4-trichlorobenzene, and naphthalene.

BD-EX-2 was located approximately 1.1 meters (3.5 feet) east of EX-2. Essentially no temperature increase was recorded at EX-2. During the pre-test characterization, PCE concentrations in EX-2 were as high as 12 and 18 mg/kg. BD-EX-2 showed PCE concentrations ranging from 0.15 to 2.46 mg/kg. There was only one small hit of TCE of 0.10 mg/kg. There were very small concentrations of toluene and 1,3-dichlorobenzene in the NFCS taken from a depth of 9.7 meters (31.7 feet) bgs, which was located approximately 0.5 meters (1.7 feet) from the nearest feature, a bedding plane fracture at 9.1 meters (30 feet) bgs.

BD-EX-3 was located approximately 1.7 meters (5.5 feet) east-southeast from EX-3. EX-3 was the extraction well farthest from the area of steam injection, and no significant temperature increase was recorded in this well. EX-3 had some of the shallowest detections of PCE, starting at a depth of 6.7 meters (22 feet) bgs, and concentrations went as high as 8 and 10 mg/kg. BD-EX-3 had PCE concentrations ranging from 0.44 to 3.34 mg/kg, and TCE concentrations ranging from 0.05 to 0.90 mg/kg. cis-1,2-DCE was detected at several locations, with the highest concentration being 0.14 mg/kg.

BD-I-3 was located approximately 1.6 meters (5.2 feet) south of I-3. During the pre-treatment characterization, the highest detections of PCE were in I-3, where the bottom three fractures sampled had concentrations of 41.8 mg/kg at 26.8 meters (88 feet) bgs, 54.4 mg/kg at 29.3 meters (96 feet) bgs, and 72 mg/kg at 29.6 meters (97 feet) bgs. During the steam injection, no temperature increases would be expected at this well; however, the temperature data show some sporadic increases. Because the pre-treatment characterization had shown that contamination existed only in the bottom of this borehole, starting at approximately 21.3 meters (70 feet) bgs, sampling during the drill back concentrated on the bottom of the borehole. This borehole contained the highest PCE concentrations found during the drill back, with 15.78 mg/kg detected at 30.1 meters (98.6 feet) bgs, and 7.02 mg/kg detected at 30.3 meters (99.5 feet) bgs. Other fractures from 26.0 to 26.3 meters (85.4 to 86.4 feet) bgs also had PCE concentrations ranging from 1.34 to 2.75 mg/kg. A fracture at 23.2 meters (76.2 feet) bgs had a smaller concentration (0.08 mg/kg), and a sample from a broken core zone at 23.7 meters (77.8 feet) bgs showed 0.73 mg/kg of PCE, as well as 0.11 mg/kg of TCE. At most places where PCE was detected, a small amount of TCE was also detected. In the most contaminated fractures, small amounts of cis- and/or trans-1,2-DCE were also detected. The most contaminated fracture at 30.1 meters (98.6 feet) bgs also contained small amounts of benzene, chlorobenzene, and naphthalene, and there was a low concentration of 1,3-dichlorobenzene at 26.3 meters (86.4 feet) bgs. Based on observation of the core in the field, it was thought that these fractures at 30.1 and 30.3 meters (98.6 and 99.5 feet) bgs were not open.

Overall, the post-treatment rock samples showed lower PCE concentrations than had been found in the pre-treatment samples. However, it must be kept in mind that it can be difficult to ensure that post-treatment borings sample the same structures as were sampled in pre-treatment borings. This is particularly true in the case of steeply-dipping fractures containing contaminant, such as those at 29.3 and 29.6 meters (96 and 97 feet) bgs in I-3. Some of the highest rock chip concentrations were found in samples from fractures that were not thought to be open based on visual observation in the field. BTEX contamination remains at approximately the depth of the water table in the eastern portion of the site. This contamination likely comes from an LNAPL plume that is known to exist to the east of the Quarry. Because the steam injection was targeting chlorinated solvent contaminants at depth, little steam was injected into the shallow zones near the water table. The shallow BTEX contamination could be remaining from before the steam injection, or it could have moved back into the area after the steam injection was completed. Despite the fact that no temperature increases were expected or noted at I-3, EX-2, or EX-3, decreases in rock concentrations were also noted at these locations. The cause of these decreases is not known.

QC Summary. The most significant QC problem noted with these samples was contamination in several of the sand blank samples that were prepared in the field. Contaminants found in the sand blanks included n-isopropylbenzene, 1,3,5-trimethylbenzene, 1,2,4-

trimethylbenzene, sec-butylbenzene, and p-isopropyltoluene, which are some of the same contaminants that were found in sand blanks during pre-treatment MERC sampling. It was determined that these contaminants were coming from a waxy coating on the lid of the sample jars. Table 9.1-1 contains only the contaminants that are known to be coming from the rock chips. Duplicate samples from the BD boreholes showed RPDs ranging from 4 to 64 percent, with 20 percent of the results outside of the criteria commonly used for evaluating duplicates of less than 40 percent difference. However, it should be kept in mind that these concentrations are low (most of them less than 1 mg/kg) and this may make the RPDs large.

Several of the samples were re-extracted with methanol for an additional week after the first methanol extraction. In virtually every case, additional contaminants were extracted by the fresh methanol. Concentrations found by re-extraction were generally 15 to 50 percent of the concentration that was found in the initial extraction. Although these data are not definitive on the extraction efficiency of the method used, they do indicate that actual rock chip concentrations are generally at least 30 percent higher than those detected by this method.

PCE concentrations were found to be high in some laboratory control samples and in MS/MSD samples, and it appeared that this was due to a discrepancy between the calibration and spiking standards. Xylenes and ethylbenzene were also high in many of the laboratory control samples; however, these compounds were generally not detected in rock chip samples. Despite these QC problems, the data quality is sufficient for the purposes of this project.

9.2. Ground Water Monitoring

For the post-treatment ground water sampling, the intention had been to sample the same ground water intervals that had been sampled prior to the steam injection in order to compare pre-treatment and post-treatment concentrations, and this was done when possible. However, not all of the intervals used for pre-treatment sampling were accessible after treatment, as several wells had been completed with grout for steam injection or monitoring purposes. Thus, adjustments were made to the sampling program. The intervals that were sampled during the three post-treatment ground water sampling rounds are shown in Tables 4.1.7.1-1 and 4.1.7.2-1. For wells I-4, I-5, I-6, I-7, and I-8, which were used as injection wells, the intervals sampled after steam injection correspond to some of the steam injection intervals, and the samples were obtained through the carbon steel standpipes that had been used to inject the steam. VEA-5 was sampled above the injection interval, which was open for extraction. All of the same intervals in the deep wells were sampled during the post-treatment sampling. Compilations of the ground water data are given in Table 9.2-1. The data are also shown on Plate 9.2-1.

Table 9.2.1-1. Post-Treatment Ground Water Sampling Results

Well I-2						
Interval, meters bgs	<13.7			>13.7		
Compounds/Date	May-03	Oct-03	May-04	May-03	Oct-03	May-04
cis-1,2-Dichloroethylene		0.00075J			0.0007J	
Chloroform		0.0016			0.0017	
Trichloroethylene		0.0042			0.0036	
Toluene		0.0016				
Tetrachloroethylene	0.0008J	0.065	0.0015	0.00096J	0.059	0.0018

Well I-3							
Interval, meters bgs	<15.2			>15.2			
Compounds/Date	May-03	Oct-03	May-04	May-03	May-03 ^d	Oct-03	May-04
Acetone				0.0011J			
cis-1,2-Dichloroethylene		0.00097J				0.00088J	
Chloroform		0.0037	0.0007J			0.0036	0.00067J
Trichloroethylene		0.0068	0.003		0.0044	0.0068	0.0026
Toluene		0.0037	0.004				0.00088J
Tetrachloroethylene	0.0012	0.13	0.044	0.0018	0.0012	0.14	0.034

Table 9.2.1-1. Continued

Well I-4			
Interval, meters bgs	21.3-33.5		
Compounds/Date	May-03	Oct-03	May-04
Acetone	0.0066	0.0048J	0.0076
Dichloromethane		0.0012	0.0026
Methyl Ethyl Ketone	0.001J		
cis-1,2-Dichloroethylene	0.0012	0.0012	0.0036
Chloroform		0.012	0.004
Benzene	0.0028	0.0024	0.0035
Trichloroethylene		0.00037J	0.00067J
Methyl Isobutyl Ketone	0.0038	0.0025	0.0023J
2-Hexanone	0.018	0.0083	0.0041J
Tetrachloroethylene	0.00097J	0.0038	0.0087
Chlorobenzene	0.0022	0.0017	0.0012
1,2,4-Trimethylbenzene			0.0006J
p-Dichlorobenzene	0.0028	0.0018	0.00082J
1,2,4-Trichlorobenzene	0.0014	0.0015	0.0024
Naphthalene	0.00086J	0.00077J	0.0016J
1,2,3-Trichlorobenzene			0.00086J

Well I-5			
Interval, meters bgs	21.3-36.6		
Compound/Date	May-03	Oct-03	May-04
Acetone	0.055	0.038	0.054
Methyl Ethyl Ketone	0.003J	0.0024J	0.0029J
cis-1,2-Dichloroethylene	0.00089J	0.0014	0.0016
Chloroform		0.0019	
Benzene	0.0029	0.003	0.0031
Methyl Isobutyl Ketone	0.00073	0.00065J	
2-Hexanone	0.0058	0.0029	
Tetrachloroethylene	0.002	0.0058	
Chlorobenzene	0.0026	0.0025	0.0022
p-Dichlorobenzene	0.0034	0.0027	0.0023
o-Dichlorobenzene	0.0006J		
1,2,4-Trichlorobenzene	0.0096	0.0095	0.0076
Naphthalene	0.014	0.0091	0.0096
1,2,3-Trichlorobenzene	0.0088	0.0056	0.0045

Well I-6			
Interval, meters bgs	9.1-15.2		
Compound/Date	May-03	Oct-03	May-04
Acetone	0.0078		
Dichloromethane	0.0024	0.0039	
Carbon Disulfide		0.0041	
Methyl Ethyl Ketone	0.00051J		
cis-1,2-Dichloroethylene	0.00059J	0.0007J	0.00075J
Chloroform	0.029	0.22	0.0019
Carbon Tetrachloride		0.074	
Benzene	0.0014	0.00091J	0.00087J
Trichloroethylene	0.006	0.039	0.026
Tetrachloroethylene	0.0011	0.0012	

Table 9.2.1-1. Continued

Well I-7			
Interval, meters bgs	23.5-30.2		
Compounds/Date	May-03	Oct-03	May-04
Vinyl Chloride	0.0012	0.0006J	
Acetone	0.0076		
1,1-Dichloroethylene	0.0035	0.00074J	
Dichloromethane	0.0018	0.0063	
trans-1,2-Dichloroethylene	0.002		
Methyl Ethyl Ketone	0.0015J		
cis-1,2-Dichloroethylene	0.028	0.014	0.0063
Chloroform	0.010	0.015	
Benzene	0.004	0.0054	0.0035
Trichloroethylene	0.031		
Toluene	0.00085J	0.00068	
Tetrachloroethylene	0.080	0.00054J	
Chlorobenzene	0.0011	0.002	0.0012
1,2,4-Trichlorobenzene	0.0013	0.0036	0.0024
Naphthalene	0.0016J	0.0024	0.0024
1,2,3-Trichlorobenzene	0.00077J	0.0019	0.00096J

Well I-8							
Interval, meters bgs	14.0-17.4				23.5-28.3		
Compound/Date	May-03	Oct-03	May-04	May-04 ^d	May-03	Oct-03	May-04
Vinyl Chloride	0.00089J		0.0022	0.0023		0.0057	0.0066
Acetone	0.019	0.28	0.037	0.040	0.71	0.0072	0.25
1,1-Dichloroethylene	0.00065J	0.0013	0.0017	0.0018	0.00059J	0.0056	0.0063
Dichloromethane	0.0017		0.0016	0.0016			
trans-1,2-Dichloroethylene		0.00067J				0.0018	0.0014
Methyl Ethyl Ketone	0.78	0.0062	0.44	0.46	0.013	0.059	0.0045J
cis-1,2-Dichloroethylene	0.018	0.031	0.042	0.042	0.0096	0.13	0.14
Chloroform	0.0063	0.0016	0.00098J	0.001	0.00064J	0.0035	0.0014
Benzene	0.0065	0.015	0.012	0.012	0.0064	0.028	0.027
Trichloroethylene	0.06	0.086	0.062	0.062	0.044	0.73	0.34
Toluene	0.0029	0.0042	0.0031	0.0031	0.0019	0.0043	0.0039
1,1,2-Trichloroethane						0.00072J	
2-Hexanone					0.0038		
Tetrachloroethylene	0.40	1.30	0.40	0.40	0.77	2.20	1.30
Chlorobenzene	0.0017	0.0086	0.0048	0.005	0.004	0.015	0.015
Ethyl Benzene	0.00073J	0.0025	0.0021	0.0021	0.00065J	0.0039	0.0041
Total Xylenes	0.004	0.011	0.0072	0.007	0.005	0.0087	0.01
Isopropylbenzene		0.00055J	0.00057J	0.00056J			0.0014
1,1,2,2-Tetrachloroethane						0.001	
n-Propylbenzene		0.00072	0.0006J	0.00062J		0.00075J	0.0016
1,3,5-Trimethylbenzene	0.00096J	0.0048	0.0029	0.0029	0.0016J	0.0016	0.0021
tert-Butylbenzene		0.00067J				0.00068J	
1,2,4-Trimethylbenzene	0.0019	0.015	0.0092	0.0087	0.0027	0.017	0.019
Sec-ButylBenzene							0.0007J
p-Isopropyltoluene		0.00069J	0.00075J	0.00074J		0.00073J	0.0023
m-Dichlorobenzene		0.00074J				0.00081J	0.0011
p-Dichlorobenzene		0.0019	0.00063J	0.0006J	0.0013	0.002	0.0023
o-Dichlorobenzene		0.0013	0.00099J		0.00059J	0.0018	0.0019
n-Butylbenzene				0.00085J		0.00057J	
1,2,4-Trichlorobenzene	0.0018	0.025	0.0071	0.0063	0.0093	0.022	0.027
Naphthalene	0.031	0.11	0.11	0.11	0.024	0.14	0.19
1,2,3-Trichlorobenzene	0.0011	0.01	0.0035	0.0031	0.004	0.011	0.012

Table 9.2.1-1. Continued

Well EX-1							
Interval, meters bgs	<12.2			>12.2			
Compound/Date	May-03	Oct-03	May-04	May-03	Oct-03	Oct-03 ^d	May-04
Chloromethane		0.0008J					
cis-1,2-Dichloroethylene					0.00058J		
Chloroform	0.00065J	0.014	0.00064J	0.00053J	0.016	0.015	0.00069J
Carbon Tetrachloride	0.00076J			0.00062J			
Trichloroethylene	0.00084J	0.0038	0.0018	0.00072J	0.004	0.0041	0.002
Toluene		0.0054	0.0038				0.00065J
Tetrachloroethylene	0.001	0.057	0.021	0.00097J	0.064	0.08	0.022

Well EX-2							
Interval, meters bgs	4.6-7.6				18.3-21.3		19.8-22.9
Compound/Date	May-03	May-03 ^d	Oct-03	May-04	May-03	Oct-03	May-04
trans-1,2-Dichloroethylene					0.00062J		
Methyl Ethyl Ketone	0.00087J	0.00069J			0.028		
cis-1,2-Dichloroethylene	0.00066J	0.00067J	0.0019		0.011	0.0016	
Chloroform			0.0018		0.005	0.0031	
Carbon Tetrachloride	0.00079J	0.00075J			0.012		
Benzene					0.0022		
Trichloroethylene	0.0063	0.0058	0.0062		0.092	0.0074	
Toluene			0.0031		0.0034		
Tetrachloroethylene	0.22	0.20	0.13	0.0051	2.60	0.20	0.0065
Chlorobenzene					0.003		
Ethyl Benzene					0.002		
Total Xylenes		0.00065J			0.0078		
Isopropylbenzene					0.00083J		
1,1,2,2-Tetrachloroethane					0.0013		
n-Propylbenzene					0.0015		
1,3,5-Trimethylbenzene	0.00092J				0.014		
1,2,4-Trimethylbenzene		0.00052J			0.033		
sec-Butylbenzene					0.00061J		
p-Isopropyltoluene					0.003		
p-Dichlorobenzene					0.0016		
o-Dichlorobenzene					0.0006J		
n-Butylbenzene					0.0032		
1,2,4-Trichlorobenzene					0.011		
Naphthalene	0.0071	0.0088	0.0006J		0.19		
1,2,3-Trichlorobenzene					0.0048		

Table 9.2.1-1. Continued

Well EX-3			
Interval, meters bgs	Upper Half		10.7-13.7
Compound/Date	May-03	Oct-03	May-04
Vinyl Chloride	0.0045	0.02	0.029
Acetone	0.0066		
1,1-Dichloroethylene	0.0024	0.0092	0.012
trans-1,2-Dichloroethylene	0.0014	0.0027	0.0035
Methyl Ethyl Ketone	0.0025J		
cis-1,2-Dichloroethylene	0.11	0.18	0.20
Chloroform	0.005	0.0073	0.0014
Benzene	0.013	0.018	0.029
Trichloroethylene	0.72	1.40	1.80
Toluene	0.0052	0.023	0.0071
Tetrachloroethylene	6.70	28.00	15.00
Chlorobenzene	0.015	0.027	0.03
Ethyl Benzene	0.0024	0.007	0.0037
Total Xylenes	0.016	0.053	0.013
Isopropylbenzene		0.0015	0.001
1,1,2,2-Tetrachloroethane	0.0024	0.0039	
n-Propylbenzene	0.00071J	0.0019	
1,3,5-Trimethylbenzene	0.0087	0.025	0.018
tert-Butylbenzene		0.00083J	
1,2,4-Trimethylbenzene	0.021	0.051	0.015
sec-Butylbenzene		0.00091J	0.00057J
p-Isopropyltoluene	0.0006J	0.0056	0.0073
m-Dichlorobenzene	0.00056J	0.0011	0.0016
p-Dichlorobenzene	0.0033	0.0061	0.0089
o-Dichlorobenzene	0.00057J	0.0012	0.0015
n-Butyl Benzene			0.0028
1,2,4-Trichlorobenzene	0.0063	0.02	0.0097
Naphthalene	0.18	0.18	0.0095
1,2,3-Trichlorobenzene	0.0033	0.0072	0.0043

Well EX-4								
Interval, meters bgs	3.0-6.1				6.1-9.1			
Compound/Date	May-03	Oct-03	Oct-03 ^d	May-04	May-03	Oct-03	May-04	May-04 ^d
Acetone								
Methyl Ethyl Ketone								
Chloroform		0.0044	0.0044	0.0016		0.0041	0.0014	0.0014
Carbon Tetrachloride		0.00079J		0.00099J		0.00068	0.0011	0.0011
Trichloroethylene		0.0044	0.0044	0.0014		0.0037	0.0011	0.001
Toluene		0.0032	0.0029			0.0071		
Tetrachloroethylene	0.00089J	0.0033	0.0029		0.0012	0.0045		

Well EX-4 Continued						
Interval, meters bgs	15.2-18.3			18.3-21.3		
Compound/Date	May-03	Oct-03	May-04	May-03	Oct-03	May-04
Acetone	0.0017J			0.0016J		
Methyl Ethyl Ketone	0.00085J			0.00085J		
Chloroform		0.0046	0.0013		0.0048	0.0014
Carbon Tetrachloride		0.00053J			0.00058J	0.00087J
Trichloroethylene	0.0044	0.0032	0.00095J		0.003	0.00093J
Toluene		0.0051			0.0015	
Tetrachloroethylene	0.0017	0.0042	0.00053J	0.0019	0.0058	0.00066J

Table 9.2.1-1. Continued

Well JBW-7817B			
Interval	Open Bore-Hole		
Compound/Date	May-03	Oct-03	May-04
Chloroform		0.00071J	
Methyl Ethyl Ketone	0.00058J		

Well VEA-5			
Interval, meters bgs	<23.5		
Compound/Date	May-03	Oct-03	May-04
cis-1,2-Dichloroethylene		0.0035	0.00066J
Benzene		0.0097	0.0055
Trichloroethylene		0.0016	0.00074J
Tetrachloroethylene	0.00066J	0.0043	0.00096J
Ethyl Benzene		0.02	0.00074J
Total Xylenes		0.0019J	0.0011J
Isopropylbenzene		0.0038	0.0018
n-Propylbenzene		0.0035	0.00074J
1,2,4-Trimethylbenzene		0.0089	0.0042
sec-Butylbenzene		0.00066J	
p-Isopropyltoluene		0.0011	0.00058J
Naphthalene			0.00065J

Well SM-1					
Interval	Interval 1		Interval 3		
Compound/Date	May-03	Oct-03	May-03	Oct-03	May-04
Acetone			0.017		
Chloroform	0.016	0.014	0.007	0.009	0.0078
Tetrachloroethylene		0.0038	0.0019	0.003	0.0025

Well SM-2						
Interval	Interval 2			Interval 3		
Compound/Date	May-03	Oct-03	May-04	May-03	Oct-03	May-04
Chloromethane		0.00053J				
Vinyl Chloride	0.0081	0.0075	0.01	0.0033	0.0016	0.0033
Acetone	0.0065	0.0054	0.0085	0.0017J		
1,1-Dichloroethylene	0.0051	0.0041	0.0046	0.0026	0.0014	0.0022
trans-1,2-Dichloroethylene	0.0022	0.0022	0.0022	0.0016	0.0012	0.0014
Methyl Ethyl Ketone	0.0013J	0.0015J	0.0019J			
cis-1,2-Dichloroethylene	0.10	0.17	0.44	0.092	0.11	0.30
Chloroform	0.0081	0.0079	0.007	0.0062	0.0057	0.0066
Benzene	0.0021	0.0021	0.0021	0.0017	0.0012	0.0014
Trichloroethylene	0.40	0.33	0.44	0.32	0.25	0.24
Toluene	0.0025	0.0025	0.0031	0.00096J	0.00059J	0.00091J
Tetrachloroethylene	0.15	0.12	0.17	0.26	0.18	0.20
Chlorobenzene	0.00079J	0.00077J	0.00069J			0.00055J
Total Xylenes			0.00089J	0.00063J		0.0007J
1,2,4-Trimethylbenzene						0.00054J
1,2,4-Trichlorobenzene						0.00058J
Naphthalene		0.00089J	0.0013J	0.0012J	0.00059J	0.0022
1,2,3-Trichlorobenzene						0.00081J

Table 9.2.1-1. Continued

Well SM-3						
Interval	Interval 1			Interval 3		
Compound/Date	May-03	Oct-03	May-04	May-03	Oct-03	May-04
Acetone				0.014		
Chloroform	0.0067	0.0052	0.0041	0.0034	0.003	0.00078J

units-mg/l

Empty cell indicates compound was not detected.

d-represents field duplicate

J - estimate

9.2.1. May 2003 Monitoring Round

The first round of post-treatment ground water samples were collected in May 2003, approximately six months after completion of the steam injection. The long period between completion of the steam injection and the first round of sampling was necessary due to problems with accessing the site during the winter. PCE concentrations were in general low during this round of sampling, especially when compared to the high concentrations that were being extracted when the steam injection was discontinued. PCE concentrations in the samples from all intervals of EX-1, EX-4, I-2, I-3, I-4, I-5, I-6, JBW-7817B, and VEA-5 that were sampled were below the MCL. For some of these intervals, that means that the concentrations dropped by as much as four orders of magnitude in the five month period immediately following the end of operations. Other samples, such as those from I-7 and I-8, showed increases in concentration from what had been extracted from these wells early in the steam injection. These concentration increases seem counterintuitive based on the fact that these wells were used for steam injection during the later part of the project. However, PCE-contaminated ground water could have entered these wells from the south or east after operations ceased. Samples from EX-3 and EX-2 remained similar to what they had been during the steam injection. Samples that had significant PCE concentrations also had significant TCE and DCE concentrations, and vinyl chloride was usually detected in these intervals.

During this sampling round, fuel components were found to have a much wider distribution than they had prior to steam injection, when they had largely been restricted to the eastern part of the site. Fuel components now also appeared in I-4, EX-2, I-8, and I-7. It appears that acetone, DCE, and vinyl chloride are now also more widely distributed.

Interval 1 of SM-1 and SM-3, both of which are below the target zone, were both nondetect for PCE during this sampling round. Small concentrations of chloroform were detected. Interval 3 of these same two wells, which are approximately at the same elevation as the treatment area, shows PCE concentrations similar to those found prior to treatment. SM-2, which had contained significant contamination in Intervals 2 and 3 prior to treatment, showed similar levels of PCE and other contaminants in this first round of post-treatment samples. These intervals are at approximately the same elevation as the treatment area.

9.2.2. October 2003 Monitoring Round

Ground water results from this second round of sampling generally show higher contaminant concentrations than were found in the first round of sampling. PCE and TCE concentrations in I-2, I-3, EX-1, and EX-2 were similar to concentrations found prior to treatment. I-8 and EX-3 have the highest concentrations of PCE and TCE in this sampling round, and these wells still show the presence of fuel components and chlorobenzenes, compounds that had not been detected prior to treatment. I-4, I-5, I-6, and I-7 have lower concentrations of PCE and TCE than they had prior to treatment, which is consistent with the fact that these wells were used for steam injection and thus saw significant temperature increases during operations. These wells now contain some of the fuel components and chlorobenzenes that were presumably mobilized during the steam injection. EX-4, which was the closest extraction well to the heated area, does not contain fuel components, and PCE concentrations have decreased since the first sampling round. PCE concentrations in this well remain lower than they had been prior to treatment. Small concentrations of carbon tetrachloride, chloroform, and toluene were detected in this well during this sampling round. VEA-5 shows small concentrations of PCE and its breakdown products. Fuel components (but not chlorobenzenes), which were not detected in the April sampling round, have now moved back into this well, likely due to the LNAPL plume that is in this area. The absence of chlorobenzenes in this sample likely indicates that the fuel components are from a different source than the fuel components found in other wells.

Interval 1 of SM-1, which is below the treatment area, now shows a small amount of PCE; however, the results for all the other intervals of the deep wells that were sampled remain very similar to the results from the first round of post-treatment sampling. Essentially wells SM-1 and SM-3 show very little or no contamination, while SM-2 has contamination in Interval 2 and 3 as it had before treatment.

9.2.3. May 2004 Monitoring Round

Ground water results from this final round of sampling generally show lower levels of contaminants than were found in the October 2003 monitoring round. This likely demonstrates some of the same type of temporal variations in ground water quality that were found prior to treatment. PCE and TCE concentrations remain high in wells I-8 and EX-3, as do fuel components and chlorobenzenes. All of the post-treatment samples from these wells show significant concentrations of TCE, DCE, and vinyl chloride, which had not been detected prior to treatment. I-3 and EX-1 appear to have ground water concentrations that are similar to pre-treatment concentrations. Lower concentrations compared to pre-treatment levels are found in wells EX-2, EX-4, and I-2. In this sample round, wells I-4, I-5, I-6, and I-7 have lower PCE concentrations than were detected prior to treatment; however, they now contain fuel components and chlorobenzenes that were not detected prior to treatment and were presumably mobilized during treatment. Borehole JBW-7817B remains clean, and VEA-5 still contains fuel components but very little chlorinated solvent.

Little change is found in the results for the deep wells. Interval 1 of SM-1 could not be sampled during this round to confirm the result for October 2003, which showed a small concentration of PCE. Although Interval 2 of SM-2 appears to contain somewhat higher contaminant concentrations now than it did prior to treatment, Interval 3 of this well seems to show a decrease in ground water concentrations. SM-3 remains clean in all sampled intervals.

9.2.4. Ground Water QC Summary

Quality control checks on the ground water data from the post treatment sampling show that there were only minor quality control problems with these analysis, and the data are of acceptable quality for the project objectives. Trip blanks indicated there were no problems with sample integrity during shipping. Mostly dedicated sampling equipment was used so that equipment blanks generally were not required; however, one equipment blank from the October 2003 sampling round had a small concentration of chloroform. There were some differences between the results of one sample and its duplicate from the May 2003 sampling round, as the RPD in PCE concentrations was 40 percent, and TCE was not detected in the sample but was detected at a concentration of 0.0044 mg/l in the duplicate. Duplicates from the October 2003 and May 2004 sampling rounds had acceptable RPDs, ranging from zero to 22 percent. MS/MSD results showed only a few analytes that were slightly out of the acceptable range. Laboratory control samples were acceptable with only a few exceptions, as were surrogate recoveries. The May 2004 data were validated, and minor quality control problems lead to the estimation of certain results. Nondetect acetone results were rejected, while positive acetone results were estimated due to low response factors. Positive or nondetect results for several analytes were estimated due to low laboratory control sample recoveries, however, of these analytes, only carbon tetrachloride was ever detected in the samples.

9.2.5. Ground Water Summary

As summarized in Chapter 2.4, Phase I and II ground water sampling, which were done in April and November 1998, seemed to identify two source zones of DNAPL in the northern portion of the upper tier. A source zone for PCE was found in JBW-7816 and JBW-7817A which appeared to extend to the west at least as far as JMW-0201. Smaller concentrations of PCE breakdown products TCE, DCE, and vinyl chloride are also found in this area. A second source that contained more unusual chemical species, including carbon disulfide, chloroform, and carbon tetrachloride, was found in JBW-7821 and JBW-7818. In addition, two LNAPLs were found in this area: what was thought to be an oil lubricant in JBW-7817A, and a mixture of weathered fuel and possibly lubricants in JBW-7820 (HLA, 1999c). Small concentrations of chlorobenzene were found in JBW-7817A and JBW-7816. This research project targeted the PCE source area, but at least one LNAPL plume was also known to exist within the target zone.

Plate 9.2.4-1 shows total VOC concentrations in ground water over the life of the project for wells that were used for extraction. Pre-treatment ground water sampling performed as part of this study in December 2001 and April 2002 showed PCE exceeding MCLs throughout the target area. Lower concentrations of PCE breakdown products were also found. Low concentrations of fuel components were found in wells at the eastern side of the site (I-4, I-5, JBW-7817B, and VEA-5). Low concentrations of BTEX were also found in the 11-14 meters (35-45 feet) depth interval of EX-3 in the December 2001 sampling round. This fuel plume appeared to be highly mobile, as it moved into Interval 3 of SM-3 between April and June of 2002. Trichlorobenzenes were detected in low concentrations in the north-central portion of the site (I-2 and I-3), and carbon tetrachloride was found in deep intervals of EX-4 and I-4.

When the extraction system was turned on prior to the initiation of the steam injection system, PCE concentrations in the extracted water were low across the site. The highest PCE concentrations were found in wells EX-1 (0.15 mg/l) and I-2 (0.12 mg/l). Within one week, PCE concentrations had increased substantially in EX-3 (1.30 mg/l) and VEA-5 (1.4 mg/l). VEA-5 also started showing low concentrations of trichlorobenzenes at that time. On September 23, what is interpreted as a plume of spent solvents, containing high concentrations of PCE, TCE, trichlorobenzenes, and other petroleum hydrocarbons, entered wells EX-2, I-2, EX-3, and EX-1. It is interpreted that the source of these spent solvents must have been in the vicinity of these wells and VEA-5, and that they were mobilized by the steam injection towards the west. Although the September 30 round of sampling once again showed relatively low contaminant concentrations, by October 7, many of these same wells, in addition to I-3 and EX-4, again showed high concentrations of PCE, TCE, chlorobenzenes, and petroleum hydrocarbons. Another large slug of these contaminants reached many of the extraction wells on November 12. By the end of steam injection, contaminant concentrations appeared to be declining in wells EX-2, I-2, I-3, JBW-7817B, and EX-4, whereas concentrations continued to increase in wells EX-1 and EX-3. Overall, the

effluent water samples showed a trend of increasing contaminant extraction rates at the time the system was shut down, including very high concentrations of DRO. The data clearly indicate that additional contaminants had already been mobilized and could have been captured by the extraction system had operations been continued beyond November 26.

Carbon tetrachloride was common in the vapor samples, and was also present in ground water samples from I-7, EX-4, and EX-1. It reached its highest concentrations during the study in well EX-1 from September 16 to November 19. Based on the Phase II characterization, the source area for carbon tetrachloride was thought to be outside of the target area for steam injection, at JBW-7821, which is approximately 7.3 meters (24 feet) to the southeast of the target area. It is possible that some of this contamination was pulled into the treatment area by pumping at EX-1, allowing it to be recovered.

It is difficult to determine any clear trends in the post-treatment ground water data. Higher contaminant concentrations were seen in wells I-8 and EX-3 than were seen in pre-treatment samples. Well EX-1 shows a similar level of contamination pre- and post-treatment. Wells I-2 and I-3 showed concentrations in May 2003 and May 2004 that were significantly lower than the initial concentrations, but the concentrations found in October 2003 were similar to pre-treatment levels. Wells I-4, EX-2, and EX-4 showed possible reductions in ground water concentrations. Wells JBW-7817B and VEA-5 were not sampled prior to steam injection, but after treatment showed essentially no chlorinated solvents. VEA-5 contained a floating NAPL composed of fuel before treatment; however, after treatment, fuel components were not seen in this well until the final sampling round. I-5 and I-7 contained no PCE or TCE in the final sample round; however, both contained low concentrations of fuel components and chlorobenzenes. In I-6, which had been used for steam injection over most of its length, PCE was completely absent in the final post-treatment sample; however, the TCE concentration increased after treatment to approximately the same concentration that PCE had been prior to treatment.

While the main contaminant found during pre-treatment sampling was PCE, ground water samples at the end of the post-treatment sampling showed higher concentrations of fuel components and chlorinated benzenes, apparently indicating that these contaminants were mobilized by the steam injection and remained mobilized a year and a half after steam injection ceased. The highest concentrations of contaminants found in post treatment samples were found in I-8 and EX-3. The high concentrations in EX-3 are likely explained by the fact that this extraction well was furthest from the injection area, and appears to have had contaminants mobilized towards it; however, there was not sufficient treatment time for the bulk of these contaminants to be extracted. In the case of I-8, it appears that water from the mobilized plume flowed into this well after the extraction system was turned off, as this well had been used for steam injection during the later half of the injection period.

Post treatment ground water sampling results were affected by several factors, including re-establishment of natural ground water gradients and flow directions after the extraction system was shut off, and perhaps seasonal changes in recharge and/or gradients. Temperature profiles of wells in the post-operational period (after November 19, see Plate 7.1-2) show a trend towards increasing temperature in wells along the southeast margin of the site (JBW-7817B and I-8 and in TC-1, VEA-7, and VEA-8) which continues until late December, after which time the temperatures decline. At the same time, wells and monitoring arrays immediately to the west of the steam injection wells (EX-4, I-9, VEA-4, and VEA-9) undergo continued heating in the period after steam injection, continuing to the final temperature measurements in February 2003. This association of heating and cooling trends may reflect the initial migration of heated water towards the southeast and northwest, along hydraulic gradients established during steam injection. The temperature decline along the southeastern edge of the site in late December 2002 may reflect the re-establishment of natural ground water flow along strike of bedding planes towards the northwest. The contrast between the relatively large increase in temperature observed in EX-4 and VEA-9 compared to that in EX-1 and I-9 may reflect the existence of somewhat better connections along strike from I-7 compared to poorer connections adjacent to I-8, and also to the poor interconnection between the eastern part of the site and the central part.

The apparent hydrogeological boundary between the eastern and central parts of the site (under normal hydraulic gradients) may have prevented a detectable migration of heat from the central axis of the site to those wells on the northern margin of the site. The interaction of heated water moved against the natural hydraulic gradient during injection conditions, and subsequently by the re-established natural gradient, may also account for the increase in temperature detected in VEA-3 in the post-treatment period. The re-establishment of natural ground water flow along strike of bedding towards the northwest (at least in the eastern, well-connected, part of the site) accounts for the relatively high contaminant concentrations found in wells I-7 and I-8 in the first post-treatment samples, despite the fact that these wells were used for steam injection. The continued migration of displaced, contaminated water along strike of bedding is reflected in the later increase in contaminant concentration in wells in the central part of the site and along its northern boundary (EX-4, VEA-5, I-3, I-2).

Chapter 10. Discussion and Interpretation

10.1. Post-Operational Conceptual Model

The extensive characterization effort that preceded steam remediation operations led to the development of a revised conceptual model of the site hydrogeology and contaminant distribution, as is discussed in Chapter 4.2. Steam injection and extraction at the site, in conjunction with an extensive temperature, resistivity and ground water monitoring program, largely served to confirm many of the assumptions inherent in that model. However, some important differences were apparent, and these have required that a further revised conceptual model of the site be constructed.

The most significant revisions to the conceptual model of the site were the recognition of several, apparently bedding-plane parallel, fracture features (designated BP1 through BP4) that appeared to have a key role in the transfer of heat from the injection wells up-dip and along strike of bedding across the site. The location and approximate orientation of these features, where they can reasonably be correlated with open fractures recorded in core or geophysical logs, are shown in Figure 10.1-1, which are summary cross-sections across the site.

It is apparent that while bedding parallel fractures were significant in localizing fluid flow in the subsurface, and while there is some evidence to support the idea that individual bedding parallel features (most probably small faults) controlled fluid movement down-dip over distances of tens of meters, it is more probable that individual bedding parallel fractures were only open over short distances and that fluid flow moved in complex pathways, utilizing intersecting fractures of many orientations. While it seems unlikely that single bedding plane fractures or closely spaced groups of parallel fractures served to control fluid movement during operations at this site, there is some suggestion of a stratigraphic localization of bedding parallel fractures that localized fluid flow (as indicated by the presence of thermal anomalies). The location of a group of fractures, extending over a vertical thickness of 18-21 meters (60-70 feet), which become shallower from about 21.3 meters (70 feet) at the east end of the site to about 9.1 meters (30 feet) at the west end of the site, closely follows bedding in the subsurface. The upper surface of this group, marked by a relatively wide, open fracture, partly filled with calcite mineralization, coincides with the feature referred to as the BB Fault (as shown in Figure 4.2.1-1).

While significant heating was restricted to the steam injection wells and to the eastern area of the site, distinct temperature anomalies are apparent on many of the temperature profiles in the remainder of the site (these data are presented in Appendix I and Plate 7.1.1-1). Plotting of first appearance of heating in individual well or boring temperature profiles suggests the presence of heating in a series of stages across the site (Figure 10.1-2). In the initial period during the first month of steam injection, through injection into wells I-4, I-5, and I-6, heating was effectively restricted to the relatively interconnected eastern area of the bedrock aquifer (AREA 1). Previous aquifer testing had established that this part of the site would be the most readily heated by steam injection. Continued injection extended heating to the northern parts of the central and western areas of the site. The restriction of pathways to heated ground water to an apparently narrow zone along the line of I-4, I-3, and I-2 to the eastern area provided additional confirmation of the existence of a zone of interconnected fractures that had been identified by aquifer testing (discussed in Chapters 4.1.6 and 4.2 and also by Stephenson et al., 2003). By mid-October 2002, while slight heating had occurred along the northern edge of the site (AREA 2), the central axis and southern edges of the central and western areas remained cool. This is assumed to indicate that, while laterally extensive ground water movement along strike of bedding planes was important in the eastern area, along bedding strike flow paths were less important in this permeability corridor along the northern edge of the site. Flow along the strike of steeply-dipping NE-striking (“axial planar”) fractures may also have been significant in the northern “corridor,” although steeply-dipping fractures associated with temperature anomalies are uncommon and only present in I-3 and I-1 along this “corridor.”

Also in mid-October, wells VEA-5, I-7, and I-8 were retrofitted for steam injection in an attempt to expand the area of significant heating at the site. The addition of these steam injection wells allowed heating to be extended to some of the central area of the site by the end of operations in late November (AREA 3). Heating was relatively modest on the north side of wells I-7 and I-8, as indicated by the temperature profiles of EX-4 and VEA-9 (Appendix I and Plate 7.1.1-1). By contrast, heating was much more pronounced towards the southeast, as seen in the temperature profile for VEA-7. This suggested that ground water flow, presumably along strike of bedding planes, was more significant away from the site towards the southeast. As noted in Chapter 7.1, temperatures in the eastern part of the central area and in the eastern area of the site continued to increase for about one month after the end of steam injection before declining in these areas. The apparent migration of peak temperature southwards with time from the vicinity of I-8 to VEA-7 was thought to indicate a generally southwards flow of ground water along the strike of bedding. By contrast, the

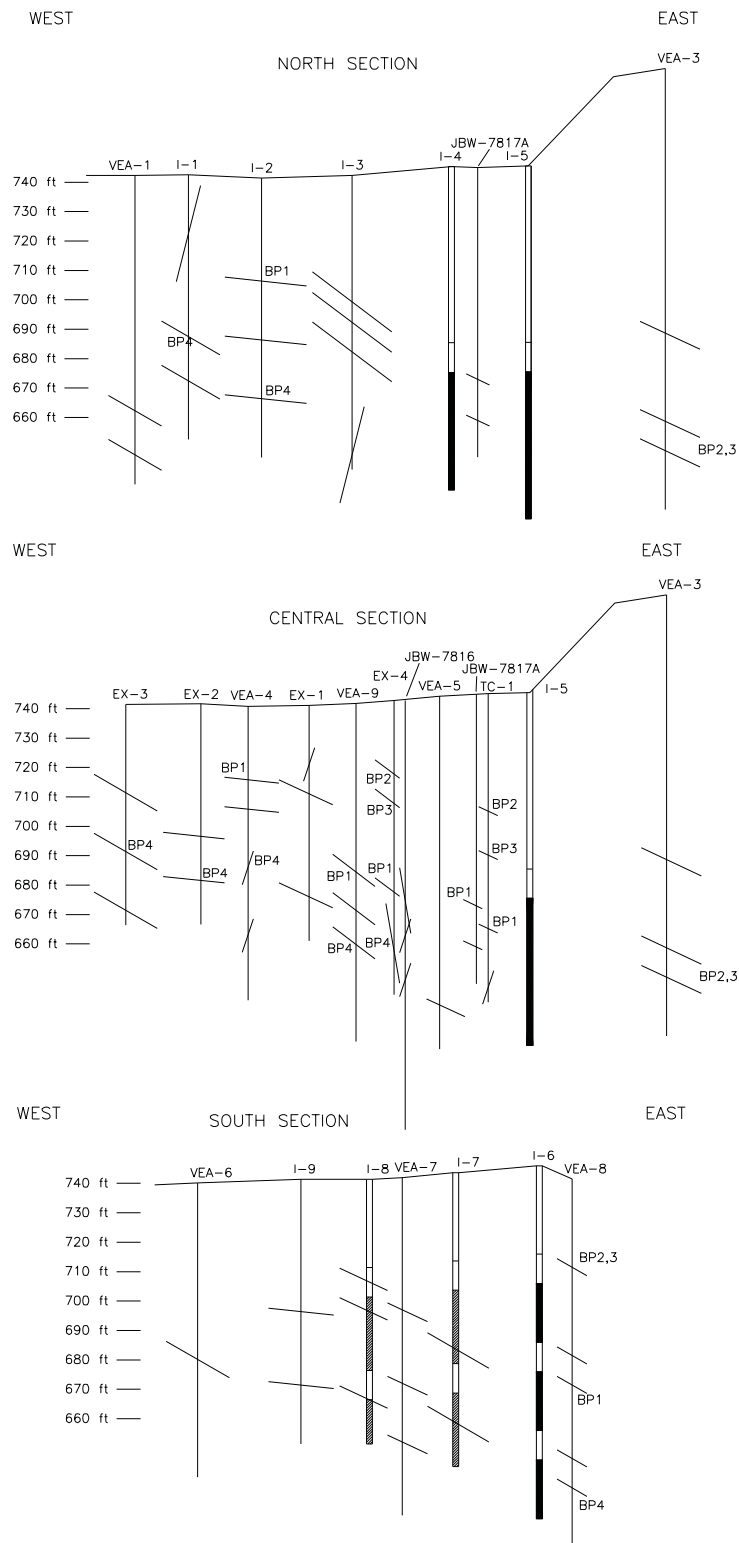


Figure 10.1-1. Schematic cross-sections of site showing those fractures that showed a temperature increase during or after operations. Fractures are correlated with structures logged in core or BIPS images where possible. BP1 – BP4 designations are from Stephenson et al. (2003).

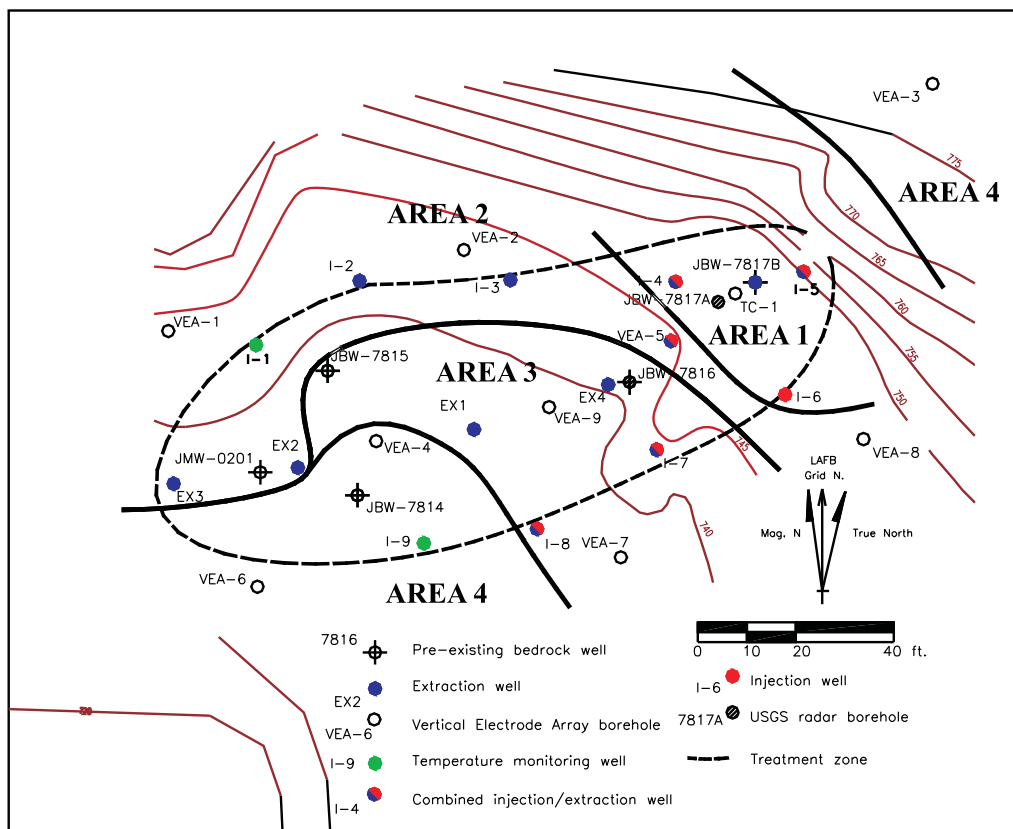


Figure 10.1-2. Progressive sequence of heating observed at site, based on first evidence of temperature increase in temperature profiles presented in Appendix I and Plate 7.1.1-1.

decline in temperature observed in VEA-8 after a peak in late December 2002 could be taken to indicate ground water flow towards the northwest. The final increases in temperature that are apparent in temperature profiles are in those areas at the southwest part of the central area and in the extreme northeast edge of the site, which had remained cool throughout steam injection (AREA 4), all of which continued to increase in temperature until the end of temperature monitoring in February 2003. The pattern of ground water flow that is suggested by the temperature trends seen in the profiles of wells along the southern and eastern parts of the site suggests that during steam injection, heated ground water was pushed towards the southeast along strike of bedding and NW-trending joints, producing the temperature peaks observed in VEA-7 and VEA-8 and also possibly causing the restricted zone of high conductivity observed in the vicinity of VEA-8 on ERT profiles (discussed in Chapter 7.2).

After steam injection was stopped, the natural ground water flow regime re-established itself. The interaction of a broadly westward hydraulic gradient (HLA, 1999c) upon the northeast-dipping bedding, which form the principal structures that control ground water flow, would be expected to produce flow towards the northwest (at least in the immediate area of the test site) as discussed by Brandon and Hoey (2004). If this local ground water flow direction under ambient conditions is accepted, the temperature trends observed suggest that heated ground water displaced laterally from I-5 and I-6 begins to re-enter the eastern end of the site along the same pathways after December 2003. The cooling trend seen in profiles in this area at later times reflects the presence of cool water from upgradient entering this area. In the southern part of the central area (I-9, VEA-9), the trend of increasing temperature beginning in December 2002 may reflect the reentry to the site, via complex pathways, of heated water displaced from I-7 and I-8 in the final month of steam injection. A complex pathway to the south of the injection wells and returning to the site under ambient conditions is suggested by the slow rate of heating in wells EX-1, I-9, and VEA-9 during steam injection.

Some additional confirmation of these general interpretations may be provided by examination of dissolved-phase concentrations of PCE in the sample rounds immediately preceding and following operations (Figure 10.1-3 a,b). The sample round in May 2003 occurred six months after the end of steam injection and five months after temperature data would suggest that the ambient ground water flow regime had been re-established. PCE concentrations at this time in the eastern area of the site and from the northern edge of the central area were substantially reduced from pre-operational levels and remained below MCL, as might be expected

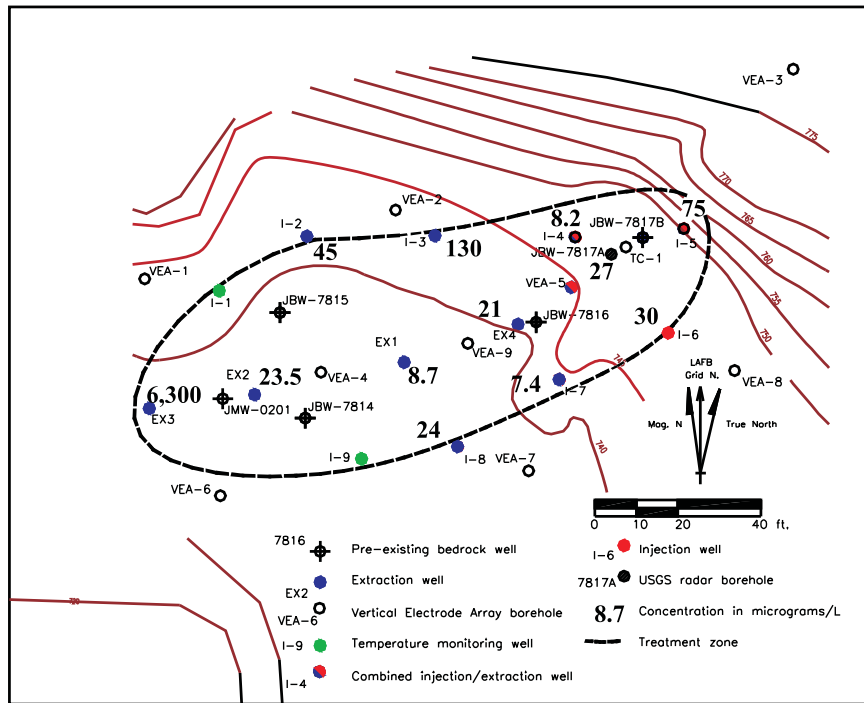


Figure 10.1-3a. PCE concentrations (micrograms/liter) in ground water, April 2002.

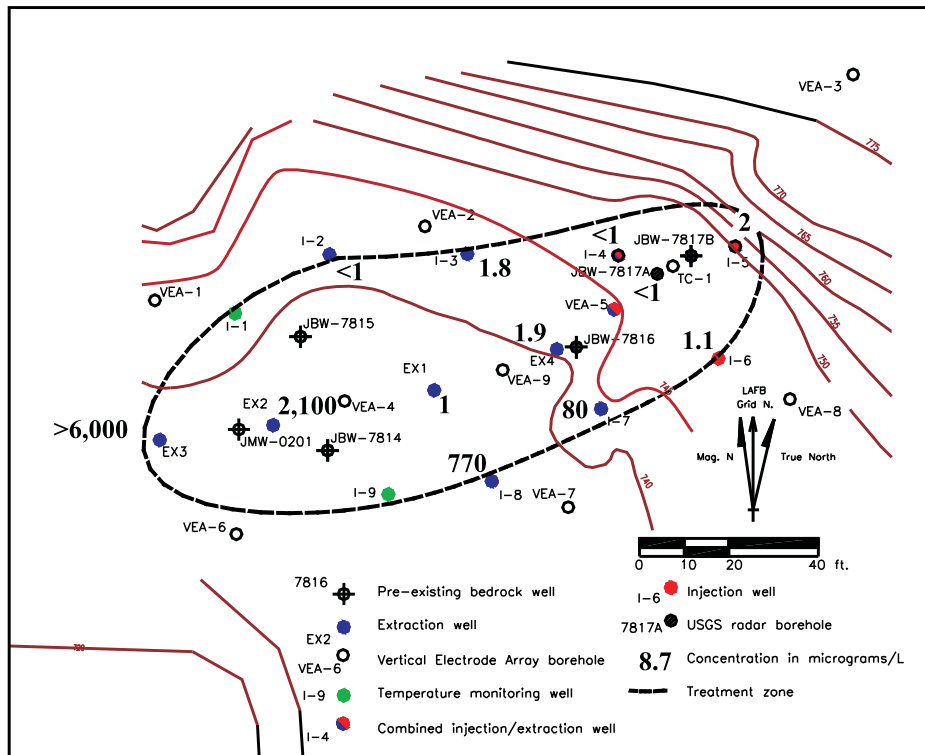


Figure 10.1-3b. PCE concentrations (micrograms/liter) in ground water, May 2003.

for samples from that part of the site that had been most effectively heated. By contrast, those wells lying along the southern and southwestern edge of the site (I-7, I-8, EX-2, and EX-3) had substantially increased PCE concentrations, in some cases considerably in excess of the pre-test concentration. The apparent paradox of wells I-7 and I-8, which displayed increased concentrations despite having been heated to steam temperatures, is most readily accounted for by the introduction of contaminated ground water to these wells from off-site. The contaminants re-introduced to these wells may have been entirely derived from material originally located within the test site; alternatively, they may also have been mixed with dissolved-phase contaminants entering the site from existing off-site source areas, along northwesterly ground water flow paths. Characterization data currently available do not allow this hypothesis to be tested.

Speculative interpretations of ground water flow paths within and across the site during the stressed conditions that prevailed during operations and under ambient conditions are presented in Figures 10.1-4 and 10.1-5. These interpretations depict the principal ground water flow paths to be located along strike of bedding. Individual flow paths can reasonably be supposed to be highly tortuous at a meter scale, with individual segments constrained by strike-parallel flow within bedding fractures (marked by yellow lines in the diagrams) linked by flow across bedding in zones of NE-striking (“axial planar”) fractures or joints.

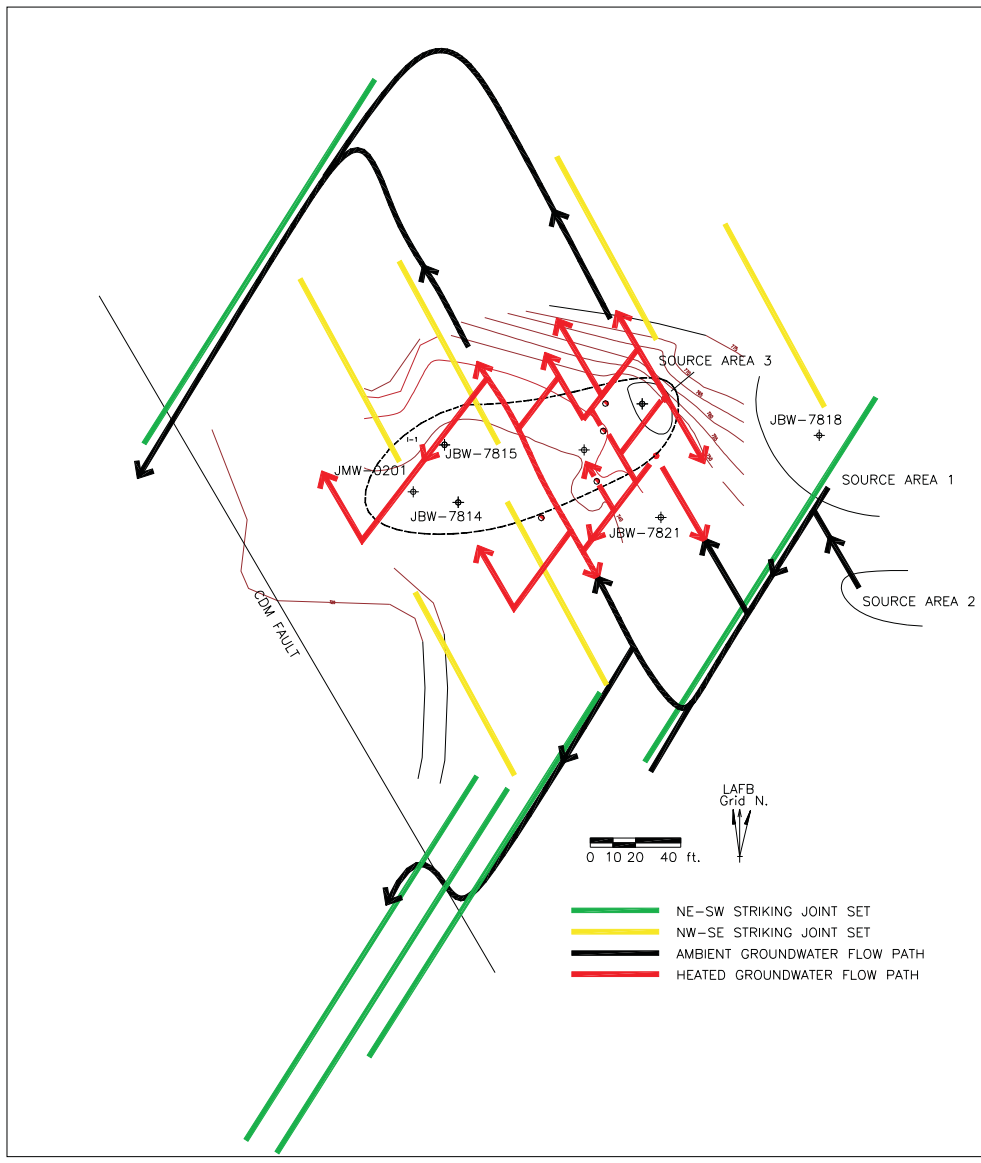


Figure 10.1-4. Interpretation of ground water flow paths under stressed conditions in effect during steam injection operations. Modified after Brandon and Hoey (2004).

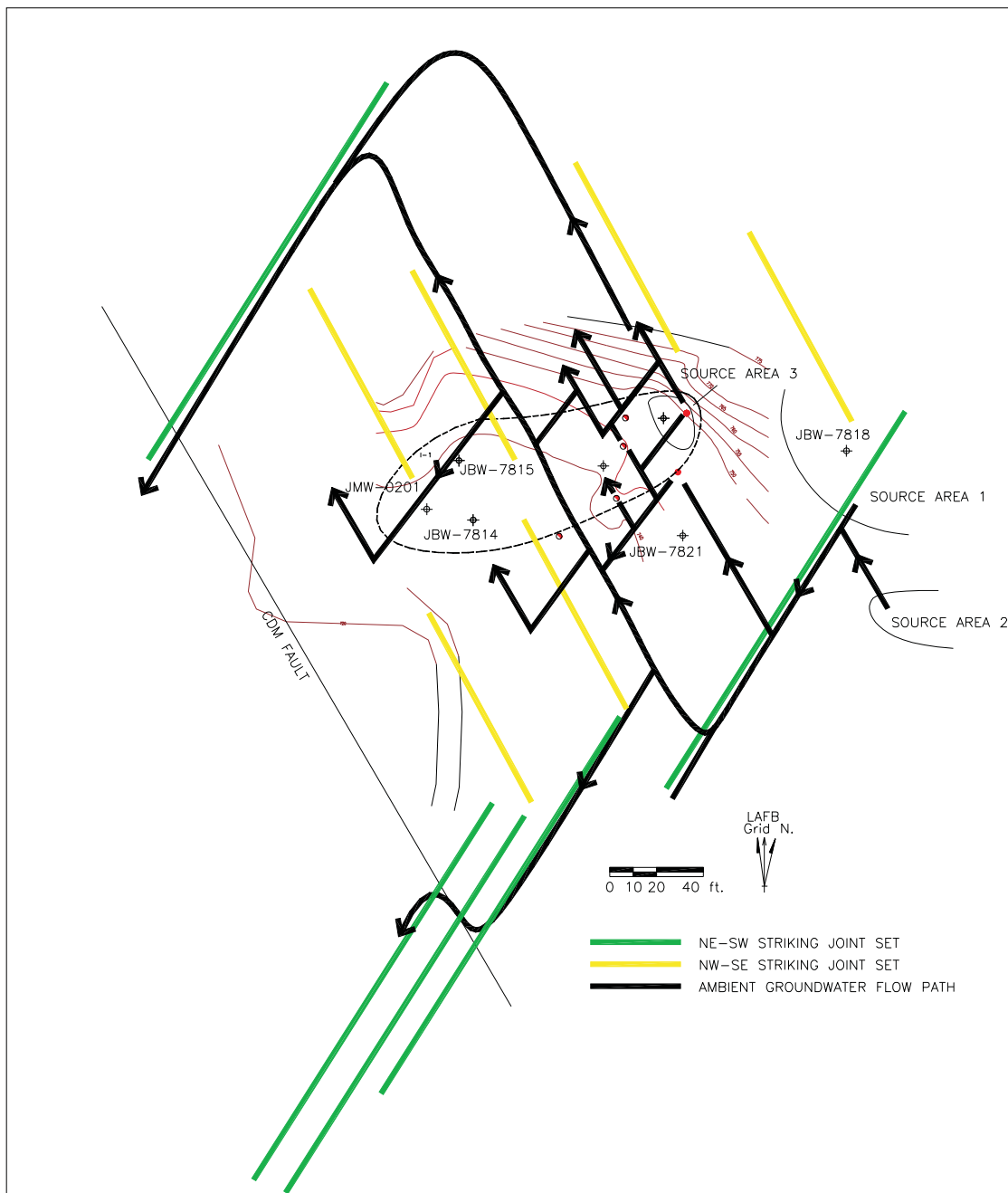


Figure 10.1-5. Interpretation of ground water flow paths under ambient conditions. Modified after Brandon and Hoey (2004).

10.2. Discussion of Removal Mechanisms

As discussed in Chapters 8.2.1 and 8.2.2, more than 3.33 kg (7.34 lbs) of VOCs were recovered in the vapor phase, and 1.71 kg (3.77 lbs) of VOCs were recovered in the aqueous phase. In addition, 0.55 kg (1.22 lbs) of GRO and 1.77 kg (3.90 lbs) of DRO contaminants were recovered in the aqueous phase. The rates of recovery in each phase were quite dependent on the operational situation. The evaluation of the effect of specific operational conditions on contaminant removal rates reveals many of the removal mechanisms that governed the observed recoveries.

Figure 8.2.1-2 shows the VOC daily recovery rates and total recovery in the extracted vapors. The VOC recovery rates began to increase somewhat during the middle of September, but generally remained low except for peaks on September 23, October 30, November 9, and after November 20. As described in Chapter 6.1.2 and illustrated in Figure 6.1.2-2, air injection occurred at times associated with the increased vapor recoveries shown in Figure 8.2.1-2. Specifically, recovery rates began to increase when air injection into I-5 began on September 14. The peak on September 23 corresponds to a time when there was no steam injection but significant air injection into the top interval of I-6 and I-4. The recovery peak on November 9 also corresponds to air injection into the top interval of I-6. Most significantly, the recovery rates increased an order of magnitude after November 20 when steam injection stopped and air injection began into each of the injection intervals. From close examination of the recovery rates versus the injection rates into various locations, one is led to a conclusion that the highest recovery was probably associated with air flow associated with air injection into the middle or bottom intervals of I-6.

The correlation between the increased vapor phase VOC recovery rates and air injection rates implies that the dominant mechanisms responsible for VOC mass removal rates are associated with processes related to air flow through contaminated regions. This inference is consistent with other sites where air co-injection with steam was practiced. Examples include the fractured rock site near Prague, Czech Republic (Dusilek et al., 2001) and the steam demonstration at Cape Canaveral, Launch Complex 34 (IWR, 2003) where vapor recovery rates were correlated with air injection rates.

As discussed in Chapter 7.1, heating was mostly local, restricted to regions near the hot steam injection wells, and adjacent to the fractures of high transmissivity. The heating itself is sufficient to vaporize the VOC NAPLs if the temperature exceeds the NAPL-water co-boiling point. The fate of the bulk of the NAPL vaporized in the heated zone is either recondensation with the steam at the edges of the heated zone, or entrainment in injected air as it passes through the cool boundary of the heated zone. If there is no air injection and the steam condenses in the fracture as it loses its energy through heat transfer to the cool rock matrix, contaminant movement is only via flow of condensate in the fracture ahead of the slowly advancing steam zone. With air injection, VOCs move via convective transport (mostly in the injected air), in steam condensate, and in original ground water displaced from the heated zones. The displaced water is also expected to see increased concentrations as the VOC-laden air flows through the otherwise water saturated fracture network, and partitions a portion of the VOCs into the aqueous phase. Also, fluids from several fractures may mix near or in the extraction wells, and VOC-laden steam can condense after contact with the cooler ground water as fluids from hot and cold fractures mix. This mixing can cause elevated VOC concentrations in the extracted water, even if the transport mechanism in between wells was vapor phase flow. These mechanisms will cause increases in contaminant concentrations in both the vapor phase and the aqueous phase during co-injection of steam and air in fractured rock systems.

Another observation of note is that the water temperatures in extraction wells began to increase after November 6, while ground water VOC concentrations began to increase after September 16. This implies that ground water velocities in fractures were high enough that convective transport in water displaced from the steam zone will overcome matrix diffusion. Theoretically, the ratio of convective transport through the fractures to diffusion into the rock matrix is related to a non-dimensional parameter similar to the Peclet number. This number is qualitatively defined by the fracture velocity times the length between wells divided by a diffusivity. High ratios correspond to conditions where the flux of water through the fractures is high enough that diffusion into the matrix is not significant. For mass transfer, the diffusivity is related to the molecular diffusion of aqueous phase VOCs in the rock matrix. Those values are of the order of 10^{-10} m²/s (10^{-9} ft²/s). For thermal diffusion, the diffusivity is of the order of 10^{-6} m²/s (10^{-5} ft²/s). Thus the contaminant transport ratio is about 10,000 greater than the thermal transport Peclet number. The fact that temperatures in the extraction wells began to increase after November 6 supports a conclusion that hot water could flow to extraction wells through fractures from the zones heated by steam without losing its energy through conduction to the rock matrix. Since the mass transport ratio is about 10,000 greater than the thermal Peclet number, the increases in ground water concentrations after September 16 are most likely due to VOC mobilization by steam near the injection wells and subsequent transport in the fractures before diffusion to the matrix could occur.

Gas phase convective transport would be even more dominant since vapor VOC mass fluxes in fractures would be higher than aqueous phase VOC fluxes while matrix diffusion would be similar. The higher overall mass recovery in the extracted vapors during air injection than those observed during water pumping is evidence of gas transport dominance.

The last mechanism that may be significant is the movement of condensed NAPL with non-condensable air bubbles away from the hot zone. Under conditions where there is condensation of NAPL with the steam at the edge of the heated zone, conditions associated with a low air to steam injection ratio and high NAPL concentrations near fractures carrying steam, NAPL may be present at the air/water interfaces. As the air bubbles move up through the fracture network toward the extraction wells, the NAPL may be carried with them, enhancing the transport and removal of the volatile NAPL contaminants originating from the heated zones.

Taken together, these transport mechanisms provide for the increased recovery rates from the fractured system observed during the steam and air injection phases of this project over those that would be expected for pump-and-treat operation. Their contributions would be expected to be increasingly important if a greater volume of the contaminated rock-fracture system were heated and optimized schedules of steam and air injection were found.

10.3. Evaluation of Objectives

A number of broad, general objectives for this research project put forth by the regulatory agencies included improving the understanding of the mechanisms that control DNAPL and dissolved phase contaminant behavior in fractured rock, evaluating characterization needs, and an improved understanding of how a remediation technology can be implemented at fractured rock sites. These were discussed in Chapter 1.3. The degree of success in meeting these objectives is the focus of this section. In the most global sense, the research project can only be considered a success in that significant strides were made towards developing, applying, and improving remedial technologies and approaches in the fractured bedrock environment, in this case SER in a sparsely fractured limestone with very low hydraulic conductivity. Significant insights were developed with respect to a number of related issues important to the regulators. These insights include improved approaches for characterizing fractured bedrock for SER (e.g., appropriate use of interconnectivity testing), better understanding of mechanisms that control DNAPL and dissolved-phase contaminant behavior (e.g., rock chip samples and discrete ground water sampling), monitoring heat movement during steam injection (e.g., temperature and ERT monitoring), and remedial technology modifications which may improve remedial performance (e.g., air co-injection). The research project must be considered a strong success in that many of these findings will have considerable technology transfer value to other fractured bedrock sites and technologies.

The more specific goal of demonstrating appreciable contaminant mass recovery could be considered a qualified success. Although the total mass recovered was somewhat limited, the starting source mass at the site is unknown, and thus the determination of mass removed does not allow assessment of removal efficiency. Perhaps more importantly, however, the upward trending removal rates which continued to be recorded even as the system was shut down are cause for optimism. It is important to note that the system was shut down due to a lack of funding to continue, not because it was believed that the technology had accomplished all that it could. It is reasonable to assume that the lessons learned from implementing SER at this site will allow future efforts to realize even greater mass removal rates and amounts with equivalent or fewer resources.

Ultimately one of the goals of remedial actions taken in source areas is always improvement of ground water quality down-gradient in the dissolved-phase plume. However, the time frames required for such assessment (typically years) were beyond the scope of this project. Additionally, there is consensus that the monitoring well network at the site beyond the target area is limited, and is likely not sufficient for a rigorous analysis of this kind. Time and funding were not available to install and sample properly placed wells. As such, assessments of whether or not ground water quality improved in the downgradient plume as a consequence of the project cannot be made. It will not be possible to determine whether or not restoration time frames have been significantly shortened, or even affected at all, as it could not be determined if the mass of contaminants in the ground has been significantly reduced.

10.3.1. Discussion of EPA SITE Program Objectives

The SITE objectives and how they were to be evaluated are described in detail in Chapter 1.3.1. How well each of these objectives was met is discussed below.

- P1. Determine the approximate reduction in contaminant of concern (COC) concentrations that occurs in ground water within the treatment zone as a result of SER treatment.*

Although data were collected to evaluate ground water concentrations in the target area before and after steam injection, this data cannot be used to fully evaluate the effectiveness of SER in fractured bedrock to reduce ground water concentrations because the treatment was incomplete. The combination of low injection rates and short treatment time limited our ability to heat the subsurface, and thus to determine the effectiveness of SER in fractured limestone. The increases in contaminant extraction rates observed during the steam injection show that contaminants were being mobilized towards the extraction wells. However, the premature termination of the project left many of these mobilized contaminants in the subsurface, and they were then re-distributed when the natural ground water flow was re-established. Also, there is a fuel plume in the area that moves around, and appears to have moved into the target area again after the steam injection was completed. Also, both pre- and post-treatment ground water data shows signs of seasonal variations in ground water concentrations. Despite these interfering processes, it does appear that some of the sampled intervals show reductions in ground water concentrations (i.e., I-4, EX-2, and EX-4); however, other intervals where mobilized contaminants remain show increased contaminant concentrations (i.e., I-8, EX-3). Thus, this project was not able to evaluate the degree to which SER can reduce VOC concentrations in ground water in fractured limestone.

- P2. Determine the mass removal of COC in all waste streams over the course of the SER treatment period.*

Daily effluent samples were collected throughout the treatment period to evaluate recovery rates and the mass recovery of VOCs by SER. Thus, strictly speaking, this objective was met. However, the fact that effluent concentrations were still increasing at the time that the system was shut down indicates that we were not able to determine how much enhancement in recovery rates is possible with this technology, or how much contaminants ultimately can be recovered. Significant increases in effluent concentrations

(approximately an order of magnitude) started approximately three weeks into the operational period in both the aqueous and vapor streams, and the recovery rates increased at least another order of magnitude when steam injection was halted and air injection rates were increased. The data collected indicate that recovery rates of VOCs from fractured limestone can be enhanced by steam injection, but the full extent of the possible enhancement was not realized. Co-air injection appears to have been important for increasing recoveries when so little energy was injected.

Although it is possible that contaminants could have been pulled in from outside of the treatment area, particularly from the western portions of the site where aggressive pumping occurred, or from the southeast where another source zone was thought to be located close to the treatment area, observation of the types of contaminants extracted from each of the wells and the timing when the contaminants reached those wells seems to indicate that the majority of the contaminants extracted came from within the target zone. Although the mass of contaminants removed was not large, the increasing extraction rates at the end of the project indicate that more contaminants could be mobilized and captured by this technology. This was discussed in Chapter 9.2.4.

S1. Determine the approximate reduction in COC concentrations in potentially open fracture intervals within the treatment zone as a result of the SER treatment.

Rock chip samples were collected before and after steam injection to evaluate whether contaminant concentrations in the rock matrix at the fracture surfaces were reduced by SER. Comparison of pre- and post-treatment concentrations in boreholes approximately 1.5 to 2.4 meters (5 to 8 feet) apart shows that there appears to have been a reduction in contaminant concentrations in the rock matrix. However, the rock chip data can only be used qualitatively for a variety of reasons: 1) significant heterogeneity in the contaminant distribution would be expected, but was not quantified; 2) data obtained during the post-operation sampling indicate that the one week extraction time was not adequate to extract all of the mobilized contaminants from the system; 3) a smaller size core was obtained during the post-treatment sampling, and this may have an effect on rock chip concentrations measured by this technique. Despite the limitations on quantifying concentrations in the rock by this technique, the data were very useful in determining where contamination resided in the system, and revealed the fact that much of the contaminant mass was in small fractures that appeared (based on visual observation in the field and on transmissivity testing of discrete intervals) to have limited permeability.

S2. Determine if contamination is mobilized below, downgradient, or to the sides of the treatment zone as a result of the SER treatment.

Three wells (designated SM-1, SM-2, and SM-3) were installed in order to determine if contaminants were mobilized horizontally or vertically from the treatment area. The rationale behind their location and construction is described in detail in Chapter 4.1.5. These wells were located and oriented in order to sample down-dip and along strike of the principal fracture sets present at the site and to intersect the projection of particular structures, where practical. Samples collected from the deepest intervals of SM-1 and SM-3 showed that there was not significant contamination below the target treatment zone before or after treatment. Intervals of wells SM-1 and SM-3 at the same elevation as the treatment area showed small concentrations of PCE both before and after treatment, indicating that there was not a significant movement of contaminants to the north or to the east by the SER process. Well SM-2 showed significant contamination at the same elevations as the target zone before (and after) steam injection, and thus could not be used to evaluate movement of contamination horizontally to the south. Thus, the data obtained from these three wells gave no indication that significant amounts of contaminants had been moved horizontally or vertically during treatment.

Although there are several pre-existing wells in the area surrounding the project site, sampling of these wells was not included as part of this research project. Extensive characterization efforts at the site and in the surrounding area had identified an overall hydraulic gradient towards the west. It was expected that injection of steam at depth in the eastern part of the site in this hydrogeological environment would lead to displacement of mobilized liquid and vapor-phase contaminants up-dip of bedding towards the west, where they would be captured by the extraction wells at the western part of the site. The closest well to the test site lying down the supposed hydraulic gradient is well JBW-7812B, which is located on the lower tier of the Quarry, approximately 52 meters (170 feet) west-southwest of JMW-0201. Data obtained by Maine DEP, as part of the long-term ground water monitoring program at the former Loring AFB, showed an increase in concentrations of PCE in well JBW-7812B in October 2002, shortly after the start of steam injection (Brandon and Steimle, 2004). Data from the period November 1999 to April 2001 showed PCE concentrations in the range of 0.079 to 0.099 mg/l and TCE of 0.023 to 0.036 mg/l, while data from July 2001 to July 2002 showed PCE concentrations ranging from 0.093 to 0.130 mg/l, and TCE concentrations of 0.037 to 0.047 mg/l. In October 2002, a month after initiation of the steam injection and aggressive ground water pumping, PCE concentrations increased to 0.320 mg/l, and subsequently remained at similar concentrations through the most recent data available (October 2003). TCE concentrations continued to increase from October 2002 to October 2003, going from 0.058 to 0.099 mg/l. Thus, while a rapid increase in concentration between July and October 2002 is apparent, the data could be interpreted as showing a perturbation imposed on an increasing trend established since at least November 1999. While order-of-magnitude variation in PCE and TCE concentrations have been observed in wells within the test site in the period prior to the test (e.g., JBW-7816 between May and November 1998) and no increase in PCE or TCE concentration was seen in wells lying further down the broad hydraulic gradient or in the SM-1, 2, or 3 wells, the close temporal association between the start of injection and extraction at the test site and the marked increase in concentration seen in JBW-7812B suggests that a causative linkage may exist between the hydrological disturbance caused by the test and the concentration increase. Two possible scenarios can be envisaged:

-
1. Steam injection displaced dissolved-phase contaminants northwards from the site to a point where they were entrained in a northeast-striking joint set and transported relatively rapidly towards the lower tier.
 2. Large-scale ground water extraction during the test (more than 832,000 liters (220,000 gallons) extracted, mostly along the northwestern edge of the site) drew dissolved-phase contaminants into permeable structures connected to the lower tier.

It can be reasonably supposed that at the eastern end of the site, where steam injection wells lay on the edge of the site, contaminants could have been displaced along permeable structures, such as bedding plane fractures, towards the northwest. However, there is no evidence from temperature or ERT monitoring to suggest that heated water, far less steam, migrated over distances in excess of 6 meters (20 feet) from the injection point. Furthermore, it was apparent that a significant fraction of the injected steam in combined injection/extraction wells (such as I-4 and I-5) was extracted from the upper intervals of the same wells, further reducing the capacity of the injected steam to physically displace contaminated ground water over large distances, although the narrow fracture widths and very low bulk porosity of the bedrock would tend to allow the effects of injection to be felt at much greater distances from the injection point than would have been the case for steam injection in porous soils (Stephenson et al., 2003). The absence of any discernible increase in concentration in any of the sample intervals in SM-1 is remarkable if it is accepted that steam injection could produce effects over a large area, yet there was no impact in any of the fractures intersected by that well. It is possible that an unconstrained and unidentified permeable feature could have had the effect of displacing a "slug" of contaminated ground water northwards from the vicinity of I-4 and I-5, underneath the upper part of SM-1, to a point where it could be entrained within a permeable feature connected to the vicinity of JBW-7812B. The data currently available are insufficient to allow this possibility to be tested.

It can safely be stated that residual or immobile NAPL, if present, could not have been mobilized outside the area of significant heating. As significant heating did not extend beyond the eastern area of the site, and no NAPL was recovered from extraction wells or detected in surrounding monitoring wells, there is no reason to suppose that this was a significant factor. Given the very low bulk porosity of the bedrock, the volume of water injected as steam could potentially have been spread in permeable fractures to considerable distances from the injection wells, potentially displacing contaminated ground water already in place, and allowing for some degree of mixing within fracture porosity. However, at the same time as steam injection was in progress, large volumes of water were being extracted from wells, principally from the western and central parts of the site. In an attempt to maintain some degree of hydraulic control over the site, a volume of water in excess of that injected as steam was extracted. As such, it seems reasonable to assume that in those parts of the site in which injection and extraction wells were in direct connection, a net extraction of water was maintained, allowing contaminant mass to be removed. In those areas of the site where there was no direct connection to an extraction well, such as north, east, and south of the I-4, I-5, I-6 group of injection wells, injected water would have mixed with and displaced existing ground water. In those areas where extraction wells formed the outer perimeter of the site, existing ground water would have been drawn into the site.

Through the same interaction of narrow fracture width and low bulk porosity of the bedrock, the extraction process could be reasonably supposed to have established inward hydraulic gradients extending to potentially large distances along permeable structures outside of the site. Conceivably, such gradients could have drawn contaminated ground water from uncharacterized areas adjacent to the site, such as immediately north of I-4 and I-5 or the area south of EX-3, into permeable structures that would have allowed the contaminated ground water to follow a pathway that could not have been used under ambient conditions. Alternatively, the perturbation to the natural ground water flow regime imposed by the test may have expedited ground water flow along pathways in addition to those postulated by Brandon and Hoey (2004), such as additional northeast trending joint sets lying to the south of the site or along the CDM fault zone. The influence of a transient episode of increased head in injection wells during the test would have been expected to produce a distinct pulse of increased contaminant concentration in down-gradient wells, which would have passed once ambient conditions were restored. That the PCE concentration in JBW-7812B should have remained at essentially the same level after the rapid increase in October 2002 is perhaps indicative of the introduction of contaminant from a stable source area to the flowpath intersected by this well. The ground water monitoring data of the area surrounding the site are currently insufficient to allow these possibilities to be tested.

The distance of well JBW-7812B from the steam injection area, the absence of discernible increases in PCE or TCE concentration in well SM-1, which is located between JBW-7812B and the steam injection wells (if speculative ground water flow paths are correct), and the excess ground water extraction from wells covering the bulk of the site, would seem to favor an interpretation that the increases observed were not a direct result of the steam injection, even though there is insufficient evidence to conclusively test this possibility. However, as discussed in Chapters 7.1 and 10.1, slight temperature effects of the steam injection were observed over much longer distances than would have been expected. During operations, steam injection at the eastern end of the target area would have been expected to displace contaminated ground water along permeable structures to the west, northwest, or southeast. At the same time, ground water extraction would have been expected to draw ground water, which may be contaminated to some degree, towards the site from the same directions. Ground water displaced by the interaction of these processes can reasonably be supposed to have been introduced to permeable structure outside the site where it could ultimately have flowed toward the lower tier under somewhat higher hydraulic gradients than exist under ambient conditions.

In conclusion, while the possibility that the increase in dissolved phase contaminant concentration seen in JBW-7812B was in some way caused by the disturbance in aquifer conditions during the test cannot be discarded, there is insufficient evidence to conclude that it was caused by steam injection and that it represents a mobilization of contaminant “below, downgradient, or to the sides of the treatment zone” as a direct consequence of SER. Also, it should be noted that any mobilization that did occur was only of dissolved phase contaminants; the concentrations measured in JBW-7818B during and after steam injection do not indicate that DNAPL was mobilized to this area.

- S3. *Determine if the rock within the treatment zone can be heated to greater than 87°C (the co-boiling point of a water and PCE mixture) in the zones containing contaminants.*

This objective overlaps with Technology Objective TO-1, which is discussed in detail in Chapter 10.3.2. This objective was not met during the research project due to lower than expected injection rates, sparse fracturing, and limited operations time. It is recognized that longer injection times would have allowed greater heating of the subsurface; however, steam injection may not be the most cost-effective means of heating sparsely-fractured, low permeability limestone, such as found at this site. Recommendations on how to heat this type of system for remediation purposes are discussed in Chapter 11.2.3.

- S4. *Document the ability of the ground water and vapor treatment system to treat the effluent streams and meet any discharge permits.*

This objective was fully met by the research project. SteamTech collected weekly samples of the treated water and vapor streams just before discharge. Only PCE was detected in the vapor samples, and this occurred twice. Both times the concentrations detected (0.021 and 0.12 ppmv) are significantly lower than the Maine DEP action level for air emissions, which is 0.581 ppm. In the water samples, PCE was detected three times, at concentrations ranging from 0.0047 to 0.00077 mg/l. Thus, PCE was never detected above the Maine DEP action level for surface water discharge of 0.005 mg/l. Carbon tetrachloride was also detected in two water samples at concentrations of 0.001 and 0.0022 mg/l. These concentrations also are below the Maine DEP action level for surface water discharge for carbon tetrachloride of 0.005 mg/l. No other contaminants were detected in the treated water. Thus, SteamTech’s effluent treatment systems for vapors and water were adequate to treat the contaminants that were recovered, and discharge requirements were met.

- S5. *Document the operating parameters during evaluation of the SteamTech SER technology.*

This objective overlaps with Technology Objective TO-3, and is discussed in more detail in Chapter 10.3.2. Basically, while this objective was successfully met during the research project, the parameters identified as governing the heating rate and steam migration at this site are not parameters that can be adjusted enough to significantly influence injection rates. Site geology and other characteristics, including fracture spacing and permeability, and heat conduction into the rock matrix - not operational parameters - were found to have the greatest influence on heating rates. Analysis of the parameters shows that heating of a site such as this with steam injection will be slow, and it is not apparent that a good sweep of the entire target area or complete heating can be achieved with steam injection alone.

- S6. *Determine the cost of treatment for the SteamTech SER technology based upon the evaluation at LAFB.*

Costs for the SteamTech SER technology as it was implemented at this site, as well as the costs for the characterization and monitoring that were done by the SITE program, are summarized in Appendix A. This objective was met by the research project.

10.3.2. Discussion of Technology Objectives

Detailed technology objectives are summarized in Chapter 1.3.2 and Table 1.3.2-1. Each of the technology objectives are discussed below.

- TO-1. *Document the application of steam injection technology and its ability to heat the fractured rock site to temperatures high enough to vaporize any DNAPL present in fractures and matrix.*

The research project as conducted did not meet this objective. The combination of the low permeability, sparse fracturing, and limited operations time available led to heating to temperatures much lower than those necessary for complete vaporization of DNAPL. For a PCE-dominated NAPL, a water-NAPL temperature of 87°C (189°F) is needed for efficient NAPL vaporization. As discussed in Chapter 7.1, the measured temperatures, in all other locations than the steam injection wells, were significantly below this target. The ERT data indicated that the steam and hot condensate migrated in relatively discrete zones, and that the bulk of the rock (including the matrix mentioned in this objective) remained relatively cool, as indicated by the relatively modest electrical resistivity changes observed (see Chapter 7.2). Furthermore, the energy balance calculations presented in Chapter 6.4 showed that the amount of energy deposited in the well-field was only sufficient to heat approximately 27 percent of the target volume within the foot-print of the target area. It became clear that the target temperatures would not be reached to satisfy this technology objective. The reasons are discussed further in Technology Objective TO-3 below.

- TO-2. *Heat a portion of the target volume from below and from three sides using multiple injection wells and intervals, and measure subsurface temperatures and electrical resistivity.*

This objective was met by the successful injection of steam into a total of ten steam injection intervals located in six different wells, and the successful and timely recording of temperature and ERT data throughout operation. The steam injection rates and

totals were monitored successfully, allowing for both water and energy balance calculations to be made. Changing temperatures recorded in the well-field showed that the temperature sensors worked satisfactorily. Changes in the electrical resistivity sensed by the ERT system were in general agreement with the recorded temperatures and miscellaneous other observations made during operation, indicating that the ERT data quality was satisfactory.

TO-3. Identify operational parameters which govern heat-up rates and steam migration.

This objective became more important as operational results started to show that the steam migration and heating were slower than anticipated. Operational parameters that are commonly adjusted during SER to control heating rates and steam migration include injection locations and depth intervals, injection pressure/rate, air co-injection rates, and vapor and ground water extraction rates. Pressure cycling is another important operational parameter in terms of contaminant recovery (see TO-10). This technology objective was met by a number of observations and implementation of the designed monitoring scheme:

- Before the operational strategy was finalized, it was necessary to determine the most appropriate injection intervals from core data, MERC data, geophysics, slug (transmissivity) tests, and pulse interference (interconnectivity) testing. The detailed characterization showed that there were only a limited number of borehole intervals that were well suited for injection. This led to a design where steam injection was conducted at the eastern end of the target area, preferentially in deep zones with limited concentrations of COCs (I-4, I-5, and I-6). In short, the site geometry, geology, and COC distribution were limiting factors themselves. This site was obviously very challenging to heat by steam injection.
- This objective included the measurement of steam and air injection pressures and the injection rates that resulted. This was achieved by a detailed monitoring program and experimentation with both air injection and steam injection pressures, using pressures as high as the limit of the steam generator (825 kPa; 8.2 atm). It became obvious that the steam injection pressure was important for the steam injection rate achieved; however, the injection pressures could not be raised sufficiently to substantially increase the heating rate. It should be noted that the injection pressures remained below pressures believed to cause fracturing of the limestone. The most effective method for accelerating the heating was to add additional injection points, as was done by converting I-7, I-8, and VEA-5 from extraction wells to injection wells. This led to a doubling of the steam injection rate.
- This objective included monitoring of extraction wells for signs of steam, condensate, or air injection effects. Since steam did not migrate to the extraction wells, and the extraction wells did not heat up in the operational time frame, no sign of steam was observed.
- This objective included determination of potential air injection benefits. While it was not positively concluded that the injection of air stimulated heating (in contrast, air injection seemed to block the flow of steam into several injection intervals, and the injection of steam and air had to be staggered), it was observed that a period of air injection following a period of steam injection had dramatic effects on the COC concentration in the extracted fluids.
- The final evaluation to support this objective regarded matrix heating which included calculations of thermal conduction time frames for site heating to be compared to observed temperatures. Since the heating was rather modest, and there was no indication that sufficient steam had been injected to raise the matrix temperatures in the majority of the site volume to temperatures high enough for effective matrix treatment, these calculations were not performed. The operational data convincingly showed that the heat migration, including the component related to thermal conduction, were insufficient at the timescale permitted by the project funding and schedule.

In summary, while this technology objective was successfully met by the implemented operational tests and the data collected, the parameters identified to govern the heating rate and steam migration are ones that are not readily adjustable, but are mostly related to the site characteristics/geology instead of operational parameters. This showed that steam enhanced remediation in this type of formation will be relatively slow, and that it is not apparent that a good sweep of the target area or complete heating can be achieved using steam and air injection alone.

TO-4. Extract liquid and vapors aggressively and recover as much of the NAPL constituents present in the test area as possible within the limitations of the technology, the resources available, and the time frame for operations.

SteamTech operated the system as designed, and made proper adjustments to the well-field and process equipment to keep the test and data collection continuous. A few equipment shut-down periods of less than 24 hours were caused by vacuum pump failures and severe weather. Overall, the equipment was running, and the research project was implemented as planned, with better than 98 percent up-time. Partial objectives were met as follows:

- *Monitor mass removal rates for NAPL, water, and vapor.* This was completed by the scheduled sampling and analysis.
- *Screen and sample individual wells for COC concentrations and headspace PID trends.* This was performed as planned and designed. Additional data were obtained by the operators, increasing the overall data density and performance on a well-specific basis.
- *Inspect extracted fluids for NAPL presence.* This was completed; however, no NAPL was observed in the water samples.

- *Evaluate if the system was operated effectively and provided a fair test of the technology at this site.* With the steam generation and distribution system operating continuously at the desired pressures and rates, this objective was met.
- *Use collected data to estimate the most appropriate full-scale approach (based on lessons learned), and evaluate how close this test came to showing the mass removal we expect when sufficient time and funds are available.* The data needed to address this issue were collected successfully. A detailed discussion of the lessons learned and a recommendation for the most appropriate operational strategy/heating technology are given in Chapter 11.

In general, this technology objective was satisfied, even though a relatively small mass of COCs was recovered from the subsurface.

TO-5. Document removal rates and mass removal by detailed sampling and analyses.

This objective overlaps with the SITE objectives (discussed in Chapter 10.3.1), and was met by the detailed flow rate and COC concentration data obtained during operation. In addition, the PID screening data provided improved data resolution and information on a well-specific basis. The additional data provided useful insights into contaminant concentration trends over time as well as between wells.

TO-6. Evaluate removal efficiency for PCE and other VOCs identified during sampling by pre- and post-test contaminant characterization.

This objective overlaps with the SITE objectives which are discussed in more detail in Chapter 10.3.1. In general, the data collection was complete and satisfactory. However, since the operational period was insufficient for achieving target temperatures, and the site remained relatively cool, the pre- and post-operational data do not reflect what the SER technology would be able to achieve at sites where the geology and/or the treatment time allows for a more complete heating.

TO-7. Identify potential barriers to full-scale implementation at this site, and at fractured rock sites in general.

The demonstration was successful in identifying several barriers to full-scale implementation of SER at sites as complex as the Loring Quarry. These include:

- SER source treatment typically intends to address the DNAPL source zone. However, DNAPL source zones are typically difficult to delineate, and it was not delineated with any certainty at this site. The characterization effort showed that high COC concentrations were found sporadically throughout the test volume, including the bottom-most samples in I-2 and I-3, and other perimeter boreholes that were hoped to be in relatively clean areas.
- The site characterization showed that the fracture connections were relatively modest, and that only three of the nine boreholes intended for steam injection were well suited for this purpose. This severely limited the amount of steam that could be injected, and thus the rate at which the site could be heated.
- The operational data indicate that heat losses into the matrix lead to steam condensation after relatively short travel distances in the formation. These heat losses lead to condensation of significant quantities of steam, creating a warm water front that had to be displaced for the steam to fill the fractures. The resulting heating for a site with sparse fracturing, and small fracture apertures which allow for only slow flow of condensate under the imposed gradients, is relatively slow.
- When perimeter steam injection wells are used, some steam always moves away from the target zone. The ERT data and discrete temperature monitoring indicated that some of the steam and/or condensate migrated towards the south, out of the target area, during this project. Fluid control and capture of COCs that are mobilized during the steam injection process will be more challenging in sites as heterogeneous and complex as this one than in unconsolidated media. The lack of fluid capture could be detrimental to the application of SER at sites with more COC mass.

Despite these identified barriers, the demonstration also resulted in several promising findings:

- Despite the modest temperatures achieved in the formation, and the fact that the water in the extraction boreholes never heated significantly, large increases in the COC mass removal rate were observed. These increases were observed towards the end of the test, and several water samples collected near the end of the project had concentrations of approximately 50 percent the solubility of PCE, indicating that DNAPL was about to be extracted.
- The injection of air into wells that had received steam for an extended period of time led to substantial increases in the COC concentrations in nearby extraction wells, indicating that an effective mechanism exists which allows the COCs to be released by the heating, then stripped from the fractures by air migrating relatively rapidly between injection and extraction boreholes.
- The ERT data and the temperature data were in general agreement with the energy balance calculations, indicating that these monitoring techniques are relatively reliable for a complex site such as this one.

Overall, the data suggest that full-scale SER at a site like the Loring Quarry would require a carefully characterized source zone, a substantial staged implementation approach which includes interconnectivity testing, a dense network of wells at modest spacing (less than 6 meters (20 feet) borehole spacing), and a relatively long period of operation (more than nine months). Furthermore, it

is not evident from the research project whether complete heating could be achieved using this technology alone, or whether COC capture can be reliably obtained at sites this complex.

10.3.3. Discussion of Additional Technology Objectives

During the field implementation, four additional technology objectives were identified (Chapter 1.3.2 and Table 1.3.2-2). The additional objectives are discussed below.

TO-8. Determine the value of borehole tests and interconnectivity tests in determining the best use of each borehole interval for operation.

The data obtained from the rock-chip sampling, depth-specific slug testing, and the interconnectivity testing were used to critically examine the original plan for steam injection and fluid extraction. Based on this analysis, the injection and extraction scheme was modified substantially. Several planned injection intervals were instead used for extraction due to high rock-chip COC concentrations. Several other intervals intended for injection proved to have low permeability and were therefore not completed as injection intervals from the start. For a site this complex, these tests, and the integration of the data prior to completion of the boreholes, were deemed to be invaluable. It is fair to say that without these tests, we would not have been comfortable moving into operations. The tests provide additional confidence that steam is injected into, and fluids are extracted from, the most favorable locations.

TO-9. Study the mechanisms and importance of using air co-injection to improve the subsurface remediation.

This was successfully completed, and the injection of steam and air in combination, or staged over different time periods, showed great promise for accelerating COC mass removal. In particular, the large increase in mass removal that occurred after cessation of steam injection and continuation of air injection near the end of the project provided compelling data to show that the air injection accelerated mass removal. Co-air injection was initially tried to stimulate the overall heating rate (as had been observed to be effective at Edwards AFB, supposedly due to development of increased fracture permeability; Earth Tech and SteamTech, 2003). However, by comparing steam injection rates with and without air injection at this site, it was established that often the co-injection of air would decrease the ability to inject steam, likely due to the air creating a vapor block in the fractures connected to the injection interval. Therefore, staggered injection of steam and air was tried, and it was observed that the PID readings from nearby extraction wells would increase significantly during the period of air injection. While the subsurface mechanisms for this can only be elucidated by theoretical examination at this point, the following explanation is offered:

- During periods of steam injection, the added energy leads to migration of COCs along the fractures away from the injection well by vaporization and re-condensation or dissolution. This transports COCs towards the extraction wells, with elevated COC concentrations in the condensate between the steam-filled zone near the injection well and the extraction wells.
- Dissolution, diffusion, distillation, and desorption can potentially also release COCs from the matrix. These COCs would then travel with the fluids towards extraction wells.
- When steam injection ceases, and air injection starts, the situation changes from one where all the injected vapor condenses to one where all the injected vapor has to flow away from the injection well. As air flows through the heated zones and through the fractures containing steam condensate, the condensate is partially displaced by the non-condensable air, and some COCs are stripped from solution (or NAPL is encouraged to vaporize).
- As the air travels in the fractures, it reaches extraction wells and mixes with the water from other depths in the boreholes. If the air is rich in COCs, both vapor-phase concentrations and the COC concentrations in the mixed water will increase.
- The COC concentrations remain elevated until the affected fractures are flushed thoroughly with air.

While these mechanisms cannot be proven, they represent the most likely explanation for the observed acceleration of mass removal during steam and air injection cycles.

The potential spread of injected air was not evaluated. This would have required detailed tracer experiments that were not included in the design of this research project. However, no signs of steam or air surfacing through surface connections were seen. After snowfall had covered the site, no signs of surface heating outside the target area were observed. This suggests that escape of COC-laden vapors was not a concern at this site.

TO-10. Develop methods for pressure cycling in fractured rock with extraction hole temperatures below steam temperatures, and assess impacts on mass removal rates.

This was successfully accomplished by using the extraction well ground water levels to induce temporal pressure changes in the extraction wells. By aggressively lowering the water level in an extraction hole, the pressure near a fracture at the bottom of the borehole could decrease as much as 18 meters (60 feet) of water column (equal to about 200 kPa; 2 atm) over a period of less than 12 hours. PID screening of vapors from such extraction wells indicated that this can increase vapor-phase COC removal substantially, in a manner similar to the pressure cycling induced by ceasing steam injection while maximizing the applied vacuum on extraction wells (SEE patent; Udell et al., 1991).

TO-11. Study the effect of SER on mass removal rates at temperatures well below boiling, caused by mixing of cold and hot extraction borehole fluids.

This objective was satisfied by an integrated analysis of the collected data. It was demonstrated that enhanced COC concentrations in extracted fluids (both vapors and water) increased the mass removal rate significantly during the study, even when the extracted water did not heat significantly. This is discussed in more detail in Chapter 10.3.1, SITE objective P2 and in Chapter 10.2.

Chapter 11. Conclusions

11.1. Lessons Learned

11.1.1. *Characterization*

The evolution of the wellfield and operational designs during the pre-treatment characterization phase of the Quarry, extending up to the beginning of operations, demonstrated the importance of understanding contaminant distribution and the hydrogeology of a remediation site thoroughly. Practical considerations, most notably the significantly greater cost required for effective characterization of a fractured rock site compared to an unconsolidated porous media site, make it particularly important that the greatest potential value must be extracted from characterization methods. A variety of characterization techniques were used at the Quarry, and while all of these provided information that was incorporated into the developing conceptual model of the subsurface, experience at this site showed a number of ways in which some relatively under-used techniques could be more effectively incorporated into future characterization efforts. Experience gained here also underscored the importance of other characterization techniques. In summary, some pertinent comments can be made:

11.1.1.1. Detailed Mapping

At this site, located in a former bedrock quarry with abundant three-dimensional exposure of rock, detailed mapping of structural geology of the site and surrounding areas had been conducted (e.g., Beane et al., 1998). This is a simple and cost-effective means of outlining the range and diversity of structures of potential hydrologic significance and of determining their possible history of development. Mapping of the site also provided a broad framework within which the subsequent characterization efforts could be accommodated. Wherever possible, mapping information from all sources, including large-scale site investigation mapping and small-scale academic, federal or state geologic maps, should be used, including fracture-trace analysis. This information should be analyzed and converted to a format suitable for direct integration with CADD plans used in subsequent characterization and wellfield design. Generating an effective base map will ensure consistent and comparable data representations.

At sites which do not offer abundant exposure of rock, a range of surface-based geophysical methods should also be considered as part of the baseline characterization effort. Surface geophysical techniques successfully used in site characterization include ground penetrating radar, electromagnetometry (EM) methods, electrical resistivity or conductivity methods, seismic refraction, and reflection methods. Electrical methods can include profiling (using a variety of array configurations) and sounding (using both linear and square-set arrays). The suitability of individual methods is dictated by the specifics of site and regional geology. A discussion of the theory and application of suitable methods is beyond the scope of this report; however, useful descriptions, case histories, and references are contained in publications such as those by EPA (1993; 2000) and USACE (1995).

11.1.1.2. Coring

At the Quarry site, a large number of wells were cored over their entire length. The high competency of the bedrock at this site ensured excellent recovery of most of the cored intervals, thereby providing a permanent record of structures intersected by boring that would be used for the remediation research project. The diamond drilling process used to collect the rock cores is relatively slow and expensive compared to other drilling methods, while the core itself is unoriented, requiring that the structures present in the core be correlated with similar structures of known orientation derived from direct mapping. In this research project, the need for coring was partly based on the need to recover material for rock matrix sampling (by the MERC method) and provided the additional benefit of smooth boring walls (in comparison to those produced by other drilling methods). The smooth boring wall allows a more effective seal to be maintained during straddle packer testing.

At sites where bedrock competency is lower or where direct sampling is not required, much of the utility of rock core can be achieved using borehole image profiling methods, which are able to directly measure the orientation of planar structures intersecting the boring, while producing “pseudo-cores” for conventional examination on computer monitors or printed images. These are discussed in more detail below.

11.1.1.3. Borehole Geophysics

At the Quarry as part of this research project, a suite of geophysical methods were used to profile each of the borings. These included caliper, fluid temperature, fluid resistivity and acoustic televiewer (ATV).

The combined caliper, fluid temperature and fluid resistance probes are commonly used borehole-logging tools. They provide a low-cost, simple measure of probable fracture locations in the borehole wall that can serve as a starting point for identifying features of interest to be correlated with visual logging methods, and which, in turn, serve as a framework on which to build an aquifer testing program. Fluid resistivity logging proved to be particularly effective at identifying features that subsequently were demonstrated to be hydraulically active. As such, this suite of probes should be used to profile all proposed operational wells as a matter of course as part of a general wellfield characterization program.

11.1.1.4. Acoustic Televiewer (ATV)

The ATV logs produced an effective record of the location and general orientation of those fractures that intersected the boring. However, no useful information could be gleaned regarding the nature or extent of fracture filling materials. Similarly, the ATV log failed to provide any detail of lithological variation or internal structure within the unfractured bedrock, such as sedimentary structures or systematic changes in mineralogy. Information of this type can be used to identify a stratigraphic sequence in core that can be correlated with adjacent borings and regional mapping, thereby serving as a tool to aid in structural analysis of bedrock. Borehole profiling methods that provide a photographic image of the boring walls, such as Optical Televiewer (OTV) or Borehole Image Profiling System (BIPS), provide greater detail (subject to potential limitations of poor color contrast in wall rocks and opacity of ground water), and are a more effective characterization tool in areas where interwell correlation is a requirement of characterization.

11.1.1.5. MERC Sampling

The methanol extracted rock chip (MERC) sampling method was originally developed for use at the Quarry (HLA, 1999c) as a means of providing fracture and location specific data on the distribution of contaminants. The procedures and assumptions used during this project are described in Chapter 4.1.2. This technique estimates the amount of contaminant mass that is extractable from the rock matrix, although it is known from the extraction of a subset of the samples that the one week extraction time used did not extract all of the contaminants from the rock matrix. In light of the very low porosity of the unfractured bedrock at the Quarry (<0.5 percent; ABB-ES, 1997), most MERC samples were collected from weathered fracture margins adjacent to a fracture with some samples (one per borehole) collected from the interior of long unfractured lengths of core.

The Phase II characterization (HLA, 1999c) had evaluated the use of MERC samples for estimating mass of contaminants in the system by considering the mass of contaminant distributed among fractures and the total potential mass contained in the impacted volume, as indicated by the average MERC mass data. It was found that the use of MERC samples, porosity, and organic carbon fraction in conjunction with the conceptual fracture model tended to underestimate the total volume of contaminant present in the rock mass, as compared to that calculated from the estimated total mass flux leaving the system in the dissolved phase. Thus, MERC sampling can only provide a qualitative means of assessing contaminant mass. However, it does provide a convenient indication of the location of contaminant within the rock mass sampled, which in turn, gives an indication of those fractures that acted as contaminant pathways, providing an understanding of contaminant transport in the system. Collectively, this provides an important piece of information that contributes towards the development of a conceptual model for any site, and its use is recommended for that reason. Contaminant distribution information is especially important for SER remediation as perimeter injection wells should be in relatively clean areas so that contaminants are not transported away from the target area by the injected steam.

11.1.1.6. Discrete Interval Ground Water Sampling

Ground water samples from completed wells within the target area were collected from short intervals of the wellbore that had been isolated by straddle or single inflatable packers. This allows particular features of interest to be sampled, thereby allowing the relative contribution to the contaminant load of a particular fracture (or group of fractures) to the contaminant concentration averaged over the length of the test interval to be determined. In conjunction with MERC sampling of matrix concentration, these data are important in developing a conceptual model of contaminant migration within the rock from an original source. It also serves to identify fractures of interest to target with steam injection, the hydraulic properties of which can then be assessed by subsequent aquifer testing.

11.1.1.7. Head Measurements

By simply recording the natural ground water head in all of the open wells at the site, three discrete zones of different head were apparent within the Quarry. This condition, lying within such a small area, was interpreted as meaning that each of the areas could be expected to contain wells that were relatively better connected to each other than were the wells of adjacent areas with significantly different head values. The discrete areas were assumed to be isolated from each other hydraulically, presumably by intervening areas of sparsely fractured rock. This model was subsequently confirmed by pulse interference testing. While the differences in head at the Quarry were relatively large because of the considerable topographic relief present across the site, the delineation of hydraulically isolated areas using such a simple method strongly recommends the use of this approach at all fractured rock sites.

11.1.1.8. Discrete Interval Transmissivity Testing

The straddle packer hydraulic testing conducted in 2001, as the first stage of aquifer testing at the site (Chapter 4.1.4), established a vertical profile of transmissivity for each proposed operational well. Each profile typically measured transmissivity in 3-meter (10-foot) increments from 3 meters (10 feet) bgs to at least 15 meters (50 feet) bgs. The deeper parts of the wells, which were generally more sparsely fractured, were more commonly isolated over longer intervals between packers or by using only a single packer. The establishment of a transmissivity profile in as many wells as practical should be regarded as a minimum standard for hydrogeological characterization in fractured rock settings. By establishing a record of transmissivity in the immediate vicinity of the boring or well, an initial correlation of aquifer properties to geological structures and geophysical anomalies can be made. This represents a first step in the hydrogeological characterization by allowing the identification of pairs of depth intervals to be investigated by pulse interference testing. In cases where more detailed pulse interference testing is beyond the project scope, the transmissivity profile alone can also serve as a template on which to select suitable injection and extraction intervals for the completed operational wells. However, it should be noted that there is no reason to assume that the optimum hydraulic connection between two wells will extend between the zones of highest transmissivity encountered in those wells. Thus, interconnectivity testing is to be strongly recommended.

11.1.1.9. Interconnectivity Testing

As discussed in Chapter 4.1.6, several phases of interconnectivity testing using pulse interference methods were employed during hydraulic characterization of the Quarry. In a wellfield of this extent with comparatively deep wells, the number of possible straddle packer-isolated intervals that could be tested is prohibitively large, and a limited number of well pairs must be selected. The characterization effort demonstrated that a longer packer interval, comparable to that used in the previous transmissivity profiling, should be used in order to reduce the total number of tests required and to allow a clearer comparison between the transmissivity profiles and the interwell connections. Size limitations of the straddle packer equipment used at this site were such that wells for monitoring could not be tested for interconnectivity. For example, the smaller diameter of well VEA-5, which had originally been intended for use as a geophysical monitoring boring, prevented straddle packer testing of interwell connections to this boring, in a part of the test site that early phases of characterization had shown to be suitable for injection. In the future when it is desirable that interconnectivity testing be conducted, all wells should be drilled at, or reamed out to, at least 0.15 meters (0.5 foot) in diameter.

The constant head pulse interference test, using pressurized injection (as described in Chapter 4.1.6), has the advantage of locating lower permeability interconnections by the injection of larger quantities of water. These lower permeability interconnections may also come into play during long-term steam injection remediations. However, logistical considerations at the Quarry, where water supply was problematic during testing, showed that in similar sites the slug interference method to be more practical than a constant head test.

In more general terms, in any fractured rock steam injection remediation site, interconnectivity testing should be regarded as an essential component of the hydrogeological characterization of the site. While all other components described above provide useful information and increase the understanding of the site beyond the level typically encountered in general characterization, only interconnectivity testing establishes the presence of real interwell fluid flow pathways and allows their transmissivity to be determined. The potential importance of this is demonstrated by the possibility of strong anisotropy in rock permeability over short distances, particularly in crystalline or metamorphic rocks of low permeability and porosity. This is seen in the head differences encountered over short distances at the Quarry and confirmed by (for example) the apparent absence of any significant connection between I-7 and I-8 and the target area at the eastern end of the site.

In an ideal setting, the potential pathways of the steam could be investigated prior to steam injection by conducting advective tracer experiments between the proposed steam injection intervals and adjacent observation (withdrawal) wells. Experience with conducting these types of experiments at similar sites (e.g., Novakowski et al., 1999), has shown that the link between hydraulic response and tracer arrival is strong; however, the effort to conduct tracer experiments is significant in comparison to the completion of interconnectivity testing. Thus, interconnectivity testing is a less resource intensive approach that should provide information of similar quality to that provided by tracer experiments. In future investigations of SER in fractured bedrock, it may be worthwhile to determine if tracer experiments can add enough value to the characterization process such that the extra expense is warranted.

11.1.1.10. Deep Well Ground Water Sampling

The deep, angled wells (SM-1, 2, and 3, described in Chapter 4.1.5) represented a departure from the conventional monitoring well approach. The intention was that they would contribute to the overall characterization effort using logging and transmissivity profiling techniques, as had been used in the vertical wells within the target area, by collecting this data from a wider area and over a greater depth. By using angled borings, it was possible to target particular groups of planar structures, such as vertical fractures, for investigation by orienting the boring to intersect the fracture at a high angle. As each of these borings was completed with multi-level sampling devices, they also served the longer term purpose of acting as monitoring wells. By having an angled orientation, they were able to intersect potential fluid pathways over long horizontal distances, effectively acting as a monitoring screen in a way that could only be duplicated by many vertical wells. In addition, at sites of suitable geometry, deep angled monitoring wells allow the rock mass underlying the remediation target volume to be sampled during operations without passing through the zone

directly affected by the remediation technique itself. At sites where mobile DNAPL may be contained in horizontal fractures, drilling from outside the source area does not have the potential to allow downward movement of the pooled DNAPL. Angled drilling in hard bedrock is more commonly required in geotechnical and mining applications than in environmental applications, thus, local environmental drilling companies may not be familiar with the technique. However, it is not technically challenging and need not be more expensive than vertical drilling if drillers familiar with the technique are employed.

11.1.2. Steam Enhanced Remediation

This section lists a number of specific lessons that were learned during the course of the field implementation of SER.

- Operation of SER in structurally complex, fractured rock sites requires a much more intensive characterization exercise than is typically the case for un lithified soils. In addition to the focused fracture interconnectivity hydraulic testing conducted during this study, it is important to determine the extent of the zone that will be influenced by injection and extraction in the remediation volume and how this likely interacts with existing flow paths to influence potential down-gradient receptors.
- SER heating was unexpectedly slow at the Loring Quarry, as discussed in Chapter 11.2.2 below. It could not be concluded that SER would have been able to meet the temperature targets set at this site, even if a much longer operational period had been allowed. Heat conduction into the rock matrix, heat losses to outside of the target zone, and heat withdrawn with the extracted fluids all will severely limited the size of the steam zone. However, despite the limited size of the steam zone, the heat in the system was mostly at the fracture surfaces (where most of the contaminants were located), and significant increases in the contaminant removal rates were achieved. It is possible that adequate treatment might have been achieved even without achieving target temperatures throughout the target zone.
- Increased steam injection pressures relative to those typically used in unconsolidated materials could be used to achieve increased injection rates and thereby accelerate heating. As a general rule, injection pressures in unconsolidated materials are limited to approximately 11 kPa/meter (0.034 atm/foot). It was observed at this site that the pressure could be more than doubled without steam excursions or other problems. The greater strength and density of the strongly lithified rock present at the Quarry allowed for injection at pressures as high as 34 kPa/meter (0.10 atm/foot) of depth to the top of the injection interval.
- Theoretical considerations suggested that thermal expansion of the rock matrix during heating could lead to shrinkage of the fracture apertures, as the rock expands and pressure builds at the contact points (Ketcheson and Zwiers, 1997). The importance of this phenomenon was evaluated by measuring steam injection rates at constant pressures. At this site, no reduction in steam injection rate was observed, suggesting that no significant shrinkage of fracture aperture caused by thermal expansion had occurred.
- At this site, the surface vapor cap proved to be relatively ineffective at preventing air infiltration to the extraction wells. This was not due to a deficiency in the cap itself, but was likely caused by the properties of the fractured bedrock system being addressed. The presence of a vertical face adjacent to the wellfield coupled with an abundance of near-horizontal interconnected fractures in the upper 6 meters (20 feet) of the subsurface, where blasting and other quarry activities had created and opened abundant fractures, likely resulted in the relatively low well-field vacuums achieved (less than 10 kPa; 0.10 atm) at the design flow rates. At other SER sites, typical vacuums in the subsurface are 17 to 50 kPa (0.17 to 50 atm). This would be a much less significant problem at sites that had not been subjected to quarrying, mining or other excavation activities.
- The steam injection rate could not, in practice, have been substantially increased above the rates achieved without a corresponding increase in the liquid recovery rate, since the water balance showed the net extraction to have been modest (when compared to net extraction rates at unconsolidated media sites). Thus, faster heating at this site could not have been achieved solely by injecting more steam. The liquid extraction rate would also have to be increased, which would likely have involved the installation of more extraction wells.
- In-ground air stripping after steam injection appeared to be very effective, as discussed under Technology Objective-9 (TO-9). At this site, it was found that a period of steam injection followed by a period of air injection increased the COC removal rates significantly (see Chapter 10.2).
- As discussed under TO-3 (Chapter 10.3.2), the heating of the subsurface at this site was severely limited by thermal conduction. Steam entering the fractures quickly gave up its energy to the rock matrix, limiting the extent of the steam zone in fractures. At the same time, with the temperature gradients present at this site, conduction rates were very low, and the entire rock matrix could not be heated. The large heat losses along fractures away from the steam injection points led to rapid condensation, and very short travel distances for the steam.
- For those wells completed with both injection and extraction intervals (e.g., I-4 and I-5), it was observed that steam short-circuiting from the lower injection interval to the upper extraction interval led to extraction of a significant fraction of the injected steam. This could have occurred through leaks in the grout seals, or by migration of steam through fracture systems near the boreholes. Cement-bond logging to detect fractures or voids in the grout in the well annulus which might permit steam short-circuiting could be a useful technique for future applications. In any case, while short-circuiting through grout seal leaks leads to a loss of energy without benefit, short-circuiting through fractures in the formation is beneficial for both heat-up and COC removal.

- Permanently installed, nested steam and air injection wells in a single boring are a simple and convenient way to inject steam at targeted depths over a large vertical interval, contacting the majority of open, permeable fractures with steam at a pressure large enough to allow flow into the fractures. Grout seals may be used successfully to separate the injection intervals, allowing higher pressures to be applied in the deeper intervals. The multiple-layered injection and extraction wells used at this site performed well (with the exception of steam short circuiting noted above), allowing multiple uses of the same boreholes and conversion of extraction wells to injection wells during operation, which increased the heating rate significantly.
- Moveable, inflatable packers would offer a more flexible solution to the need for making adjustments to injection and extraction intervals, provided that bladder polymers of suitable temperature and chemical resistance could be used. Initial development work by inflatable packer manufacturers suggested that suitable materials could be produced; however, it proved impossible to reliably produce polymers of suitable performance during the course of the project. Thus, the project proceeded with fixed installations.
- The steam generation and effluent treatment systems were purposely oversized for the project, in order to provide spare capacity. As the observed flow rates were between 10 and 30 percent of the design rates, systems of 25-33 percent of the capacity of those used could be employed at similar sites with consequent cost reductions in construction and operation.
- Downward mobilization of DNAPL due to lowering of interfacial tensions is a significant concern of any flushing/displacement technology. However, the interfacial tension of the PCE-water system is not reduced substantially by heating (Heron et al., 1998b). The reduction is less than 15 percent during heating from 10 to 88°C (50 to 190°F), and thus does not lead to a significantly increased mobility of the DNAPL. Significant details of the downward mobilization issue are provided in Heron et al. (1998b). However, it is likely that the interfacial tension of the spent solvents at this site was significantly different from that of pure liquid PCE, and the effect of temperature on the interfacial tension of NAPLs in the subsurface has not commonly been measured. For this site, three deep monitoring wells were installed and sampled for the purpose of determining if contamination existed below the treatment area before or after treatment. Although these wells did not indicate that contaminant concentrations increased below the target treatment zone (see Chapter 10.3.1), this is a limited number of sampling points on which to evaluate downward movement. Also, a low permeability zone at approximately 33 meters (100 feet) bgs at this site may have aided in limiting downward movement of contaminants. We can only conclude that the monitoring points that we had did not indicate that downward movement had occurred.
- Monitoring during SER could include subsurface pressure monitoring, which may include the use of pressure transducers or water level monitoring in suitable wells. Subsurface pressure monitoring could be conducted in both active wells used in the application of SER and in dedicated monitoring wells within and surrounding the remediation volume. The location and number of monitoring points will be dependent on the complexity of the site and the conceptual model of ground water flow available at the time of installation. Subsurface pressure monitoring should begin during site characterization, as part of the establishment of ambient conditions in the subsurface, and continue during remediation operations and during the recovery phase. The network of pressure monitoring wells surrounding the remediation volume should cover an area sufficient to encompass the zone of potential hydraulic influence. At Loring Quarry, possibly a much larger area was affected by ground water extraction than the zone of heating, and this may have been detected by subsurface pressure monitoring.

Overall, the impression of the leading experts in SER application was that this site may be the most complex and difficult site ever attempted using SER, and that the technology was severely challenged by the hydrogeology and COC distribution at this site. It is believed that while several promising indications of remedial progress were seen, the impressive results achieved at other sites may not be practically achievable at a site of this complexity using SER alone.

11.2. Technology Application

11.2.1. General Challenges for SER Applications in Fractured Rock

This section discusses challenges and general difficulties relevant to the application of SER in fractured rock. Despite the impressive results obtained at sites with unconsolidated materials and at the two first SER applications at fractured rock sites in Prague (Dusilek et al., 2001) and at Edwards AFB (Earth Tech and SteamTech, 2003), fractured rock sites with more complex geology and hydrology have characteristics which make it difficult for the geologists and engineers to provide a robust design. These characteristics include:

1. It is extremely difficult, and arguably impractical, to fully characterize the spatial distribution and physical properties of all fractures in any real geological setting. The location, geometry, and morphology of individual fractures in areas not directly sampled are often largely unknown. Even with careful site characterization, the highly variable properties of the fractures make prediction of flow direction of injected fluids difficult.
2. The vertical extent of DNAPL penetration is extremely difficult to establish, and may never be fully understood. For the design and cost estimates to be realistic, a target treatment depth needs to be established. This is more challenging at rock sites due to the “hit- or miss” results of typical characterization efforts.

3. Typically, weathering or human activity increases fractures near the surface, but fractures become less abundant with increasing depth. This makes it more difficult to heat the bottom of a treatment volume with techniques based on fluid flow, which was true at both Loring Quarry and Edwards AFB Site 61 (Earth Tech and SteamTech, 2003).
4. Fractures larger than $1\text{-}3 \times 10^{-4}$ meters ($3\text{-}10 \times 10^{-4}$ feet) are not likely to retain DNAPL effectively (Schwille, 1977), but will be preferential paths for injected fluids. This research has shown that significant contaminant concentrations can be found in fractures that appear to be closed, and do not appear to be active in the ground water flow system. The smaller and potentially dead-end fractures that may contain DNAPL residuals are much less permeable to steam, air, and hot water, and therefore, the flow system is not favorable for displacement of NAPL from injection to extraction points.
5. Rock porosity and matrix diffusion may limit the rate at which contaminants can be removed by vaporization. A significant fraction of the contaminant mass may be situated in the rock matrix. For example, a study of PCE contamination at the Smithville fractured rock site estimated that two thirds of the mass was contained in the porous limestone matrix rock, and only one third of the mass was in the open fractures (MacFarlane et al., 1997). At the Quarry site, small contaminant concentrations were found in the rock matrix approximately 0.30 meters (1 foot) from the nearest fracture. This complicates any technology that relies on contaminant flow through fractures during remediation. For SER, when the fractures are filled with steam or hot condensate, temperature gradients will be inward towards the matrix block centers during heat-up, potentially discouraging diffusion out of the matrix. After heat-up, pressure cycling is hoped to enhance removal by creating boiling of the pore water in the matrix. However, the effects of heat transport from fractures on contaminants within the rock matrix have not been the subject of research studies, and the effects are largely unknown. The remedial efficiency for the COCs that exist within the matrix should be a topic of future investigations, as discussed in Chapter 12.
6. Small fracture apertures, clay lining of fractures, and infrequent occurrence of fractures may severely limit the achievable rate of steam injection, and thereby, the heating rate.
7. Hydraulic and pneumatic control is always important for SER. In fractured rock, such control is much more challenging to achieve than in unconsolidated materials, as well as very difficult to document.

While these are general challenges for the designers and implementers, it should be noted that many fractured rock sites lend themselves to SER applications without presenting all these difficulties. Properties that make sites more amenable to SER include:

1. A relatively permeable formation overlying a permeability barrier such as a tight, competent shale.
2. Crystalline rock of low porosity and negligible matrix diffusion with a large number of open fractures.
3. Formations with predictable fracture pattern and angles, such as the roof sequence joints in the Valley and Ridge province of the U.S. Appalachians (excluding areas of karst features; Perry, 1978; Engelder, 2004).
4. Formations with strongly developed bedding fracture systems (such as the paleozoic limestones of the Niagara region, e.g., Novakowski and Lapcevic, 1988).
5. Formations with a high degree of fracture connectivity but lacking karst features.
6. Sites with a thick vadose zone in weathered rock, residual soil, or unconsolidated porous deposits where contaminant capture is achievable (as Edwards AFB Site 61; Earth Tech and SteamTech, 2003).
7. Large sites where SER can be very economical per unit volume in the target treatment zone.

In conclusion, while rock sites are more challenging than most unconsolidated media sites, they represent a continuum from relatively easy to practically impossible for the application of SER. In the following sections, approaches for SER in fractured rock and potential amendments and alternatives are discussed.

11.2.2. Recommended Approach for SER Implementation at Fractured Rock Sites

Ideally, site characterization would be completed before work began on a remediation design. Many years of experience in unconsolidated porous media by different researchers has shown that steam remediation designs can use two basic operational strategies:

1. Where the true lateral extent of a contaminated aquifer is known, the treatment area can be surrounded by injection wells, and extraction can proceed from the interior, utilizing a conventional steam-drive approach to maximum effect.
2. Where the true lateral extent of a contaminated aquifer is not known (as at the Loring Quarry) or full remediation is beyond the scope of the project (as in a pilot test), the treatment area will likely consist of a cell within a larger impacted area. The treatment design must then use a perimeter of extraction wells in order to provide the best circumstances for maintaining hydraulic control of the site and preventing lateral spreading of contaminant, and to control recontamination of the treatment cell after the end of treatment.

At the Loring Quarry, insufficient characterization data were available at the time of the original design to allow an adequate understanding of the contaminant distribution and hydrogeology. However, due to budget and time constraints, the decision was made

that operational wells would be used for the detailed characterization effort that was needed. Unfortunately, the operation wells could not also provide characterization of the larger scale hydrogeology surrounding the site. This prevented an effective assessment of the location and extent of any migration of steam, hot water, or mobilized contaminant away from the site during the project and also precluded the possibility of assessing the impact of the hydrologic manipulations conducted during the test on the ambient ground water flow regime. In many, if not all, “real-world” sites, funding is likely to be limited; thus, embarking on a lengthy and expensive characterization of a site is likely to be impossible. With that in mind, it makes practical sense to make operational wells an integral part of the characterization effort. It is apparent that a phased approach to characterization and well installation is appropriate, thereby allowing the understanding of the site conditions to be incrementally increased and the remediation design to be adapted to site conditions. To this end, flexibility in design is important, and all wells should be constructed in such a way as to allow them to be used for injection, extraction, or monitoring with a minimum of modification, as may be dictated at a later stage in implementation by the findings of the characterization effort.

The following sequence of events describes the characterization effort needed in order to truly understand a fractured rock environment such as the Loring Quarry.

1. Desk study – Use all existing data to develop a conceptual model and preliminary remediation design, including provisional characterization and operational well locations. This should include all available site investigation and characterization work. An attempt should be made to incorporate the site into a broader hydrogeological conceptual model.
2. 2-Dimensional (2-D) electrical resistivity (ER) survey – This should consist of a minimum of two lines of a length that is not less than six times the depth of interest. The lines should form an intersecting grid pattern covering the proposed treatment cell and the surrounding area and provide cross-sections of resistivity data to a depth at least as deep as the proposed target body of rock. The survey can provide an indication of the presence and orientation of major resistivity anomalies, which may correspond to hydraulically significant features such as faults, fracture zones, and highly permeable lenses or beds. In so doing, this survey can contribute to the overall understanding of the site geology and provide a broad framework into which subsequent borehole characterization efforts can be placed.
3. Phase I drilling – Core drilling should be completed to a total depth equivalent to the base of the target bedrock zone (at 0.15 meter (0.5 foot) boring diameter) in two borings located in areas of different resistivity, based on the findings of the 2-D ER survey. It is recommended that one of these should be a centrally-located boring. The soil profile (at sites where there is overburden) should be logged, tested for NAPL using Sudan IV, and sampled where NAPL is present or at mid-screen depths for VOCs if NAPL is not present. Bedrock geology should also be cored at HQ size from auger refusal to the total depth. The recovered core should be logged and tested for NAPL presence using Sudan IV dye. If NAPL is detected or suspected in discrete fractures or geological features in core, a rock chip sample should be collected using MERC protocols. These borings should also be subjected to geophysical logging prior to completion.

The completion of all wells is dependent on the requirements of the site owner and regulatory agencies. If possible, borings in bedrock should remain open during all phases of characterization. At sites where a substantial thickness of overburden is present, a temporary casing may be required to stabilize the upper part of the boring. At some sites, it may be unacceptable to leave borings open for the extended period necessary to conduct all characterization activities, because of the potential for downward mobilization of DNAPLs and cross-contamination of dissolved-phase or LNAPL contamination. In such cases, a temporary impermeable textile liner such as the FLUTE system should be everted into the well to block fracture intersections within the wellbore. The liner can be removed when the well is ready for final completion. At sites where a temporary liner is unacceptable, or where there are concerns regarding its ability to prevent cross-contamination, the wells should be completed as multiple screened wells according to the requirements of the remediation design. If this approach is followed, the diversity of characterization data and degree of flexibility in final well completion are substantially reduced. Useful characterization data can, however, still be gathered.

4. Phase II drilling – The remaining 0.15 meter (0.5 foot) borings should be drilled to completion depth. Coring or sampling need not be carried out. The completed borings should be fitted with a temporary casing to bedrock to maintain the integrity of the upper boring. All wells should then be profiled using standard geophysical logging methods, which should include, at a minimum, caliper, fluid temperature and resistivity, and OTV/BIPS or similar. In some settings, natural gamma (TD), electric (SP/SPR/8-32-in normal resistivity), ATV, and heat pulse flow meter (HPFM) may also be beneficial. Upon completion of geophysical logging, the well should be installed with a temporary liner or, if deemed necessary, completed according to their final remediation design.
5. Phase III drilling – If employed, Vertical Electrode Array (VEA) borings for cross-borehole ERT sensors should be drilled to completion depth at 0.10 meter (0.33 foot) diameter. Unless these borings are intended for use in further characterization activities, the pre-fabricated VEA/temperature probes should be installed and grouted into place after completion of any characterization activities.

6. Phase IV drilling –Any vertical or angled monitoring wells should be drilled and installed at this time. New monitoring wells should be drilled at 0.15 meter (0.5 foot) diameter and logged for the full suite of geophysical profiling methods as described above. Upon completion of geophysical logging, the well should be installed with a temporary liner or, if deemed necessary, completely installed as described in the remediation design. Any wells that may lie within the treatment zone, where significant heating can be expected, must be completed with all steel components to prevent failure if contacted by steam during operations. Angled wells that are located and oriented in such a way as to be expected to remain relatively cool during remediation operations can be completed with PVC materials, including multi-level sampling systems.
7. Development of all new monitoring wells – Pre-existing wells within the treatment cell should also be developed if found to be impacted by drilling of adjacent new wells. All wells should be gauged at the completion of development and head distribution maps produced.
8. Ground water sampling and transmissivity profiling – In open wells, intervals isolated by straddle packer assemblies should be sampled for COCs using low-flow techniques. Upon completion of sampling, slug tests may be conducted in the same packer-isolated intervals to measure transmissivity. Where multiple-screen completion wells have been installed, the screened intervals could be sampled as conventional monitoring wells, and slug tests could be used to determine transmissivity adjacent to the screened intervals.
9. Interconnectivity testing – Where open wells are available, individual pairs of transmissive fractures can be tested using the pulse interference method described in Chapter 4.1.6. Short depth intervals, isolated by straddle packer assemblies, and identified on the basis of previous geological interpretation and transmissivity profiling, should be selected for testing. Whenever practical, observations of response to pulse interference testing in adjacent, open wells should also be attempted. This approach serves to identify interwell connections that may be analyzed in subsequent tests, thereby augmenting the hydrogeological interpretation of previously acquired characterization data. At sites where wells cannot remain open for extended periods, the pulse interference method can also be used to quantify the transmissivity of interwell connections between the fixed, screened depth intervals.
10. Additional hydraulic testing – If deemed appropriate, additional conventional aquifer tests can also be conducted. Such tests might include step-drawdown tests, constant rate drawdown tests, and additional slug tests or pumping tests in overburden. While these tests were not conducted at the Loring site and add considerable expense and difficulty to the overall characterization effort, they would address questions of hydraulic control and ground water migration paths over a larger area than can be addressed by pulse interference testing alone. Also, they may elucidate low transmissivity interconnections that are not readily detected by short term slug interference tests.
11. Final well installation – At sites where wells have been left open during hydraulic testing, final completion as multiple screen injection/extraction wells can begin after final remediation design modifications have been made in response to findings of the characterization effort.
12. Aquifer recovery – The aquifer should then be allowed to recover for a period of several months after completion of hydraulic testing. The length of time at any particular site will vary, dependent on the local hydrogeological conditions. After the aquifer or aquifers have recovered, the first round of background ground water samples can be collected from the treatment and surrounding monitoring wells. During the recovery period, characterization data can be analyzed and the design and work plan modified where necessary.
13. Start of operations – Remediation operations can now begin.

11.2.3. Amendments and Alternative Approaches

As described in the discussion of Technology Objective 1 (TO-1; Chapter 10.3.2), the application of SER at this site did not lead to the expected and needed heating of the target treatment zone, and the maximum temperatures achieved were significantly below the target temperature. The most likely reasons for this were discussed under TO-3 and TO-6, and included:

- The widely-spaced fractures and low transmissivity of the target intervals.
- Only a limited number of borehole intervals were well suited for steam injection. This led to a design where steam injection was conducted at the eastern end of the test area, preferentially in deep zones with limited concentrations of COC. The site geometry, geology, and COC distribution were limiting factors themselves.
- The observed steam injection rates were relatively low, and raising the injection pressures to the limit of the steam generator did not lead to substantially faster heating. The most effective method that served to accelerate the heating of the subsurface was to increase the number of steam injection points by converting some extraction wells to injection wells, as was done with wells I-7, I-8, and VEA-5, about half way through the operational phase.
- The operational data convincingly showed that the heat migration, including the component related to thermal conduction, was insufficient at the timescale permitted by the project funding and schedule.
- The operational data indicate that heat losses into the matrix lead to steam condensation after relatively short travel distances in the formation. These heat losses lead to condensation of significant quantities of steam, creating a warm water front that had

to be displaced for the steam to fill the fractures. The resulting heating rate for a site with sparse fracturing and low fracture apertures is very slow.

Two alternatives are suggested for improving the completeness of heating at a site comparable to the Loring Quarry:

1. Operate SER over much longer periods, using smaller steam injection and effluent treatment systems. The maximum steam injection rate achieved for the whole site was approximately 500 kg/hour (1,200 lbs/hour), while the steam generator had a capacity of 3,600 kg/hour (8,000 lbs/hour). Similarly, the water extraction rates were below 20 lpm (5 gpm), and the treatment system had a capacity greater than 75 lpm (20 gpm). By operating over a longer period, improved heat distribution would have been achieved, even with the low heat-up rates observed. By reducing the size of the above ground equipment, the system could be run more cost effectively. However, it should be noted that the data collected during this project failed to show that the target temperatures could be achieved using this approach. Other factors, such as increased overall heat losses when operating for longer periods and the increased sensitivity to cold water moving through the target area, must be evaluated before a conclusive recommendation could be made.
2. Heat the site using different methods such as Electrical Resistance Heating (ERH) or Thermal Conduction Heating (TCH). ERH is limited by the electrical resistivity of the rock. A site-specific analysis on the applicability of ERH would have to be made, including a determination of acceptable electrode separations. For sites with very resistive rock such as limestone, it is likely that the electrodes would have to be placed close together (less than 4.5 meters (15 feet) separation) in order to achieve sufficient current flow through the formation to reach target temperature. The application of TCH is dependent on the thermal conductivity of the rock. Since the thermal diffusivities of limestone and quartz minerals are similar, it may be assumed that TCH can be used to heat limestone. Typical TCH heater well temperatures are in the 700°C (1,300°F) range, which significantly increases the conductive heating rate over that observed during SER, where maximum temperatures were 100-130°C (212-266°F). Using TCH, inter-well temperatures above 100°C can be achieved within an operational period of less than one year using well separations between 3.5 and 6 meters (12 and 20 feet).

The second option is attractive from a different standpoint as well: It is possible to extract fluids from all the TCH and ERH heating boreholes, which increases the chance of capturing COCs during heating by contacting and extracting from all the fractures that are penetrated by the boreholes. This keeps fluids moving inward towards the heated zone during operation, and reduces or eliminates the risk of spreading COCs.

One potential disadvantage of ERH and TCH is that the energy demand is larger for heating, since the entire matrix would be heated. However, the energy necessary to heat limestone is on the order of 65-130 kWh per cubic meter (6,300-12,600 Btu/cubic foot), which equals between \$6.5 and \$13 per cubic meter (\$0.20 and \$0.40 per cubic foot) at typical power costs.

While SER could probably reach target temperatures with a modified approach and more limited scope, and no claims are made regarding the alternative heating approaches as they have not yet been tested in fractured limestone, our collected experience indicates that for sites as complex as the Loring Quarry, the ostensibly more predictable heating of energy intensive methods such as ERH or TCH have promise. The use of these technologies in fractured rock warrants research in the future.

11.2.4. Conceptual Comparison of SER and TCH/ERH Costs for a Range of Site Complexity

The choice of heating technology depends on the complexity and size of the site. Likewise, the cost of both the remediation and the associated characterization necessary to design, implement, and document the remedial results, depend on site complexity and size. The following generalizations are offered:

- For complex sites such as the Loring Quarry, the effort necessary to fully define the source zone to be targeted for remediation would be substantial. For this project, the cost of the characterization effort exceeded the cost of the SER implementation (however, it should be kept in mind that SER costs were reduced by using boreholes that had been used for characterization). Yet, there is general consensus among the project team that while our understanding of the site was greatly increased by the characterization efforts, the subsurface distribution of COCs and the location of ground water flowpaths were only partly constrained and ultimately remained undefined.
- Assuming that a perfect source removal action were to be completed, the amount of data needed to document that the cleanup objectives had been met would be as substantial and expensive to collect as the pre-removal characterization had been. For many complex sites the available funding may not be sufficient for the characterization effort necessary to fully document that the remediation objectives have been met.
- When a more predictable remediation method (i.e., one that is not sensitive to subsurface properties that can vary significantly within the treatment zone) is used, less characterization efforts are necessary. Since there would be greater confidence that heat-up would be achieved, fewer thermocouples and sampling locations would be necessary. This reduces the cost of monitoring and characterization during and after remediation using a predictable heating method when compared to SER.
- Simple sites require less characterization and are easier to remediate using SER than complex sites, since steam flow and heating are more predictable in simple sites. This leads to relatively low cost per unit volume (see for example the predicted costs for scale-up application of SER at Edwards AFB; Earth Tech and SteamTech, 2003).

- SER application costs are strongly dependent on site complexity. As the complexity increases more boreholes are needed, there are more critical steps during implementation, longer operation times may be needed, and significantly more monitoring and adjustments may be needed during operation.
- The heating approach and cost for sites treated using more predictable heating methods such as TCH or ERH are relatively insensitive to complexity, since the heater wells or electrodes are placed throughout the target zone, and the heating occurs primarily by thermal conduction or electrical conduction. Complexity does not affect thermal or electrical conduction as much as it affects permeability.

Figure 11.2.3-1 qualitatively indicates how the cost of any source removal technology is higher for complex sites than for simple ones. For very complex sites, the characterization cost can be prohibitive. For a range of sites, including the simple to moderately complex sites, the cost of treatment dominates over the characterization costs. SER costs are likely to be lower than TCH costs for very simple sites where an inexpensive SER system can be used. However, the costs of a more predictable heating method such as TCH or ERH become more and more favorable compared to SER costs as the complexity of the site increases.

While these are merely speculative interpretations based on our knowledge of these technologies, the indication is that for a complex site such as the Loring Quarry, more predictable heating methods such as ERH or TCH, that do not rely on fluid movement to deliver the heat, would likely be more cost-effective.

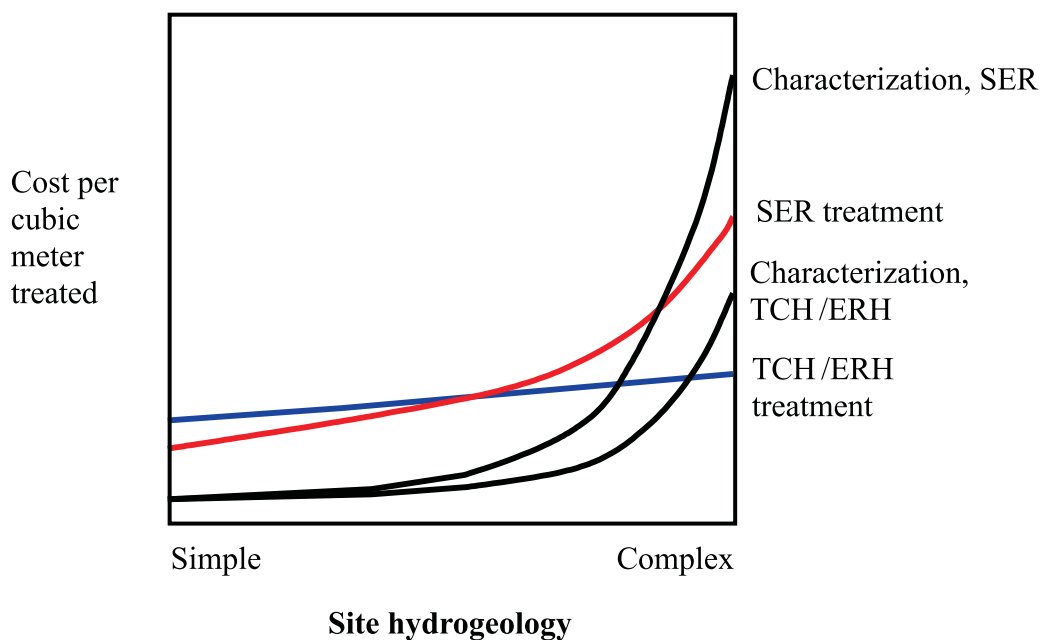


Figure 11.2.4-1. Sketch of comparative cost of site characterization and treatment costs for SER and TCH/ERH applications to sites with varying complexity.

Chapter 12. Recommendations for Future Research Related to Thermal Remediation in Fractured Rock

Although steam injection remediation in unconsolidated media has been studied extensively in the laboratory and in the field, and several full scale remediations have been successfully completed (see Chapter 3), very little research has been carried out to date on the use of thermal remediation to recover volatile contaminants from fractured rock. To the authors' knowledge, only three steam injection studies involving fractured rock have been conducted, of which this study was the first field-based research project on the use of steam injection for the remediation of volatile contaminants from fractured limestone. Short summaries of the other two projects are included in Chapter 3. Also, very little laboratory research has been done to date to support this field research. A search of the literature revealed one paper on a laboratory study of steam injection into fractured rock (Keller, 1998). Examination of the data collected during this project raises several questions, and additional research is recommended to further our understanding of how contaminants flow in and are trapped by fractures, how steam and heat flow in fractures, the mechanisms by which contaminants were released from the fracture surface or rock matrix by the steam or heat, and methods of tracking the movement of heat and/or steam in the fractured rock system via geophysical methods (such as ERT or cross-borehole radar tomography). Also, the extensive data set provided by this project on heat flow in fractures should be used to determine the adequacy of existing models for steam and heat flow in fractured rock systems. Each of these research needs is discussed in more detail below.

12.1. Rock Chip Samples to Determine Contaminant Distribution

Rock chip samples extracted by methanol were first used at this site in an attempt to determine the distribution of contaminants in the fractured rock system during the Phase I characterization in 1998. As part of this project, an attempt was made to standardize the procedures for obtaining rock chips, the amounts of rock and methanol to use, and the extraction period, in an effort to make the data a more quantitative measure of the concentration of contaminants. However, this was not actually achieved. Re-extraction of some of the samples during the back drill showed that the one week extraction time chosen was not adequate to extract all of the contaminants from the rock chips, as approximately 15 to 50 percent more contaminants were recovered by the second extraction. Although the data acquired by the method used was invaluable for determining the distribution of contaminants in the subsurface, laboratory research on extraction efficiency for various times and different techniques may identify improved methods for acquiring the samples and for the extraction process, and will aid in interpreting field data.

A question was raised by the rock chip data due to the fact that some of the highest contaminant concentrations in the rock samples were found in fractures that did not appear through visual examination of cores and by extensive transmissivity testing to have significant permeability. This is consistent with rock chip sampling results from other sites, where it was found that the active contaminant transport pathways identified using rock samples were greater than the active ground water flow pathways identified using hydrophysical or geophysical methods (Parker et al., 2004). Laboratory studies on the movement of NAPL contaminants in fractures would aid in determining the fate and transport of NAPLs in fractured rock systems.

12.2. Monitoring Methods

It is important during steam injection to be able to monitor the location and movement of hot water and steam and the associated heating of the media, both within and surrounding the remediation volume. This is even more important in the fractured rock setting because of the channelized nature of steam and fluid flow in only a limited number of fractures. Thermocouple strings placed in boreholes, as used here, provide data at specific points. Fiber optic temperature sensors would allow more closely spaced vertical data collection points; however, an adequate number of measurement points to understand the flow system would entail a large number of boreholes and would be excessively costly. Geophysical techniques such as ERT or cross-borehole radar tomography, both of which were tested during this project, may provide data on steam and/or heat movement using less invasive techniques, and thus would require fewer monitoring wells. The borehole radar tomography data were collected by USGS, and a short summary of their work is provided in Appendix G. A full report on their research will be presented in a separate report.

ERT has been used with considerable success at various other steam injection sites to monitor steam movement in unconsolidated media (e.g., LaBrecque et al., 1996; Newmark, 1994; Newmark and Aines, 1998; SteamTech, 1999), as well as at the Edwards Air Force Base steam injection treatability study (Earth Tech and SteamTech, 2003). At Loring, extensive ERT data were collected across the entire site throughout the steam injection and presented as 2-D images showing changes in resistivity and conductivity. Although there is some indication that plotted linear resistivity anomalies are consistent with geological structures observed in cores and known to be hydraulically significant, the resources available to date do not allow a full interpretation of the data collected.

The limited interpretation that has been done identified some significant anomalous signals. Specifically, the interpreted changes in resistivity are much greater than our current understanding of the relationship between formation resistivity and temperature would predict. While this may indicate that ERT is considerably more sensitive to temperature changes than previously supposed and hence, potentially of great usefulness, the difficulty in correlating observed temperature to interpreted resistivity has made geological interpretation of ERT data problematic. Detailed comparisons between what is known about the geology of the site should be compared with virtual cross sections of planar features seen in the resistivity data. This will serve to 'ground truth' the resistivity anomalies with real geological structures of hydrologic significance and will test the ability of ERT to map such structures. This process will be greatly aided by the ability to collect resistivity data in 3-D, thereby reducing the amount of data reduction needed prior to geological interpretation.

The next step in evaluating the use of ERT to monitor steam and heat flow in fractured rock is a detailed comparison of the ERT data with the temperature data collected from the thermocouples during steam injection. A simultaneous inversion of the interpreted heat flow and ERT data should be undertaken to provide a formal statistical assessment of the degree of agreement between these data sets in areas where there is uncertainty in the ERT signal. Also, laboratory measurements of the electrical resistance of cores taken from the site at various temperatures are needed to support this interpretation of the field data.

12.3. Evaluation of Existing Heat Flow Data

Although a considerable amount of heat flow data were collected during the project, the field data have yet to be reconciled with existing conceptual models for ground water flow and steam flow in fractures. Existing numerical models could be used to evaluate the potential propagation of steam and heat in the complex fracture network at Loring under the injection and extraction conditions that were employed.

12.4. Mechanistic Laboratory Studies of Steam Flow in Fractures

The laboratory work completed to date on steam flow in fractures is very limited. Questions remain on the rate of steam propagation in fractures, the effect of steam injection and condensation on NAPL within the fractures, the effects of non-condensable gases on steam and NAPL movement in fractures, and the fate of NAPL after it has been vaporized by the advancing steam front. Laboratory experiments of steam injection into fractures created using two glass slabs would allow visualization of the mechanisms occurring in an idealized system as well as quantification of steam and heat flow for the development of refined models of heat flow in fractures. The next step in understanding steam, heat, and contaminant flow in fractures is steam injection into actual fractured rock samples, which would allow the effects of matrix diffusion to be studied. Currently we have an hypothesis on the mechanisms that enhanced the recovery of the contaminants from the fractured rock system at the Loring Quarry, and laboratory experiments of this type would aid in determining what the actual mechanisms were and the relative importance of different mechanisms under different conditions, thus allowing optimization of the operation of these systems in the field.

12.5. Mechanistic Studies of TCH and ERH in Rock Settings

Since the delivery of heat by steam injection can be difficult and slow, related thermal techniques for heating and treating subsurface materials should be studied. Electrical Resistant Heating can deliver the energy directly to the rock and fracture fluids, as current flows through the formation. However, most rock sites have very low porosity and therefore also low water content. Low water content rock has significantly higher electrical resistance than typical unconsolidated material, and it is uncertain whether sufficient current can be passed through the rock to achieve heating to the boiling point of water throughout the treatment area. Laboratory studies into this topic, leading to tools for selecting electrode spacing and necessary voltage, would aid in extending the application of ERH to fractured rock. Thermal Conductive Heating is relatively predictable in rock systems; however, for both of these heating technologies, the fate of dissolved and adsorbed COCs located in the rock matrix is uncertain. The ability of vacuum extraction systems to capture all the vaporized and/or desorbed COCs, and strategies for extraction during field applications, should also be studied.

12.6. Effects of SER on the Dissolved Phase Plume

Within the environmental community today, considerable emphasis is being placed on studying the effects of source reduction on plume longevity. Indeed, one of the goals of many NAPL remediations is to reduce the size of and ultimately to eliminate the downgradient dissolved phase plume. Team members involved in this research project recommended that the objectives include studying the effects of SER in fractured rock on the dissolved phase plume. However, it was not possible to include this objective in this project because: 1) incomplete information prior to SER implementation on where the plume is, its extent, and pre-treatment concentration levels, 2) insufficient funding for the installation of additional monitoring wells to find and evaluate the downgradient plume, and 3) insufficient time to define the plume prior to and after treatment, as it is recognized that it may take years for the effects of SER to be seen and confirmed in the downgradient plume. Also, the fact that this project did not address the entire source area that was potentially creating the dissolved phase plume, and the fact that insufficient funding was available to fully treat the target area (resulting in increasing concentrations in the effluent even as the system was shut off), make it inappropriate to evaluate the effects of SER on the downgradient plume as part of this research project. However, it is certainly a topic that should be addressed by future research on thermal remediation in fractured rock.

12.7. Effects of Injection and Extraction on a Larger Area

During discussions within the research team on the increased contaminant concentrations observed in well JBW-7812B, it became apparent that SER implementation may have impacted a much larger area than was being monitored as part of this research project. In fractured rock systems such as that found in the Loring Quarry, the bedrock matrix may be of sufficiently low permeability that it does not contribute to ground water flow to a measurable extent. Thus, the fractures, which are only a small portion of the volume, dominate ground water flow, and their low porosity means that if a significant volume of water is moved in the system, the effect may be felt over great distances. Considering the large amounts of water that were injected and extracted as part of this research project, it is likely that a large area was impacted by the project, much larger than the spatial extent that would be expected to be effected in an unconsolidated media system. It is recommended that future research on the use of SER in fractured rock systems evaluate a larger area by employing an expanded hydraulic monitoring system to determine the spatial extent of the effects of the injection and extraction.

12.8. Use of Moveable, Inflatable Packers in Injection Wells

The original proposal for this research project included the use of moveable, inflatable packers in the wells to allow greater flexibility in injection and extraction well intervals during the course of the project. This would have reduced significantly the time and effort required to convert extraction wells to injection wells after steam injection began. However, packers that could withstand the expected temperatures and pressures could not be constructed in time for this project. Thus, fixed completions in the injection wells were used instead, and flexibility in system operation was lost. A potential area for future research would be on the potential costs and benefits of using these inflatable packers if they can be produced to withstand the expected subsurface conditions.



Chapter 13. References

- ABB Environmental Services, Inc. (ABB-ES). *Operable Unit (OU) 12 Final Remedial Investigation Report, Loring Air Force Base*, Limestone, Maine, 1997.
- Archie, G.E. Electrical resistivity log as an aid in determining some reservoir characteristics. *Am. Inst. Mining and Metal, (Engr. Transl.)* 146: 54-62 (1942).
- Basel, M., and K.S. Udell. Two-dimensional study of steam injection into porous media. *Multiphase Transport in Porous Media*, 127: 39-46 (1989).
- BERC. *Steam Enhanced Extraction Demonstration at Site 5, Alameda Point*. Field Feasibility Demonstration for the U.S. Navy, DO-9. Berkeley, CA: Environmental Restoration Center, University of California at Berkeley, 2000.
- Beane, W. Brandon, and R. Behre. Quarry Site—Former Loring Air Force Base, Orientation of Joints East and West of CDM Fault. State of Maine: Department of Environmental Protection, (Unpublished Map), 1998.
- Betz, C., A. Farber, C.M. Green, H.P. Koschitzky, and R. Schmidt. *Removing Volatile and Semivolatile Contaminants from the Unsaturated Zone by Injection of Steam/Air Mixture in Contaminated Soil*, London: Thomas Telford, 1998.
- Brandon, W., and R. Hoey. “Examination of the relationship of rock structure to groundwater flow in a fractured limestone aquifer.” Poster presented at the *USEPA/National Ground Water Association Fractured Rock Conference: State of the Science and Measuring Success in Remediation, Portland, ME*, September 13-15, 2004.
- Brandon, W.C., and R. Steimle. “Issues Identified From Several Remedial Pilot Studies in Fractured Rock.” Poster presented at the *Fourth International Conference on Remediation of Chlorinated and Recalcitrant Compounds, Battelle Memorial Institute, Monterey, CA*, May 2004.
- Butler, J.J., Jr. *The Design, Performance, and Analysis of Slug Tests*, Boca Raton, Florida: Lewis Publishers, 1998.
- CDM. *Fracture and Fault Analysis of the Quarry Site, Loring Air Force Base, Limestone, Maine*, CDM Federal Programs Corp., 1992.
- Cooper, H. H., Jr., J.D. Bredehoeft, and I.S. Papadopoulos. Response of a finite diameter well to an instantaneous charge of water. *Water Resources Research* 3(1): 263-269 (1967).
- Davis, E.L. *How Heat Can Accelerate In-situ Soil and Aquifer Remediation: Important Chemical Properties and Guidance on Choosing the Appropriate Technique*, EPA/540/S-97/502. Cincinnati, OH: U.S. Environmental Protection Agency, 1997.
- Davis, E.L. *Steam Injection for Soil and Aquifer Remediation*, EPA/540/S-97/505. Cincinnati, OH: U.S. Environmental Protection Agency, 1998.
- Davis, E.L. *Wyckoff/Eagle Harbor Steam Injection Treatability Studies*, Report to Region X, U.S. Environmental Protection Agency, 2002.
- DeVoe, C., and K.S. Udell. “Thermodynamic and hydrodynamic behavior of water and DNAPLs during heating.” In *Proceedings from the First Conference on Remediation of Chlorinated and Recalcitrant Compounds, Monterey CA*, 1998.
- Dusilek, P., P. Kvapil, and K.S. Udell. “Remediation of a partially fractured aquifer system containing a TCE source using steam enhanced extraction.” Paper presented at the 2001 *International Containment and Remediation Technology Conference & Exhibition*, Orlando, FL, June 10-13, 2001.
- Eaker, C. *Full-scale steam enhanced extraction at Visalia Pole Yard*. Personal communication, 2003.
- Earth Tech and SteamTech. *Site 61 Treatability Study Report, Steam Injection. Northwest Main Base, Operable Unit 8*. Edwards AFB, CA: Draft report submitted to U.S. Air Force Flight Test Center, Environmental Restoration Division, 2003.
- Engelder, T. Tectonic implications drawn from differences in the surface morphology on two joint sets in the Appalachian Valley and Ridge, Virginia. *Geology*, 32: 413-416 (2004).
- Gildea, M.L., and L.D. Stewart. *Demonstration of Steam Injection as an Enhanced Source Removal Technology for Aquifer Restoration*. Tyndall AFB, FL: Report for U.S. Air Force Research Laboratory, ARA Project #5241, 1997.

-
- Golder Associates, Inc. "Fracman: Interactive discrete feature data analysis." *Geometric Modeling and Exploration Simulation, Version 2.6*, 1998.
- Harding Lawson Associates, Inc. (HLA) *Phase I Data Report and Interpretation, Additional Site Characterization, Quarry Pilot Study*, 1998.
- Harding Lawson Associates, Inc. *Final Basewide Groundwater Operable Unit (OU 12) Feasibility Study Report, Installation Restoration Program, Loring Air Force Base*, 1999a.
- Harding Lawson Associates, Inc. *Final Proposed Plan for Operable Unit (OU) 12, Installation Restoration Program, Loring Air Force Base*, 1999b.
- Harding Lawson Associates, Inc. *Loring Air Force Base, Phase II Data Report and Interpretation, Additional Site Characterization, Quarry Pilot Study*, 1999c.
- Heron, G., M. Van Zutphen, T.H. Christensen, and C.G. Enfield. Soil heating for enhanced remediation of chlorinated solvents: A laboratory study on resistive heating and vapor extraction in a silty, low-permeable soil contaminated with trichloroethylene. *Environmental Science and Technology* 32 (10): 1474-1481 (1998a).
- Heron, G., T.H. Christensen, T. Heron, and T.H. Larsen. "Thermally enhanced remediation at DNAPL sites: The competition between downward mobilization and upward volatilization." In *Proceedings of the First International Conference on Remediation of Chlorinated and Recalcitrant Compounds*, Monterey, CA, 1998b.
- Heron, G., D. LaBrecque, and H. Sowers. "Steam stripping/hydrous pyrolysis oxidation for in-situ remediation of a TCE DNAPL spill." In *Proceedings of the 2000 Battelle Conference on Chlorinated and Recalcitrant Compounds*, Monterey, CA, 2000.
- Heron, G., S. Carroll, and S.G. Nielsen. Full-scale removal of DNAPL constituents using steam enhanced extraction and electrical resistance heating. *Ground Water Monitoring and Remediation* (In Press, Winter 2005).
- Hilberts, B. "In-situ steam stripping." In *Proceedings of the First International TNO Conference on Contaminated Soil*, Dordrecht, NL, 1986.
- Hunt, J.R., N. Sitar, and K.S. Udell. Nonaqueous phase liquid transport and cleanup 1. Analysis of mechanisms. *Water Resources Research* 24 (8): 1247-1258 (1988a).
- Hunt, J.R., N. Sitar, and K.S. Udell. Nonaqueous phase liquid transport and cleanup 2. Experimental Studies. *Water Resources Research* 24 (8): 1259-1269 (1988b).
- Hvorslev, M.J. *Time Lag and Soil Permeability in Groundwater Observations*, Bulletin 36. Vicksburg, MS: U.S. Army Corp of Engineers Waterways Experiment Station, 1951.
- Imhoff, P.T., A. Frizzell, and C.T. Miller. Evaluation of thermal effects on the dissolution of a nonaqueous phase liquid in porous media. *Environmental Science & Technology* 31: 1615-1622 (1997).
- Integrated Water Resources. *Deployment of a Dynamic Underground Stripping-Hydrous Pyrolysis/Oxidation System at the Savannah River Site 321-M Solvent Storage Tank Area, Final Report*. Prepared for Westinghouse Savannah River Company, 2002.
- Itamura, M.T., and K.S. Udell. "An analysis of optimal cycling time and ultimate chlorinated hydrocarbon removal from heterogeneous media using cyclic steam injection." In *Proceedings of the ASME Heat Transfer and Fluids Engineering Divisions*, 1995.
- IWR. *Deployment of a Steam Injection/Extraction System at LC34, Cape Canaveral Air Station, Final Report*. Prepared for MSE-Technology Applications, Inc., 2003.
- Jeffers, P.M., L.M. Ward, L.M. Woytowitch, and N.L. Wolfe. Homogeneous hydrolysis rate constants for selected chlorinated methanes, ethanes, ethenes, and propanes, *Environmental Science & Technology* 23 (8): 965-969 (1989).
- Kaslusky, S.F., and K.S. Udell. A theoretical model of air and steam co-injection to prevent downward migration of DNAPLs during steam enhanced extraction. *Journal of Contaminant Hydrology* 55: 213-232 (2002).
- Keller, A.A. "Steam injection to displace DNAPLs from fractured media." In *International Association of Hydrological Science*, Oxfordshire, UK, 1998.
- Ketcheson, D.R., and W.G. Zwiers. "Evaluation of in-situ restoration technologies for a DNAPL impacted fractured carbonate rock site at Smithville, Ontario. In *Proceedings of the Air & Water Management Association's 90th Annual Meeting & Exhibition*, Toronto, Ontario, Canada, 1997.
- Konopnicki, D.T., E.F. Traverse, A. Brown, and A.D. Deibert. Design and evaluation of the Shiells Canyon field steam-distillation drive pilot project. *JPT: Journal of Petroleum Technology* 31: 546-552 (1979).
- LaBrecque, D.J., A.L. Ramirez, W.D. Daily, A.M. Binley, and S.A. Schima. ERT monitoring of environmental processes. *Measurement Science and Technology* 7: 375-383 (1996).
- Leif, R.N., M. Chiarappa, R.D. Aines, R.L. Newmark, K.G. Knauss, and C. Eaker. "In situ hydrothermal oxidative destruction of DNAPLs in a creosote contaminated site." In *Proceedings of the First International Conference on Remediation of Chlorinated and Recalcitrant Compounds*, Monterey, CA, 1998.

-
- Llera, F.J., M. Sato, K. Nakatsuka, and H. Yokoyama. Temperature dependence of the electrical resistivity of water-saturated rocks. *Geophysics* 55: 576-585 (1990).
- MacFarlane, S., D. Mackay, and W.Y. Shiu. "Application of screening model for assessing subsurface NAPL contamination and remediation. In *Proceedings of the Air & Water Management Association's 90th Annual Meeting & Exhibition*, Toronto, Ontario, Canada, 1997.
- Mackie, B.E. "Interconnectivity study of a fractured rock aquifer." In *Remediation in Rock Masses*, Reston, Virginia: ASCE Press, 2000, 56-67.
- Mandl, G., and C.W. Volek. Heat and mass transport in steam-drive processes. *Soc. Pet. Eng. J.* 9: 59-79 (1969).
- Mercer, J.W., and R.M. Cohen. A review of immiscible fluids in the subsurface: properties, models, characterization and remediation. *Journal of Contaminant Hydrology* 6: 107-163 (1990).
- Michalski, A., and R. Britton. The role of bedding fractures in the hydrology of sedimentary bedrock – Evidence from the Newark Basin, New Jersey. *Ground Water* 35: 318-327 (1997).
- Michalski, A., and G.M. Klepp. Characterization of transmissive fractures by simple tracing of in-well flow, *Ground Water* 28:191-198 (1990).
- Morin, R.H., L.A. Senior, and E.R. Decker. Fractured-aquifer hydrogeology from geophysical logs: Brunswick Group and Lockatong Formation, Pennsylvania. *Ground Water* 38: 182-192 (2000).
- Newmark, R.L. *Demonstration of Dynamic Underground Stripping at the LLNL Gasoline Spill Site, Vol. 1-4*, UCRL-ID-116964. Livermore, CA: Lawrence Livermore National Laboratory, 1994.
- Newmark, R.L., and R.D. Aines. *Dumping Pump and Treat: Rapid Cleanups Using Thermal Technology*, UCRL-JC-126637. Livermore, CA: Lawrence Livermore National Laboratory, 1997.
- Newmark, R.L., and R.D. Aines. They all like it hot: Faster cleanup of contaminated soil and groundwater. *Science and Technology Review* (1998).
- Novakowski, K.S. Analysis of pulse interference tests. *Water Resources Research* 25 (11): 2377-2387 (1989).
- Novakowski, K.S., and P.A. Lapcevic. Regional hydrogeology of the Silurian and Ordovician sedimentary rock underlying Niagara Falls, Ontario, Canada. *Journal of Hydrology* 104: 211-236 (1988).
- Novakowski, K., P. Lapcevic, G. Bickerton, J. Voralek, L. Zanini, and C. Talbot. *The Development of a Conceptual Model for Contaminant Transport in the Dolostone Underlying Smithville, Ontario*, Smithville Phase IV Bedrock Remediation Program, 1999.
- Oochs, S.O., R.A. Hodges, R.W. Falta, T.F. Kmetz, J.J. Supar, N.N. Brown, and D.L. Parkinson. Predicted heating patterns during steam flooding of coastal plain sediments at the Savannah River Site. *Environmental & Geological Geoscience* 9 (1): 51-60 (2003).
- Pankow, J.F., and J.A. Cherry. *Dense Chlorinated Solvents and Other DNAPLs in Groundwater: History, Behavior, and Remediation*. Portland, Oregon: Waterloo Press, 1996.
- Parker, B., J. Cherry, K.J. Goldstein, A.R. Vitolins, D. Navon, G.A. Anderson, J.P. Wood, Matrix influence on contaminant mass distribution in a fractured shale, Abstract 1B-34, A.R. Gavashar & A.S.C. Chen, eds., *Remediation of Chlorinated and Recalcitrant Compounds, Proceedings of the Fourth International Conference on Remediation of Chlorinated and Recalcitrant Compounds*, Monterey, CA, Battelle Press, Columbus OH, May 2004.
- Perry, W.J. Sequential deformation in the central Appalachians. *American Journal of Science* 278: 518-542 (1978).
- Ramey Jr., H.J. "A current review of oil recovery by steam injection." In *Proceedings of the Seventh World Petroleum Congress*, 1966.
- Roy, D.C. *Geologic Map of the Caribou and Northern Presque Isle 15' Quadrangles, Maine*, 1987.
- Schmidt, R., J. Gudbjerg, T.O. Sonnenborg, and K.H. Jensen. Removal of NAPLs from the unsaturated zone using steam: Prevention of downward migration by injecting mixtures of steam and air. *Journal of Contaminant Hydrology* 55: 233-260 (2002).
- Schwille, F. *Dense Chlorinated Solvents in Porous and Fractured Media*. Chelsea, M: Lewis Publishers, 1977.
- Shapiro, A.M. Cautions and suggestions for geochemical sampling in fractured rock. *Ground Water Monitoring and Remediation* 22 (3): 151-164 (2002).
- She, H.Y., and B. Sleep. The effect of temperature on capillary pressure-saturation relationships for air-water and perchloroethylene-water systems. *Water Resources Research* 34: 2587-2597 (1998).
- Sleep, B.E., and Y. Ma. Thermal variation of organic fluid properties and impact on thermal remediation feasibility. *Journal of Soil Contamination* 6 (3): 281-306 (1997).

-
- Sleep, B.E., and P.D. McClure. The effect of temperature on adsorption of organic compounds to soils. *Can. Geotech. J.* 38: 46-52 (2001).
- SteamTech Environmental Services. *Steam Stripping and Hydrous Pyrolysis Pilot Project for the Portsmouth Gaseous Diffusion Plant, Portsmouth, Ohio*, DOE/OR/11-3032&D1. Department of Energy, 1999.
- SteamTech Environmental Services. *Pilot Study of Steam Enhanced Remediation for Mitigation of Residual DNAPL in Fractured Rock, Limestone, Maine*, Preliminary Draft Work Plan, 2001; Final Draft Work Plan, 2002.
- SteamTech Environmental Services. *In-Situ Remediation to Remove Non-Aqueous Phase Liquids Located in the Subsurface at the North-East Site Area A, Young-Rainey STAR Center, Largo, Florida*, SM Stoller and Department of Energy, 2003.
- Stephenson, K.M., and K.S. Novakowski. The Analysis of Pulse Interference Tests Conducted in a Fractured Rock Aquifer Bounded by a Constant Free Surface. *Journal of Contaminant Hydrology* (Accepted for publication 2004).
- Stephenson, K.M., K.S. Novakowski, E. Davis, and G. Heron. Hydraulic characterization for steam enhanced remediation conducted in fractured rock. *Journal of Contaminant Hydrology* (Submitted 2003).
- Stewart, L.D., and K.S. Udell. Mechanisms of residual oil displacement by steam injection. *SPE Reservoir Engineering* 1233-1242 (1988).
- Thiem, G. *Hydrologische Methoden*, Gebhardt, Leipzig, 1906.
- Udell, K.S., and L.D. Stewart. *Field Study of In Situ Steam Injection and Vacuum Extraction for Recovery of Volatile Organic Solvents*, UCB-SEEHRL Report No. 89-2. Berkeley, CA: University of California, 1989.
- Udell, K.S., N. Sitar, J.R. Hunt, and L.D. Stewart. *Process for In Situ Decontamination of Subsurface Soil and Groundwater*, United States Patent #5,018,576, 1991.
- Udell, K.S., and L.D. Stewart, Jr. *Combined Steam Injection and Vacuum Extraction for Aquifer Cleanup*, "In *Proceedings of the First International Conference on Subsurface Contamination by Immiscible Fluids*, Rotterdam, Netherlands: Weyer (ed.) Balkema, 327-336, 1992.
- Udell, K.S., and M.T. Itamura. *Pilot Demonstration of Steam Enhanced Extraction to Remediate Soils Containing JP-5 Jet Fuel*, Port Hueneme, CA: NAS Lemoore Final Technical Report, Department of the Navy, 1995.
- Udell, K.S. "Heat and mass transfer in clean-up of underground toxic wastes." In *Annual Reviews of Heat Transfer, Vol. 7*, New York: Chang-Lin Tien, Begell House, Inc., 333-405, 1996.
- Udell, K.S., M. Itamura, and L. Alvarez-Cohen. *NAS Lemoore JP-5 Cleanup Demonstration*. <http://www.abacus.me.berkeley.edu/BERC/projects/Lemoore> 1997
- USACE. *Geophysical Exploration for Engineering and Environmental Investigation*, EM1110-1-1802, 1995.
- U.S. Department of Energy. *Pinellas Environmental Restoration Project. Northeast Site Area A NAPL Remediation*, Grand Junction, CO: Young - Rainey STAR Center. U.S. Department of Energy, 2003.
- U.S. EPA. *Use of Airborne, Surface, and Borehole Geophysical Techniques at Contaminated Sites*, EPA/625/R-92/007. Cincinnati, OH: U.S. Environmental Protection Agency, 1993.
- U.S. EPA. *In Situ Steam Enhanced Recovery Process, Hughes Environmental Systems, Inc., Innovative Technologies Report*, EPA/540/R-94/510. Cincinnati, OH: U.S. Environmental Protection Agency, 1995.
- U.S. EPA. *Record of Decision, Operable Unit 12, Loring Air Force Base, Limestone, Maine*, EPA/ROD/R01-99/118. Cincinnati, OH: U.S. Environmental Protection Agency, 1999.
- U.S. EPA. *Innovations in Site Characterization: Geophysical Investigation at Hazardous Waste Sites*, EPA/542/R-00/003. Cincinnati, OH: U.S. Environmental Protection Agency, 2000.
- U.S. EPA. *Final Quality Assurance Project Plan for the SteamTech Environmental Services Inc. Steam Enhanced Remediation Technology Demonstration at Loring Air Force Base, Maine*, Cincinnati, OH: Including Amendments 1- 4 (March 28, 2002; August 7, 2002; October 2002).
- Volek, C.W., and J.A. Pryor. Steam distillation drive - Brea Field, California. *JPT: Journal of Petroleum Technology* 24: 899-906 (1972).
- Yuan, Z.G., and K.S. Udell. Steam distillation of a single component hydrocarbon liquid in porous media. *International Journal of Heat Transfer* 36 (4): 887-897 (1993).



Please make all necessary changes on the below label, detach or copy, and return to the address in the upper left-hand corner.

If you do not wish to receive these reports CHECK HERE ; detach, or copy this cover, and return to the address in the upper left-hand corner.

PRESORTED STANDARD
POSTAGE & FEES PAID
EPA
PERMIT No. G-35

State of Maine
Department of Environmental Protection
Augusta, Maine 04333

United States
Environmental Protection Agency
National Risk Management
Research Laboratory
Cincinnati, OH 45268

Official Business
Penalty for Private Use
\$300

EPA/540/R-05/010
August 2005



Recycled/Recyclable
Printed with vegetable based ink on paper that contains a minimum of 50% post-consumer fiber content processed chlorine free